IJAE

Italian Journal of Anatomy and Embryology

Official Organ of the Italian Society
of Anatomy and Histology

Vol. 127
N. 2
2023
ISSN 1122-6714

FIRENZE
UNIVERSITY
PRESS

IJAE
Italian Journal of Anatomy and Embryology
Official Organ of the Italian Society of Anatomy and Histology

Founded by Giulio Chiarugi in 1901

Journal e-mail: ijae@unifi.it – Web site: http://www.fupress.com/ijae

2023 Firenze University Press
Firenze University Press
via Cittadella, 7
I-50144 Firenze, Italy
E-mail: journals@fupress.com
Available online at
http://www.fupress.com/ijae

Italian Journal of Anatomy and Embryology

IJAE

Vol. 127, n. 2 - 2023

Firenze University Press

Italian Journal of Anatomy and Embryology
Published by
Firenze University Press – University of Florence, Italy
Via Cittadella, 7 - 50144 Florence - Italy
http://www.fupress.com/substantia
Direttore responsabile: **Ferdinando Paternostro, University of Firenze, Italy**
Direttore scientifico: **Domenico Ribatti, University of Bari, Italy**

IJAE
ITALIAN JOURNAL OF ANATOMY AND EMBRYOLOGY

Firenze University Press
www.fupress.com/ijae

Citation: Guidolin, D., Tortorella, C., De Caro, R., & Agnati, L.F. (2023). On the connectivity in the central nervous system and the age-induced changes of its network organization. *Italian Journal of Anatomy and Embryology* 127(2): 3-11. doi: 10.36253/ijae-14574

Data Availability Statement: All relevant data are within the paper and its Supporting Information files.

Competing Interests: The Author(s) declare(s) no conflict of interest.

On the connectivity in the central nervous system and the age-induced changes of its network organization

Diego Guidolin[1,*], Cinzia Tortorella[1], Raffaele De Caro[1], Luigi F. Agnati[2]

[1] *Department of Neuroscience, Section of Anatomy, University of Padova, 35121 Padova, Italy*
[2] *Department of Biomedical Sciences, University of Modena and Reggio Emilia, 41125 Modena, Italy*
*Corresponding author. E-mail: diego.guidolin@unipd.it

Abstract. Intercellular communication plays a crucial role as the structural substrate for the brain functions. It occurs according to two main processes, namely wiring transmission, i.e. the transmission of signals through physical contacts between cells, and volume transmission, i.e. the chemical signal diffusion along the interstitial fluid pathways. Intercellular communication represents the main rationale for the emerging field of connectomics, defined as the comprehensive study of all aspects of central nervous system connectivity, aimed at creating a comprehensive map (connectome) of the cellular networks in the brain to better understand brain functions. A consensus exists that the brain connectome structure follows a hierarchical or nested architecture, and macro-, meso- and microscales have been defined. Available data on network organization at these different miniaturization levels will be here briefly reviewed. The connectome, however, is also a dynamical entity, undergoing changes during lifetime. Thus, a specific focus will be maintained on the changes the network organization undergoes during normal aging.

Keywords: intercellular communication, brain networks, brain aging, connectome, molecular networks.

INTRODUCTION

The central nervous system (CNS) can be well described as an interaction-dominant dynamics system (Anderson et al., 2012; Guidolin et al., 2017) where interaction processes among cells and regions determine virtually all aspects of its integrative function, making difficult, and sometimes impossible, to assign tightly defined and unique roles to each specific component. The key role played by the network architecture as a structural substrate for the CNS functions represents the main rationale for the emerging field of connectomics, the comprehensive study of all aspects of CNS connectivity (Sporns, 2012). This idea has a quite long history behind it (see Schmahmann

and Pandya, 2007). Early neuroanatomists, indeed, were aware of the inappropriateness of their anatomical techniques to unravel the complex brain organization, and mapping the connections within the CNS has been a scientific goal for centuries. A significant example is represented by the 1685 Steno's far-sighted lecture "On the anatomy of the brain" (see Steno, 1965) where he emphasized the need of a program aimed at detailing brain anatomy in particular for what it concerns the fibers course through the white matter, since "it is impossible to explain the movements of a machine if the contrivance of its parts is unknown".

The characterization of inter-neuronal pathways, however, became possible only when new methods able to stain and trace neuronal connections were developed (Flechsig, 1901; see Sporns, 2013, for a thoughtful historical summary on this topic), and a significant advancement in the field occurred in the 1990s with the development of noninvasive magnetic resonance-based imaging methods and the related computational techniques (see Le Bihan and Johansen-Berg, 2011, for a review). Thus, the idea emerged of creating a comprehensive map of the brain structural connections to better understand brain function based on the structural features of neuronal networks, leading to the definition of the NIH 'Human connectome project' (www.humanconnectomeproject.org) aimed at providing an unparalleled compilation of neural data and the opportunity to achieve never realized conclusions about the living human brain (Van Essen et al., 2012). As pointed out by Sporns (2013), the emphasis on structure is important because anatomically determined connections among CNS elements embody a large (but finite) set of properties that (at least in principle) can be objectively mapped and represented by appropriate network models characterized by well-defined geometrical, biophysical and functional features. Defining the connectome, however, involves a careful analysis of the communication processes existing between CNS elements and of the pathways they exploit.

In this respect, it has to be observed that although networks of neurons interconnected by synapses represent the fundamental structural substrate of the CNS function, they do not deal exhaustively with the issue. In the last decades, indeed, a broadened view on the connectivity in the CNS came with the proposal (Agnati et al., 1986; Nicholson, 2001) of the existence of two main modes of intercellular communication in the CNS (see Guidolin et al., 2017 for a recent review), that have been called wiring transmission (WT: point-to-point communication via private channels, as, for instance, synaptic transmission) and volume transmission (VT: communication by diffusion in the extracellular fluid and in the cerebrospinal fluid). Experimental evidence suggested that these communication processes involve not only neurons but also other types of cells in the CNS (Syková and Chvátal, 2000; Färber and Kettenmann, 2005; Guidolin et al., 2022), allowing the formation of 'complex cellular networks' including neurons and glial cells (in particular astrocytes), in addition to the extracellular matrix.

A further aspect deserving consideration concerns the hierarchical structure exhibited by CNS networks. It is well known, indeed, that all anatomic systems exhibit the pivotal property to form multiscale structures (Jacob, 1970) each of which forms "a whole in relation to its parts and is simultaneously part of a larger whole" (Grizzi and Chiriva-Internati, 2005). In the CNS this feature is of particular relevance, being its architecture extending over a range of up to five orders of magnitude of scales: from microns for cell structures at one end to centimeters for inter-areal neuronal connections at the other. Thus, a hierarchical or nested architecture has been suggested as a suitable model to describe the CNS network organization (Agnati and Fuxe, 1984; Sporns et al., 2005; Sporns, 2013; Guidolin et al., 2016). From the point of view of connectomics this structural feature poses a significant challenge (see Zalesky et al., 2010), that concerns an unambiguous identification of the significant levels of organization. In this respect, an almost general consensus exists (see Agnati and Fuxe, 1984; Sporns et al., 2005) in defining at least three nested levels (see Guidolin et al., 2017 for details), namely the "macroscale" (where CNS areas and neuronal populations represent the basic elements), the "mesoscale" (the level of complex cellular networks forming a CNS area) and the "microscale" (where single cells and intercellular contacts, such as synapses, can be found). They are schematically illustrated in Figure 1 and briefly discussed in the sections that follow. Furthermore, being age one of the arguably most robust sources of neurobiological variation in the connectome, a specific focus will be on available data illustrating the changes the CNS network organization undergoes during normal aging.

MACROSCALE: CNS NETWORKS AND PATHWAYS

Basic elements at this level are CNS areas, neuronal populations and the pathways connecting them. A number of anatomical regions on the order of 100 or more (Van Essen et al., 1998; Glasser et al., 2016), for instance, can be defined in the human cerebral cortex on the basis of several different criteria (see Wig et al., 2011). Despite the limitation associated with the lack of

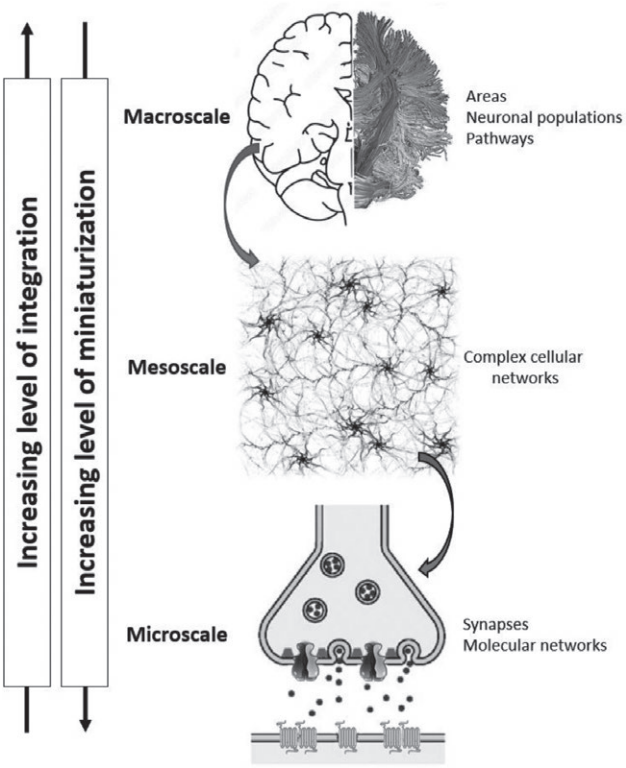

Figure 1. Schematic representation of the hierarchic structure of CNS networks, characterized by at least three nested levels of increasing miniaturization.

a single universally accepted parcellation scheme, the macroscale level is considered the most feasible organizational level for a first draft of a connectome (Sporns et al., 2005). In this respect, direct, invasive, techniques for localizing brain regions and tracing anatomical connections have been available for many decades and used in animal studies. They involve the use of tracers and the post-mortem analysis of the distribution of labeled axons (Markov et al., 2011). For mapping neuronal connections non-invasively in the human brain two approaches are currently used (see Behrens and Sporns, 2012), both involving magnetic resonance imaging (MRI), but relying on very different principles. 'Diffusion tractography' (tMRI) aims to infer the tracks of axon bundles in the white matter, while 'resting state functional MRI' (rfMRI) measures spontaneous fluctuations in the blood-oxygenation-level-dependent (BOLD) signal in grey matter regions and estimates statistical dependencies between these time series. Although methodological issues (see Behrens and Sporns, 2012; Mohanty et al., 2020), such as reduction of artifacts and improvement of accuracy by using more appropriate metrics, still deserve further development, the analysis by methods from network science and graph-theory (Rubinov and Sporns, 2010; Fornito et al., 2013) of available MRI datasets obtained in animals (see Hilgetag et al., 2000) and humans revealed a convergence on some key features of brain architecture. Concerning the neural connections between different cortical areas, for instance, they were shown to possess an organization in the form of 'small-world networks' (Watts and Strogatz, 1998; Liao et al., 2017), characterized by clusters of nearby cortical areas connected by short links, which in turn have long-range connections to other clusters (Sporns and Zwi, 2004; Stam and Reijneveld, 2007). Within clusters, the network topology identified by functional MRI is the type called 'scale-free' (Eguiluz et al., 2005), in which some nodes (hubs of connectivity) have a high number of connections to other nodes, whereas most nodes have just a handful. These basic architectures are schematically illustrated in Figure 2. VT pathways at macroscale were also proposed (see Fuxe et al., 2013; Illes, 2018). The proposal was based on the hypothesis that cyclic pressure oscillations (associated to intracranial arterial pulses) exist in the subarachnoid space leading to "tide" movements (Agnati et al., 2005) in the fluid of the Virchow-Robin spaces. Such convective movements would generate long-distance VT signals (Picard and Zanardi, 2015). As indicated by experimental studies on β-endorphin (Bjelke and Fuxe, 1993; MacMillan et al., 1998), peptidergic neurons appear able to operate via long-distance VT with distances in the range of millimeters (Jansson et al., 2002).

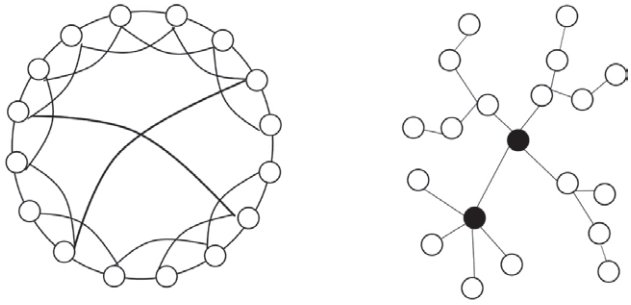

Figure 2. Schematic representation of the two basic network topologies identified in the CNS. The left panel illustrates a 'small-world network' and the right panel a 'scale-free network' (see text for details).

This research effort provided important insights into how anatomical connections shape and constrain brain dynamics, how this relation varies across individuals, and applications to clinical disorders are under development (Siddiqi et al., 2023). Concerning MRI-based life span studies (see Zuo et al., 2017 for a detailed review on the topic), tMRI approaches largely confirmed early findings indicating an inverted-U trajectory for white matter

development (Mwangi et al., 2013). In particular, phylogenetically primitive sensorimotor brain structures were found to exhibit the most rapid development and greatest preservation, while more phylogenetically advanced structures (e.g., prefrontal cortex) showed slower development and faster declines, suggesting a first-in-last-out pattern of development across the life span (Imperati et al., 2011). Complementing structural perspectives of life span development for the connectome are those emerging from rfMRI, suggesting, in young brains, age-related increases in long-range connectivity when compared to both short-range and interhemispheric connectivity (Fair et al., 2007). By contrast, aging studies revealed consistent patterns of decreases in long-range connectivity (Andrews-Hanna et al., 2007), leading to a reduction in network modularity (Chen et al., 2011; Varangis et al., 2019), i.e. in the propensity for a network to be divisible in subnetworks or modules. The interpretation of this pattern of results is contentious, with some suggesting that this pattern represents a compensatory process which allows an optimization of the wiring cost in older adults (Cabeza, 2002), while others posit that it simply reflects network dedifferentiation (Colcombe et al., 2005), a process that could be associated with some decline of cognitive functions (Varangis et al., 2019).

MESOSCALE: COMPLEX CELLULAR NETWORKS

Within each brain region, segregated neuronal subcircuits can be recognized. A classic example is provided by cortical columns (Lorente de Nò, 1938) consisting of an array of cooperating neuronal groups extending radially across the cortical layers and representing units of operation (Rakic, 2008). They appear loosely delimitated in morphological terms, being dynamic entities changing according to functional needs. A role in delimiting them is probably played by astrocytes, since the astroglial cells, especially in mammalian brains, define the microarchitecture of the parenchyma by dividing the gray matter into relatively independent structural units through a process known as 'tiling' (Bushong et al., 2004).

The relationship between neurons and astrocytes, however, is much more significant than this (see Guidolin et al., 2023 for a recent review). Evidence, indeed, exists highlighting the involvement of 'neuron-astroglial interactions' in the higher brain functions (Pereira and Furlan, 2010). As a matter of fact, the concept of 'tripartite synapse' has been introduced (Araque et al., 1999), since in most glutamatergic central synapses, the extremity of a protoplasmic astrocyte process wraps the synaptic cleft. Since astrocytes express membrane receptors to neurotransmitters and can release their own chemical messengers (gliotransmitters), this arrangement allows them to establish a cross-talk with both pre- and postsynaptic neurons. Several astrocytes participate in this functional organization, coupled with each other by gap junctions, leading to the formation of real neuroastroglial networks (Fellin and Carmignoto, 2004).

A further broadening of this view can be appreciated when VT-based intercellular communication processes are considered. In fact, this signaling backbone involves almost all the types of cells in the CNS (Syková and Chvátal, 2000). Hence, the concept of 'complex cellular networks' has been introduced to indicate the set of cells of any type that exchanging signals in a certain volume of brain tissue are capable not only of integrating multiple inputs to give out appropriate outputs but also of supporting each other's survival (Agnati et al., 2000).

On this basis, it can be proposed that the basic network elements at mesoscale should be defined by considering not only neuronal networks but also whole compartments of brain tissue where different cell types and the extracellular matrix work as an integrated 'functional module' (Agnati et al., 2009; Guidolin et al., 2017).

Age-related changes in brain cell number received a significant attention in the last century. Early studies (reviewed in Pannese, 2011) led to the idea that a significant loss of neurons occurred during normal aging, suggesting such a substantial loss as the origin of the cognitive decline often associated with brain aging. However, subsequent studies (see von Bartheld, 2018; Pannese, 2011 for reviews), exploiting more accurate morphometric methods, have evidenced that during normal aging neuronal loss is limited to restricted regions of the central nervous system and is quite small (probably no more than 10%). Similar concepts apply to astrocytes as well (see Pannese, 2021) and changes with aging in astrocyte number were detected only in specific brain regions. Moreover, the idea of an overabundance of glial cells as compared to neurons also changed with the development of modern counting methods and the concept that glial cells are not more abundant than neurons in human brains is now becoming increasingly accepted in the field (von Bartheld, 2018).

During aging, however, evident morphological changes have been reported in both neurons and glial cells. The most common age-related structural changes undergone by neurons involve a reduction in the complexity of dendrite arborization and dendritic length, and the myelin sheaths of axons may become less compact (Dickstein et al., 2007; Pannese 2011). Concerning glial cells, astrocytes may become hypertrophic and accumulate intermediate filaments, oligodendrocytes

and Schwann cells exhibit alterations consistent with the observed changes to the myelin sheaths, while in microglia, proliferation in response to injury, motility of cell processes, ability to migrate and phagocytic capabilities are often reduced (Rodriguez-Arellano et al., 2015; Pannese, 2021). Possible age-related modifications affecting VT processes in the cortex were also investigated (Nicholson, 2005) indicating no significant changes of the extracellular space in terms of volume and tortuosity, suggesting that, at least in the cortex, diffusion properties for small signaling molecules should not change dramatically with age.

Altogether these changes likely may modify the pattern of intercellular interactions at this scale, probably contributing to the behavioral impairment and cognitive decline often associated with normal aging.

MICROSCALE: SYNAPSES AND MOLECULAR NETWORKS

At this scale, single cells and synapses can be found. Of particular interest at this level are the so-called synaptic clusters (SC), in which multiple synapses act cooperatively to modulate their strength (Golding et al., 2002). SC are often organized around the dendritic spines and partially isolated from the surrounding environment by glial cells (Golding et al., 2002; Cutsuridis et al., 2009).

As pointed out by Sporns et al. (2005), drawing the connectome at microscale is infeasible, at least in the near future. Even considering the single neurons as the basic element, the connections to map would be in the order of 10^{15}, a technically impossible task. If we also consider other cell types and VT connections, the connectome size would become even greater. However, it must be said that such a level of structural detail may be unnecessary and a simple characterization of mechanisms remodeling connectivity at this scale could represent a sufficiently significant dataset for a deeper description of CNS functions. In particular, to better capture properties concerning the strength and plasticity of synapses, looking at the cell membrane can be useful. At this level molecular networks can be found. They are made of molecules (in particular proteins) that function as a metabolic and/or regulatory signaling pathway in a cell (Bhalla and Iyengar, 1999). For our discussion of particular interest are the 'receptor mosaics', i.e. macromolecular complexes formed at the membrane level by receptors as a consequence of direct (structural) allosteric receptor-receptor interactions (see Guidolin et al., 2019; 2023 for recent reviews). The cooperativity that emerges in the actions of orthosteric and allosteric ligands of the monomers forming the assembly provides the cell decoding apparatus with sophisticated dynamics in terms of modulation of recognition and signal transduction. Thus, the formation of the receptor mosaics allows an integration of the incoming signals already at the plasma membrane level and can significantly contribute to set and tune the efficiency of the connections between cells and, in particular, the synaptic strength (Agnati et al., 2003). Interestingly, methods from graph and network theory appear appropriate also to describe the dynamic behavior of interacting receptors (Guidolin et al., 2007), further suggesting the possibility of including these structures in the context of connectomics. In particular, the possible existence of receptors acting as 'hubs' in the receptor assembly has been suggested (Agnati et al., 2016). Due to their position in the network of receptor interactions, hub receptors could play a key role in the integrative action of the assembly and represent a target of primary importance from the pharmacological perspective.

As mentioned before, with increasing age the dendritic tree undergoes progressive regression. In this context, it has been known for a long time that the number of dendritic spines significantly decreases (Nakamura et al. 1985; Nunzi et al., 1987). These changes have been assessed quantitatively in certain regions of the nervous system. For instance, the reduction in spine number in monkey cerebral cortex ranges from 25 to 50% according to the area considered (Dumitriu et al. 2010), while in the CA1 region of the rat hippocampus the reported reduction was of about 12% (Nunzi et al., 1987). Being dendritic spines important sites of synapse formation, these findings are consistent with observations indicating a decrease of neuronal connectivity at microscale during normal aging (Morrison and Baxter, 2013). A tendency to reduced inter-astroglial coupling has also been reported (Cotrina et al., 2001). However, during aging astrocytes seem to conserve their ability to express spontaneous and neurotransmitter-dependent intracellular Ca^{2+} signals. Moreover, gliotransmission resting levels, and astrocyte-neuron interactions also appear largely conserved (Gomez-Gonzalo et al., 2017).

From the functional standpoint, one of the general hallmarks of aging is the decline of a number of physiological functions in response to a variety of stimuli. These observations led to an emerging hypothesis attributing aging to loss of cell communications (see Robert and Fulop, 2014) mainly associated either to some receptor loss in aging cells and tissues or to their uncoupling from their specific signaling pathways (Santos-Otte et al., 2019). Several examples of these processes have been

documented in the CNS. They include decline in muscarinic responsiveness with age (Joseph and Roth, 1990), loss of D_2/D_3 dopamine receptors in extrastriatal regions (Kaasinen et al., 2020), and alterations in the expression and activity of $G_{i/0}$ protein-coupled receptors in the human frontal cortex, hippocampus, substantia nigra and striatum (de Oliveira et al., 2019). The involvement of G protein coupled receptors (GPCRs) is of particular interest for the present discussion, in view of their well-documented (see Guidolin et al. 2007; 2019; 2023) capability to form receptor complexes at the cell membrane through direct allosteric receptor-receptor interactions. In fact, due to oligomerization of GPCRs at the membrane and their cooperative signaling, downregulation of some specific GPCR may affect signaling and drug targeting of other types/subtypes of GPCRs with which it interacts, opening the possibility that the dynamics of molecular networks could exhibit significant age-associated changes.

CONCLUDING REMARKS

The rapid increase of studies addressing connectomics clearly indicates that the anatomical mapping of the relationship among CNS components may lead to a deeper level of understanding of CNS functions. The CNS, indeed, is believed to accomplish its activity mainly through the integrative action of networks in which functions emerge from collections of elementary units (nodes), linked by connections and bound together dynamically (Bullmore and Sporns, 2012). Thus, drawing the connectome is much more than collecting a large descriptive dataset. It strongly implies the adoption of network models for brain function, including but not limited to the quantitative methods offered in abundance by network science (Sporns, 2013).

This research effort has been so far focused mainly on neuronal connectivity at a macroscale level, exploiting the possibilities offered by magnetic resonance imaging to evaluate the inter-regional structural and functional connectivity patterns. The obtained data demonstrated a number of nontrivial architectural features of the human neuronal networks (Behrens and Sporns, 2012). Brain integrative actions, however, strongly depend, but certainly not only, on the wiring diagram of neurons, since additional networks and processes exist modulating neuronal activity (Brezina, 2010). In this respect, two aspects should deserve consideration.

The first refers to the increasing evidence indicating that synaptic transmission is significantly complemented by cell types other than neurons. As illustrated above, neurons and glial cells form complex cellular networks communicating via two modes of connection, WT and VT, which are not mutually exclusive. From the connectomics point of view, it is also of interest to observe that both modes can be identified, mapped, characterized in terms of their neuroanatomical and biophysical features (Syková and Chvátal, 2020) and included in formal network models (Guidolin et al., 2007; 2017). The second concerns the level of highest miniaturization of the CNS network organization, where protein-protein allosteric interactions generate molecular networks performing integrative functions already at the plasma membrane level, suggesting they could be of relevance for connectomics (Sala et al., 2023). In this respect, of the greatest importance are direct (structural) receptor-receptor interactions, playing a role in setting synaptic efficacy and in memory processes (Agnati et al., 2003; Guidolin et al., 2007).

Finally, it must be observed that the connectome is a dynamical entity, undergoing changes during lifetime. A number of connectomics-based studies concerning typical and atypical development of human brain neuronal networks from birth to early adulthood are presently available (see Cao et al., 2016, for a review) and, as briefly discussed above, the number of studies on the modifications induced by the normal aging process is increasing (see Zuo et al., 2017). In this respect, however, a better understanding of the relationship between brain structure (at all the organizational levels) and behavior across the whole life span still represents a defining agenda for the next future. This effort, indeed, may help to better discriminate the effect that pathologic aging and disease processes have on the declining CNS architecture, as well as the interventions aimed at targeting these conditions.

REFERENCES

Agnati LF, Fuxe K (1984). New concepts on the structure of the neuronal networks: the miniaturization and hierarchical organization of the central nervous system. (Hypothesis). Biosci Rep 4: 93–98.

Agnati LF, Fuxe K, Zoli M, Ozini I, Toffano G, Ferraguti F (1986). A correlation analysis of the regional distribution of central enkephalin and beta endorphin immunoreactive terminals and of opiate receptors in adult and old male rats. Evidence for the existence of two main types of communication in the central nervous system: the volume transmission and the wiring transmission. Acta Physiol Scand 128: 201–207.

Agnati LF, Fuxe K, Nicholson C, Sykova E, eds. (2000). Volume transmission revisited. Progress in Brain Research, Elsevier, Amsterdam.

Agnati LF, Franzen O, Ferré S, Leo G, Franco R, Fuxe K (2003). Possible role of intramembrane receptor-receptor interactions in memory and learning via formation of long-lived heteromeric complexes: focus on motor learning in the basal ganglia. J Neural Transm Suppl. 65: 1–28.

Agnati LF, Genedani S, Lenzi PL, Leo G, Mora F, Ferré S, Fuxe K (2005). Energy gradients for the homeostatic control of brain ECF composition and for VT signal migration: introduction of the tide hypothesis. J Neural Transm 112: 45–63.

Agnati LF, Baluška F, Barlow PW, Guidolin D (2009). 'Mosaic', 'self-similarity logic', and 'biological attraction' principles: three explanatory instruments in biology. Commun Integr Biol 2: 552–563.

Agnati LF, Guidolin D, Cervetto C, Borroto-Escuela DO, Fuxe K (2016). Role of iso-receptors in receptor-receptor interactions with a focus on dopamine iso-receptor complexes. Rev Neurosci 27: 1–25.

Anderson ML, Richardson MJ, Chemero A (2012). Eroding the boundary of cognition: implications of embodiment (1). Top Cogn Sci 4: 717–730.

Andrews-Hanna JR, Snyder AZ, Vincent JL, Lustig C, Head D, Reichle ME, et al. (2007) Disruption of large-scale brain systems in advanced aging. Neuron 56: 924–935.

Araque A, Parpura V, Sanzgiri RP, Haydon PG (1999). Tripartite synapses: glia, the unacknowledged partner. Trends Neurosci 22: 208–215.

Behrens TEJ, Sporns O (2012). Human connectomics. Curr Opin Neurobiol 22: 144-153.

Bjelke B, Fuxe K (1993). Intraventricular beta-endorphin accumulates in DARPP-32 immunoreactive tanycytes. Neuroreport 5: 265–268.

Bhalla US, Iyengar R (1999). Emergent properties of networks of biological signaling pathways. Science 283, 381–387.

Brezina V (2010). Beyond the wiring diagram: signalling through complex neuromodulator networks. Phil Trans R Soc B 365: 2363–2374.

Bullmore E, Sporns O (2012). The economy of brain network organization. Nat Rev Neurosci 13: 336–349.

Bushong EA, Martone ME, Ellisman MH (2004). Maturation of astrocyte morphology and the establishment of astrocyte domains during postnatal hippocampal development. Int J Dev Neurosci 22, 73–86.

Cabeza R (2002). Hemispheric asymmetry reduction in older adults: the HAROLD model. Psychol Aging 17: 85–100.

Cao M, Huang H, Peng Y, Dong Q, He Y (2016). Toward developmental connectomics of the human brain. Front Neuroanat 10: 25.

Chen ZJ, He Y, Rosa-Neto P, Gong G, Evans AC (2011). Age-related alterations in the modular organization of structural cortical network by using cortical thickness from MRI. Neuroimage 56: 235–245.

Colcombe SJ, Cramer AF, Erickson AI, Scalf P (2005). The implications of cortical recruitment and brain morphology for individual differences in inhibitory function in aging humans. Psychol Aging 20: 363–375.

Cotrina ML, Gao Q, Lin JH, Nedergaard M (2001). Expression and function of astrocytic gap junctions in aging. Brain Res 901: 55-61.

Cutsuridis V, Wennekers T, Graham BP, Vida I, Taylor JG (2009). Microcircuits: their structure, dynamics and role for brain function. Neural Netw 22: 1037–1038.

de Oliveira PG, Ramos MLS, Amaro AJ, Dias RA, Vieira SI (2019). $G_{i/0}$-protein coupled receptors in the aging brain. Front Aging Neurosci 11: 89.

Dickstein DL, Kabaso D, Rocher AB, Luebke JI, Wearne SL, Hof PR (2007). Changes in structural complexity of the aged brain. Aging Cell 6: 275-284.

Dumitriu D, Hao J, Hara Y, Kaufmann J, Janssen WGM, Lou W, Rapp PR, Morrison JH (2010). Selective changes in thin spine density and morphology in monkey prefrontal cortex correlate with aging-related cognitive impairment. J Neurosci 30:7507–7515

Eguiluz VM, Chialvo DR, Cecchi GA, Baliki M, Apkarian AV (2005). Scale-free brain functional networks. Phys Rev Lett 94: 018102.

Fair DA, Dosenbach NU, Church JA, Cohen AL, Brahmbhatt S, Miezin FM, et al. (2007). Development of distinct control networks through segregation and integration. Proc Natl Acad Sci USA 104: 13507–13512.

Färber K, Kettenmann H (2005). Physiology of microglial cells. Brain Res Rev 48: 133–143.

Fellin T, Carmignoto G (2004). Neurone-to-astrocyte signaling in the brain represents a distinct multifunctional unit. J Physiol 559: 3–15.

Flechsig P (1901). Developmental (myelogenetic) localization of the cerebral cortex in the human subject. Lancet 158: 1027–1030.

Fornito A, Zalesky A, Breakspear M (2013). Graph analysis of the human connectome: promise, progress and pitfalls. Neuroimage 80: 426-444.

Fuxe K, Borroto-Escuela DO, Tarakanov A, Romero Fernandez W, Manger P, Rivera A et al. (2013). Understanding the balance and integration of volume and synaptic transmission. Relevance for psychiatry. Neurol Psych Brain Res 19: 141–158.

Glasser MF, Coalson TS, Robinson EC, Hacker CD, Harwell J, Yacoub E et al. (2016). A multi-modal parcellation of human cerebral cortex. Nature 536: 171–178.

Golding NL, Staff NP, Spruston N (2002). Dendritic spikes as a mechanism for cooperative long-term potentiation. Nature 418: 326–331.

Gomez-Gonzalo M, Martin-Fernandez M, Martinez-Murillo R, Mederos S, Hernandez-Vivanco A, Jamison S, et al. (2017). Neuron- astrocyte signaling is preserved in the aging brain. Glia 65: 569-580.

Grizzi F, Chiriva-Internati M (2005). The complexity of anatomical systems. Theor Biol Med Model 2: 26.

Guidolin D, Fuxe K, Neri G, Nussdorfer GG, Agnati LF (2007). On the role of receptor-receptor interactions and volume transmission in learning and memory. Brain Res Rev 55: 119–133.

Guidolin, D., Tortorella, C., De Caro, R., and Agnati, L.F. (2016). Does a self-similarity logic shape the organization of the nervous system? In: Di Ieva A (ed.) The Fractal Geometry of the Brain. Springer, New York.

Guidolin D, Marcoli M, Maura M, Agnati LF (2017). New dimensions of connectomics and network plasticity in the central nervous system. Rev Neurosci 28: 113-132.

Guidolin D, Marcoli M, Tortorella C, Maura G, Agnati LF (2019). Receptor-receptor interactions as a widespread phenomenon: novel targets for drug development. Front Endocrinol 10: 53.

Guidolin D, Tortorella C, Marcoli M, Maura G, Agnati LF (2022). Intercellular communication in the central nervous system as deduced by chemical neuroanatomy and quantitative analysis of images: impact on neuropharmacology. Int J Mol Sci 23: 5805.

Guidolin D, Tortorella C, Marcoli M, Cervetto C, Maura M, Agnati LF (2023). Receptor-receptor interactions and microvesicle exchange as mechanisms modulating signaling between neurons and astrocytes. Neurophamacology 231: 109509.

Hilgetag CC, Burns GAPC, O'Neill MA, Scannell JW, Young MP (2000). Anatomical connectivity defines the organization of clusters of cortical areas in the macaque monkey and the cat. Phil Trans R Soc Lond B Biol Sci 355: 91–110.

Illes S (2018). More than a drainage fluid: the role of CSF in signaling in the brain and other effects on brain tissue. In: Deisenhammer F, Teunissen CE, Tumani H, eds. Cerebrospinal fluid in neurologic disorders. Handbook Clin Neurol 146: 33-46.

Imperati D, Colcombe S, Kelly C, Di Martino A, Zhou J, Castellanos FX, et al. (2011) Differential development of human brain white matter tracts. PLoS One 6: e23437.

Jacob F (1970). La logique du vivant. Une histoire de l'hérédité. Gallimard, Paris.

Jansson A, Descarries L, Cornea-Hebert V, Riad M, Verge D, Bancila M et al. (2002). Transmitter receptor mismatches in central dopamine serotonin and neuropeptide systems. In: Walz W, Totowa NJ, eds. The Neuronal Environment, Brain Homeostasis in Health and Disease. Humana Press, New York, pp. 83–107.

Joseph JA, Roth GS (1990). Loss of agonist-receptor efficacy in senescence: possible decrements in second messenger function and calcium mobilization. In: Bergener M, Emini M, Stahelin HB, eds. The 1990 Sandoz Lectures in Gerontology. Challenges in Aging. Academic Press, New York, pp 167–184.

Kaasinen V, Vilkman H, Hietala J, Nogren K, Helenius H, et al. (2000). Age-related dopamine D2/D3 receptor loss in extrastriatal regions of the human brain. Neurobiol Aging 21: 683–688.

Le Bihan D, Johansen-Berg H (2011). Diffusion MRI at 25: exploring brain tissue structure and function. NeuroImage 61: 324–341.

Liao X, Vasilakos AV, He Y (2017). Small-world networks: perspectives and challenges. Neurosci Biobehav Rev 77: 286-300.

Lorente de Nò R (1938). Architectonics and structure of the cerebral cortex. In: Fulton JF, ed. Physiology of the Nervous System. Oxford University Press, New York, pp. 291–330.

MacMillan SJ, Mark MA, Duggan AW (1998). The release of β-endorphin and the neuropeptide-receptor mismatch in the brain. Brain Res. 794: 127–136.

Markov NT, Misery P, Falchier A, Lamy C, Vezoli J, Quilodran R, et al. (2011). Weight consistency specifies regularities of macaque cortical networks. Cereb Cortex 21:1254-1272.

Mohanty R, Sethares WA, Nair VA, Prabhakaran V (2020). Rethinking measures of functional connectivity via feature extraction. Sci Rep 10: 1298.

Morrison JH, Baxter MG (2013). The aging cortical synapse: hallmarks and implications for cognitive decline. Net Rev Neurosci 13: 240-250.

Mwangi B, Hasan KM, Soares JC (2013). Prediction of individual subject's age across the human lifespan using diffusion tensor imaging: a machine learning approach. Neuroimage 75: 58–67.

Nakamura S, Akiguchi I, Kameyama M, Mizuno N (1985). Age-related changes of pyramidal cell basal dendrites in layers III and V of human motor cortex: a quantitative Golgi study. Acta Neuropathol 65:281–284.

Nicholson C (2001). Diffusion and related transport mechanisms in brain tissue. Rep Prog Phys 64: 815–884.

Nicholson C (2005). Factors governing diffusing molecular signals in brain extracellular space. J Neural Transm 112: 29-44.

Nunzi MG, Milan F, Guidolin D, Toffano G (1987). Dendritic spine loss in hippocampus of aged rats. Effect of brain phosphatidylserine administration. Neurobiol Aging 8: 501-510.

Pannese E (2011). Morphological changes in nerve cells during normal aging. Brain Struct Funct 216: 85-89.

Pannese E (2021). Quantitative, structural and molecular changes in neuroglia of aging mammals: a review. Eur J Histochem 65: 3249.

Pereira A, Furlan FA (2010). Astrocytes and human cognition: modeling information integration and modulation of neuronal activity. Progr Neurobiol 92, 405–420.

Picard NA, Zanardi CA (2015). Brain motion and volume transmission: keeping the interstice flowing. Med Hypotheses 85: 41–44.

Rakic P (2008). Confusing cortical columns. Proc Natl Acad Sci USA 105: 12099–12100.

Robert L, Fulop T (2014). Aging of cell communication: loss of receptor function. Interdiscipl Top Gerontol 39: 142-162.

Rodriguez-Arellano JJ, Parpura V, Zorec R, Verkhratsky A (2015). Astrocytes in physiological aging and Alzheimer's disease. Neuroscience 323: 170-182.

Rubinov M, Sporns O (2010). Complex network measures of brain connectivity: uses and interpretations. Neuroimage 52: 1059–1069.

Sala A, Lizarraga A, Caminiti SP, Calhoun VD, Eickhoff SB, Habeck C, et al. (2023). Brain connectomics: time for a molecular imaging perspective ? Trends Cogn Sci 27: 353-366.

Santos-Otte P, Leysen H, van Gastel J, Hendrickx JO, Martin B, Maudsley S (2019). G protein-coupled receptor systems and their role in cellular senescence. Comp Struct Biotech J 17: 1265-1277.

Schmahmann JD, Pandya DN (2007). Cerebral white matter – historical evolution of facts and notions concerning the organization of the fiber pathways of the brain. J Hist Neurosci 16: 237–267.

Siddiqi SH, Taylor JJ, Horn A, Fox MD. Bringing human brain connectomics to clinical practice in psychiatry. Biol Psych 98: 386-387.

Sporns O (2012). Discovering the Human Connectome. MIT Press,. Cambridge, MA.

Sporns O (2013). The human connectome: origins and challenges. NeuroImage 80: 53–61.

Sporns O, Zwi JD (2004). The small world of the cerebral cortex. Neuroinformatics 2: 145–162.

Sporns O, Tononi G, Kötter R (2005). The human connectome: a structural description of the human brain. PLoS Comput Biol 1: 245–251.

Stam CJ, Reijneveld JC (2007). Graph theoretical analysis of complex networks in the brain. Nonlinear Biomed Phys 1: 3.

Steno N. (1965). Lecture on the Anatomy of the Brain: Nordisk Forlag Brusck, Copenhagen.

Syková E, Chvátal A (2000). Glial cells and volume transmission in the CNS. Neurochem Int 36: 397–409.

Van Essen DC, Drury HA, Joshi S, Miller MI (1998). Functional and structural mapping of human cerebral cortex: solutions are in the surfaces. Proc. Natl. Acad. USA 95: 788–795.

Van Essen DC, Ugurbil K, Auerbach E, Barch D, Behrens TEJ, Bucholz R et al. (2012). The Human Connectome Project: a data acquisition perspective. NeuroImage 62: 2222–2231.

Varangis E, Habeck CG, Razlighi QR, Stern Y (2019). The effect of aging on resting state connectivity of predefined networks in the brain. Front Aging Neurosci 11: 234.

von Bartheld CS (2018). Myths and truths about the cellular composition of the human brain: a review of influential concepts. J Chem Neuroanat 93: 2-15.

Watts D, Strogatz S (1998). Collective dynamics of small world networks. Nature 393: 440–442.

Wig GS, Schlaggar BL, Petersen SE (2011). Concepts and principles in the analysis of brain networks. Ann NY Acad Sci 1224: 126–146.

Zuo X-N, He Y, Betzel RF, Colcombe S, Sporns O, Milham MP (2017). Human connectome across the life span. Trends Cogn Sci 21: 32-45.

IJAE
ITALIAN JOURNAL OF ANATOMY AND EMBRYOLOGY

Firenze University Press
www.fupress.com/ijae

OPEN ACCESS

Citation: Malerba, S., Puglisi, G.R., Panzera, P., Pasculli, A., Prete, F.P., Gurrado, A., & Testini, M. (2023). Wandering gallbladder wrapping hepatoduodenal ligament and mimicking gastrointestinal stromal tumor at imaging. Case report and literature review. *Italian Journal of Anatomy and Embryology* 127(2): 13-17. doi: 10.36253/ijae-14548

Data Availability Statement: All relevant data are within the paper and its Supporting Information files.

Competing Interests: The Author(s) declare(s) no conflict of interest.

Wandering gallbladder wrapping hepatoduodenal ligament and mimicking gastrointestinal stromal tumor at imaging. Case report and literature review

Silvia Malerba, Giuliana Rachele Puglisi, Piercarmine Panzera, Alessandro Pasculli, Francesco Paolo Prete, Angela Gurrado, Mario Testini*

Department of Precision and Regenerative Medicine and Ionian Area. University of Bari, Italy
*Corresponding author. E-mail: mario.testini@uniba.it
The first two authors contributed equally to the work

Abstract. Wandering or free-floating gallbladder is a rare anomaly of position of the gallbladder, characterized by an unusually long or absent mesentery. This condition may present clinically as an emergency case of gallbladder torsion or as part of a complex clinical picture, where patients may present symptoms that trace to gallbladder pathology, but show morphologic features that are distant from gallbladder disease. We present a case where a wandering gallbladder wrapping around the hepatoduodenal ligament adhered to the stomach mimicking features of a gastrointestinal stromal tumor at preoperative imaging.

Keywords: ectopic gallbladder, cholecystectomy, anatomical variant, position anomaly; gastrointestinal stromal tumor.

INTRODUCTION

Cholelithiasis is one of the most common surgical diseases; its estimated overall prevalence is 10–15% in the general population, with some differences across Countries, and the majority of patients are asymptomatic [1, 2].

Laparoscopic cholecystectomy (LC) is considered worldwide the gold standard for the treatment of symptomatic gallbladder lithiasis, and it is currently one of the most frequently performed procedures in general surgery [3]. However, this procedure has rare but potentially very serious complications[4].

Guidelines and technical suggestions have been published to offer indications for a safe cholecystectomy, although this body of evidence most commonly refers to the normal anatomical situation of the gallbladder with its most common variants[5]. Some anomalies of the gallbladder position may present unexpected challenges to the surgeon but also to the physician investigating symptoms that may involve gallbladder pathology.

There are different types of anomalies and anatomic variants of gallbladder: agenesis, duplication, anomalies of shape, of size, and position. For what concerns the defects of position, they are divided in wandering gallbladder, gallbladder torsion and ectopic gallbladder. An ectopic gallbladder usually can be intrahepatic, suprahepatic, retrohepatic, supradiaphragmatic, and retroperitoneal; left-sided gallbladders may occur in *situs inversus* or as an isolated finding [6]. Ectopic gallbladder can also lie in the falciform ligament, transverse mesocolon, and anterior abdominal wall. When the gallbladder has an unusually long mesentery, it can "wander" or "float" (wandering or free-floating gallbladder, WG), increasing the risk for torsion, as it can twist around its pedicle, leading to subsequent necrosis. In the literature, over 500 cases of gallbladder torsion, but less than 10 reports of WG [7] have been reported at the time of writing.

We describe a case where we detected intraoperatively a WG, which wrapped around the hepatoduodenal ligament. The patient was brought to the operating theatre with working diagnosis of a gastrointestinal stromal tumor (GIST), supported by CT scan.

CASE REPORT

A 77-year-old male with a medical history of hypertension, carrier of an aortic prosthesis for thoracic aneurysm, treated with endovascular techniques, with prior excision of *Kaposi*'s sarcoma of the glans and of the leg, was admitted as an emergency case for abdominal pain, fever, and obstructive jaundice (hyperbilirubinemia, 3.30 mg/dL), with no biochemical signs of acute pancreatitis. An abdominal ultrasound showed a distended gallbladder with a large gallstone in the fundus, and a marked dilation of the intra and extra-hepatic biliary tract. A subsequent CT-scan confirmed the gallstone disease, and the distention of the proximal segment of the biliary tract, evidencing a normal size of the distal choledochus. Furthermore, CT-imaging (Figure 1) showed a thickening in the context of the submucosa of the anterior wall of the distal stomach that suggested a GIST of the gastric antrum. The working diagnosis was cholangitis in a patient with suspected GIST of the stomach. After initiating antibiotic therapy and restoring the hydro-electrolyte balance, the patient underwent an Endoscopic Retrograde Cholangio Pancreatography (ERCP). ERCP showed absence of gallstones in the common bile duct, the mid segment of which appeared thinned, while there was proximal dilation before the biliary *carrefour*. Moreover, a swelling of the gastric antrum wall in the presence of a normal mucosa was confirmed. A cholangio-

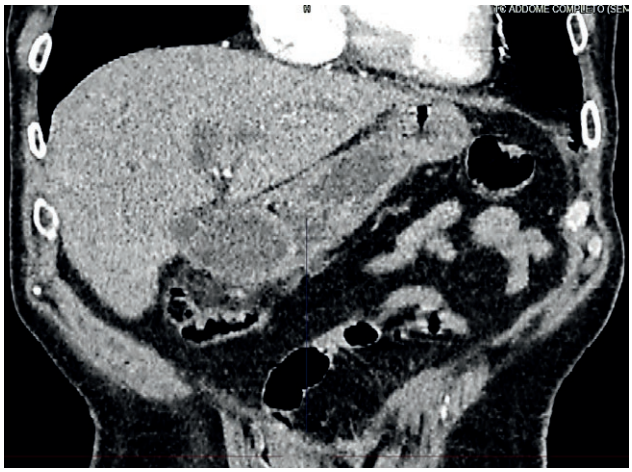

Figure 1. Coronal CT scan of the abdomen showing a tumor at the distal stomach with hypodense core, which was interpreted as suspect GIST.

MRI could not be performed due to the presence of a non-titanium prosthesis of the hip, and an endoscopic US was not exhaustive regarding the gastric wall. Based on this diagnostic picture, the patient was referred to laparoscopic surgery for a cholecystectomy and resection of the stomach. Intraoperatively, anatomical subversion of the standard anatomy was evident by a marked pattern of abdominal adhesions with diffuse post-inflam-

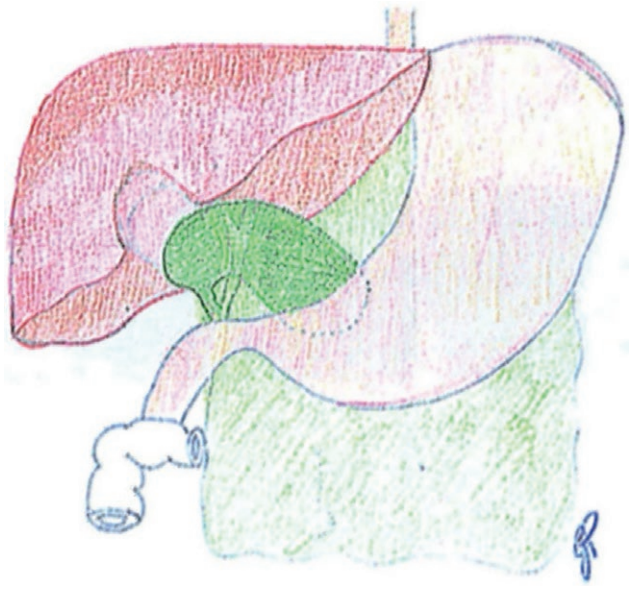

Figure 2. Schematic drawing depicting the gallbladder free from attachments to the liver and wrapped around the hepatic pedicle. The fundus of the gallbladder rests on the posterior portion of the gastric antrum.

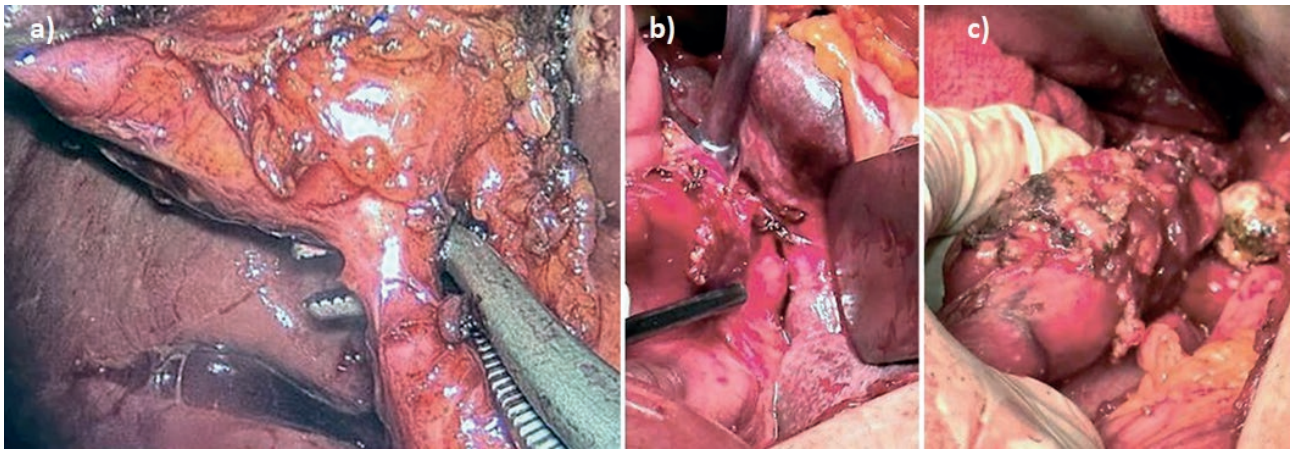

Figure 3. Intraoperative picture showing: a) laparoscopic view of the hepatic pedicle; b) adhesion of the gallbladder fundus to the gastric antrum in a fashion that suggested a fistulation process; c) gallbladder mobilized from the gastric fundus and repositioned to its original site.

matory scar tissue, resulting in the complete obfuscation of the hepatoduodenal ligament and the hepatic hilum (Figure 2). An intraoperative, laparoscopic US-scan was performed, documenting an area of fusion of the walls of the gallbladder and of the gastric antrum, with the interposition of a fluid-containing area of 2.5 cm of maximum diameter. This intraoperative picture suggested a cholecysto-gastric fistulation process, contraindicating further laparoscopy, so the procedure was converted to laparotomy (Figure 3).

Therefore, following the opening of the gastro-colic and gastro-hepatic ligament, gentle adhesiolysis, from the stomach and duodenum to the hepatic hilum, evidenced a wandering bulky gallbladder, wrapping anteriorly the hepatoduodenal ligament and the hepatic hilum. The fundus of the gallbladder containing a large stone appeared fused with the prepyloric antrum, forming a gallbladder-gastric fistula, mimicking the gastric swelling already demonstrated at preoperative imaging. Surgery was completed by standard cholecystectomy after repositioning the gallbladder to its natural location to the right of the common bile duct. An intra-operative trans-cystic duct cholangiogram showed normal anatomy of the biliary tract. Postoperative course was uneventful and the patient was discharged four days after surgery with normal serum bilirubin. Pathology confirmed inflammatory changes of the portion of gallbladder wall adherent to the stomach, representing the early stage of a cholecysto-gastric fistula.

DISCUSSION

Cholecystectomy for gallstone disease represents one of the most common procedures in routine surgical practice, with a risk for post-operative mortality that has been estimated to be between 0.1 and 0.7% [8]. However, mortality increases to 3.6% when cholecystectomy is performed for acute cholecystitis[9, 10]. Mortality rates were not substantially affected by the introduction of a LC; LC is a widely accepted procedure, because postoperative recovery is rapid, it is more acceptable to patients and, consequently, it has replaced open cholecystectomy as the procedure of choice for the treatment of symptomatic gallbladder disease[10]. On the other hand, LC is the most frequent cause of injury to the bile duct, and more rarely to the hepatic artery and portal vein, duodenum, small bowel, and colon. These injuries tend to occur when the operation is difficult as a result of inflammation or subversion of anatomy, or resulting from trocar punctures, thermal injury, and difficult adhesiolysis[10-12].

Congenital anomalies of the gallbladder, its duct, and its blood supply, are sufficiently common for the surgeons that they need to be aware of these vagaries. Indeed, most postoperative complications of cholecystectomy may be related to a combination of inadequate anatomical knowledge or poor visualization of the operative field [13]. This determines a high rate of perioperative complications, but also of mortality. So, the results can be additional surgeries, long recovery time, loss of time from work, and reduction in the quality of life [14] [15] [16].

In WG there is no adhesion or even a loose attachment to the liver, so the gallbladder is only connected to the cystic duct and its mesentery. The first report of free-floating or wandering gallbladder was by Wendel in 1898 with a torsion of the gallbladder complicated by perforation [17]. Gallbladder torsion is largely acquired and secondary to aging but it may also be congenital. Generally, there is an abnormal migration of the *pars cystica*

Table 1. Wandering gallbladder.

N.	Author	Year of publication	Publication type	Age	Presenting signs/symptoms	Hospital admission
1	*Wendel A.V.*	1898	Case report	33	Abdominal pain	Emergency
2	*Ziegler H.*	1952	Case report	-	-	-
3	*Maki et al*	1962	Case report	-	-	-
4	*Chiavarini RL et al*	1975	Case report	22	Abdominal pain	Elective
5	*Faso F.J. et al*	1989	Case report	81	-	Emergency
6	*Mathonnet et al*	2001	Case report	-	-	-
7	*Marano A. et al*	2002	Case report	90	Abdominal pain, nausea, vomiting	Emergency
8	*Otani et al*	2007	Case report	57	Abdominal pain, pyrexia	Emergency
9	*Morales A.M. et al*	2008	Case report	70	Acute diarrhoea, back pain	Emergency
10	*Boer J.*	2011	Case report	89	Abdominal pain, nausea	Emergency
11	*Warfe S. R. et al*	2013	Case report	69	Acute epigastric pain, nausea	Emergency
12	*Wu W-C et al*	2013	Case report	40	Abdominal pain	Emergency
13	*Kopp et al*	2019	Case report	51	Hypertension, GE reflux, abdominal pain	Emergency
14	*Miroslav K. et al*	2019	Case report	51	Abdominal pain	Emergency

from the hepatic diverticulum during the fourth to seventh weeks of embryologic development. Aside an early description in 1952, a handful of articles on WG have since appeared (Table 1).

The clinical presentation varies among individuals. It can be asymptomatic, it may cause recurrent episodes of abdominal pain and transient hyperbilirubinemia, or present acutely with potential fatal torsion and necrosis due to its predisposition to twist around its vascular pedicle leading to ischemic necrosis[18] . The incidence of torsion is higher in the elderly population, with male to female ratio of 1:3 [19].

Preoperative diagnosis is difficult and rarely made by ultrasonography, and also CT**.** However, there are no specific radiologic signs, but a gallbladder with a long cystic duct that is not in its normal anatomic position can be suggestive [7]. A delay in the diagnosis may end up in rupture and peritonitis.

When a complete torsion occurs, a scenario of acute abdomen could appear. The mechanisms leading to torsion are poorly understood [7]. Three anatomic variants are believed to be responsible for torsion. The first variant is a free-floating gallbladder, suspended only by the cystic mesentery, where the gallbladder may rotate around its vascular axis represented by the cystic artery. Another variant is when the gallbladder hangs from the liver through an elongated, narrow-based and freely mobile mesentery, possibly due to age-related visceroptosis. Here rotation may occur around an axis represented by the gallbladder itself or its liver mesentery. A third variant described is extremely rare and consists of a normally fixed gallbladder to a mobile liver lobe free of its coronary and triangular ligaments[13]. Various triggering mechanisms have been mentioned including visceroptosis, weight loss, gastric or colonic hyperperistalsis, constipation or diarrhoea, sigmoid volvulus, cholelithiasis, kyphosis, or iatrogenic manipulation. Patients with wandering gallbladder can present biliary colic-like symptoms attributed to torsion and de-torsion around the cystic duct as well as acute cholecystitis secondary to persistent obstruction[17-19]. In this reported case the encirclement of the hepatoduodenal ligament and adhesion to the stomach was evidently the result of a long and chronic process, with no acute signs of ischaemia.

A further peculiarity of this case was the misunderstanding of the gastric wall at imaging. So that the inflammatory reaction of the gallbladder wall with initial involvement of the adjacent stomach mimicked a swelling of the gastric wall, looking like a GIST.

Accurate knowledge of anatomical variants of the biliary anatomy is important when elaborating differential diagnosis for suspect gallbladder pathology and even more so when operating complex cases with a working diagnosis that may be misleading. In fact, a routine cholecystectomy may harbour unexpected and at times severe complications that may be anticipated and prevented when a complex picture can be reverted to normal anatomy.

CONCLUSION

A case is reported of wandering gallbladder wrapped around the hepatoduodenal ligament and adherent to the gastric fundus. Anomalies of position of the gallbladder are rare and should be suspected when gallblad-

der is not found in its classical position. Reverting to normal anatomy by careful dissection is the key to recognize anatomical variants and to prevent complications at surgery.

REFERENCES:

1. Lammert F, Gurusamy K, Ko CW, et al., Gallstones. 2016. **2**(1): p. 1-17.
2. Pisano M, Allievi N, Gurusamy K, et al., 2020 World Society of Emergency Surgery updated guidelines for the diagnosis and treatment of acute calculus cholecystitis. 2020. **15**(1): p. 1-26.
3. Törnqvist B, Strömberg C, Persson G, et al., Effect of intended intraoperative cholangiography and early detection of bile duct injury on survival after cholecystectomy: population based cohort study. 2012. **345**.
4. Fletcher DR, Hobbs MS, Tan P, et al., Complications of cholecystectomy: risks of the laparoscopic approach and protective effects of operative cholangiography: a population-based study. 1999. **229**(4): p. 449.
5. Sgaramella LI, Gurrado A, Pasculli A, et al., The critical view of safety during laparoscopic cholecystectomy: Strasberg Yes or No? An Italian Multicentre study. 2021. **35**: p. 3698-3708.
6. Gui D, Magalini S, Prete F, et al., What's right when the gallbladder's left? Surgical Endoscopy, 2002. **16**(11): p. 1637-1637.
7. Kopp M, Cornish NA, and Nazir SJIS, Wandering Gallbladder: A Case Report. 2019. **104**(7-8): p. 371-374.
8. Sandblom G, Videhult P, Crona Guterstam Y, et al., Mortality after a cholecystectomy: a population-based study. 2015. **17**(3): p. 239-243.
9. González-Castillo AM, Sancho-Insenser J, Miguel-Palacio D, et al., Mortality risk estimation in acute calculous cholecystitis: beyond the Tokyo Guidelines. 2021. **16**(1): p. 1-10.
10. Kwon A-H, Inui H, and Kamiyama YJWjos, Laparoscopic management of bile duct and bowel injury during laparoscopic cholecystectomy. 2001. **25**: p. 856-861.
11. El-Banna M, Abdel-Atty M, El-Meteini M, et al., Management of laparoscopic-related bowel injuries. 2000. **14**: p. 779-782.
12. Ress AM, Sarr MG, Nagorney DM, et al., Spectrum and management of major complications of laparoscopic cholecystectomy. 1993. **165**(6): p. 655-662.
13. Berger HJBMJ, Wandering Gall Bladders. 1975: p. 193.
14. Törnqvist B, Waage A, Zheng Z, et al., Severity of acute cholecystitis and risk of iatrogenic bile duct injury during cholecystectomy, a population-based case–control study. 2016. **40**: p. 1060-1067.
15. Melton GB, Lillemoe KD, Cameron JL, et al., Major bile duct injuries associated with laparoscopic cholecystectomy: effect of surgical repair on quality of life. 2002. **235**(6): p. 888.
16. Testini M, Piccinni G, Lissidini G, et al., Management of descending duodenal injuries secondary to laparoscopic cholecystectomy. 2008. **25**(1): p. 12-15.
17. AV W, A case of floating gallbladder and kidney complicated by cholelithiasis with perforation of the gallbladder. Ann Surg, 1898. **27**: p. 199-202.
18. Morales AM and Tyroch AHJTAjos, Wandering gallbladder. 2008. **196**(2): p. 240-241.
19. Quinn SF, Fazzio F, and Jones EJAjor, Torsion of the gallbladder: findings on CT and sonography and role of percutaneous cholecystostomy. 1987. **148**(5): p. 881-882.

IJAE
ITALIAN JOURNAL OF ANATOMY AND EMBRYOLOGY

Firenze University Press
www.fupress.com/ijae

OPEN ACCESS

Citation: Melovitz-Vasan, C., McBride, A., Huff, S., & Vasan, N. (2023). Megaureter and hydronephrosis: Consequences of ureteric dysfunction. *Italian Journal of Anatomy and Embryology* 127(2): 19-28. doi: 10.36253/ijae-14545

Data Availability Statement: All relevant data are within the paper and its Supporting Information files.

Competing Interests: The Author(s) declare(s) no conflict of interest.

Megaureter and hydronephrosis: Consequences of ureteric dysfunction

Cheryl Melovitz-Vasan[1], Amanda McBride[1], Susan Huff[2], Nagaswami Vasan[1,*]

[1] *Department of Biomedical Sciences, Cooper Medical School of Rowan University, Camden, New Jersey 08103, USA*
[2] *Medical Education Research Collaborator and Instructional Designer, Rowan University, Glassboro, New Jersey 08028, USA*
*Corresponding author. E-mail: vasan@rowan.edu

Abstract. The prevalence of "megaureter" among children can be as high as 20-25% and can be bilateral or unilateral; in some cases, the contralateral kidney is either absent or dysplastic. Megaureters can be categorized as obstructed, refluxing, obstructed and refluxing, or neither obstructing nor refluxing. Megaureter is likely to either transiently or permanently involve the kidneys, resulting in hydronephrosis or other medullary and cortical derangement. During routine student dissection of an 86-year-old female donor who died of atherosclerotic cardiovascular disease, we observed the presence of large ureters on both kidneys with the right-side ureters comparatively much larger than the left side. The upper and lower lobes of the right kidney were drained by independent ureters, which were encased in a thin, membranous connective tissue structure. Additionally, we also observed thinning of the renal cortex, renal pelvis, and caliceal dilation with total loss of medulla and lack of corticomedullary delineation. Importantly, reproductive structures such as uterus, fallopian tubes, ovaries. cervix and vagina were normal. This paper, in addition to providing a description of what was observed on dissection, will discuss various causes, pathophysiology, and alterations in the matrix composition of the ureter and kidney.

Keywords: hydronephrosis, megaureter, altered ureteric matrix, reflux, obstruction, anomaly, dysfunction, ureterovesical junction.

INTRODUCTION

This paper starts with a review of the development of the renal system, followed by a report of the association between megaureter and hydronephrosis and, finally, various ways megaureter develops and is classified. Analysis deliberating whether megaureter or hydronephrosis occurred first follows a description of the findings and morphometric measurements of the renal system in this case. The introduction and discussion provide solid foundations about the complications observed in the case.

Embryologically, the permanent kidneys develop from two sources: the ureteric bud (aka metanephric diverticulum) and the metanephric blastema

(aka metanephric mass). The ureteric bud is a diverticulum or an outgrowth from the mesonephric duct. The ureteric bud is the primordium of the ureter, renal pelvis, calices, and collecting tubules. The extending ureteric bud penetrates the metanephric blastema that forms the nephrons. The stem of the ureteric bud becomes the ureter, of which the cranial part undergoes repetitive branching to form the collecting tubules. The initial four branches enlarge and coalesce to form major calices, while the subsequent four coalesce to form minor calices (Moore et al., 2020). Additionally, the ureter undergoes changes in its matrix components, including types of collagen and longitudinal and smooth muscle content (Friedrich et al., 1987; Hanna et al., 1976; Hanna et al., 1977; Vlad, et al., 2007).

Congenital ureteric abnormalities, specifically megaureter, are a common and widespread pathology (Sharif, 2021); frequency varies between 20% and 40% of all malformations related to the urinary system. Megaureter is most often diagnosed in children and is also discovered in incidental findings when other problems are investigated. More common in boys than girls, megaureter occurs more frequently on the left side (Wilcox and Mouriquand, 1998), but arises bilaterally in 25% of cases (Shokeir and Nijman 2000; Manzoni 2002; Wilcox and Mouriquand, 1998). The disruption of urodynamics affected by megaureter makes possible the subsequent development of pyelonephritis or scarring of renal tissue that causes loss of physiological functions. A ureter is considered a megaureter if the lumen diameter is larger than 7-8 mm (Hodges et al., 2010; Baskin et al., 1994).

In general, an obstruction to the flow of urine, due either to intrinsic or extrinsic compression, produces hydronephrosis. The causes of intrinsic obstruction include renal stones, tumor, ureteropelvic junction narrowing, ureteral strictures from earlier infections, posterior urethral valves, prostatic hyperplasia, and neurogenic bladder, etc. The causes of extrinsic compression include pregnancy, pelvic/perineal cysts, malpositioned ureter, tumor, pelvic fibrosis, etc. (Thotakura and Anjum, 2022). Anatomic abnormalities, such as urethral valves or strictures, stenosis at the ureterovesical or ureteropelvic junction, or vesicourethral reflux, account for most cases in children (Capriotti and Frizzell, 2016). In pregnancy, rotation to the right (dextrorotation) of the uterus can cause compression of the right ureter, thus making hydronephrosis more common in the right kidney than left (Rasmussen and Nielsen, 1988).

Based on the international classification of nomenclature, the megaureters can be classified as obstructive, refluxing, obstructed and refluxing, or neither obstructing nor refluxing (Report of working party to establish an international nomenclature for the large ureter 1977). Primary obstructive megaureter occurs when the ureter is too narrow at the point where it enters the bladder; peristalsis of the ureter proves insufficient and blockage results. An obstructive process characterizes **secondary obstructive** megaureter occurring secondary to elevated intravesical pressure of some other cause such as neurogenic bladder, ectopic ureter, ureteral vesicular junction problem, retroperitoneal mass and enlarged prostate and others (Shokeir and Nijman, 2000; Khoury and Bagli, 2007; Berrocal et al., 2002). The **primary and secondary refluxing** megaureters represent a refluxing ureter that happens to be dilated. This may be associated with abnormalities of uretero-vesicular junction problem. In the **refluxing obstructed megaureter,** some degree of obstruction occurs, perhaps due to ectopic insertion of the ureter into the neck of the bladder (Weiss and Lytton, 1974).

In the light of what is known about megaureter and hydronephrosis and what is observed in the present case, the authors will attempt to explain the possible causes of the megaureter and hydronephrosis seen in the female donor.

MATERIALS AND METHODS

Case report

We report on pathology seen in a donated body that was obtained from the willed body program; it was intended for medical student dissection and learning at Cooper Medical School of Rowan University. During students' dissection of an 86-year-old female Caucasian donor who died of atherosclerotic cardiovascular disease, we observed megaureter of both kidneys; the right ureter was much larger with hydronephrosis of the right kidney. Unfortunately, the students randomly dissected the kidneys before the authors had a chance to carefully dissect, document and display the abnormalities. Despite this, we performed a detailed study of the anomalous renal system presented here.

Declaration: The authors state that every effort was made to follow all local and international ethical guidelines and laws that pertain to the use of human cadaveric donors in anatomical research.

Results and observations

The right kidney was primarily affected; the magnitude became noticeable when comparing it with the less-involved left kidney and its ureter. An Illumifun elec-

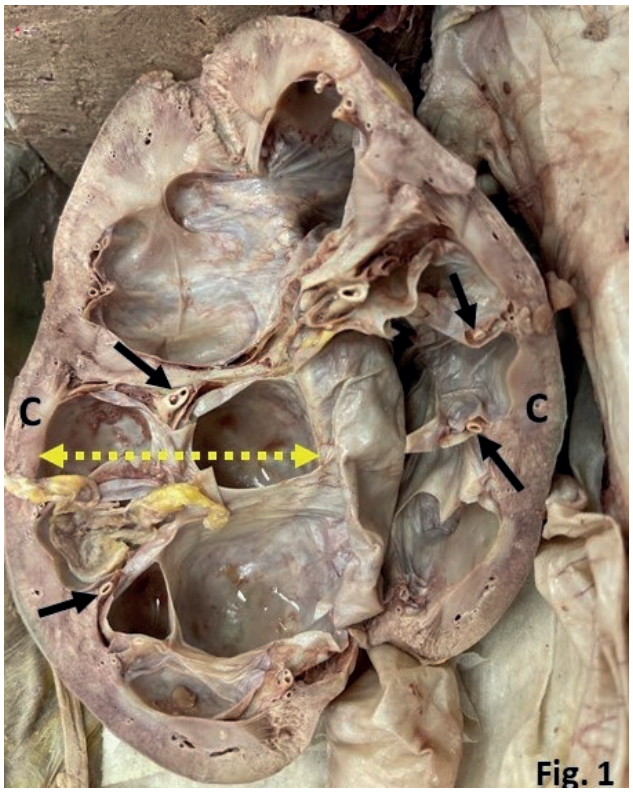

Figure 1. Longitudinal section of the right kidney showing hydronephrosis, cortex thinning, renal pelvis and caliceal dilation with total loss of medulla and lack of corticomedullary delineation. C=Cortex; Short black arrows pointing to vasculatures and double headed yellow arrow indicates renal pelvis and caliceal dilation with total loss of medulla and lack of corticomedullary delineation.

Table 1.

	R. Kidney	L. Kidney
Length	122.2 mm	139.9 mm
Width	51.3 mm	55.4 mm
Thickness	44.8 mm	60.6 mm
Medulla	Non-existent	Fairly defined
Cortex at Hilum	8.3 mm	19.4 mm
Ureter Luminal Diameter		
Lower lobe: proximal part	247 mm	201 mm
Lower lobe: middle part	316 mm	n/a
Lower lobe: distal part	119 mm	15.1 mm
After uniting	146 mm	n/a
Upper lobe	21.3 mm	n/a
Ureter Length		
Length:		241.5 mm
Upper lobe	132 mm	n/a
Lower lobe	130 mm	n/a
After uniting	63 mm	n/a
Bladder		
Wall thickness		1.4-1.7 mm
Inter ureteral orifices distance		21.7 mm
Ureteral orifice to internal urethral opening		34.7 mm

tronic digital vernier caliper was used to make all measurements reported here.

The right kidney was slightly smaller compared to the left kidney in all the dimensions measured (see Table 1: length (122.2 mm vs 139.9 mm); width at the hilum (51.3 mm vs 55.4 mm); and thickness measured at the hilum (44.8 mm vs 60.6 mm). The right kidney additionally exhibited medullary cavitation due to loss of the integrity of pyramid and caliceal systems and cortical thinning [see Figure 1].

Both right and left ureters exhibited dilation and contortion, the right far more than the left [see Figure 2].

Measurements listed in Table 1 clearly show that the right ureter luminal diameter was considerably larger (mega) and more misshapen in comparison to the left ureter, though that was also enlarged [see Table 1 and Figure 1].

Though initially separate, a clear, thin membranous connective tissue sheath wrapped the ureters from the upper and lower lobes of the right kidney together. Distally, the ureters joined as a single ureter prior to reaching the bladder posterolaterally. Ureter length of the upper lobe is 130 mm; the lower lobe was 130 mm before uniting and 63 mm after uniting. The left ureter length was 241 mm, was less contorted and ran parallel with the large left ovarian vein, which drained into the left renal vein.

In the medulla of the right kidney, the renal pyramid and papilla were unrecognizable [see Figure 1].

The renal caliceal system of minor and major calices and the renal pelvis appear to have lost their histology and physical configurations. The interlobular vascular system appears intact, allowing a viable cortex, even though the thickness of the cortex is diminished in size (see Figure 1). Cortex thickness across from the hilum was 8.3 mm on the right and 19.4 mm on the left [see Figures 1 and 3].

The medulla of the left kidney is acceptably well defined and the caliceal system is recognizable when viewed with higher magnification (see Figure 4). Measured at two different sites, the bladder wall thickness was between 1.4 and 1.7 mm. Normally, bladder wall thickness is 2.76 mm when the bladder is almost empty and 1.55 mm when it is distended. The inter-ureteral orifice was 21.7 mm apart (normal 13-41 mm) and the distance between the ureteral orifice and the urethral opening was 34.7mm (normal 17-40 mm) (see Figure 4).

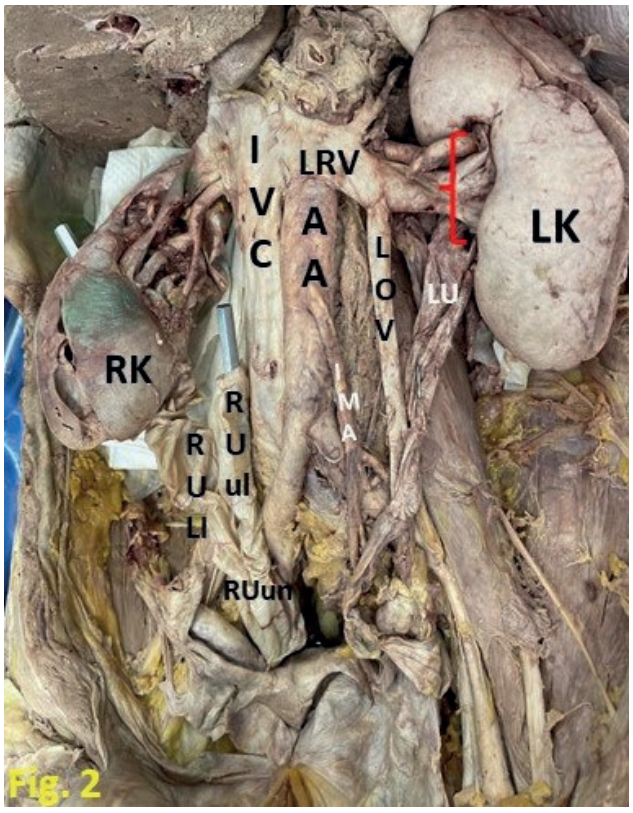

Figure 2. Megaureter –Right kidney: In situ view showing markedly large and tortuous ureters of both upper and lower lobes that fused distally forming a single ureter that entered the bladder posterolaterally. Left kidney (LK) Ureter is less large and less twisted. RK= Right kidney; RULl= Right ureter lower lobe; RUul=Right ureter upper lobe; RUun= Right kidney upper and lower lobe ureters united; IVC=Inferior Vena Cava; AA=Abdominal aorta; IMA=Inferior mesenteric artery; LRV-Left renal vein; LU=Left ureter; LK=Left kidney.

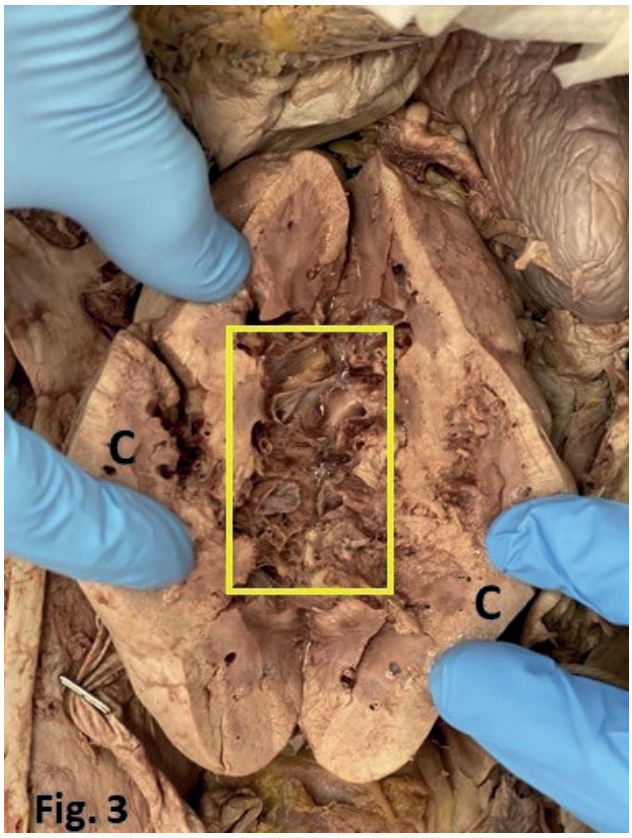

Figure 3. Left kidney: vertical section showing normal caliceal system and cortex and in general larger than the right kidney. C=Cortex; The vertical block of medulla is enlarged and shown in figure 4.

The trigone (or Lieto Triangle), which is the triangular portion of the bladder floor, was the site of the anti-reflux mechanism [see Figure 5].

One ovary showed fibrosis and the uterus showed age-related reduction in size; otherwise, the reproductive structures were within normal limits.

DISCUSSION

Megaureter

Epidemiologically, occurrence of congenital primary megaureter (PM) is unclear; however, it is the second most common cause of neonatal hydronephrosis (Younsi 2020). A primary congenital megaureter means a dilatation of the ureter with a ureteric diameter ≥7 mm (normal 3-5 mm) due to a structural or functional obstruction of the ureterovesical junction (Younsi 2020). The male to female ratio is nearly 4:1 and the left side is more often affected than right (1.6-4.5 times) (Braga et al., 2016). Most cases are non-refluxing and unobstructed. The frequency of obstructed megaureter is 1/10,000 (Farrugia et al., 2014). Primary megaureter has been classified in many ways, based on functional impediment. The Pfister–Hendren classification established in 1978 was based on the morphological appearance: Type I involved the distal ureter without associated hydronephrosis; Type II extended to both ureter and pelvis; and Type III was associated with severe hydroureteronephrosis and ureteric tortuosity (Pfister and Hendren, 1978; Weber et al., 1971). Using the Pfister–Hendren classification, we assign the findings in this case as Type III hydronephrosis with megaureter and ureteric tortuosity.

The Society for Fetal Urology (SFU) classification specified five grades of hydronephrosis which, in addition to renal parenchyma, describes the ureter (Fernbach et al., 1993). Based on the SFU classification, the findings in

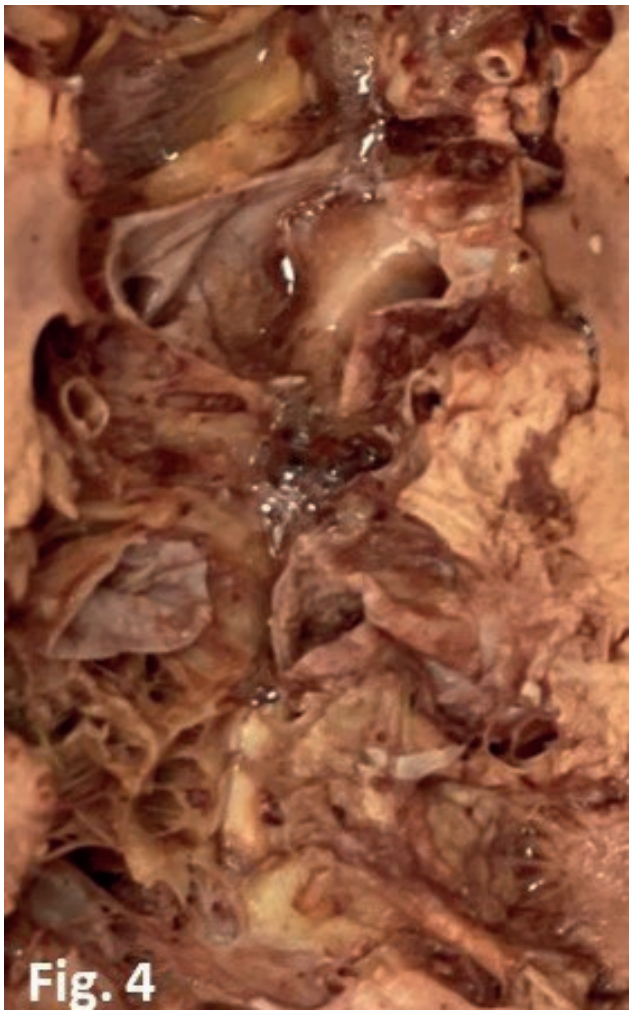

Figure 4. Left kidney= An enlarged vertical section from figure 3 showing normal caliceal system.

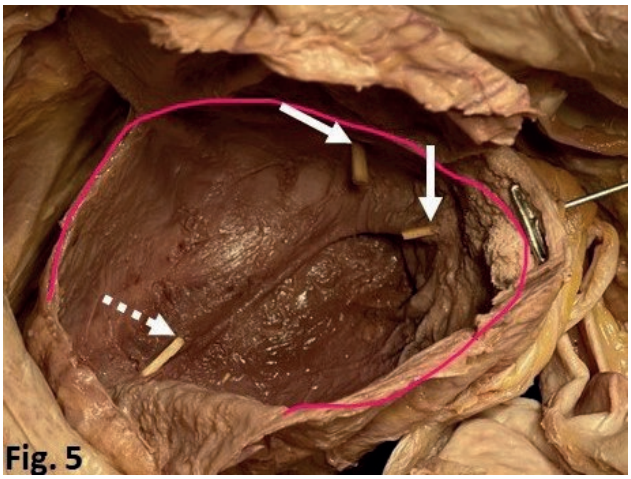

Figure 5. Urinary bladder= The ventral wall removed to display the dorsal 'trigone' region. The open bladder wall is marked by red outline. The solid white arrows pointing to the ureteral entrance with wooden picks. The dotted white line and wooden picks indicate the urethral opening.

Figure 6. Schematic diagram based on the actual dissection showing gross dilation of the ureter, pelvis, and calyces; loss of papillary impressions; thinning of cortex and ureteral tortuosity.

this case can be classified as grade V hydronephrosis with megaureter and ureteric tortuosity [see Figure 6]. Figure 6 here was drawn to show what was observed during the dissection, similar to what is seen in Fernbach et al.

According to Baskin et al., primary megaureter results from a functional or anatomical abnormality involving the ureterovesical junction, whereas secondary megaureter results from abnormalities that involve the bladder or urethra. It appears to be most commonly due to an abnormality or delay in the development of the muscle in the distal ureter adjacent to the ureterovesical junction at 20 weeks gestation. This results in the formation of an aperistaltic segment which leads to functional obstruction (Baskin et al., 1994).

Primary obstructive megaureter (POM) is a congenital dilatation of the ureter due to an adynamic segment of vesicoureteral junction obstruction (Hamid et

al 2022). Megaureters may be primary or secondary and the dilatation may be due to obstruction or reflux or both. Hamid et al. found that refluxing or obstructive types of megaureter occurred 58% and 18.5% of time respectively and the distribution of ureteral diameter varied from 5-30 mm (Hamid et al., 2022). The cause of primary obstructed megaureter is the aperistaltic and narrowed pre-vesical portion of the ureter. The inner sheath of the terminal ureter generally shows a reduced amount of longitudinal smooth muscle bundles and an increased amount of collagen (Merlini and Spina, 2005). Primary obstructive megaureter (POM) is an uncommon disease in adults, it is defined as an intrinsic congenital abnormality at the lower segment of the ureter in the ureterovesical junction (Ibrahimi and Ziani, 2020). Refluxing PM is caused by a short or absent intravesical ureter, congenital para-ureteric diverticulum or other derangement of the vesico-ureteric junction. Obstructed PM is a functional obstruction arising from an aperistaltic jucstavesical segment 0.5-4cm long that is unable to transport urine at acceptable rates. Causal theories include excessive collagen deposition, hypertrophy of ureter muscle, thick periureteral tissues or a circumferential segment devoid of muscle (Merlini and Spina, 2005). Primary megaureter is not known to be hereditary, but families with more than one affected member have been described (Farrugia et al., 2014). A recent publication (Ayad Y Khudair, 2020) brings to light numerous studies related to both embryology and pathophysiology of megaureter. Sharif writes, "It is believed that the ureters has an aperistaltic jucstavesical (adynamic) segment, which leads to insufficient peristalsis of the ureter and, therefore, to urinary outflow. This distal segment was examined histologically, and it was found to contain elevated collagen levels of types I and III (mainly type I). It is this increased fibrosis that is connected with the disturbance of intercellular connections and leads to arrhythmias and ureteric obstruction. Some scientists have proved the atrophy of internal longitudinal muscles in these segments of the ureter (longitudinal muscles transmit peristalsis) and hypertrophy of external compressive circular muscles, which leads to obstruction. " (Sharif, 2021) (Hanna et al., 1976; Merlini and Spina, 2005, Hill, 2015). The muscular layer of the ureter consists of longitudinal and circular smooth muscles that create the peristaltic contractions to move the urine into the bladder without the aid of gravity (Hill, 2015).

While there are many scientific studies explaining the histological origin of megaureter, the results often varied from one another. However, they all showed an increase of connective tissue in the megaureter (Hanna et al., 1977; Vlad et al., 2007). A quantitative study showed that the collagen to smooth muscle ratio in the normal ureter is 0.52, while in obstructive and reflux megaureters, it is 0.78 and 1.99 respectively (Lee et al., 1998). Other researchers have shown the presence of smooth muscle cells in these ureters, which produce abnormally increased amount of collagen (Hanna et al., 1977). It has also been shown that muscles in these segments of the ureter have an abnormal response to neurotransmitters, emphasizing the atypical behavior of these cells (Hanna et al., 1977; Vlad et al., 2007; Lee et al., 1998; Mackinnon, 1977; Mackinnon et al., 1970).

Congenital megaureter is considered to be related to the expression of transforming growth factor β, which might lead to a lack of post-natal muscle dysplasia (Ozturk et al., 2012; 2016). According to Nicótina et al., the primary megaureter should be attributed to a segmental developmental delay of the terminal ureter arising at about 20 weeks of gestation, with a possible pathogenetic involvement of autocrine TGF-β overexpression (Nicótina et al., 1997). Mackinnon et al. theorized that an absence of longitudinal muscle in the distal ureter led to the functional obstruction, which was accepted by number of other researchers (Mackinnon et al., 1970). Notley utilized an electron microscope to observe the normal nerve distribution and hyperplasia of collagen fiber in the muscular layer of megaureters, which was believed to be the primary cause of megaureter (Notley 1972). Furthermore, Tokunaka and Koyanagi and Tokunaka et al. described a small subgroup of megaureters with muscle dysplasia that affected the dilated part of the ureter; and the muscle dysplasia was thought to be the primary cause leading to the dilatation (Tokunaka and Koyanagi, 1982; Tokunaka et al., 1984). In light of the evidence, we, like other researchers, believe that multiple factors contributed to the congenital megaureter.

Hydronephrosis

The renal parenchyma, which produces urine, and the pelvicalyceal system, which collects and conveys the urine into the ureter, comprise the two functional segments of the kidney. Hydronephrosis occurs due to two distinct causes: ureteropelvic junction problems or vesicoureteral reasons (Onen 2020). It happens when there is either a blockage of the outflow of urine or reverse flow of urine that is already in the bladder (vesicoureteral reflux), contraction of bladder detrusor muscles (neurogenic bladder) that can cause the renal pelvis to become enlarged (Thotakura and Anjum, 2022). Furthermore, structural defects of the connections between the kidney, ureter and bladder can also lead to hydronephrosis. Oth-

er causes that result in hydronephrosis are due to renal stone, congenital causes, scarring from infections or earlier surgery, cancer, enlarged prostate, and pregnancy, to name a few (Thotakura and Anjum, 2022). Common causes of upper urinary tract obstruction include kidney stones at the ureteropelvic junction (UPJ) and blockages caused by intrinsic narrowing of the ureters or extrinsically caused by overlying renal blood vessels. Ureteropelvic junction obstruction (UPJO) is primarily a congenital condition that results in diminished urine flow from the renal pelvis into the ureter; this can cause hydronephrosis and, if untreated, may result in complete functional loss of the affected kidney (Jackson et al., 2018; Sulemanji and Vaklit, 2013). Reflux of urine into the kidney (e.g., neurogenic bladder or ureteral obstruction) causes impairment in the lower urinary tract (Thotakura and Anjum, 2022). In pregnancy, towards the end of 2nd trimester, physiological dextrorotation (rotation to the right) of the gravid uterus and engorged right ovarian vein that drain into the right renal vein can cause compression on the right ureter, thus making hydronephrosis more common in the right kidney than the left (Rasmussen and Nielsen, 1988). Hydronephrosis or hydroureter is a normal finding in pregnant women. The renal pelvises and caliceal systems may be dilated due to effects of progesterone and mechanical compression of the dilated ureters against the bony pelvic brim (Rasmussen and Nielsen, 1988. According to Rasmussen and Nielsen (1988), pregnancy-induced hydronephrosis recedes in 80% of women, but persists in 20%. It is possible that, in the case of the female donor, it did not return to normal, as seen in the right-side kidney.

Other congenital causes of hydronephrosis include ureteral hypoplasia that may lead to an aperistaltic segment of the ureter due to abnormal arrangement of the smooth muscle layer, which in turn will impair the urine drainage from the renal pelvis into the ureter and cause functional obstruction, rather than mechanical [Jackson et al., 2018; Sulemanji and Vaklit, 2013]. High insertion of the ureter into the renal pelvis can result in urine failing to empty from the pelvis into the ureter. Entrapment of the ureter by a crossing accessory renal vessel occurs most commonly from the lower pole. This results in kinking of the proximal ureter, interrupting the free flow of the urine and, rarely, a malrotated kidney can cause UPJO. UPJO is estimated to occur 1 in 1000-1500 cases. [Jackson et al., 2018; Sulemanji and Vaklit, 2013].

No matter what causes hydronephrosis, staging of the condition is important in planning a treatment protocol. With ultrasound (US), it has become possible to detect and stage hydronephrosis. Onen and his group studied the hydronephrosis for several years; in 2020, they published an article with staging of hydronephrosis (Onen 2020). From the US images in Onen, it is easy for us to stage the donor kidney's functional status and explain what has been exposed in our dissection (see Figures 5 and 6). The anterior-posterior thinning (44.4 mm vs 60.6 mm) parenchymal thinning indicates a possible severe functional loss. Onen (2020) further distinguished the parenchymal thinning into medullary thinning and cortical thinning. In the right kidney of the donor (see Figure 1), we also observed pelvis plus caliceal dilation, total medulla loss, cortical thinning, and no recognizable corticomedullary differentiation, resulting in progressive and permanent damage to the right kidney.

ANALYSIS

The following analysis pertains to the case presented here; it is based on our observations, findings and on available published research studies on megaureter and hydronephrosis. Deciding which came first, the megaureter or hydronephrosis, is analogous to the "chicken or egg" conundrum. Resolving the question requires consideration of the following: the donor was an 86-year-old female with complete internal reproductive structures whose right side of the renal system was primarily involved. Due to donor confidentiality, we do not know whether she was married or had children. Any conclusion drawn in the discussion is the authors' assumption or based on available published materials.

As mentioned earlier, megaureter may be caused by a structural or functional obstruction of the ureterovesical junction; it represents the second most likely cause of neonatal hydronephrosis (Younsi 2020). According to Merlini and Spina (2005), abnormality or delay in the development of the longitudinal muscle bundle and an increased amount of collagen in the distal ureter adjacent to the ureterovesical junction results in the formation of an aperistaltic segment that leads to functional obstruction. It is believed (Ayad Y Khudair, 2020) that the ureters have an aperistaltic jucstavesical (adynamic) segment, which leads to insufficient peristalsis of the ureter and, therefore, to urinary outflow (Ayad Y Khudair, 2020). Other reasons such as expression of transforming growth factor β, which might lead to a lack of post-natal muscle dysplasia (Ozturk et al. (2012; 2016); a possible pathogenetic involvement of autocrine TGF-β overexpression (Nicótina et al., 1997), or abnormal changes in the collagen to smooth muscle ratio (Lee et al., 1998). In agreement with other researchers, we feel that multiple factors contributed to the development of the congenital megaureter in this donor.

Hydronephrosis occurs for two reasons: ureteropelvic junction or vesicoureteral causes (Onen 2020). Any number of reasons can cause the renal pelvis to become enlarged: a blockage of the outflow of urine or reverse flow of urine already in the bladder (vesicoureteral reflux), contraction of bladder detrusor muscles (neurogenic bladder) at the ureteropelvic junction (UPJ); renal stone, congenital cause, scarring from infections or earlier surgery, cancer, enlarged prostate, pregnancy, etc. (Thotakura and Anjum, 2022).

Based on the Pfister–Hendren classification and what was observed in this donor, we consider that the findings in the case presented here can be classified as type III hydronephrosis with megaureter and ureteric tortuosity of the right-side renal system (Pfister and Hendren 1978). Additionally, we also observed Onen's Grade 4 hydronephrosis with cortex thinning, renal pelvis and caliceal dilation with total loss of medulla and lack of corticomedullary delineation (Onen 2020).

Our report does not include histological appearance of the vesicoureteral junction or distal ureter due poor preservation of such details in an embalmed cadaver tissue. However, there are studies that report that defective vesicoureteral junction and loss of muscles at the distal ureter and increased connective tissues caused aperistaltic distal ureter and retrograde flow of urine from the bladder towards kidney, resulted in dilated ureter and hydronephrosis (Nicótina et al., 1997; Lee et al., 1998).

CONCLUSION

With the available information about the donor, who lived for 86 years, had complete reproductive structures to ovulate, conceive, and carry a fetus to full term, and the fact her megaureter and hydronephrosis are on the right side, we assume that she carried a fetus to full-term. In pregnancy, in the late second semester, the gravid uterus rotated to the right side, causing compression of the right ureter and gonadal vein. This compression of the right ureter initiated the hydronephrosis. Hence, we believe that the megaureter came first and caused the hydronephrosis.

FUNDING

This study was supported by the Faculty Development Funds administered by the Cooper Medical School of Rowan University.

ACKNOWLEDGEMENTS

The authors sincerely thank the donor and her family for their generosity, which made this study possible and facilitated scientific and medical innovations in patient care. To our families and the families of our donor who inspire us to enrich and further our knowledge we are indebted.

The authors state that every effort was made to follow all local and international ethical guidelines and laws that pertain to the use of human donors in anatomical research.

For research using human subjects, American Association for Anatomy endorses the protections embodied in the Basic Principles of the Declaration of Helsinki and their expansion in the regulations governing research supported by the U.S. Government (45 CFR Part 46; 56 FR 28003).

REFERENCES

1. Ayad yas Khudair (2020) Modern issues of diagnosis and treatment megaureter in children. European Journal of Molecular & Clinical Medicine. 7: 7056-7065.
2. Baskin L.S., Zderic S.A., Snyder H.M., Duckett J.W. (1994) Primary dilated megaureter: long-term follow-up. J Urol. 152(2 Pt 2): 618-621.
3. Berrocal T., López-Pereira P., Arjonilla A., Gutiérrez J. (2002) Anomalies of the distal ureter, bladder, and urethra in children: embryologic, radiologic, and pathologic features. Radiographics 22: 1139–1164.
4. Braga L.H., D'Cruz J., Rickard M., Jegatheeswaran K., Lorenzo A.J. (2016) The fate of primary nonrefluxing megaureter: A prospective outcome analysis of the rate of urinary tract infections, surgical indications and time to resolution. J Urol. 195(4 Pt 2): 1300–1305.
5. Capriotti T., Frizzell J.P. (2015) Pathophysiology: Introductory Concepts and Clinical Perspectives. F.A. Davis Company, Philadelphia.
6. Farrugia M.K., Hitchcock R., Radford A., Burki T., Robb A., Murphy F. (2014) British Association of Paediatric Urologists consensus statement on the management of the primary obstructive megaureter. J Pediatr Urol. 10: 26-33.
7. Fernbach S.K., Maizels M., Conway J.J. (1993) Ultrasound grading of hydronephrosis: introduction to the system used by the Society for Fetal Urology. Pediatr Radiol. 23: 478–480.
8. Friedrich U., Schreiber D., Gottschalk E., Dietz W. (1987) Ultrastructure of the distal ureter in congeni-

tal malformations in childhood. Eur J Pediatr Surg. 42: 94–102.
9. Hamid R., Bhat N.A., Baba A.A., Mufti G.N., Sheikh K.A., Bashir M.I. (2022) Primary obstructive megaureter in children; 10 years' experience from a tertiary care center. Urol Ann. 14: 252–258.
10. Hanna M.K., Jeffs R.D., Sturgess J.M., Barkin M. (1976) Ureteral structure and ultrastructure. Part II. Congenital ureteropelvic junction obstruction and primary obstructive megaureter. J Urol. 116: 725–730.
11. Hanna M.K., Jeffs R.D., Sturgess J.M., Barkin M. (1977) Ureteral structure and ultrastructure. Part III. The congenitally dilated ureter (megaureter). J Urol. 117: 24–27.
12. Hill W.G. (2015) Control of urinary drainage and voiding. Clin J Am Soc Nephrol. 10: 480-492.
13. Hodges S.J., Werle D., McLorie G., Atala A. (2010) Megaureter. ScientificWorldJournal. 10: 603-612.
14. Ibrahimi A., Ziani I. (2020) Primary obstructive megaureter. Pan Afr Med J. 37: 296.
15. Jackson L., Woodward M., Coward R.J. (2018) The molecular biology of pelvi-ureteric junction obstruction. Pediatr Nephrol. 33: 553-571.
16. Khoury A., Bagli D. (2007) Reflux and megaureter. In: Wein A.J., Kavoussi L.R., Novick A.C., Partin A.W., Peters C.A.: Campbell-Walsh Urology. 9th ed. WB Saunders, Philadelphia. Pp. 3423-3481
17. Lee B.R., Silver R.I., Partin A.W., Epstein J.I., Gearhart J.P. (1998) A quantitative histologic analysis of collagen subtypes: the primary obstructed and refluxing megaureter of childhood. Urology 51: 820–823.
18. Mackinnon, K.J. (1977) Primary megaureter. Birth Defects Orig. Artic. Ser. 13: 15–16.
19. Mackinnon K.J., Foote J.W., Wiglesworth F.W., Blennerhassett J.B. (1970) The pathology of the adynamic distal ureteral segment. J Urol. 103: 134–137.
20. Manzoni, C. (2002) Megaureter. Rays 27: 83–85.
21. Merlini E., Spina P. (2005) Primary non-refluxing megaureters. J Pediatr Urol. 1: 409-417.
22. Moore K.L., Persaud T.V.N., Torchia M.G. (2020) Urogenital System. In: Moore K.L., Persaud T.V.N., Torchia M.G. The Developing Human: Clinically Oriented Embryology. 11th Ed. Elsevier, Edinburgh. Pp 223-262.
23. Nicótina P.A., Romeo C., Arena F., Romeo G. (1997) Segmental up-regulation of transforming growth factor-beta in the pathogenesis of primary megaureter. An immunocytochemical study. Br J Urol. 80: 946-949.
24. Notley R.G. (1972) Electron microscopy of the primary obstructive megaureter. Br J Urol. 44: 229–234.
25. Onen A. (2020) Grading of hydronephrosis: An ongoing challenge. Front Pediatr. 8: Article 458.
26. Öztürk E., Burgu B., Gülpınar Ö., Soygür T. (2012) Effects of transforming growth factor on the developing embryonic ureter: An in-vitro megaureter model in mice. J Urol. 187(4S): e297-e298.
27. Öztürk E., Telli O., Gokce M.I., Ozcan C., Okutucu T.M., Soygur T., Burgu B. (2016) Effects of transforming growth factor on the developing embryonic ureter: An in-vitro megaureter model in mice. J Pediatr Urol. 12: 310.e1-310.e4.
28. Pfister R.C., Hendren W.H. (1978) Primary megaureter in children and adults. Clinical and pathophysiologic features of 150 ureters. Urology 12: 160-176.
29. Rasmussen P.E., Nielsen F.R. (1988) Hydronephrosis during pregnancy: a literature survey. Eur J Obstet Gynecol Reprod Biol. 27: 249-259.
30. Report of working party to establish an international nomenclature for the large ureter. (1977) Birth Defects Orig. Artic. Ser. 13: 3-8.
31. Sharif H. (2021) Modern issues of diagnosis and treatment megaureter in children. Sys Rev Pharm. 12: 16-19.
32. Shokeir A.A., Nijman R.J.M. (2000) Primary megaureter: current trends in diagnosis and treatment. BJU International. 86: 861–868.
33. Sulemanji M., Vakili K. (2013) Neonatal renal physiology. Semin Pediatr Surg. 22: 195-198.
34. Thotakura R., Anjum F. (2022 Sep 26) Hydronephrosis and Hydroureter. In: StatPearls. Treasure Island (FL): StatPearls Publishing.
35. Tokunaka S., Gotoh T., Koyanagi T., Miyabe N. (1984) Muscle dysplasia in megaureters. J Urol. 131: 383–390.
36. Tokunaka S., Koyanagi T. (1982) Morphologic study of primary nonreflux megaureters with particular emphasis on the role of ureteral sheath and ureteral dysplasia. J Urol. 128: 399–402.
37. Vlad M., Ionescu N., Ispas A.T., Ungureanu E., Stoica C. (2007) Morphological study of congenital megaureter. Rom J Morphol Embryol. 48: 381–390.
38. Weber A.L., Pfister R.C., James A.E. Jr., Hendren W.H. (1971) Megaureter in infants and children: roentgenologic, clinical, and surgical aspects. Am J Roentgenol Radium Ther Nucl Med. 112: 170-177.
39. Weiss R.M., Lytton B. (1974) Vesicoureteral reflux and distal ureteral obstruction. J Urol. 111: 245–249.
40. Wilcox D., Mouriquand P. (1998) Management of megaureter in children. Eur Urol. 34: 73–78.
41. Younsi N. (2020) Diagnostisches Management des primären Megaureters: Miktionszysturethrog-

raphie obligat, Szintigraphie sinnvoll? [Diagnostic management of primary megaureter: Voiding cystourethrography obligatory, scintigraphy useful?]. Urologe A. 59: 261-265.

IJAE
ITALIAN JOURNAL OF ANATOMY AND EMBRYOLOGY

Firenze University Press
www.fupress.com/ijae

OPEN ACCESS

Citation: Siwek, K., Wieczorek, W., Łopińska, M., Polak-Boroń, K., Saniotis, A., Galassi, F.M., & Suchanecka, M. (2023). Developmental and surgical anatomy of pathologies of the craniovertebral junction: a much-needed problematization of efficacy and long-term outcomes. *Italian Journal of Anatomy and Embryology* 127(2): 29-37. doi: 10.36253/ijae-14666

Data Availability Statement: All relevant data are within the paper and its Supporting Information files.

Competing Interests: The Author(s) declare(s) no conflict of interest.

Developmental and surgical anatomy of pathologies of the craniovertebral junction: a much-needed problematization of efficacy and long-term outcomes

Katarzyna Siwek[1], Wiktoria Wieczorek[6], Marcelina Łopińska[2], Katarzyna Polak-Boroń[2], Arthur Saniotis[3,4], Francesco M. Galassi[3,5,*], Małgorzata Suchanecka[1]

[1] *Division of Anatomy, Department of Human Morphology and Embryology, Wroclaw Medical University, Wrocław, Poland*
[2] *Department of Anatomy, Collegium Medicum, Faculty of Medicine, University of Warmia and Mazury, Olsztyn, Poland*
[3] *Biological Anthropology and Comparative Anatomy Research Unit, School of Biomedicine, The University of Adelaide, Australia*
[4] *Bachelor of Doctor Assistance Department, DDT College of Medicine. Gaborone, Botswana*
[5] *Department of Anthropology, Faculty of Biology and Environmental Protection, University of Lodz, Lodz, Poland*
[6] *Faculty of Stomatology, Wrocław Medical University, Wrocław, Poland*
*Corresponding author. E-mail: francesco.galassi@biol.uni.lodz.pl

Abstract. Introduction. Due to its complex anatomy and function the craniovertebral junction (CVJ) is prone to several pathological conditions. The unique topography of neuro-vascular and bony structures makes surgical management of this area particularly challenging. Methods. A systematic online literature search was conducted in *PubMed*, *Google Scholar, Scopus, and Web of Science* with keywords relating to Chiari malformation, Wallenberg syndrome, Syringomyelia, and atlantoaxial dislocations. Results. This paper presents an up-to-date summary of the pathogenesis and surgical management of Chiari malformation, Wallenberg syndrome, syringomyelia, and atlantoaxial dislocation with particular emphasis on developmental and surgical anatomy. Conclusion. In such complex pathologies of the CVJ, the many factors contributing to the patient's condition and the aspects playing a key role in the treatment process are all difficult to be considered concurrently. A better and universal surgical technique is impossible to be established.

Keywords: craniovertebral junction, Chiari malformation, Wallenberg syndrome, syringomyelia, atlantoaxial dislocations, surgical management.

INTRODUCTION

The human head contributes to approximately 6% of total body weight. Therefore, an average 80 kg male individual carries five kilograms of weight

at the top of his torso throughout his lifetime (Szczygieł et al., 2020). The cranium transitions through the craniovertebral junction into the spine. Several structures contribute to the junction including 6 joints in total: the upper joint of the head comprises two atlantooccipital joints, while the lower joint of the head contains four joints: two lateral atlantoaxial joints and two median atlantoaxial joints anterior and posterior (Gworys, 2012, Standring, 2021) these joints are supported by muscles, ligaments, and membranes which serve two functions: allowing movement in the upper cervical region and protecting vital structures, such as the spinal cord, nerves and vessels supplying the cerebrum. Both congenital and acquired diseases develop in this area. The complexity of the region and its anatomical variability among individuals provide challenges to surgical management.

The multistage diagnostic process usually begins with computer tomography (CT scan imaging), which has questionable accuracy and poor image resolution (Takami et al., 2014; Chi et al.,2019). In contrast, magnetic resonance imaging (MRI) and its parameters provide physicians with a more precise image of a patient's current stage. A further advantage of MRI is its ability to depict soft tissue (Winklhofer et al., 2014). A more invasive diagnostic examination is a myelogram (Kular & Cascella, 2022). This paper focuses on the pathogenesis of diseases of the craniovertebral junction and provides a comparison of specific procedures which were performed during each pathological study.

METHODS

This review was based on an internet search of *PubMed*, *Google Scholar*, *Scopus*, and *Web of Science* in order to find pathological cases based on a specific word search. Word search entries included 'Chiari malformation', 'Chiari malformation types', 'Wallenberg syndrome', 'lateral medullary syndrome', 'posterior inferior cerebellar artery syndrome', 'Syringomyelia', and 'atlantoaxial dislocations'.

RESULTS

Etiology and classification

Chiari malformation (CM, previously known as Arnold-Chiari malformation) was first observed and described by Julius Arnold (1835-1915), a German pathologist, along with his Austrian colleague Hans Chiari (1851-1916). They discovered a general deformation of the hindbrain accompanied by ectopic cerebellar tonsils. Currently, CM is classified according to four types (Table 1). Type 1 is the most prevalent type of CM, which involves a caudal displacement of the cerebellar tonsils through the foramen magnum. The displacement must be 5mm or greater with no involvement of spinal herniation to be classified as type 1 CM. Nevertheless, a spinal herniation may also appear in other types of CM. Another common characteristic of type 1 CM is its late appearance in adolescents, whereas type 2 CM can be diagnosed much earlier. Furthermore, type 2 CM is typically diagnosed with ectopy of the cerebellar vermis, fourth ventricle as well as brainstem, and myelodysplasia. Type 3 and 4 CM are extremely rare (Kular & Cascella, 2022; Fric et al., 2019; Brito et al., 2019; Milhorat, 2009). Type 0/0,5 CM has recently been identified as having no symptoms of type 1 CM in children, however, in this type, the cerebellar tonsils wrapped around the medulla oblongata. Type 1.5 combines symptoms of type 1 and 2. Additionally, there is no evident spine herniation in type 1.5 CM (Fric et al., 2019; Morgenstern et al., 2020).

No specific or supported mechanism of the pathogenesis in CM has been supported by research. Some arguments purport that CM is a genetic disease with association with alleles located on the 9th and 15th chromosomes (Boyles et al., 2006). Alternatively, counterarguments highlight that CM is rarely identified in families and that late diagnosis in infants may be asymptomatic (Fric et al., 2019). Although type 2 and 3 CM derive from neuro-ectodermal defects, type 1 CM is believed to be an effect of a para-axial mesoderm lesion leading to impaired development of the posterior cranial fossa. Interestingly enough, type 1 CM can occur alongside cases in which no cranial hypoplasia is observed, such as tethered cord syndrome, hydrocephalus, or acromegaly (Milhorat, 2009). Thus, CM can be diagnosed as a secondary condition to other diseases. Iatrogenic CM has also been reported (Kular & Cascella, 2022).

Table 1. Epidemiology of the craniovertebral junction pathologies.

Disease		Epidemiology
Chiari malformation	Type 1	1 per 1280 live births (Capra et al., 2019)
	Type 2	1 per 1000 live births (Kuhn and Emmady, 2022)
	Type 3	51 cases reported (Elbaroody et al., 2021)
	Type 4	no data available
Wallenberg syndrome		60 000 cases a year only in the United States (Venti, 2012)
Syringomyelia		8.4 per 100000 live births (Sharma et al., 2006)

Wallenberg Syndrome (WS) otherwise known as the lateral medullary syndrome was first mentioned in 1808 by Gaspard Vieusseux (1746-1814), with a more precise description of WS being presented by the German neurologist Adolf Wallenberg (1862-1949) in 1895 (Wallenberg, 1895). Vieusseux described WS as an occlusion of the vertebral artery or the posterior inferior cerebellar artery (PICA) followed by infarction of the lateral medulla oblongata (Lui et al., 2022). Lateral medullary syndrome (LMS) is the non-eponym designation of WS. In WS the lateral region of the medulla oblongata, posterior to the olivary nucleus is affected.

In order to understand the mechanism of WS a brief description of PICA is necessary. The posterior inferior cerebellar artery is a branch of the vertebral artery, arising 1,6-1,7 cm below the vertebrobasilar junction. The main trunk of PICA is the source of branches supplying the lower cerebellar hemispheres, the vermis, the fourth ventricle, and the tonsils. As mentioned, blood clots can develop in PICA or even in the vertebral artery. Moreover, PICA is important when aneurysms are involved since they are prone to rupture during surgical procedures (Lui et al., 2022). Risk factors of WS include hypertension, smoking, diabetes, or arteriosclerosis. Also, head trauma may contribute to the evolution of WS, as well as Marfan syndrome, Wegener's granulomatosis, or during a cocaine overdose (Lui et al., 2022; Gasca-González et al., 2020)

Syringomyelia which is the subsequent pathology in focus, is a condition in which a cavity filled with fluid in the parenchyma of the spinal cord occurs (Wichmann et al., 2020). It was originally described by Brunner et. al. in 1688 (Hart, 2014). The fluid-filled cavity is called the syrinx. A vital aspect of the fluid filling the cavity is that it is isotonic or close to isotonic with the CSF but with a much lower protein content (Rusbridge et al., 2006). That fluid-filled cavities must be separated from protein-filled tumor cavities which may resemble the syrinx (Rusbridge et al., 2006). Specialists describe the syrinx as a secondary lesion to another aforementioned disease of CM or myelomeningocele but with higher prevalence as it is associated with high-energy trauma (Wichmann et al., 2020; Fischbein et al., 1999). Syringomyelia can also develop in patients with no history of trauma due to cervical spondylostenosis or arachnoiditis.

Although an accurate mechanism remains unclear, the consensus is that it is caused by impaired cerebrospinal fluid (CSF) flow and partial obstruction. The theory of syringomyelia proposes that it occurs due to hypertension in the arachnoid matter the CSF is pumped through perivascular spaces into the parenchyma and accumulates in the central canal of the spinal cord. If the CSF remains in the parenchyme the condition is called presyrinx (Fischbein et al., 1999). An alternate theory argues that a cascade of this kind would rather cause increased pressure on the spinal cord; second, the differential pressure between the spinal cord and the subarachnoid space provides the driving force for such action. However, these theories do not explain the lowered protein level in the syrinx. Yet another hypothesis is described by Clare Rusbridge et al. to explore the relationship between syringomyelia and the principles of thermodynamics, specifically investigating fluid dynamics in the context of CM. The authors delve into the potential implications of fluid flow and energy considerations on the development and progression of syringomyelia, providing valuable insights into the underlying mechanisms of this neurological condition (Rusbridge et al., 2006). The authors suggested a division between communicating and non-communicating types of syringomyelia in reference to the connection between the syrinx and the fourth ventricle. The first type is diagnosed in less than 10% of patients and has received little theoretical attention (Rusbridge et al., 2006). However, some authors have speculated that the first type of syringomyelia may run in families (Busis & Hochberg, 1985).

Previous research has highlighted the vital connection between the cervical vertebrae C1 and C2 vertebrae in relation to mobility as well as instability. The principal joints of this region the atlantooccipital joint and atlantoaxial joints have various functions. While the atlantooccipital joint provides a positioning function, the atlantoaxial joint performs head rotation. That unfortunately makes it highly prone to any defects and damages. Some researchers consider that the atlantooccipital joint is a highly vulnerable structure (Goel, 2019; Salunke, 2018; Ibrahim et al., 2021).

Even small forces like a tap on the head in early childhood may lead to instabilities and minimal deformation of the upper cervical region (Goel, 2019). Instability and dislocations are frequently diagnosed in elderly people with weakened muscle tonus and children due to their smooth and slippery articular cartilages.

These conditions may contribute to the loss of correct stabilization (Goel, 2019). It has also been observed that any inborn asymmetry or malformation of the lateral masses of the atlas will lead to increased forces on one side of the joint (Salunke, 2018). Charles Bell in 1830 described a case in which a patient developed spinal cord compression secondary to pharyngitis and syphilis (Grisel, 1951). After two more cases of nontraumatic atlantoaxial dislocations (AAD), it was defined as Grisel syndrome. The mechanism of this condition remains unknown (Barcelos et al., 2014). Atlantoaxial disloca-

tions are a frequent outcome of high-energy trauma with a high mortality rate. Odontoid fracturing often occurs in such situations (Sánchez-Ortega et al., 2021). Other risk factors include rheumatoid arthritis, tuberculosis, Hirayama disease, or myelopathy which is related to the ossification of the posterior longitudinal ligament (Goel, 2021). Some researchers claim that atlantoaxial instability itself can cause basilar invagination or the CM (Wagner et al., 2020). Two classifications of atlantoaxial dislocations have been developed. The first classification focuses on the direction and surface of the malformation therefore we have anterio-posterior dislocation, rotary, central, and mixed one. The second one is clinically divided by surgeons into reducible (RAAD) and irreducible (IAAD) atlantoaxial dislocations.

Symptoms

Since pathologies occurring in the craniovertebral junction show similarity, they are difficult to distinguish.

Symptoms of CM derive from impaired CSF flow through a very constricted foramen magnum during any neck maneuvers. Pain accompanies coughing and sneezing. Suboccipital pain radiates to the frontal and parietal areas. Other symptoms include nausea and cognitive disorders. Intracranial pressure can cause disorders of the autonomic nervous system manifested as loss of consciousness, bradycardia, tinnitus, or swallowing problems. Children with CM suffer from sleep apnea and difficulties in food intake due to CNIX and CNX dysfunction (Kular & Cascella, 2022; Fric et al., 2019).

Nystagmus, dizziness, dysphagia, ataxia, and Horner's syndrome occurring on the side of the lesion, as well as contralateral loss of pain and temperature of the body and ipsilateral loss of pain and temperature to the face are signature symptoms of WS. Another noticeable symptom of WS is hiccupping (Lui et al., 2022; (16) (17). The progression of WS can be both rapid and gradual. In both cases the symptoms are similar.

Syringomyelia is a disease that can be symptomatic and asymptomatic. Due to the individual location of the cysts, the symptoms will vary in intensity and area of radiation (Wichmann et al., 2020). Generally, patients experience pain, oversensitivity, impaired muscle function, and spasticity (Schurch et al., 1996). Some patients report loss of temperature and nociception but with intact proprioception and sense of vibration (Wichmann et al., 2020). Muscular dysfunction of one limb or neurogenic bladder is also spotted in patients with syringomyelia (La Haye & Batzdorf, 1988). Interestingly, the time between trauma and the appearance of symptoms varies from 2 months to even 30 years (Schurch et al., 1996).

Atlantoaxial dislocations, especially in children tend to be asymptomatic. This unfortunately delays diagnosis and treatment. No specific neurological symptoms have been assigned to this pathology, but a cock-robin position of the head can be an indication. In this position, the head inclines to one side and tilts to the other side (Goel, 2019; Štulík et al., 2022). The literature also mentions acute neck pain and numbness of the limbs (Ibrahim et al., 2021). Dislocations occurring after high-impact trauma may cause breathing difficulties (Koljonen & Cheung, 2021; Liu et al., 2022). It is difficult for patients in the cock-robin position to turn their heads contralaterally.

Surgical management

As in most spinal defects, a patient's individual anatomy and general condition must be taken into consideration while clinical treatment of CM is being established. Though surgical management is usually a method of choice, some ideas of conservative treatment also occur in literature. This depends on whether the symptoms exacerbate, or the disease is prone to development. The Pediatric Section of the American Association of Neurological Surgeons stated that there is no need for surgical decompression procedures in asymptomatic children (Siasios et al., 2012). Conservative treatment includes non-steroidal anti-inflammatory drugs and muscle relaxants which provide minimal results in patients with more intensified symptoms.

Surgical procedures aim to re-establish equal pressure between the intracranial subarachnoid space and the intramedullary area. The cerebral spinal fluid (CSF) should have normal pressure. The main procedure performed in almost 99% of cases was the posterior fossa decompression (PFD) which focuses on widening the cisterna magna with one or two posterior arches of the cervical vertebrae and opening the dura matter but leaving the cerebellar tonsils in herniation (Fric et al., 2019; Arnautovic et al., 2015; Siasios et al., 2012; Lou et al., 2019). However, this is not a flawless procedure since the side effects may include cephalomeningitis or CSF leakage. Moreover, 17% of patients require repeated surgery (Lou et al., 2019). To decrease the side effects of PFD, a posterior fossa reconstruction (PFR) with duroplasty can be performed in type 1 CM with syringomyelia. An advantage of PFR is that it does not interfere with the CSF flow due to the remained continuity of the arachnoid matter. Currently, there is no consensus on a 'better' method for PFR. Advantages of PFD include shorter operating times and lower hospitalization costs. Research carried out on 582 patients provides information about

similar outcomes of PFD with or without duroplasty (Lou et al., 2019; Mohanty, 2019). A less invasive technique does not involve craniectomy removal of subdural tonsil herniation with a reconstruction of cisterna magna in patients with type 1 CM with syringomyelia. However, some side effects were also observed (Kular & Cascella, 2022; Lou et al., 2019). If the CSF flow does not return to its proper level after any of those procedures or the intracranial pressure increases, then a ventriculoperitoneal shunt is recommended (Fric et al., 2019).

Regarding WS, diagnostic tools are worth mentioning. MRI with diffusion-weighted imaging (DWI) is a prescribed method since it allows early detection of ischemic lesions (Lui et al., 2022; Heinemann et al., 2009). Rare cases like vertebral artery dissection can be dismissed due to the use of a CT or MRI angiogram followed by a precise location of the damaged area (Lui et al., 2022; Saleem & Das, 2022). The best-case prognosis is where a quick diagnosis is established. Some research mentions similar steps, beginning with an intravenous (IV) thrombolysis with IV tissue plasminogen activator (Lui et al., 2022; Saleem & Das, 2022). Endovascular revascularization performed with modern devices is recommended if large intracranial vessels have been impaired. Patients who have undergone this procedure tend to have improved recovery (Lui et al., 2022). Secondary prevention includes statins, antiplatelets (i.e., aspirin and antihypertensive drugs).

Using phase-contrast MRI to measure blood flow in large vessels is considered an optimal diagnostic method in syringomyelia. A benefit of this method is that it is free from side effects and provides physicians with qualitative and quantitative data. Moreover, it is less invasive than lumbar puncture or neuroendoscopy (Wichmann et al., 2020; Fischbein et al., 1999).

Surgical treatment is performed in symptomatic cases in which patients' mobility is impaired and limited or where there is inordinate pain. Conservative treatment is sparsely used in symptomatic cases (Schurch et al., 1996). An interesting position among surgical maneuvers is the syringo-subarachnoid-peritoneal shunt with a T-tube. According to some authors, this method differs from syringe-subarachnoidal or syringe-pleural shunts which are also used to siphon off CSF. Unfortunately, a drawback of syringe-subarachnoidal or syringe-pleural shunts is their tendency to fail. In the case of syringe-pleural shunts repeat surgery may be required within a year (Kim et al., 2012). Other disadvantages of shunts are their incidence of displacement and obstruction. For example, a linear catheter in syringostomia runs a high risk of dislocation. The method presented in the article included high perforation of the T-tube and allocation of only one arm of the tube in the syrinx and the second in the subarachnoid space to avoid injuring the spinal cord during its removal. In one patient who received this treatment, his syrinx decreased with subsequent improvement in motor function in his upper right arm (Kim et al., 2012).

Other articles which mention the T-tube as a shunt of choice do not evaluate any specifics of the procedure. Syringostomia tends to have a positive outcome in patients most of whom report decreased symptoms (Schurch et al., 1996). In one of the positions available after individual assessment doctors performed: suboccipital decompression with partial resection of cerebellar tonsils or C3 through C7 laminectomy with sectioning the dentate ligament at C3-C4 and lysis of subdural adhesions or VP shunting. Even though some patients had suffered from other disorders aside from syringomyelia, in most of them, an improvement was observed (Fischbein et al., 1999). Another research used cyst-to-peritoneal shunt in most patients all of whom regained physical strength and their pain decreased (La Haye & Batzdorf, 1988).

In Goel and Desai's research, an interesting aspect was that a syringe-subarachnoidal shunt was used to treat syringomyelia secondary to CM and basilar invagination (Goel & Desai, 2000). Here, the shunt was a fundamental procedure. Although the operation may succeed in decreasing the size of the syrinx, symptoms caused by the pressure on the brainstem and cervical spinal cord may increase. The authors point out that the syrinx might have evolved as a protective phenomenon to protect vital structures prone to any damage because of the CM and not as a pathological condition (Goel, 2001).

Between 2002-2015, a series of surgical procedures containing laminectomy, lysis of adhesions, cyst fenestration, and duraplasty was performed in patients with post-traumatic syringomyelia. The outcome was ambiguous since some patients reported improvement and some claimed that the symptoms declined (Li et al., 2021). Patients often required a repeated operation after surgical management in syringomyelia, in some cases there is a need for even 10 re-operations when spine fusion is performed. Circumferential spine surgery, lysis of adhesions, or duraplasty are believed to be the most effective in decreasing the risk of repeated operation (Li et al., 2021).

Before proceeding with the surgical methods in atlantoaxial dislocations, some discussion on the aims of treatment is necessary. The inclination should be reduced with traction (closed method) and if not possible by opening the joints (open method). No pressure on any vital structures should remain post-operation. Usually, an arthrodesis is recommended (Jain, 2012). In

most reported cases, a reduction followed by fixation is performed (Jain, 2012; Štulík et al., 2022).

Among techniques used in RAAD treatment after the repositioning of the joint and bone graft, is sub-laminar wiring. In this procedure, complications may occur involving cutting the posterior arch of the atlas with the wire. Titanium is often used due to its pliability when compared to steel rods. It should be pointed out that a fusion from the occiput to C4 should be performed only when a patient requires it. Another disadvantage of such fusion from the occiput to C4 is the high force impacting the structures at both ends. The C1-C2 spacer jamming is a further option but should be executed along with sub-laminar wiring or C1-C2 fusion to strengthen the connection. A trans-articular screw with sub-laminar wiring by the Magerl technique is also considered functional, stable, and efficient (Jain, 2012).

Atul Goel proposes that the first approach to reducing a dislocation can be cervical halter or halo-gravity traction. If after 3-4 weeks no improvement is observed, an open procedure can be implemented. The Goel method allows the patient to have greater freedom of movement in the cervical region (Goel, 2019). This method has proven to be successful. Prevalent procedures are C1-C2 posterior fixations executed by transarticular Magerl or the above-mentioned Goel technique. New solutions include transpendicular axis mass fixation and an anterior transarticular fixation with the Vaccaro method (Sánchez-Ortega et al., 2021).

Not many papers mention the management of atlantoaxial instabilities in the Grisel syndrome. In this case, conservative treatment precedes surgical intervention. A protocol of conservative treatment in atlantoaxial dislocations is mentioned by Wetzel and La Rocca who discuss the management of dislocations emerging in children in relation to a 7-year-old male patient. Due to the patient's age and body build, a fusion would have had a high risk considering the size of the child's bones and soft tissues. The authors mention Menezes who proposes, in this case, a subtle craniectomy with laminectomy of the upper cervical region and a bilateral interlaminar followed by occipital rib graft. This is fixed with a titanium wire (Barcelos et al., 2014).

Harms-Goel and Magerl techniques are mentioned along with the Wright method in which the screw is allocated through the lateral masses of the atlas and intralaminarly of the axis (Marcon et al., 2012). In the case of IAAD, a transoral odontoidectomy is performed, although some surgeons prefer a more applicable method of transoral decompression. A transoral odontoidectomy is aimed at delivering the neurological structures (Jain, 2012). This procedure has a high risk of CSF leakage and meningitis (Liu et al., 2022). Halo traction and vest are listed again as ways for managing acute atlantoaxial dislocations in children with no guarantee of reduction. Surgical operations involved here are Magerl, Harms-Goel technique, and Brooks or Gallie wiring (Koljonen & Cheung, 2021).

DISCUSSION

Undoubtedly, the complexity of the cranio-vertebral junction has several drawbacks which need to be considered before surgery. Their etiology is probably an outcome of many factors including a genetic base possible in the development of CM or syringomyelia (Boyles et al., 2006; Busis & Hochberg, 1985). High-impact trauma, on the other hand, may contribute to the increase of syringomyelia or atlantoaxial dislocations (Wichmann et al., 2020; Fischbein et al., 1999; Sánchez-Ortega et al., 2021). The occurrence of one pathology in this area does not exclude others. For example, syringomyelia may be secondary to CM. Symptoms of both diseases often resemble each other.

As for the treatment, milestone steps have been made. A posterior fossa reconstruction aims at eliminating side effects of PFD in CM which is found in the literature. Nevertheless, many surgeons perform a PFD with various levels of success (Lou et al., 2019; Mohanty, 2019).

Magnetic resonance imaging with diffusion-weighted imaging (DWI) which is used in Wallenberg syndrome diagnostics allows a fast and accurate diagnosis (Lui et al., 2022; Heinemann et al., 2009). Additionally, endovascular revascularisation provides a patient with a higher rate of recovery (Lui et al., 2022).

The treatment of syringomyelia offers several tools that can be employed in the treatment process. The syringo-subarachnoid-peritoneal shunt, as the authors propose, is a questionable option since the obstruction and moveability of shunts have to be taken into consideration (Kim et al., 2012). Other surgeons perform a series of cyst-to-peritoneal shunt placements with a highly positive outcome (La Haye & Batzdorf, 1988). Laminectomy, lysis of adhesions, cyst fenestration, and duraplasty used in the treatment of patients found in one article had questionable results (Li et al., 2021). The idea that syringomyelia is an evolutionary development for decreasing pressure still requires more research (Goel, 2001).

In relation to atlantoaxial dislocation, the Goel and Magerl method in posterior fixation is often preferred (Goel, 2019; Koljonen & Cheung, 2021). Other aspects have been addressed in the medical literature, including

the unnecessary occiput to C4 fusion which can limit a patient's movements. This systematic review found few papers discussing the treatment of Grisel syndrome. In relation to children's atlantoaxial dislocations, Menezes management has been examined (Barcelos et al., 2014).

CONCLUSIONS

The aim of this paper was to review the surgical aspects of cranio-vertebral junction pathologies. Current knowledge of each disease's etiology and treatments was included. Although several surgical techniques are currently in use, more research is necessary to identify any long-term effects. Fortunately, due to ongoing developments in medical technology, surgeons have an increasing number of resources to use. A conclusion drawn from this paper is that a universal technique for correcting pathologies of the craniovertebral junction is not possible. This is due to the complex nature of pathologies, as well as various other factors contributing to a patient's condition which play a vital role in the treatment process, and which are difficult to be considered concurrently.

REFERENCES

Arnautovic A, Splavski B, Boop FA, Arnautovic KI. 2015. Pediatric and adult Chiari malformation Type I surgical series 1965-2013: a review of demographics, operative treatment, and outcomes. J Neurosurg Pediatr. 2015 Feb;15(2):161-77. [PubMed]

Barcelos AC, Patriota GC, Netto AU. 2014. Nontraumatic atlantoaxial rotatory subluxation: grisel syndrome. Case report and literature review. Global Spine J. 2014 Aug;4(3):179-86. doi: 10.1055/s-0033-1363936. Epub 2014 Jan 13. PMID: 25083360; PMCID: PMC4111947.

Boyles AL, Enterline DS, Hammock PH, Siegel DG, Slifer SH, Mehltretter L, Gilbert JR, Hu-Lince D, Stephan D, Batzdorf U, Benzel E, Ellenbogen R, Green BA, Kula R, Menezes A, Mueller D, Oro' JJ, Iskandar BJ, George TM, Milhorat TH, Speer MC.2006. Phenotypic definition of Chiari type I malformation coupled with high-density SNP genome screen shows significant evidence for linkage to regions on chromosomes 9 and 15. Am J Med Genet A.Dec 15;140(24):2776-85. doi: 10.1002/ajmg.a.31546. PMID: 17103432.

Brito JNPO, Santos BAD, Nascimento IF, Martins LA, Tavares CB. 2019. Basilar invagination associated with chiari malformation type I: A literature review. Clinics (Sao Paulo). 2019;74:e653. doi: 10.6061/clinics/2019/e653. Epub 2019 Apr 8. PMID: 30970117; PMCID: PMC6448527.

Busis NA, Hochberg FH. 1985. Familial syringomyelia. J Neurol Neurosurg Psychiatry. 1985 Sep;48(9):936-8. doi: 10.1136/jnnp.48.9.936. PMID: 4045487; PMCID: PMC1028499.

Capra V, Iacomino M, Accogli A, Pavanello M, Zara F, Cama A, De Marco P. Chiari malformation type I: what information from the genetics? Childs Nerv Syst. 2019 Oct;35(10):1665-1671. doi: 10.1007/s00381-019-04322-w. Epub 2019 Aug 5. PMID: 31385087.

Chi J, Zhang Y, Yu X, Wang Y, Wu C. 2019. Computed Tomography (CT) Image Quality Enhancement via a Uniform Framework Integrating Noise Estimation and Super-Resolution Networks. Sensors (Basel). 2019 Jul 30;19(15):3348. doi: 10.3390/s19153348. PMID: 31366173; PMCID: PMC6696205.

Elbaroody M, Mostafa HE, Alsawy MFM, Elhawary ME, Atallah A, Gabr M. Outcomes of Chiari Malformation III: A Review of Literature. J Pediatr Neurosci. 2020 Oct-Dec;15(4):358-364. doi: 10.4103/jpn.JPN_135_19. Epub 2021 Jan 19. PMID: 33936298; PMCID: PMC8078634.

Fischbein NJ, Dillon WP, Cobbs C, Weinstein PR. 1999. The "presyrinx" state: a reversible myelopathic condition that may precede syringomyelia. AJNR Am J Neuroradiol. Jan;20(1):7-20. PMID: 9974051.

Fric R, Ringstad G, Eide PK.2019. Chiari-malformasjon type 1 – diagnostikk og behandling [Chiari malformation type 1 – diagnosis and treatment]. Tidsskr Nor Laegeforen. 2019 Jun 11;139(10). Norwegian. doi: 10.4045/tidsskr.18.0455. PMID: 31238671.

Gasca-González OO, Pérez-Cruz JC, Baldoncini M, Macías-Duvignau MA, Delgado-Reyes L. 2020. Neuroanatomical basis of Wallenberg syndrome. Cir Cir; 88(3):376-382. English. doi: 10.24875/CIRU.19000801. PMID: 32539005.

Grisel P. Enucleation of the atlas and nasopharyngeal torticollis. Presse Med. 1951;59:1647–8. [PubMed] [Google Scholar]

Goel A, Desai K. 2000. Surgery for syringomyelia: an analysis based on 163 surgical cases. Acta Neurochir (Wien). 2000;142(3):293-301; discussion 301-2. doi: 10.1007/s007010050038. PMID: 10819260.

Goel A.2001 Is syringomyelia pathology or a natural protective phenomenon?. J Postgrad Med ;47:87

Goel A. 2019. Torticollis and rotatory atlantoaxial dislocation: A clinical review. J Craniovertebr Junction Spine. 2019 Apr-Jun;10(2):77-87. doi: 10.4103/jcvjs.JCVJS_40_19. PMID: 31404132; PMCID: PMC6652258.

Goel A. 2021. Indicators of atlantoaxial instability. J Craniovertebr Junction Spine. 2021 Apr-Jun;12(2):103-106. doi: 10.4103/jcvjs.jcvjs_55_21. Epub 2021 Jun 10. PMID: 34194154; PMCID: PMC8214233.

Grisel P. 1951. Enucleation of the atlas and nasopharyngeal torticollis. Presse Med. 1951;59:1647–8.

Gworys B. 2014. Kompendium anatomii prawidłowej człowieka tom 1

Hart DJ.2014. Encyclopedia of the Neurological Sciences (Second Edition)

Ibrahim Y, Zhao Y, Liu W, Yuan S, Tian Y, Wang L, Liu X. 2021. An unusual injury mechanism of atlantoaxial dislocation: illustrative case. J Neurosurg Case Lessons. 2021 Jun 14;1(24):CASE21134. doi: 10.3171/CASE21134. PMID: 35855094; PMCID: PMC9245838.

Jain VK. 2012. Atlantoaxial dislocation. Neurol India ;60:9-17

Kim SH, Choi SW, Youm JY, Kwon HJ.2012. Syringo-subarachnoid-peritoneal shunt using T-tube for treatment of post-traumatic syringomyelia. J Korean Neurosurg Soc. 2012 Jul;52(1):58-61. doi: 10.3340/jkns.2012.52.1.58. Epub 2012 Jul 31. PMID: 22993681; PMCID: PMC3440506.

Koljonen PA, Cheung KM.2021. Concomitant atlantoaxial and atlanto-occipital rotatory dislocation in children: Radiological features, diagnostic pitfalls, and long-term outcome. Journal of Orthopaedic Surgery. 2021;29(1_suppl). doi:10.1177/23094990211015502

Kuhn J, Emmady PD. Chiari II Malformation. In: StatPearls. StatPearls Publishing, Treasure Island (FL); 2022. PMID: 32491430.

Kular S, Cascella M. 2022. Chiari I Malformation. [Updated 2022 Feb 5]. In: StatPearls [Internet]. Treasure Island (FL): StatPearls

La Haye PA, Batzdorf U. 1988. Posttraumatic syringomyelia. West J Med. 1988 Jun;148(6):657-63. PMID: 3176472; PMCID: PMC1026203.

Li YD, Therasse C, Kesavabhotla K, Lamano JB, Ganju A. 2021. Radiographic assessment of surgical treatment of post-traumatic syringomyelia. J Spinal Cord Med. 2021 Nov;44(6):861-869. doi: 10.1080/10790268.2020.1743086. Epub 2020 Mar 30. PMID: 32223591; PMCID: PMC8725754.

Liu HD, Li N, Miao W, Su Z, Cheng HL. 2022. Traumatic posterior atlantoaxial dislocation without fracture of the odontoid process: illustrative case. J Neurosurg Case Lessons. 2022 Nov 7;4(19):CASE22330. doi: 10.3171/CASE22330. PMID: 36345203; PMCID: PMC9644412.

Lou Y, Yang J, Wang L, Chen X, Xin X, Liu Y. 2019. The clinical efficacy study of treatment to Chiari malformation type I with syringomyelia under the minimally invasive surgery of resection of Submeningeal cerebellar Tonsillar Herniation and reconstruction of Cisterna magna. Saudi J Biol Sci. 2019 Dec;26(8):1927-1931. doi: 10.1016/j.sjbs.2019.07.012. Epub 2019 Jul 25. PMID: 31885484; PMCID: PMC6921303.

Lui F, Tadi P, Anilkumar AC. 2022. Wallenberg Syndrome. Oct 21. In: StatPearls [Internet]. Treasure Island (FL): StatPearls Publishing; 2022 Jan. PMID: 29262144.

Marcon RM, Cristante AF, Teixeira WJ, Narasaki DK, Oliveira RP, de Barros Filho TE. 2013. Fractures of the cervical spine. Clinics (Sao Paulo). 2013 Nov;68(11):1455-61. doi: 10.6061/clinics/2013(11)12. PMID: 24270959; PMCID: PMC3812556.

Milhorat TH, Nishikawa M, Kula RW, Dlugacz YD. 2010. Mechanisms of cerebellar tonsil herniation in patients with Chiari malformations as guide to clinical management. Acta Neurochir (Wien). 2010 Jul;152(7):1117-27. doi: 10.1007/s00701-010-0636-3. Epub 2010 May 4. PMID: 20440631; PMCID: PMC2887504.

Mohanty A. 2019. Chiari I malformation: Surgical considerations. Neurol India 2019;67:662-3

Morgenstern PF, Tosi U, Uribe-Cardenas R, Greenfield JP.2020. Ventrolateral Tonsillar Position Defines Novel Chiari 0.5 Classification. World Neurosurg. 2020 Apr;136:444-453. doi: 10.1016/j.wneu.2020.01.147. PMID: 32204296.

Rusbridge C, Greitz D, Iskandar BJ. 2006, Syringomyelia: Current Concepts in Pathogenesis, Diagnosis, and Treatment. Journal of Veterinary Internal Medicine, 20: 469-479. doi: 10.1892/0891-6640(2006)20[469:sccipd]2.0.co;2. PMID: 16734077.

Saleem FM, Das J. 2022. Boczny zespół rdzeniasty. StatPearls [Internet]. Treasure Island (Floryda): Wydawnictwo StatPearls; -https://www.ncbi.nlm.nih.gov/books/NBK551670/

Salunke P.2018. Congenital Atlantoaxial Dislocation: Nature's Engineering Gone Wrong and Surgeon's Attempt to Rectify It. J Pediatr Neurosci. 2018 Jan-Mar;13(1):1-7. doi: 10.4103/JPN.JPN_73_17. PMID: 29899764; PMCID: PMC5982474.

Sánchez-Ortega JF, Vázquez A, Ruiz-Ginés JA, Matovelle PJ, Calatayud JB.2021. Longitudinal atlantoaxial dislocation associated with type III odontoid fracture due to high-energy trauma. Case report and literature review. Spinal Cord Ser Cases. 2021 May 25;7(1):43. doi: 10.1038/s41394-021-00407-4. PMID: 34035212; PMCID: PMC8149632.

Schurch B, Wichmann W, Rossier AB. 1996. Post-traumatic syringomyelia (cystic myelopathy): a prospec-

tive study of 449 patients with spinal cord injury. J Neurol Neurosurg Psychiatry. 1996 Jan;60(1):61-7. doi: 10.1136/jnnp.60.1.61. PMID: 8558154; PMCID: PMC486191.

Sharma, M., Coppa, N., & Sandhu, F. A. (2006). Syringomyelia: A Review. Seminars in Spine Surgery, 18(3), 180–184. doi:10.1053/j.semss.2006.06.008

Siasios J, Kapsalaki EZ, Fountas KN. 2012. Surgical management of patients with Chiari I malformation. Int J Pediatr. ;2012:640127. doi: 10.1155/2012/640127. Epub 2012 Jun 28. PMID: 22811732; PMCID: PMC3395248.

Standring, S. (Ed.). (2021). Gray's Anatomy (42nd ed.). Elsevier.

Štulík J, Rybárová M, Barna M, Klézl Z. 2022. Atlantoaxial rotatory dislocation: Surgical treatment in a pediatric patient cohort. Brain Spine. 2022 Nov 1;2:101667. doi: 10.1016/j.bas.2022.101667. PMID: 36506286; PMCID: PMC9729819.

Szczygieł E, Fudacz N, Golec J, Golec E.2020. The impact of the position of the head on the functioning of the human body: a systematic review. Int J Occup Med Environ Health. 2020 Sep 17;33(5):559-568. doi: 10.13075/ijomeh.1896.01585. Epub 2020 Jul 23. PMID: 32713947.

Takami M, Nohda K, Sakanaka J, Nakamura M, Yoshida M.2014. Usefulness of full spine computed tomography in cases of high-energy trauma: a prospective study. Eur J Orthop Surg Traumatol. 2014 Jul;24 Suppl 1:S167-71. doi: 10.1007/s00590-013-1268-0. Epub 2013 Jul 6. PMID: 23832413.

Ueda M, Nishiyama Y, Abe A, Katayama Y. 2013. Hemorrhagic Wallenberg syndrome. Intern Med. 2013;52(20):2383-4. doi: 10.2169/internalmedicine.52.1141. PMID: 24126409.

Venti M, Cerebellar infarcts and hemorrhages. Frontiers of neurology and neuroscience. 2012; [PubMed PMID: 22377889]

von Heinemann P, Grauer O, Schuierer G, Ritzka M, Bogdahn U, Kaiser B, Schlachetzki F. 2009. Recurrent cardiac arrest caused by lateral medulla oblongata infarction. BMJ Case Rep.;2009:bcr02.2009.1625. doi: 10.1136/bcr.02.2009.1625. Epub 2009 Oct 12. PMID: 21991295; PMCID: PMC3027905.

Wagner A, Grassner L, Kögl N, Hartmann S, Thomé C, Wostrack M, Meyer B.2020. Chiari malformation type I and basilar invagination originating from atlantoaxial instability: a literature review and critical analysis. Acta Neurochir (Wien). 2020 Jul;162(7):1553-1563. doi: 10.1007/s00701-020-04429-z. Epub 2020 Jun 6. PMID: 32504118; PMCID: PMC7295832.

Wallenberg, A. (1895). Die akute Bulbärparalyse: Eine Monographie [Acute Bulbar Paralysis: A Monograph].

Wichmann TO, Pedersen M, Ringgaard S, Rasmussen MM.2022. Cerebrospinal fluid flow dynamics and the potential of phase-contrast MRI in syringomyelia. Ugeskr Laeger. 2020 May 5;182(22):V12190730. Danish. PMID: 32515330.

Winklhofer S, Thekkumthala-Sommer M, Schmidt D, Rufibach K, Werner CM, Wanner GA, Alkadhi H, Hodler J, Andreisek G.2013. Magnetic resonance imaging frequently changes classification of acute traumatic thoracolumbar spine injuries. Skeletal Radiol. Jun;42(6):779-86. doi: 10.1007/s00256-012-1551-x. Epub 2012 Dec 27. PMID: 23269516.

IJAE
ITALIAN JOURNAL OF
ANATOMY AND EMBRYOLOGY

Firenze University Press
www.fupress.com/ijae

Special Issue PhD course in Innovative Technologies in Clinical Medicine & Dentistry (University G. d'Annunzio, Chieti-Pescara)

The PhD course in Innovative Technologies in Clinical Medicine & Dentistry (InTEchMed) of the "G. d'Annunzio" of Chieti-Pescara aims to address some of the main challenges of personalized medicine through "the pursuit of multidisciplinary research" and "the internationalization of PhD programme". The PhD students are encouraged to work synergistically with their supervisors, interfacing with the national and international scientific communities in order to build and develop the skills and knowledge necessary for their research activity. This special issue collects the oral presentation of the preliminary data of the research projects presented by PhD students at 2nd IntechMed Conference (20 July 2023).

Coordinator of PhD program
Prof. Oriana Trubiani

Italian Journal of Anatomy and Embryology 127(2): 39-39, 2023
ISSN 1122-6714 (print) | ISSN 2038-5129 (online) |

IJAE
ITALIAN JOURNAL OF ANATOMY AND EMBRYOLOGY

Firenze University Press
www.fupress.com/ijae

OPEN ACCESS

Citation: Angiolani, F., Piattelli, M., Rinaldi, F., Trubiani, O., & Varvara, G. (2023). Prevalence and localization of *Canalis Sinuosus*: a mini review. *Italian Journal of Anatomy and Embryology* 127(2): 41-45. doi: 10.36253/ijae-14680

Data Availability Statement: All relevant data are within the paper and its Supporting Information files.

Competing Interests: The Author(s) declare(s) no conflict of interest.

Prevalence and localization of *Canalis Sinuosus*: a mini review

Francesca Angiolani*, Maurizio Piattelli, Fabiola Rinaldi, Oriana Trubiani, Giuseppe Varvara

Department of Innovative Technologies in Medicine & Dentistry, University of Chieti-Pescara 'Gabriele d'Annunzio', Via dei Vestini 11, 66100 Chieti, Italy
*Corresponding author. E-mail: angiolanif@gmail.com

Abstract. In recent years, scientific literature has been focusing on the study of the *Canalis Sinuosus* (CS); this canal contains the *anterior superior alveolar nerve* (ASAN), together with bundles. Accordingly, the CS may vary its frequency and anatomical features. These variations can be identified through imaging technologies such as *cone beam computed tomography* (CBCT). The aim of this mini review is to present the current understanding of the CS, its prevalence and localization in order to decrease the potential surgical risk associated with this region. As revealed by the analysis of the international literature available, presence of CS is a crucial factor to consider in implantology and generally in oral surgery procedures in this area. In conclusions the use and analysis of CBCT imaging in the diagnosis stage is fundamental to preserve the most important anatomical structures which are present in the jaws.

Keywords: canalis sinuosus, maxillary anatomy, CBCT.

INTRODUCTION

Replacement of single or multiple missing teeth with dental implants in the anterior maxilla is a reliable treatment option, with success rates reaching as high as 95% [1]. However, the occurrence of complications remains a concern, needing an accurate preoperative planning [2]. The anterior region of the jaw exhibits significant variability in innervation and blood supply and high trabecular density, emphasizing the need for Cone Beam Computed Tomography (CBCT) and highlighting the importance of three-dimensional diagnostics.

Compared to two- dimensional radiographic techniques, CBCT is considered the most informative method for comprehensive pre and postoperative analysis of the maxillary anatomy [3]. It is crucial in avoiding complications [4], such as bleeding and neurological symptoms [5,6].

Oliveira-Santos et al. reported the relative frequent occurrence of foramina and canals in the anterior superior maxillary region underlining the need for dental surgeons to be well trained in identifying these variations [7]. One significant anatomical structure in this region is the *Canalis Sinuosus*

(CS) whose damage can lead to the aforementioned complications [8]. The CS is a small branch of the infraorbital canal that contains the anterior superior alveolar nerve and vessels, providing innervation and nutrition to the anterior maxilla [7,9]. It runs below the inferior wall of the orbit, passing below the infraorbital foramen and skirting the lateral and inferior borders of the nasal fossa, with its opening located in front of the nasopalatine canal [10,11]. The CS innervates dental elements such as incisors and the canines, as well as the corresponding soft tissues. Despite being under-discussed in scientific articles, CS and other jaw structures are still unfamiliar to most oral surgeons and dental students [12]. The aim of this study was to evaluate the course of the CS using CBCT and emphasize the importance of identifying the CS before performing surgical procedures near the canal. This awareness and knowledge of CS variability allows for increased safety during such procedures

MATERIALS AND METHODS

Study design

Literature searches were conducted trough PubMed and Web of science databases.

The terms used to identify studies were: *"canalis sinuosus"*, *"maxillary anatomy"* and "CBCT". These reporting items for the research was performed by using combinations of the following Boolean operators: *"AND", "OR"*.

The mini review included only English language articles and the electronic search of publications was conducted in the last 10 years.

Inclusion criteria were: trials investigated using 3D radiographs (CBCT) that presented data on the prevalence and location of canalis sinuosus as main result.

All articles, presenting secondary results connected only to accessories canalis sinuosus (AC), canalis sinuosus orientation and meta-analysis, were ruled out.

RESULTS

The Table 1 below sum up the results of the study.

The search identified 19 articles in which the most common percentage, location and anatomical size of canalis sinuosus found, were examined, through detailed CBCT image.

The average and frequency of these values can be defined in detail by analyzing Table 1.

DISCUSSION

The increased and continuos use of implants for oral rehabilitation, together with the wider availability of CBCT imaging, has provided valuable information regarding important anatomical structures in the anterior maxillary region, where most surgeries are performed [7]. Within this area, the anterior superior alveolar nerve (ASAN) can be found, supplying innervation to the incisors, canines and their adjacent soft tissues. The ASAN is an intraosseous branch of the infraorbital nerve, originating from the maxillary nerve. The canalis sinuosus (CS) is a bony canal through which the infraorbital nerve passes to facilitate the passage of the ASAN [10]. In 1939, Frederic Wood Jones firstly described the CS, a bony canal containing neurovascular bundles that conveys the anterior superior alveolar nerve and vessels to the premaxilla [10]. The CS runs beneath the inferior margin of the orbit, medial to the anterior wall of the maxillary sinus, passing below the infraorbital foramen and skirting the lateral and inferior limits of the nasal fossa, ultimately opening into the nasal septum in front of the nasopalatine canal [13]. CBCT imaging is the most effective method for determining the location of the CS, making it highly valuable for diagnosis and implant planning [14].

In our search for studies on CS, we identified 19 publications in the PubMed database, comprising 11 case report and 6 prospective studies. These studies investigated the existence of the CS using CBCT with the number of subject ranging from 1 to 1460.

The frequency of CS occurrence varied significantly, ranging from 15.7% to 100%.

Regarding its specific locations, according to Oliveira-Santos et al's classification, the end of the CS trajectory, was found in several sites, with the highest occurrence observed in the maxillary intercentral region, particularly close to the lateral incisor, followed by the central incisor, between the central and lateral incisors, canine, posterior to the incisive foramen, and first premolar [7,10,15,16].

The majority of the studies in the literature describe cases of CS with diameter greater than or equal to 1 mm. However, Ghandourah et a, Fernandes et al and Khojastepour et al, reported cases with a diameter less than 1 mm.

Gender and age did not appear to influence the diameter, spatial location or and of the CS trajectory. While some studies suggests a higher prevalence of CS in males compared to females, no statistically no statistically significant differences were found [3,10,16,17].

Oliveira-Santos et al concluded that: "over 15% of the population studied had additional foramina in the ante-

Table 1.

Author	Year	Type of article	CBCT images evalueted	Presence of at least one CS	%	Localization End of CS	Size diameter
Aoki at al	2019	Prospective study	200	133	66.5	Central incisor (*n* = 91; 44.39%), Lateral incisor (*n* = 45; 21.95%) Canine (*n* = 29; 14.15%)	1 mm (*n* = 198/205; 96.6%) > 1 mm (*n* =6; 3.4%)
Anatoly at al	2019	Prospective study	150	101	67	Central incisor (*n=36;* 24.2%) Between central and lateral incisors (n=16; 10.7%) Lateral incisor (n=50; 33.5%) Canine (n=32; 21.5%) First premolar (n=14; 9.4%) Lateral to incisive foramen (n=1; 0.7%) Posterior to incisive foramen (n=0; 0%)	0.5-1 mm
Manhaes et al	2015	Prospective study	500	181	36.2	Central incisor (n=8;4.42%). Between central and lateral incisors (n=51;28.18%) Lateral incisor (n=28;15.46%) Canine (n=38;21%) First premolar (n=50;2762%) Lateral to Incisive foramen (n=35;19.33%) Posterior to incisive foramen (n=15;8.3%)	NS
Gurler et al	2017	Prospective study	111	111	100	Central incisor (n=1;1%) Between central and lateral incisors (n=o;o%) Lateral incisor (n=o;o%) Canine (n=o;o%) First premolar (n=0;0%) Lateral to incisive foramen (n=110;99%). Posterior to incisive foramen (n=o;o%)	(0.75-2.25 mm) 1.37 mm
Ruso et al	2017	Case report	1	1	100	NS	NS
Ghandourah et al	2017	Prospective study	219	144	65.75	NS	<1 mm
Wanzeler et al	2014	Prospective study	100	88	88	NS	0.7-0.8 mm
Machado et al	2016	Prospective study	1000	521	52.1		1.0-1.5 mm
Leven et al	2018	Case report	1	1	100	Lateral incisor	1.5 mm
McCrea et al	2017	Case report	1	1	100	Canine Posterior to incisive foramen	
Von Arx et al	2013	Prospective study	176	97	55.1	NS	NS
Oliveira-Santos et al	2013	Prospective study	178	28	15.7	Incisor Canine	(1-1.9 mm) 1.4 mm
Torres et al	2015	Case report	1	1	100	Medial at canine	2.5mm
Orhan et al	2018	Prospective study	1460	1460	100	Maxillary intercentral region	NS
Fernandes et al	2022	Prospective study	100	18	18	Palatal to the maxillary lateral incisor	<1 mm
Rosano et al	2020	Case report	1	1	100	Central incisor	NS
Harumiti Shintaku et al	2020	Case report	3	3	100	Canine Central incisor Lateral incisor	NS
Khojastepour et al	2023	Prospective study	485	380	78.35	Lateral incisor	<1 mm
Shan et al	2020	Prospective study	1007	372	36.9	Central incisor Lateral incisor	1.2 ± 0.1 mm

rior palate, ranging from 1 mm and 1.9 mm in width and located variably. In most cases, the canals associated with these foramina either served as a direct extension of the CS or traveled towards the nasal cavity floor [7]." Torres et al presents a case of dental implant placement in the anterior maxilla. The patient experienced neurovascular dis-

turbances, profuse postoperative nasal bleeding, pain, subnasal swelling, and a sense of "blockage" and "ethmoidal sinusitis" after 6 months [18]. When postoperative bleeding and prolonged paresthesia occur following dental implant placement in the anterior maxilla, neurovascular injury should be suspected [19] Shelley A et al, discussed a case in which an accessory canal (AC) was encountered during surgical implant placement, which could potentially result in persistent postoperative pain [3].

The presence of CS should be highlighted not only when planning surgery in the maxillary anterior, as it can affect implant success, but also when interpreting intraoral radiographs, as it may be mistaken for a periapical pathologic condition [20].

In conclusions, the CS is an anatomical structure which presence is relevant for oral surgery procedures in the anterior maxillary area. The awareness of it from clinicians lead to a more accurate diagnosis and treatment planning.

REFERENCES

1. Misje K, Bjørnland T, Saxegaard E, Jensen JL. Treatment outcome of dental implants in the esthetic zone: a 12- to 15-year retrospective study. Int J Prosthodont. 2013 Jul-Aug;26(4):365-9. doi: 10.11607/ijp.3097. PMID: 23837168.
2. L. R. C. Manhães Júnior, M. F. L. Villaça-carvalho, M. E. L. Moraes, S. L. P. d. C. Lopes, M. B. F. Silva, and J. L. C. Junqueira, "Location and classification of Canalis sinuosus for cone beam computed tomography: avoiding misdiagnosis," *Brazilian Oral Research*, vol. 30, no. 1, p. e49, 2016.
3. Anatoly A, Sedov Y, Gvozdikova E, Mordanov O, Kruchinina L, Avanesov K, Vinogradova A, Golub S, Khaydar D, Hoang NG, Darawsheh HM. Radiological and Morphometric Features of Canalis Sinuosus in Russian Population: Cone-Beam Computed Tomography Study. Int J Dent. 2019 Dec 16;2019:2453469. doi: 10.1155/2019/2453469. PMID: 31933643; PMCID: PMC6942815.
4. L. Maestre-Ferrín, S. Galán-Gil, C. Carrillo-García, and M. Peñarrocha-Diago, "Radiographic findings in the maxil- lary sinus: comparison of panoramic radiography with computed tomography," *The International Journal of Oral & Maxillofacial Implants*, vol. 26, no. 2, pp. 341–346, 2011.
5. R. Ferlin, B. S. C. Pagin, and R. Y. F. Yaedú, "Canalis sinuosus: a systematic review of the literature," *Oral Surgery, Oral Medicine, Oral Pathology and Oral Radiology*, vol. 127, no. 6, pp. 545–551, 2019.
6. F. O. Azhari and I. Fariska, "Normal value of cortical and mandibular trabecular bone density using cone beam com- puted tomography (CBCT)," *Journal of International Dental and Medical Research*, vol. 12, no. 1, pp. 160–164, 2019.
7. Oliveira-Santos C, Rubira-Bullen IRF, Monteiro SAC, Léon JE, Jacobs R. Neurovascular anatomical variations in the anterior palate observed on CBCT images. Clin Oral Implants Res. 2013;24(9):1044-8. doi:10.1111/j.1600-0501.2012.02497.x
8. L. Tolstunov, *Horizontal Alveolar Ridge Augmentation in Implant Dentistry: A Surgical Manual*, Wiley-Blackwell, Hoboken, NJ, USA, 2016.
9. de Machado VC, Chrcanovic BR, Felippe MB, Manhães Júnior LRC, de Carvalho PSP. Assessment of accessory canals of the *canalis sin- uosus*: a study of 1000 cone beam computed tomography examinations. *Int J Oral Maxillofac Surg*. 2016;45:1586-1591.
10. Jones FW. The anterior superior alveolar nerve and vessels. J Anat. 1939 Jul;73(Pt 4):583-91. PMID: 17104781; PMCID: PMC1252464.
11. Wanzeler AM, Marinho CG, Junior SM, Manzi FR, Tuji FM (2014) Anatomical study of the canalis sinuosus in 100 cone beam computed tomography examinations. Oral Maxillofac Surg. doi:10.1007/s10006-014-0450-9
12. Lopes-Santos G, Ikuta CRS, Salzedas LMP, Miyahara GI, Tjioe KC. *Canalis sinuosus*: an anatomic repair that may prevent suc- cess of dental implants in anterior maxilla. *J Prosthodont*. 2020;29:751-755.
13. Ghandourah AO, Rashad A, Heiland M, Hamzi BM, Friedrich RE (2017) Cone-beam tomographic analysis of canalis sinuo- sus accessory intraosseous canals in the maxilla. Ger Med Sci 15:1–12
14. Rusu MC, Săndulescu M, Bichir C, Muntianu LAS (2017) Com- bined anatomical variations: the mylohyoid bridge, retromolar canal and accessory palatine canals branched from the canalis sinuosus. Ann Anat 214:75–79
15. Von Arx T, Lozanoff S, Sendi P, Bornstein MM. Assessment of bone channels other than the nasopalatine canal in the anterior maxilla using limited cone beam computed tomography. Surg Radiol Anat. 2013;35:783-790.
16. Aoki R, Massuda M, Zenni LTV, Fernandes KS. Canalis sinuosus: anatomical variation or structure? Surg Radiol Anat. 2020 Jan;42(1):69-74. doi: 10.1007/s00276-019-02352-2. Epub 2019 Oct 12. PMID: 31606782.
17. Shelley A, Tinning J, Yates J, Horner K. Potential neurovascular damage as a result of dental implant placement in the anterior maxilla. Br Dent J. 2019

May;226(9):657-661. doi: 10.1038/s41415-019-0260-4. PMID: 31076691.
18. Torres MG, de Faro Valverde L, Vidal MT, Crusoé-Rebello IM. Branch of the canalis sinuosus: a rare anatomical variation--a case report. Surg Radiol Anat. 2015 Sep;37(7):879-81. doi: 10.1007/s00276-015-1432-9. Epub 2015 Jan 24. PMID: 25616849.
19. McCrea SJJ. Aberrations Causing Neurovascular Damage in the Anterior Maxilla during Dental Implant Placement. Case Rep Dent. 2017;2017:5969643. doi: 10.1155/2017/5969643. Epub 2017 Jul 13. PMID: 28785491; PMCID: PMC5530455.
20. Leven AJ, Sood B. Pathosis or Additional Maxillary Neurovascular Channel? A Case Report. J Endod. 2018 Jun;44(6):1048-1051. doi: 10.1016/j.joen.2018.02.025. Epub 2018 Apr 18. PMID: 29680725.

IJAE
ITALIAN JOURNAL OF ANATOMY AND EMBRYOLOGY

Firenze University Press
www.fupress.com/ijae

OPEN ACCESS

Citation: Rinaldi, F., Piattellli, M., Angiolani, F., Bernardi, S., Rastelli, E., & Varvara, G. (2023). Volumetric evaluation of maxillary sinuses using CBCTS: radiographic study. *Italian Journal of Anatomy and Embryology* 127(2): 47-50. doi: 10.36253/ijae-14681

Data Availability Statement: All relevant data are within the paper and its Supporting Information files.

Competing Interests: The Author(s) declare(s) no conflict of interest.

Volumetric evaluation of maxillary sinuses using CBCTS: radiographic study

Fabiola Rinaldi[1,*], Maurizio Piattellli[1], Francesca Angiolani[1], Sara Bernardi[2], Elena Rastelli[2], Giuseppe Varvara[1]

[1] *Department of Innovative Technologies in Medicine & Dentistry, University of Chieti-Pescara 'Gabriele d'Annunzio', Via dei Vestini 11, 66100 Chieti, Italy*
[2] *Department of Life, Health and Environmental Sciences, University of L'Aquila, 67100 L'Aquila, Italy*
*Corresponding author. E-mail: fabiola.rinaldi@unich.it

Abstract. The evaluation of maxillary sinus volumes is fundamental for pre-surgical planning in this area, as well as for the diagnosis of sinusitis and the diagnosis and treatment of maxillary hypoplasia. This study aimed to assess changes in sinus volume over time as a function of different conditions, such as sex, orthodontic treatments like rapid palate expansion, and the presence of edentulism. The Cone-Beam Computed Tomographies of eighteen patients were selected, and their entire sinus volumes were segmented, enabling the measurement of the sinus volume in three spatial dimensions. The collected data were statistically analyzed using the T-Student test and ANOVA. The mean size of the measured right sinus volume was 14.42 cm^3, and that of the left sinus was 14.17 cm^3. No statistically significant difference was identified between the right and left maxillary sinus volumes, even in correlation with the considered factors (p-value > 0.05). The values found in the present study agreed with those in the literature, confirming the importance of radiographic evaluation of this structure for diagnosis and treatment planning.

Keywords: maxillary sinus, maxillary antrum, Cone Beam Computed Tomography, innovation technology, health.

INTRODUCTION

The paranasal sinuses serve both skeletal and respiratory functions. They lighten the skull and provide a structure that can withstand facial trauma while conferring resonance to speech and warming inspired air (Amine et al., 2020). Therefore, it is crucial to study the anatomy and volumetric extension of the maxillary sinus for diagnosis, verification of response to chemo- and radiotherapy in malignant tumors, and surgical planning (Thariat et al., 2021). Surgical treatments requiring a study of the full volume of the maxillary sinuses include endoscopy sinus surgery and maxillary floor lift for graft and implant placements (Giovannetti et al., 2019; Raponi et al., 2021). The literature reports that breathing patterns, dental problems, anatomical features,

gender, and age influence the maxillary sinus volume (Iturralde-Garrote et al., 2023).

This study aimed to measure in vivo the volumetric dimensions of maxillary sinuses in a European population and see if there is any association between the morphometric data with gender, orthopaedic treatment on the palate (rapid palatal expansion), and presence of edentulism.

MATERIAL AND METHODS

Eighteen Cone Beam Computed Tomography (CBCT) scans were collected from patients requiring surgical treatment in maxillary sinuses. The CT scans had a reading area measuring 23.8 cm in width and 19.3 cm in height, a grayscale of 14 bit, voxel dimension of 0.4/0.3/0.25/0.2 mm, and a field of view of 16.5 cm x 17 cm. The DICOM files were segmented using the open-source software INVESALIUS vers. 3.1, highlighting the airspace of the maxillary antrum on the three direction (axial, sagittal and coronal) in each sections (Figure 1).

Finally, the 3D volume rendering of the maxillary sinus was obtained (Figure 2).

Statistical analysis of the obtained data was performed using SAS University edition software. T-Student and One Way ANOVA tests were performed in the statistical analysis, with statistical significance assumed at p-value < 0.05.

RESULTS

The mean value of the right side was higher than the left side. The mean and standard deviation of the measured volume of the right maxillary sinus resulted in 14.42 $\pm$ 4.73 cm^3, and that of the left maxillary sinus was 14.17$\pm$ 4.79 cm^3. The minimum and maximum values found for the right maxillary sinus were 6.44 and 29.3 cm^3, and for the left sinus were 6.32 and 27.53 cm^3. The difference assessed by the T-Student test between the right and left sinuses was not statistically significant (p-value> .05). From the association of the volumetric values of the right and left maxillary sinus with the established categories (Rapid Palatal Expansion, presence of edentulism, and presence of sinusitis), it was possible to see how the edentulism and the sinusitis decrease the volume of maxillary sinuses, both left and right. However, the patients who underwent palatal expansion had different results from the left and right maxillary sinus (Table 1).

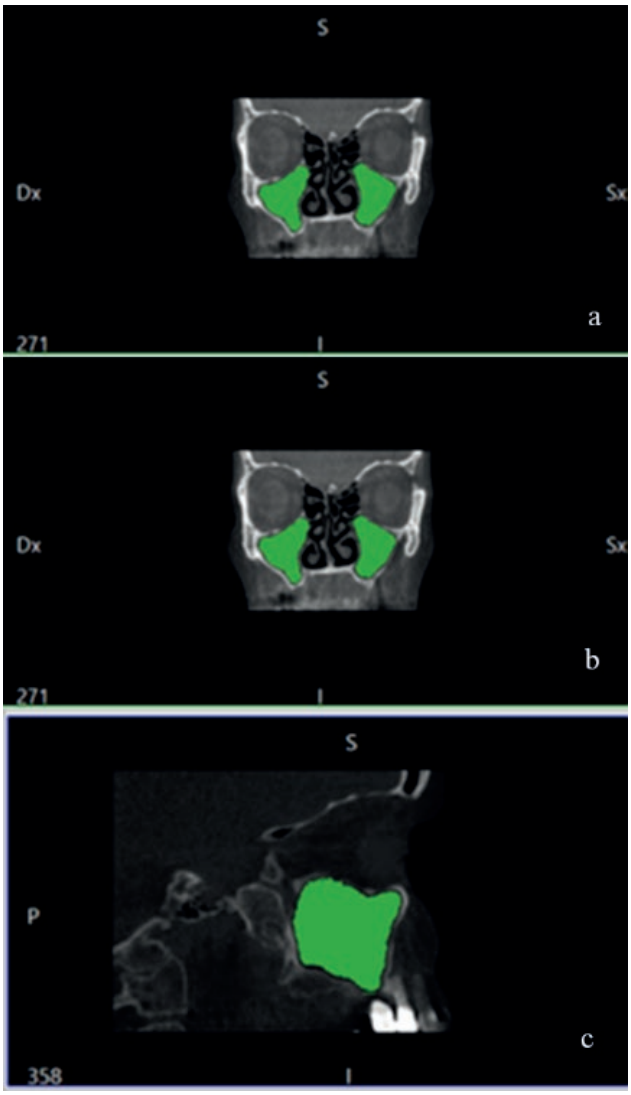

Figure 1. a. CBCT frontal section of the maxillary sinus; b. CBCT axial section of the maxillary sinus; CBCT sagittal section of the maxillary sinus.

DISCUSSION

The present study aimed to assess whether certain factors could influence the size of the right and left maxillary sinuses individually. The study referred to previous research that evaluated maxillary sinus size considering various factors. Emirzeoglu et al. (2007) evaluated 39 males and 38 females using computed tomography scans, which showed that the average size of the maxillary sinuses was 11.6 + 0.8 cm^3, smaller than the present study's findings. Pirner et al. (2009) conducted a study for pre-operative anatomical assessment in sinus surgery and found that the volume of the right maxillary sinus

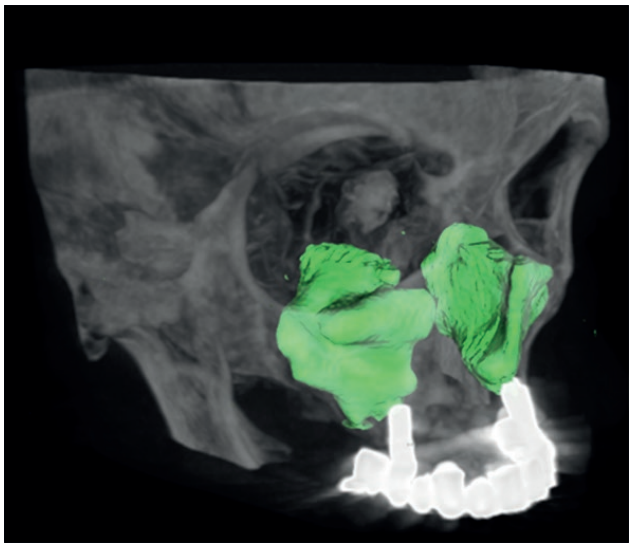

Figure 2. 3D rendering of the maxillary sinus segmentation's.

Table 1. One Way ANOVA statistical analysis of the association of right and left maxillary sinus volumetric values with the factors RPE (rapid palate expansion), presence of edentulism, and presence of sinusitis.

RIGHT MAXILLARY SINUS		ANOVA (P value)	LEFT MAXILLARY SINUS		ANOVA (P value)
Male	Female	>.05	Male	Female	>.05
14.038	14.597		14.281	14.125	
RPE YES	RPE NO	>.05	RPE YES	RPE NO	>.05
13.351	14.621		14.321	13.390	
EDENTULISM YES	EDENTULISM NO	>.05	EDENTULISM YES	EDENTULISM NO	>.05
13.694	18.295		13.564	17.424	
SINUSITIS YES	SINUSITIS NO	>.05	SINUSITIS YES	SINUSITIS NO	>.05
12.918	15.513		12.897	15.103	

was 17.4 cm^3, while the left was 17.9 cm^3, larger measurements than those reported in the present study. Urooge et al. (2017) reported a mean value of maxillary sinus volume of 16 cm^3, and Bangi et al. (2017) reported an average volume of 15.3 cm^3 in the right maxillary sinus and an average volume of 13 cm^3 in the left maxillary sinus, values that were in line with the present study's findings. Giacomini et al. (2018) experimented to determine the best method for measuring maxillary sinus volumes in a sample of 30 subjects, finding a mean value of 14.7 cm^3 between the right and left maxillary sinuses.

The literature has also investigated whether there is a dimensional variation of the maxillary sinus between oral and nasal breathing patients. Tikku et al. (2013) found that oral breathers had a smaller maxillary sinus volume than nasal breathers. Agacayak et al. (2017) analyzed 239 subjects, finding that the maxillary sinus of oral breathers was significantly smaller than that of nasal breathers. Additionally, studies have investigated the change in maxillary sinus volume following orthognathic surgery. Panou et al. (2013) evaluated 16 patients who underwent cone beams before and after surgical treatment for third classes, showing a significant reduction in the volume of the maxillary sinus. Okşayan et al. (2017) compared the volume of the maxillary sinuses in patients with high, low, or normal vertical size, finding a greater maxillary sinus size in the group with low vertical dimension compared to the group with high vertical dimension.

The present study found that the average volume of the maxillary sinuses was 14 cm^3 and emphasized the importance of studying maxillary sinus volumes for presurgical planning in the case of surgery in these areas and for the diagnosis and treatment of maxillary hypoplasia in oral respiratory patients.

CONCLUSION

The study of maxillary sinus volume is crucial because of its variability and essential in the diagnosis process of suspected sinusitis, to plan any endoscopic surgery in this area, to determine if the maxillary sinus lift is reliable and to quantify the amount of volume graft in case of alveolar bone regeneration surgery.

REFERENCES

Agacayak K.S., Gulsun B., Koparal M., Atalay Y., Aksoy O., Adiguzel O. (2015) Alterations in maxillary sinus volume among oral and nasal breathers. Med Sci Monit. 21:18-26

Amine K., Slaoui S., Kanice F.Z., Kissa J. (2020) Evaluation of maxillary sinus anatomical variations and lesions: A retrospective analysis using cone beam computed tomography. J Stomatol oral Maxillofac Surg 121:484–489.

Bangi B.B., Ginjupally U., Nadendla L.K., Vadla B. (2017) 3D Evaluation of Maxillary Sinus Using Computed Tomography: A Sexual Dimorphic Study. Int J Dent. 2017:9017078.

Emirzeoglu M., Sahin B., Bilgic S., Celebi M., Uzun A. (2007) Volumetric evaluation of the paranasal sinuses in normal subjects using computer tomography images: a stereological study. Auris Nasus Larynx. 34(2):191-5.

Giacomini G., Pavan A.L.M., Altemani J.M.C., Duarte S.B., Fortaleza C.M.C.B., Miranda J.R.A., de Pina D.R. (2018) Computed tomography-based volumetric

tool for standardized measurement of the maxillary sinus. PLoS One. 13(1):e0190770.

Giovannetti F., Raponi I., Priore P., Macciocchi A., Barbera G., Valentini V. (2019) Minimally-Invasive Endoscopic-Assisted Sinus Augmentation. J Craniofac Surg. 30:e359–e362.

Iturralde-Garrote A., Sanz J.L., Forner L., Melo M., Puig-Herreros C. (2023) Volumetric Changes of the Paranasal Sinuses with Age: A Systematic Review. J Clin Med. 12(10):3355.

Okşayan R., Sökücü O., Yeşildal S. (2017) Evaluation of maxillary sinus volume and dimensions in different vertical face growth patterns: a study of cone-beam computed tomography. Acta Odontol Scand. 75(5):345-349.

Panou E., Motro M., Ateş M., Acar A., Erverdi N. (2013) Dimensional changes of maxillary sinuses and pharyngeal airway in Class III patients undergoing bimaxillary orthognathic surgery. Angle Orthod. 83(5):824-31.

Pirner S., Tingelhoff K., Wagner I., Westphal R., Rilk M., Wahl F.M., Bootz F., Eichhorn K.W. (2009) CT-based manual segmentation and evaluation of paranasal sinuses. Eur Arch Otorhinolaryngol. 266(4):507-18.

Raponi I., Giovannetti F., Buracchi M., Priore P., Battisti A., Scagnet M., Genitori L., Valentini V. (2021) Management of orbital and brain complications of sinusitis: A practical algorithm. J cranio-maxillo-facial 49:1124–1129.

Thariat J., Carsuzaa F., Marcy P.Y., Verillaud B., Gabory L. de, Ferrand F.R. (2021) Precision Postoperative Radiotherapy in Sinonasal Carcinomas after Endonasal Endoscopic Surgery. Cancers (Basel). 13(19): 4802.

Tikku T., Khanna R., Sachan K., Srivastava K., Munjal N. (2013) Dimensional changes in maxillary sinus of mouth breathers. J Oral Biol Craniofac Res. 3(1):9-14.

Urooge A., Patil B.A. (2017) Sexual Dimorphism of Maxillary Sinus: A Morphometric Analysis using Cone Beam Computed Tomography. J Clin Diagn Res. 11(3): ZC67-ZC70.

IJAE
ITALIAN JOURNAL OF ANATOMY AND EMBRYOLOGY

Firenze University Press
www.fupress.com/ijae

OPEN ACCESS

Citation: Mazzone, M., Di Marcantonio, M.C., Mincione, G., & Muraro, R. (2023). First year of life: the *Golden Age* of gut microbiota. *Italian Journal of Anatomy and Embryology* 127(2): 51-56. doi: 10.36253/ijae-14682

Data Availability Statement: All relevant data are within the paper and its Supporting Information files.

Competing Interests: The Author(s) declare(s) no conflict of interest.

First year of life: the *Golden Age* of gut microbiota

Mariangela Mazzone*, Maria C. Di Marcantonio, Gabriella Mincione, Raffaella Muraro

Department of Innovative Technologies in Medicine & Dentistry, University "G. d'Annunzio" Chieti-Pescara, 66100, Chieti, Italy
*Corresponding author. E-mail: mariangela.mazzone@unich.it

Abstract. During the first year of life, development and balance of newborn gut microbiota are strongly influenced by external factors such as delivery mode, breastfeeding, duration of pregnancy, mother diet and lifestyle, siblings and pets, environment, and antibiotics administration. Gut microbiota colonization starts with facultative anaerobes and continues with the establishment of anaerobic genera of which *Bifidobacteria* are the *gold standard* of a healthy gut neonatal microbiota. Scientific literature traditionally describes the fetus as sterile in the womb and identifies the membranes rupture as the beginning of microbial colonization. Vaginal delivery is an important source for the onset of infant colonization which will then continue with the transfer of a new selection of intestinal bacteria with breastfeeding. During cesarean delivery a direct contact of the mouth of newborn with the vaginal and intestinal microbiota is absent, and environmental bacteria play an important role for infants intestinal colonization. Nature has ensured that newborns receive other specific maternal bacteria, through a subsequent method of transfer: breastfeeding. We present a brief and comprehensive state-of-the-art in order to encourage natural childbirth and breastfeeding whenever possible and discuss innovative directions for develop new *ad hoc* personalized treatments in order to restore physiological microbiota.

Keywords: gut microbiota, newborn microbiota, bifidobacteria, breastfeeding, vaginal delivery, cesarean delivery.

INTRODUCTION

The intestinal microbiota is essential for the development and maturation of the immune, metabolic, and cognitive systems. According to current knowledge, it is crucial to ensure its balance in the first year of life in order to guarantee a well-being even in adulthood. In full-term infants, natural delivery and breastfeeding represent the most important drivers for the early composition of the intestinal microbiota, but the overall composition of neonatal gut microbiota is influenced by additional factors such as mother's diet and lifestyle, siblings, pets, environment, and antibiotics administration (Yasmin F. et al., 2017; Stewart C.J. et al., 2018) (Figure 1).

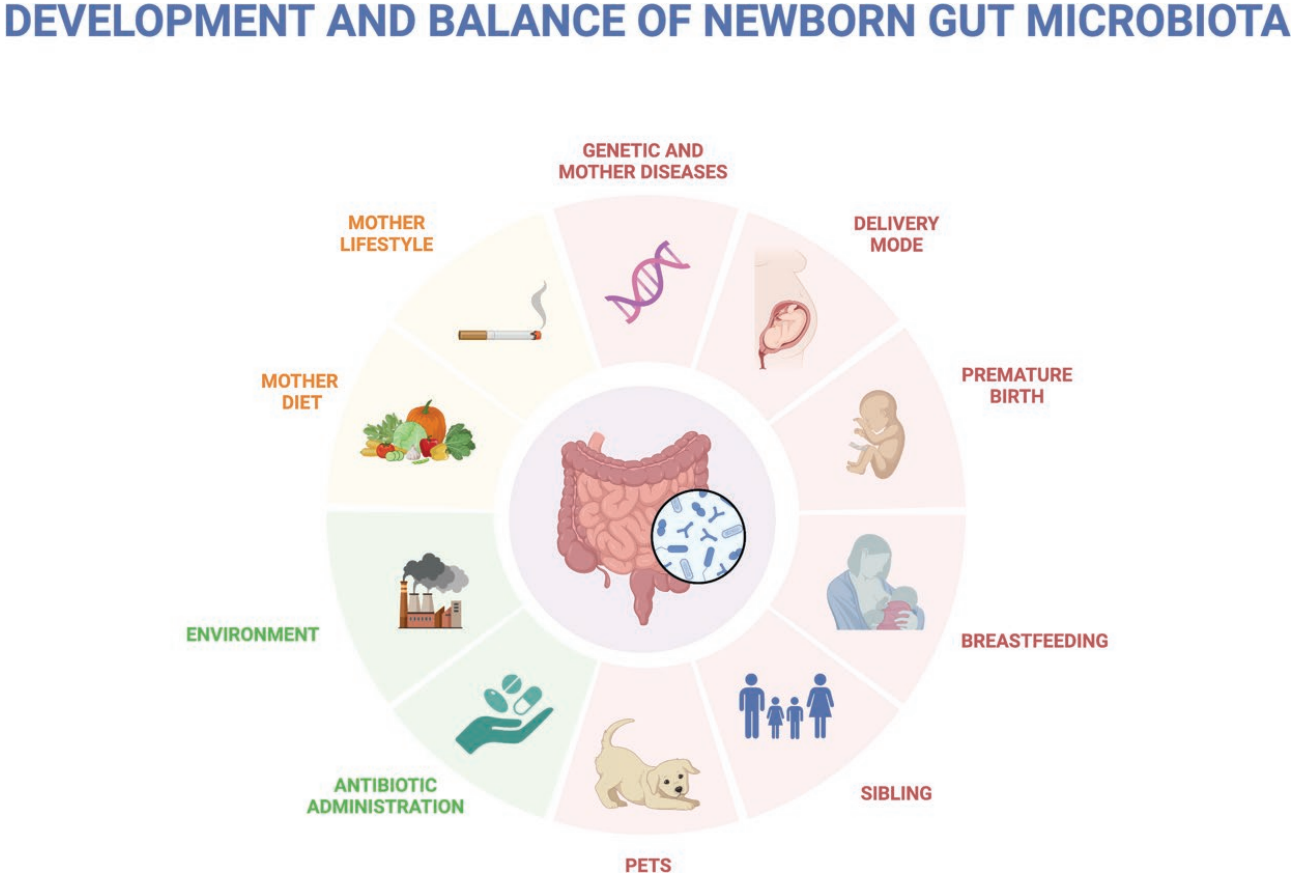

Figure 1. Determinants of development and balance of newborn gut microbiota. Created with BioRender.com.

Natural birth provides a greater bacterial richness and variety with a clear overlap with the maternal microbial profile. An interesting systematic analysis showed significant domain of *Bifidobacterium* and *Bacteroides* in naturally delivered compared with cesarean section delivered newborn, colonized by *Clostridium* and *Lactobacillus* (Rutayisire E. et al., 2016). *Bifidobacteria* are also transmitted to infants with breastfeeding. Thus, children born by cesarean section and/or not breastfed, commonly develop a bifidobacterial dysbiosis. Tojo R. et al. showed that neonatal bifidobacterial dysbiosis, as well as in adulthood, correlates and increases the risk of atopy, allergy, irritable bowel syndrome, inflammatory bowel disease, celiac disease, and obesity (Tojo R. et al., 2014).

An "upstream" hypothesis suggests that fetus already encounters initial microbial colonization at intrauterine level (Collado M.C. et al., 2016).

What's new? Interesting novel studies highlight how the evolution has been able to ensure the microbes transfer from mother to child. Vatanen T. et al. discovered that maternal gut microbioma influence the infant microbioma through mobile genetic elements from the late pregnancy (Vatanen T. et al., 2022). Bogaert T. et al. suggest the presence of auxiliary routes of mother-to-infant microbial seeding (Bogaert T. et al., 2023).

NATURAL DELIVERY: THE *GOLDEN WAY*

Over the last twenty years, elective or emergency cesarean delivery (CD) increased worldwide (Arboleya S. et al., 2018). This delivery mode, undoubtedly mandatory in most cases, led to alterations of newborn intestinal microbial profile, lacking the classical vaginal microbiota transmission route. In addition, antibiotic prophylaxis, following CD, directly impacts, on the newborn intestinal microbiota.

In physiological conditions, in pregnant women intestinal microbiota undergoes a process of bacterial inflammatory drift resulting in an increase of *Proteobacteria* and a decrease of butyrate-producing species, in order to increase the supply an adequate maternal fat reserve for breastfeeding.

Infant intestinal microbiota composition is mostly derived from different maternal body districts: intestine (22.1%), vagina (16.3%), oral cavity (7.2%), and skin (5%) (Cardelli E. et al., 2021). Vaginal delivery (VD), as compared to CD, confers different and more stable microbial colonization, containing mainly *Lactobacilli*, *Prevotella* and *Bifidobacteria*. Childs from CD, on the contrary, acquire a microbiota similar to the skin microbiota, with a greater expression of *Clostridium*, *Staphylococcus* and *Enterococcus* (Figure 2). This results in a delayed colonization of *Lactobacilli*, *Bifidobacterium* and *Bacteroides* and a consequent reduction of Th1 lymphocytes or *Bacteroides*-dependent cytokines during the first two years of life (Jakobsson H.E. et al., 2014).

In the vaginal area, *Lactobacilli* produce lactic acid from glucose derived by glycogen catabolism, an essential function for the pH maintenance of pH to avoid infections; furthermore, through the α-galactosidase, are able to catabolize milk lactose. *Lactobacilli* also stimulate pulmonary growth and alveolarization process in the lungs of newborns and exert a protective effect, probably due to their anti-inflammatory and immunostimulatory properties, with a reduced incidence of inflammatory airways diseases (Stokholm J. et al., 2020; Cardelli E. et al., 2021). In addition, during VD, contractions and oxygen hypoxia promote the development of stress hormones such as catecholamine and cortisol. Cortisol increase at birth is a predictor of hypothalamic-pituitary-adrenal axis activation of the immune system, lung, and organ maturation and neurogenesis. In contrast, in CD the use of synthetic oxytocin, antibiotics correlates with higher global DNA methylation in cord blood derived leukocytes, which could be involved in T-helper type 1 and 2 T-helper cells imbalance, leading to an increased risk of immune diseases (Cho C.E. and Norman M., 2013).

HUMAN MILK: THE *WHITE GOLD*

Differences in gut microbial composition between breast-fed and formula-fed infants are well-established. Mammary glands are colonized by fecal bacteria through the entero-mammary circulation and thus release "contaminated milk". Indeed, maternal intestine, mammary gland and milk show the same strains that are then traced in newborn intestine. Specifically, breastfeeding has been associated with the presence of *Bifidobacterium* and *Lactobacillus* present in breast milk and *Staphylococcus* present on the skin surrounding the nipple (Stewart C.J. et al., 2018) (Figure 2).

Since the maternal microbiota shapes the antibody "repertoire" of breast milk, breastfeeding contributes to the transfer of immune memory from the mother to the child. Once infants begin weaning, the protective effects of milk disappear (Ganal-Vonarburg S.C. et al., 2020).

Exclusive breast-fed newborns present an eubiosis characterized by a lower biodiversity, primary focused on *Bifidobacteria*, by a slower microbiota maturation and progressive diversification until weaning. On the contrary, formula-fed newborn are exposed to different substances that promote different patterns of intestinal microbial colonization and resulting in an anticipated divergence towards the typical adult composition (Figure 2). Both formula-fed and mixed-fed infants microbiota are characterized by an anticipated decrease in *Bifidobacteria*, with a consequent immune immaturity that has both immediate and delayed effects.

A study by Stewart C.J. et al. showed a clear increase of *Bifidobacteria* in early stages of life associated with breastfeeding, while its interruption leads to an anticipated decrease of *Bifidobacteria* and therefore to immune immaturity (Stewart C.J. et al., 2018). To note, *Bifidobacteria* are capable to metabolize Human Milk Oligosaccharides (HMO), and to produce aromatic lactic acids, bacterial post-biotic metabolites able to strengthen the intestinal barrier, protect against infection, influence the host's metabolism, and modulate immune function (Laursen M.F. et al., 2021).

It is important to emphasize that milk microbiome is far from stable: a maternal wrong diet can decrease the benefits and/or cause newborn dysbiosis resulting in gastrointestinal and metabolic disorders. For example, varying the glycemic index or the energy source influences the composition of the HMO and, consequently, the bacterial strains involved in their metabolism. Therefore, it is crucial to consider the dynamics and possible factors influencing milk microbiome, in order to safeguard the newborn health (Seferovic M.D. et al., 2020).

In summary, breast milk can act as a dynamic "incubator" that enriches, protects, and transports specific bacteria in the newborn intestinal tract. Exclusivity, duration, and modality (directly or using breast pump) of breastfeeding shape infants gut microbiota and its overall composition (Moossavi S. et al., 2019; Fehr K. et al., 2020).

CONCLUSION

Pregnant women should be properly informed by medical staff about the actual consequences of VD or

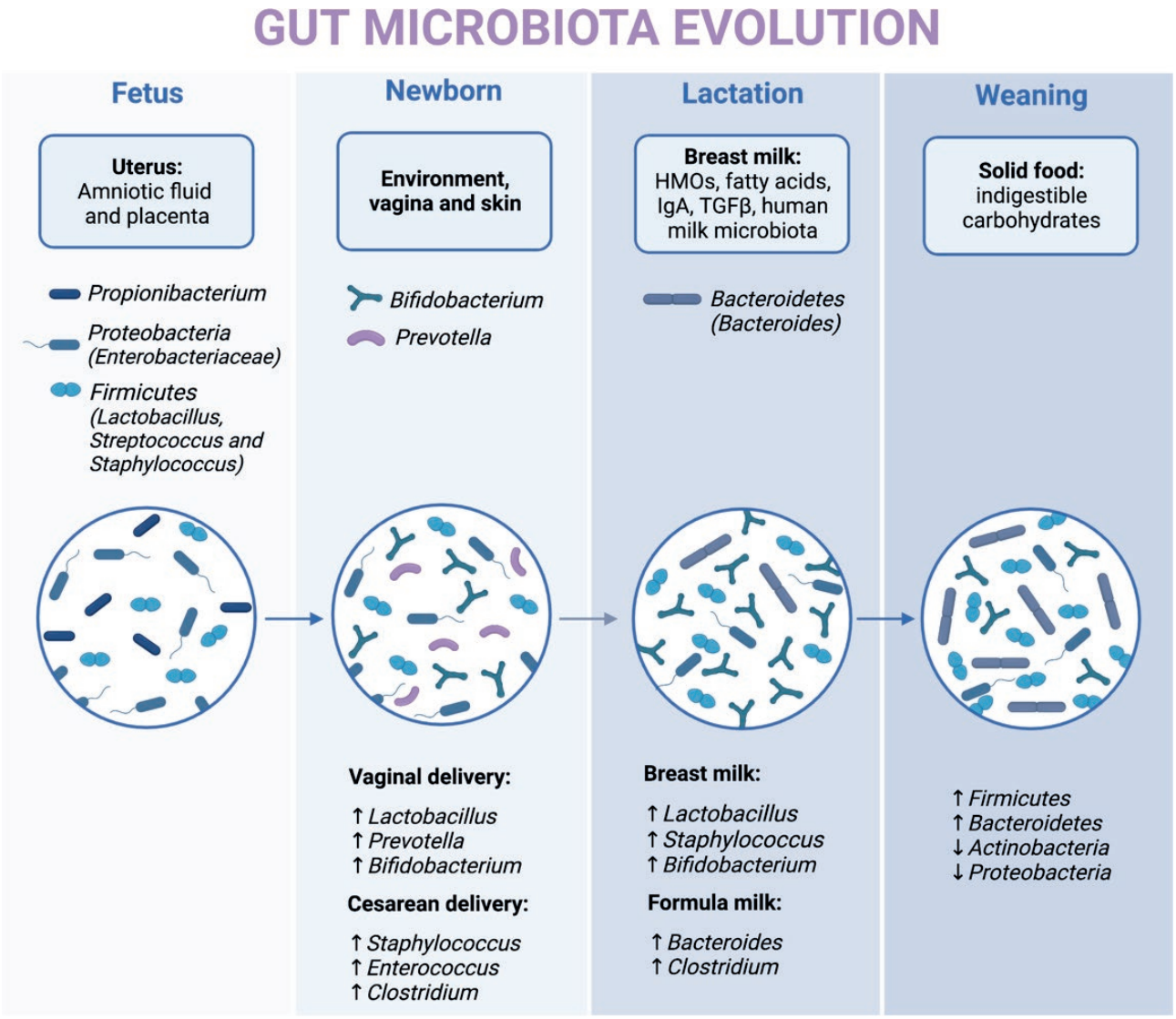

Figure 2. Development of gut microbiota in human infant. Diversity of gut microbiota increases with age. Arrow represents an increase/decrease. Created with BioRender.com.

CD delivery modes on child health, limiting CD to peculiar conditions.

Breastfeeding becomes even more important after CD, since newborn do not inherit maternal vaginal and intestinal microbiota.

Currently, it is possible genetically identify bacterial microbiota in maternal feces and breast milk and transfer specific selected strains to newborn to help developing a physiological microbiota.

It will be crucial to determine the best way to transfer mother microbiota to her caesarean-born children, through vaginal seeding or fecal microbiota transplantation, as well as to develop a universal cocktail of bacteria to reproduce the healthy microbiota (Mueller N.T. et al., 2019; Korpela K. et al., 2020).

REFERENCES

1. Arboleya S., Suárez M., Fernández N., Mantecón L., Solís G., Gueimonde M., de Los Reyes-Gavilán C.G. (2018) C-section and the Neonatal Gut Microbiome Acquisition: Consequences for Future Health. Ann Nutr Metab. 73 Suppl 3:17-23.
2. Bogaert D, van Beveren GJ, de Koff EM, Lusarreta Parga P, Balcazar Lopez CE, Koppensteiner L, Clerc

M, Hasrat R, Arp K, Chu MLJN, de Groot PCM, Sanders EAM, van Houten MA, de Steenhuijsen Piters WAA. Mother-to-infant microbiota transmission and infant microbiota development across multiple body sites. Cell Host Microbe. 2023 Mar 8;31(3):447-460.e6.
3. Cardelli E., Calvigioni M., Vecchione A., Macera L., Mazzantini D., Celandroni F., Panattoni A., Pistello M., Maggi F., Ghelardi E., Mannella P. (2021) Delivery Mode Shapes the Composition of the Lower Airways Microbiota in Newborns. Front Cell Infect Microbiol. 23;11:808390.
4. Cho C.E., Norman M. (2013) Cesarean section and development of the immune system in the offspring. Am J Obstet Gynecol. 208(4):249-54.
5. Collado M.C., Rautava S., Aakko J., Isolauri E., Salminen S. (2016) Human gut colonisation may be initiated in utero by distinct microbial communities in the placenta and amniotic fluid. Sci Rep. 22;6:23129.
6. Fehr K., Moossavi S., Sbihi H., Boutin R.C.T., Bode L., Robertson B., Yonemitsu C., Field C.J., Becker A.B., Mandhane P.J., Sears M.R., Khafipour E., Moraes T.J., Subbarao P., Finlay B.B., Turvey S.E., Azad M.B. (2020) Breastmilk Feeding Practices Are Associated with the Co-Occurrence of Bacteria in Mothers' Milk and the Infant Gut: the CHILD Cohort Study. Cell Host Microbe. 28(2):285-297.e4.
7. Ganal-Vonarburg S.C., Hornef M.W., Macpherson A.J. (2020) Microbial-host molecular exchange and its functional consequences in early mammalian life. Science. 368(6491):604-607.
8. Jakobsson H.E., Abrahamsson T.R., Jenmalm M.C., Harris K., Quince C., Jernberg C., Björkstén B., Engstrand L., Andersson A.F. (2014) Decreased gut microbiota diversity, delayed Bacteroidetes colonisation and reduced Th1 responses in infants delivered by caesarean section. Gut. 63(4):559-66.
9. Korpela K., Helve O., Kolho K.L., Saisto T., Skogberg K., Dikareva E., Stefanovic V., Salonen A., Andersson S., de Vos W.M. (2020) Maternal Fecal Microbiota Transplantation in Cesarean-Born Infants Rapidly Restores Normal Gut Microbial Development: A Proof-of-Concept Study. Cell. 183(2):324-334.e5.
10. Laursen M.F., Sakanaka M., von Burg N., Mörbe U., Andersen D., Moll J.M., Pekmez C.T., Rivollier A., Michaelsen K.F., Mølgaard C., Lind M.V., Dragsted L.O., Katayama T., Frandsen H.L., Vinggaard A.M., Bahl M.I., Brix S., Agace W., Licht T.R., Roager H.M. (2021) Bifidobacterium species associated with breastfeeding produce aromatic lactic acids in the infant gut. Nat Microbiol. 6(11):1367-1382.
11. Moossavi S., Sepehri S., Robertson B., Bode L., Goruk S., Field C.J., Lix L.M., de Souza R.J., Becker A.B., Mandhane P.J., Turvey S.E., Subbarao P., Moraes T.J., Lefebvre D.L., Sears M.R., Khafipour E., Azad M.B. (2019) Composition and Variation of the Human Milk Microbiota Are Influenced by Maternal and Early-Life Factors. Cell Host Microbe. 25(2):324-335.e4.
12. Mueller N.T., Hourigan S.K., Hoffmann D.E., Levy L., von Rosenvinge E.C., Chou B., Dominguez-Bello M.G. (2019) Bacterial Baptism: Scientific, Medical, and Regulatory Issues Raised by Vaginal Seeding of C-Section-Born Babies. J Law Med Ethics. 47(4):568-578.
13. Rutayisire E., Huang K., Liu Y., Tao F. (2016) The mode of delivery affects the diversity and colonization pattern of the gut microbiota during the first year of infants' life: a systematic review. BMC Gastroenterol. 16(1):86.
14. Seferovic M.D., Mohammad M., Pace R.M., Engevik M., Versalovic J., Bode L., Haymond M., Aagaard K.M. (2020) Maternal diet alters human milk oligosaccharide composition with implications for the milk metagenome. Sci Rep. 10(1):22092.
15. Stewart C.J., Ajami N.J., O'Brien J.L., Hutchinson D.S., Smith D.P., Wong M.C., Ross M.C., Lloyd R.E., Doddapaneni H., Metcalf G.A., Muzny D., Gibbs R.A., Vatanen T., Huttenhower C., Xavier R.J., Rewers M., Hagopian W., Toppari J., Ziegler A.G., She J.X., Akolkar B., Lernmark A., Hyoty H., Vehik K., Krischer J.P., Petrosino J.F. (2018) Temporal development of the gut microbiome in early childhood from the TEDDY study. Nature. 562(7728):583-588.
16. Stokholm J., Thorsen J., Blaser J., Rasmussen M.A., Hjelmsø M., Shah S., Christensen E.D., Chawes B.L., Bønnelykke K., Brix S., Mortensen M.S., Brejnrod A., Vestergaard G., Trivedi U., Sørensen S.J., Bisgaard H. (2020) Delivery mode and gut microbial changes correlate with an increased risk of childhood asthma. Sci Transl Med. 12(569):eaax9929.
17. Tojo R., Suárez A., Clemente M.G., de los Reyes-Gavilán C.G., Margolles A., Gueimonde M., Ruas-Madiedo P. (2014) Intestinal microbiota in health and disease: role of bifidobacteria in gut homeostasis. World J Gastroenterol. 20(41):15163-76.
18. Vatanen T., Jabbar K.S., Ruohtula T., Honkanen J., Avila-Pacheco J., Siljander H., Stražar M., Oikarinen S., Hyöty H., Ilonen J., Mitchell C.M., Yassour M., Virtanen S.M., Clish C.B., Plichta R., Vlamakis H., Knip M., Xavier R.J. (2022) Mobile genetic elements from the maternal microbiome shape infant gut microbial assembly and metabolism. Cell. 185(26):4921-4936.e15.
19. Yasmin F., Tun H.M., Konya T.B., Guttman D.S., Chari R.S., Field C.J., Becker A.B., Mandhane P.J.,

Turvey S.E., Subbarao P., Sears M.R.; CHILD Study Investigators; Scott J.A., Dinu I., Kozyrskyj A.L. (2017) Cesarean Section, Formula Feeding, and Infant Antibiotic Exposure: Separate and Combined Impacts on Gut Microbial Changes in Later Infancy. Front Pediatr. 5:200.

IJAE
ITALIAN JOURNAL OF ANATOMY AND EMBRYOLOGY

Firenze University Press
www.fupress.com/ijae

OPEN ACCESS

Citation: Marinacci, B., Pellegrini, B., & Roos, S. (2023). A mini-review: valuable allies for human health: probiotic strains of *Limosilactobacillus reuteri*. *Italian Journal of Anatomy and Embryology* 127(2): 57-60. doi: 10.36253/ijae-14684

Data Availability Statement: All relevant data are within the paper and its Supporting Information files.

Competing Interests: The Author(s) declare(s) no conflict of interest.

A mini-review: valuable allies for human health: probiotic strains of *Limosilactobacillus reuteri*

Beatrice Marinacci[1,2,*], Benedetta Pellegrini[1], Stefan Roos[3,4]

[1] *Department of Pharmacy, "G. d'Annunzio" University of Chieti-Pescara, Chieti, Italy*
[2] *Department of Innovative Technologies in Medicine & Dentistry, "G. d'Annunzio" University of Chieti-Pescara, Chieti, Italy*
[3] *Department of Molecular Sciences, Swedish University of Agricultural Sciences, Uppsala, Sweden*
[4] *BioGaia AB, Stockholm, Sweden*
*Corresponding author. E-mail: beatrice.marinacci@unich.it

Abstract. The World Health Organization defines probiotics as "live microorganisms which, when administered in adequate amounts, confer a health benefit on the host". One of the most well studied probiotics is *Limosilactobacillus reuteri*, a Gram-positive, rod-shaped bacterium that colonizes the mucosal surfaces of mammals and birds and is considered autochthonous to the human microbiome. Genetic analyses have confirmed that this microorganism has co-evolved with its host, a prerequisite for the development of a mutualistic relation. On the one hand, *L. reuteri* contributes to the health of the host by releasing antimicrobial compounds, such as reuterin, and numerous active metabolites that can cross the epithelial barrier and reach different targets. Secondly, it can directly prevent the mucosal colonization by pathogenic bacteria helping in the prevention and restoration of dysbiosis due to the capability of forming biofilm. The characterization of numerous effector molecules produced by *L. reuteri* has provided a broad understanding of the mechanisms by which it not only displays antimicrobial and immunomodulatory activities within the gastrointestinal tract but can also influence the correct balance of distal locations of the body. This mini-review carries out a brief overview relating to the most well-known properties of *L. reuteri* highlighting the main biological processes involved.

Keywords: *Limosilactobacillus reuteri*, probiotic, postbiotic, immunomodulation.

INTRODUCTION

Named after Gerhard Reuter, the German microbiologist who conducted pioneering studies on the subject, *Lactobacillus reuteri* has recently been reclassified as *Limosilactobacillus reuteri* (Zheng et al., 2020). This Gram-positive bacterium is currently one of the widely-used probiotics, in which an increased number of studies support its ability to elicit health benefits to the host (Mu et al., 2018). As confirmed by Oh et al., *L. reuteri* colonizes the Gastrointestinal Tract (GIT) of different vertebrates and can be considered autochthonous to the human gut. Their phylogenetic analysis speculates the

fact that, between this microorganism and the host, there is a symbiotic relationship developed from a long-term evolutionary process (Oh et al., 2009; Walter et al., 2011).

As a member of the gut microbiota, *L. reuteri* strains are involved in a complex interplay within the host and can exert different antimicrobial, immunostimulatory and anti-inflammatory activities (Abuqwider et al., 2022). In addition to lactic acid and different low-molecular mass compounds, *L. reuteri* produces a small aldehyde, known as reuterin, which is effective in inhibiting numerous bacterial pathogens (Castellani et al., 2021). At the same time, *L. reuteri* produces biofilm that provides a successful colonization of host-tissues, thus limiting the adhesion of pathogens (Grande et al., 2017). The purpose of this mini-review is to provide an overview of the most well-known properties of *L. reuteri* describing its potential role in health and disease.

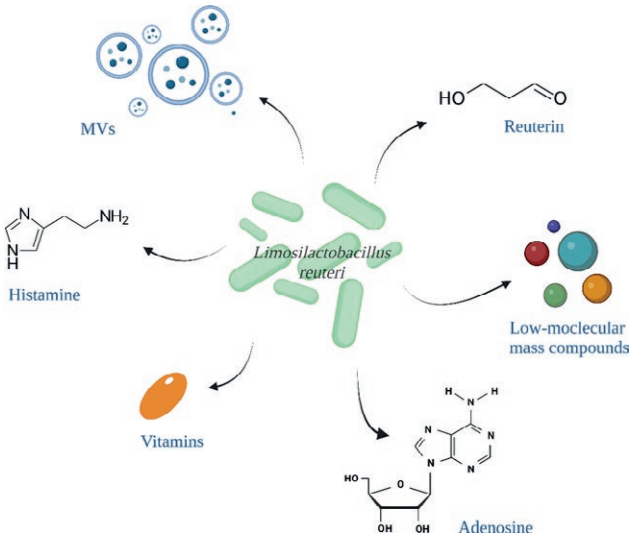

Figure 1. Graphical summary of *Limosilactobacillus reuteri* bioactive compounds. Created with BioRender.com.

L. REUTERI BIOACTIVE COMPOUNDS

According to the definition provided by the International Scientific Association of Probiotics and Prebiotics, the term "postbiotics" defines a "preparation of inanimate microorganisms and/or their components that confers a health benefit on the host" (Salminen et al., 2021). In line with this definition, several metabolites produced by *L. reuteri* can be mentioned for their bioactivities and they could be part of preparations with postbiotic properties (Figure 1).

Reuterin is a water-soluble mixture of different forms of 3-hydroxypropionaldehyde synthesized only in the presence of glycerol. It shows antimicrobial activity against Gram-positive and Gram-negative bacteria maintaining this effect in a wide range of pH (Cleusix et al., 2007). Then, Thomas and colleagues characterized the function of *L. reuteri* 6475-derived histamine. This compound is the result of the L-histidine metabolism and exerts anti-inflammatory activity via tumor necrosis factor suppression (Thomas et al., 2012). Similarly, several authors reported that *L. reuteri* can produce adenosine which can also reduce inflammation by interacting with T-cell receptors (Pang et al., 2022; Liu et al., 2023). Moreover, some strains, such as *L. reuteri* CRL1098 and *L. reuteri* JCM1112, can produce vitamins including vitamin B12 and vitamin B9 (Mu et al., 2018).

However, it is reasonable to assume that all the health promoting properties could be related to a synergy between the compounds released by this bacterium. For instance, Maccelli et al. found that the Cell Free Supernatant (CFS) of *L. reuteri* DSM 17938 displayed antimicrobial and antibiofilm activities versus different pathogens, although it was almost impossible to attribute these functions to a single compound. In fact, the metabolomic analysis revealed the complexity of the CFS composition making its characterization a challenging issue (Maccelli et al., 2020; Vitale et al., 2023). Furthermore, these studies focused on *L. reuteri*-derived Membrane Vesicles (MVs) which can be produced in the planktonic and biofilm phenotypes. As reviewed by Krzyżek et al., the MVs secreted by *L. reuteri*, as well as other probiotics strains, are likely one of the effectors of the probiotic activity in maintaining physiological homeostasis and ameliorate disease conditions (Krzyżek et al., 2023).

HEALTH PROMOTING PROPERTIES OF *L. REUTERI*

It is widely known that a balanced gut microbiota promotes the health of the host and that probiotics play a key role in maintaining tissue homeostasis. Given their resistance to low pH and bile salts, multiple *L. reuteri* strains have the potential to colonize the GIT; the adherence to epithelial cells is guaranteed by the expression of mucus-binding proteins and the production of exopolysaccharides which result in the biofilm formation (Mu et al., 2018). *L. reuteri* competes for nutrients and space with other microorganisms, thus limiting their growth. As mentioned above, it can release antimicrobial compounds that directly kill pathogens. This probiotic is also known for enhancing the function of the intestinal epi-

thelial barrier by reversing altered transepithelial electrical resistance and increasing the expression of tight junction proteins (Gao et al., 2022). It is interesting to note that in 2022 Lee and colleagues demonstrated that *L. reuteri* DS0384 accelerated the maturation of fetal intestine in stem cell-derived models as well as *in vivo* models. The results obtained using different strains gave way to the conclusion that the effect is strain-dependent rather than species-dependent (Lee et al., 2022).

The colonization of the GIT mucosa and the immunomodulatory properties attribute *L. reuteri* as having key function that may be effective for the management of inflammatory bowel disease. Numerous studies reported that the treatment with *L. reuteri* decreased the levels of pro-inflammatory markers, in both *in vitro* and *in vivo* models, by regulating Treg and dendritic cells (Abuqwider et al., 2022). At the same time, Liu and colleagues demonstrated that four *L. reuteri* strains can differentially modulate the release of cytokines and chemokines from cultured intestinal cells and rat intestine resulting in both immunosuppression and immunostimulation (Liu et al., 2010).

As extensively studied, the cross-talk between probiotics and immune system does not only impact the gastrointestinal tissue, but correlates with the homeostasis of different areas of the body. Fang et al. documented the efficacy of *L. reuteri* treatment in alleviating atopic dermatitis in mice (Fang et al., 2022), while, in 2023 Lu et al. investigated whether maternal *L. reuteri* supplementation could restore detrimental neurological alterations in offspring. Given that maternal inflammatory states can induce Blood-Brain Barrier (BBB) dysfunction and neurodevelopment deficits in children, they employed rodent models of maternal immune activation and demonstrated that *L. reuteri* treatment during lactation rescued the BBB deficits in offspring improving their spatial learning later in life. Even though the detailed mechanisms are still unknown, it is plausible that these effects are mediated by metabolites and neurotransmitters systemically released by *L. reuteri* (Lu et al., 2023). Thus, as documented for other probiotics, *L. reuteri* participates in the balance of the gut-brain axis (Abuqwider et al., 2022).

CONCLUSION

The existing body of literature concerning *L. reuteri* allowed its characterization in terms of sites of colonization, capability of forming biofilm and release of bioactive compounds. Therefore, all these findings highlighted the numerous health promoting properties related to this probiotic. This mini-review summarizes some of the most well studied *L. reuteri* strains that are involved in health and disease conditions and widely described are some of the mechanisms related to their properties. In conclusion, studies in this area of research are constantly evolving with the purpose of continuous learning relating to this probiotic.

REFERENCES

Abuqwider, J., Altamimi, M., and Mauriello, G. (2022). *Limosilactobacillus reuteri* in Health and Disease. *Microorganisms* 10, 522. doi: 10.3390/MICROORGANISMS10030522.

Castellani, C., Obermüller, B., Kienesberger, B., Singer, G., Peterbauer, C., Grabherr, R., et al. (2021). Production, Storage Stability, and Susceptibility Testing of Reuterin and Its Impact on the Murine Fecal Microbiome and Volatile Organic Compound Profile. *Front. Microbiol.* 12, 699858. doi: 10.3389/FMICB.2021.699858/BIBTEX.

Cleusix, V., Lacroix, C., Vollenweider, S., Duboux, M., and Le Blay, G. (2007). Inhibitory activity spectrum of reuterin produced by *Lactobacillus reuteri* against intestinal bacteria. *BMC Microbiol.* 7, 1–9. doi: 10.1186/1471-2180-7-101/TABLES/2.

Fang, Z., Pan, T., Wang, H., Zhu, J., Zhang, H., Zhao, J., et al. (2022). *Limosilactobacillus reuteri* Attenuates Atopic Dermatitis via Changes in Gut Bacteria and Indole Derivatives from Tryptophan Metabolism. *Int. J. Mol. Sci.* 23, 7735. doi: 10.3390/IJMS23147735/S1.

Gao, J., Cao, S., Xiao, H., Hu, S., Yao, K., Huang, K., et al. (2022). *Lactobacillus reuteri* 1 Enhances Intestinal Epithelial Barrier Function and Alleviates the Inflammatory Response Induced by Enterotoxigenic *Escherichia coli* K88 via Suppressing the MLCK Signaling Pathway in IPEC-J2 Cells. *Front. Immunol.* 13. doi: 10.3389/FIMMU.2022.897395/PDF.

Grande, R., Celia, C., Mincione, G., Stringaro, A., Di Marzio, L., Colone, M., et al. (2017). Detection and physicochemical characterization of membrane vesicles (MVs) of *Lactobacillus reuteri* DSM 17938. *Front. Microbiol.* 8, 1040. doi: 10.3389/FMICB.2017.01040/BIBTEX.

Krzyżek, P., Marinacci, B., Vitale, I., and Grande, R. (2023). Extracellular vesicles of probiotics: shedding light on the biological activity and future applications. *Pharmaceutics* 15, 522. doi: 10.3390/PHARMACEUTICS15020522/S1.

Lee, H., Jung, K. B., Kwon, O., Son, Y. S., Choi, E., Yu, W. D., et al. (2022). *Limosilactobacillus reu-*

teri DS0384 promotes intestinal epithelial maturation via the postbiotic effect in human intestinal organoids and infant mice. *Gut Microbes* 14. doi: 10.1080/19490976.2022.2121580.

Liu, Y., Armbrister, S. A., Okeugo, B., Mills, T. W., Daniel, R. C., Oh, J.-H., et al. (2023). Probiotic-derived ecto-5'-nucleotidase produces anti-inflammatory adenosine metabolites in Treg-deficient scurfy mice. *Res. Sq.* doi: 10.21203/RS.3.RS-2781715/V1.

Liu, Y., Fatheree, N. Y., Mangalat, N., and Rhoads, J. M. (2010). Human-derived probiotic *Lactobacillus reuteri* strains differentially reduce intestinal inflammation. *Am. J. Physiol. Gastrointest. Liver Physiol.* 299. doi: 10.1152/AJPGI.00124.2010.

Lu, J., Fan, X., Lu, L., Yu, Y., Markiewicz, E., Little, J. C., et al. (2023). *Limosilactobacillus reuteri* normalizes blood-brain barrier dysfunction and neurodevelopment deficits associated with prenatal exposure to lipopolysaccharide. *Gut Microbes* 15. doi: 10.1080/19490976.2023.2178800.

Maccelli, A., Carradori, S., Puca, V., Sisto, F., Lanuti, P., Crestoni, M. E., et al. (2020). Correlation between the antimicrobial activity and metabolic profiles of cell free supernatants and membrane vesicles produced by *Lactobacillus reuteri* DSM 17938. *Microorganisms* 8, 1653. doi: 10.3390/MICROORGANISMS8111653.

Mu, Q., Tavella, V. J., and Luo, X. M. (2018). Role of *Lactobacillus reuteri* in human health and diseases. *Front. Microbiol.* 9, 315828. doi: 10.3389/FMICB.2018.00757/BIBTEX.

Oh, P. L., Benson, A. K., Peterson, D. A., Patil, P. B., Moriyama, E. N., Roos, S., et al. (2009). Diversification of the gut symbiont *Lactobacillus reuteri* as a result of host-driven evolution. *ISME J.* 4, 377–387. doi: 10.1038/ismej.2009.123.

Pang, Y., Ermann Lundberg, L., Mata Forsberg, M., Ahl, D., Bysell, H., Pallin, A., et al. (2022). Extracellular membrane vesicles from *Limosilactobacillus reuteri* strengthen the intestinal epithelial integrity, modulate cytokine responses and antagonize activation of TRPV1. *Front. Microbiol.* 13. doi: 10.3389/FMICB.2022.1032202.

Salminen, S., Collado, M. C., Endo, A., Hill, C., Lebeer, S., Quigley, E. M. M., et al. (2021). The International Scientific Association of Probiotics and Prebiotics (ISAPP) consensus statement on the definition and scope of postbiotics. *Nat. Rev. Gastroenterol. Hepatol.* 18, 649–667. doi: 10.1038/s41575-021-00440-6.

Thomas, C. M., Hong, T., van Pijkeren, J. P., Hemarajata, P., Trinh, D. V., Hu, W., et al. (2012). Histamine Derived from Probiotic *Lactobacillus reuteri* Suppresses TNF via Modulation of PKA and ERK Signaling. *PLoS One* 7, e31951. doi: 10.1371/JOURNAL.PONE.0031951.

Vitale, I., Spano, M., Puca, V., Carradori, S., Cesa, S., Marinacci, B., et al. (2023). Antibiofilm activity and NMR-based metabolomic characterization of cell-free supernatant of *Limosilactobacillus reuteri* DSM 17938. *Front. Microbiol.* 14. doi: 10.3389/FMICB.2023.1128275.

Walter, J., Britton, R. A., and Roos, S. (2011). Host-microbial symbiosis in the vertebrate gastrointestinal tract and the *Lactobacillus reuteri* paradigm. *Proc. Natl. Acad. Sci. U. S. A.* 108 Suppl 1, 4645–4652. doi: 10.1073/PNAS.1000099107.

Zheng, J., Wittouck, S., Salvetti, E., Franz, C. M. A. P., Harris, H. M. B., Mattarelli, P., et al. (2020). A taxonomic note on the genus *Lactobacillus*: Description of 23 novel genera, emended description of the genus *Lactobacillus beijerinck* 1901, and union of *Lactobacillaceae* and *Leuconostocaceae*. *Int. J. Syst. Evol. Microbiol.* 70, 2782–2858. doi: 10.1099/IJSEM.0.004107/CITE/REFWORKS.

IJAE
ITALIAN JOURNAL OF ANATOMY AND EMBRYOLOGY

Firenze University Press
www.fupress.com/ijae

OPEN ACCESS

Citation: Sorrentino, E., Della Rocca, Y., Marconi, G.D., Iezzi, G., Trubiani, O., D'Arcangelo, C., De Angelis, F., & Diomede, F. (2023). A mini-review on different polymerization protocols for resin-based dental composites. *Italian Journal of Anatomy and Embryology* 127(2): 61-64. doi: 10.36253/ijae-14686

Data Availability Statement: All relevant data are within the paper and its Supporting Information files.

Competing Interests: The Author(s) declare(s) no conflict of interest.

A mini-review on different polymerization protocols for resin-based dental composites

Edoardo Sorrentino[1,*], Ylenia Della Rocca[1], Guya Diletta Marconi[1], Giovanna Iezzi[2], Oriana Trubiani[1], Camillo D'Arcangelo[2], Francesco De Angelis[2], Francesca Diomede[1]

[1] *Department of Innovative Technologies in Medicine & Dentistry, University "G. d'Annunzio" Chieti and Pescara*
[2] *Department of Medical, Oral and Biotechnological Sciences, University "G. d'Annunzio" Chieti and Pescara*
*Corresponding author. E-mail: edoardo.sorrentino@unich.it

Abstract. Biocompatibility is one of the major prerequisites for safe clinical application of materials. Dental resin composites may release their components into oral environment, which can lead to adverse reactions. Several studies have identified that many organic components of composites resin, such as bisphenol-A-glycidyl-methacrylate (Bis-GMA), triethylene glycol dimethacrylate (TEGDMA), urethane dimethacrylate (UDMA) and 2-hydroxyethyl methacrylate (HEMA) show a cytotoxic profile. Cytotoxicity is mainly sustained by free monomers released after polymerization process. Direct restorations are polymerized at body temperature by visible light emitting lamps, but the conversion from monomer to polymer after light-curing is never complete. To improve the degree of conversion of resin-based composites, additional curing protocols performed at increased temperatures, such as heat-curing, can be employed. Polymerization reaction plays a key role in the conversion of the free monomers into polymers and resin-based composites with high degree of conversion might show higher biocompatibility. The aim of this mini-review is to report current knowledge about the cytotoxicity of different composite resins, cured in two different ways. Further studies are necessary to better understand the relationship between the cytotoxicity and the degree of polymerization of resin-based composites.

Keywords: composite, cytotoxic, polymerization.

INTRODUCTION

In restorative dentistry decayed tooth tissues and dental defects can be replaced by direct and indirect dental composite. Direct composite restorations are light-cured at body temperature, while indirect restorations can be subjected to supplementary heat-curing cycles. Resin composites are widely used in restorative dentistry, although their safety in terms of biocompatibility is not yet completely understood (Yang et al. 2018).

Biocompatibility, which is defined as the ability of a material to induce an appropriate biological response following a specific application, is con-

sidered a key property for any material used in contact with human tissues. In the oral cavity, biocompatibility depends on the host, the material and the function performed. The polymerization process and the intra-oral degradation are considered two main factors able to influence the free-monomer release from a polymeric matrix (Goldberg 2008). Biocompatibility and degree of monomer conversion seem to be correlated as the cytotoxic effect is directly affected by the monomers released by uncured resin in the composite (Inoue et al. 1988). Intra-oral degradation is defined as a chemical degradation caused by hydrolysis or enzyme catalysis and by the interactions between the composite resins and the human saliva-derived esterases and pseudocholinesterases (Goldberg 2008). Polymeric weight loss occurs as a result of water and solvents entering and eroding the polymer, while free monomers spread as a result of the expansion of the polymer network (Goldberg 2008). These monomers showed a cytotoxic effect *in vitro* for dental pulp and gingival cells (Goldberg 2008). Some ions as Cu2+, Al3+, and Fe2+ could be also implicated in the production of reactive oxygen species (ROS) (Goldberg 2008). The purpose of this mini-review is to report current knowledge about the cytotoxicity of resin-based dental composites subjected to two different polymerization protocols: light-curing and heat-curing.

COMPOSITE RESINS

Resin composites are composed by polymer matrix, filler, silane coupling agents and chemicals that catalyse or inhibit the curing reaction. Biocompatibility of the composite resins can be affected by the organic matrix components as bisphenol-A-glycidyl-methacrylate (Bis-GMA), triethylene glycol dimethacrylate (TEGDMA), urethane dimethacrylate (UDMA), and 2-hydroxyethyl methacrylate (HEMA) (Yang et al. 2018; Goldberg 2008). Bis-GMA is the mainly used monomer in dental resins, due to its mechanical properties and relatively low curing shrinkage (Gajewski et al. 2012). Salivary hydrolysis may promote the release of small amounts of Bisphenol A (BPA) in Bis-GMA based materials (Kingman et al. 2012) (Fig. 1). BPA estrogenic potential effects can affect the human health (Söderholm and Mariotti 1999). After composite placement in oral cavity, short-term increases in BPA levels were observed (Kingman et al. 2012). Promising results have been obtained by Bis-GMA-free composites, but to appreciate stability of these materials over time, further research is needed (Pérez-Mondragón et al. 2020). Moreover, according to the literature, the combined action of many monomers

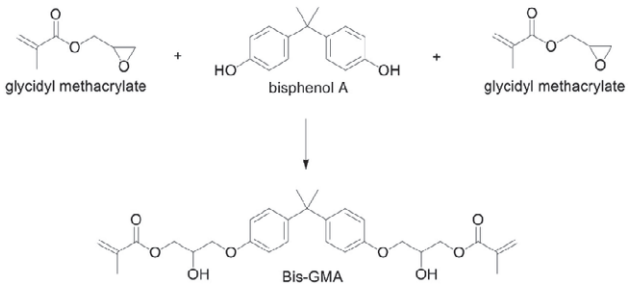

Figure 1. Chemical structure of Bis-GMA. The original figure has been published in: "Šimková M, Tichý A, Dušková M, Bradna P. Dental composites - a low-dose source of bisphenol A? Physiological research. 2020;69(Suppl 2):S295-s304."

included inside a commercial composite formulation may produce different cytotoxic and genotoxic effects compared to their single action (Wisniewska-Jarosinska et al. 2011), suggesting that biocompatibility of complex materials should not be assessed based on the effect of single specific components (De Angelis et al. 2021). The *in vitro* elution of resin-based dental composites seems to be influenced by organic and water-based solvents, molecular mass, volume and surface area of the composite restoration (De Angelis et al. 2022). Also, the type of inorganic filler should be considered. The inorganic filler content positively enhances mechanical properties of current resin-based composites (Ferracane 2011), but a potential cytotoxic risk related to modern nanoscale fillers has been pointed out with concern by some authors (Nel et al. 2006).

POLYMERIZATION

The extent of polymerization is defined as the degree of conversion of monomers into polymers. Direct composite restorations are light-cured at body temperature, while indirect restorations are subjected to further curing cycles. During polymerization reaction, an amount of monomeric methacrylate groups ranging between 15% and 50% may remain unreacted (Ferracane 1994). Unbounded monomers may be released to external environment by an incomplete polymerization and possibly cause irritation, inflammation, and allergic reactions of oral mucosa (Goldberg 2008). As a result of the incomplete polymerization reaction, the residues of free methacrylate monomers may promote the production of prostaglandin E2 (PGE2), cyclooxygenase 2 (COX2), and the increase of interleukin-1β (IL-1β), IL-6, and nitric oxide (NO), triggering a pro-inflammatory response (Kuan et al. 2013). The curing time, the intensity and the distance of the light-curing

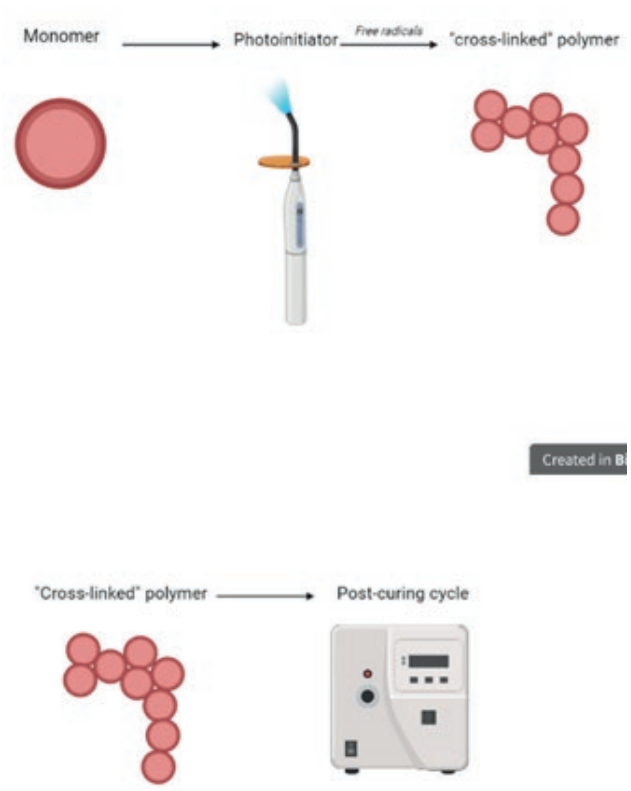

Figure 2. Light-curing and heat-curing process. The figure has been created in biorender.com.

lamp from the specimens are factors affecting the monomer conversion (Leloup et al. 2002), which inadequate conversion may jeopardise the mechanical properties of dental-based resin composites (Ferracane 1994). Additional heat-curing cycles, providing light at increased temperatures ranging between 50 and 170 °C, can be performed to increase the degree of monomer conversion of composite resins, reducing the amount of unreacted material at the composite surface, simultaneously improving the material mechanical properties (Magne et al. 2015) (Fig. 2). Higher amounts of eluted monomers are correlated to a lower extent of monomer to polymer conversion (Miletic and Santini 2008). According to Caughman and coll. (Caughman et al. 1991), the percentage of increased monomer conversion should be proportional to a decreased cellular toxicity. However, to our knowledge, no previous study was able to demonstrate a difference in cytotoxicity between heat- and light-cured composites. Moreover, according to Säilynoja and coll. (Säilynoja et al. 2004), cytotoxicity would not be affected by heat-curing process due to the slow release of molecules from the matrix, although UTMA-based materials were considered in their study (Table 1).

Table 1. Factors affecting the polymerization. The table has been published in: "Hervás-García A, Martínez-Lozano MA, Cabanes-Vila J, Barjau-Escribano A, Fos-Galve P. Composite resins. A review of the materials and clinical indications. Medicina oral, patologia oral y cirugia bucal. 2006;11(2):E215-20."

Factor	Clinical repercussions
Curing time	It depends on: resin shade, light intensity, box deep, resin thickness, curing through tooth structure, composite filling.
Shade of resin	Darker composite shades cure more slowly and less deeply than lighter shades (60 seconds at a maximum depth of 0.5 mm).
Temperature	Composite at room temperature cure more completely and rapidly.
Thickness of resin	Optimum thickness in 1-2 mm.
Type of filler	Microfine composites are more difficult to cure than heavily loaded composites.
Distance between light and resin	Optimum distance < 1 mm, with the light positioned 90 degrees from the composite surface.
Light source quality	Wavelength between 400 to 500 nm. A power density about 600 mW/cm^2 is required to ensure that 400 mW/cm^2 reaches the first increment of composite in a posterior box.
Polymerization shrinkage	Depends on the amount of organic phase.

Similar results were obtained by Vallittu and coll (Vallittu and Ekstrand 1999). Thus, the correlation between degree of conversion and cytotoxicity of resin composites seems to need further investigations.

CONCLUSIONS

In conclusion, from a clinical point of view, resin-based dental composites should demonstrate the lowest possible citoxicity, preserving their mechanical properties and clinical performance after the polymerization process. The present mini-review evidenced the importance of polymerization reaction for the release of residual monomers. However, the correlation between the cytotoxicity of dental resins composite and the degree of monomer conversion or the composite chemical formulation seems still to be better understood.

REFERENCES

Caughman, W. F., G. B. Caughman, R. A. Shiflett, F. Rueggeberg, and G. S. Schuster. 1991. 'Correlation of cytotoxicity, filler loading and curing time of dental composites', *Biomaterials*, 12: 737-40.

De Angelis, F., D. Mandatori, V. Schiavone, F. P. Melito, S. Valentinuzzi, M. Vadini, P. Di Tomo, L. Vanini, L. Pelusi, C. Pipino, P. Del Boccio, C. D'Arcangelo, and A. Pandolfi. 2021. 'Cytotoxic and Genotoxic Effects of Composite Resins on Cultured Human Gingival Fibroblasts', *Materials (Basel)*, 14.

De Angelis, F., N. Sarteur, M. Buonvivere, M. Vadini, M. Šteffl, and C. D'Arcangelo. 2022. 'Meta-analytical analysis on components released from resin-based dental materials', *Clin Oral Investig*, 26: 6015-41.

Ferracane, J. L. 1994. 'Elution of leachable components from composites', *J Oral Rehabil*, 21: 441-52.

———. 2011. 'Resin composite--state of the art', *Dent Mater*, 27: 29-38.

Gajewski, V. E., C. S. Pfeifer, N. R. Fróes-Salgado, L. C. Boaro, and R. R. Braga. 2012. 'Monomers used in resin composites: degree of conversion, mechanical properties and water sorption/solubility', *Braz Dent J*, 23: 508-14.

Goldberg, M. 2008. 'In vitro and in vivo studies on the toxicity of dental resin components: a review', *Clin Oral Investig*, 12: 1-8.

Inoue, K., H. Arikawa, K. Fujii, A. Niihara, R. Fujita, G. Tsukada, K. Kuroki, T. Oka, and C. Uchiyama. 1988. 'Composite restorative resins. Part 3. Cytotoxicity test to mouse fibroblasts in culture of UV and visible light-activated composite resins', *Dent Mater J*, 7: 55-61.

Kingman, A., J. Hyman, S. A. Masten, B. Jayaram, C. Smith, F. Eichmiller, M. C. Arnold, P. A. Wong, J. M. Schaeffer, S. Solanki, and W. J. Dunn. 2012. 'Bisphenol A and other compounds in human saliva and urine associated with the placement of composite restorations', *J Am Dent Assoc*, 143: 1292-302.

Kuan, Y. H., F. M. Huang, S. S. Lee, Y. C. Li, and Y. C. Chang. 2013. 'Bisgma stimulates prostaglandin E2 production in macrophages via cyclooxygenase-2, cytosolic phospholipase A2, and mitogen-activated protein kinases family', *PLoS One*, 8: e82942.

Leloup, G., P. E. Holvoet, S. Bebelman, and J. Devaux. 2002. 'Raman scattering determination of the depth of cure of light-activated composites: influence of different clinically relevant parameters', *J Oral Rehabil*, 29: 510-5.

Magne, P., D. A. Malta, R. Enciso, and S. Monteiro-Junior. 2015. 'Heat Treatment Influences Monomer Conversion and Bond Strength of Indirect Composite Resin Restorations', *J Adhes Dent*, 17: 559-66.

Miletic, V. J., and A. Santini. 2008. 'Remaining unreacted methacrylate groups in resin-based composite with respect to sample preparation and storing conditions using micro-Raman spectroscopy', *J Biomed Mater Res B Appl Biomater*, 87: 468-74.

Nel, A., T. Xia, L. Mädler, and N. Li. 2006. 'Toxic potential of materials at the nanolevel', *Science*, 311: 622-7.

Pérez-Mondragón, A. A., C. E. Cuevas-Suárez, J. A. González-López, N. Trejo-Carbajal, M. Meléndez-Rodríguez, and A. M. Herrera-González. 2020. 'Preparation and evaluation of a BisGMA-free dental composite resin based on a novel trimethacrylate monomer', *Dent Mater*, 36: 542-50.

Säilynoja, E. S., A. Shinya, M. K. Koskinen, J. I. Salonen, T. Masuda, A. Shinya, T. Matsuda, T. Mihara, and N. Koide. 2004. 'Heat curing of UTMA-based hybrid resin: effects on the degree of conversion and cytotoxicity', *Odontology*, 92: 27-35.

Söderholm, K. J., and A. Mariotti. 1999. 'BIS-GMA--based resins in dentistry: are they safe?', *J Am Dent Assoc*, 130: 201-9.

Vallittu, P. K., and K. Ekstrand. 1999. 'In vitro cytotoxicity of fibre-polymethyl methacrylate composite used in dentures', *J Oral Rehabil*, 26: 666-71.

Wisniewska-Jarosinska, M., T. Poplawski, C. J. Chojnacki, E. Pawlowska, R. Krupa, J. Szczepanska, and J. Blasiak. 2011. 'Independent and combined cytotoxicity and genotoxicity of triethylene glycol dimethacrylate and urethane dimethacrylate', *Mol Biol Rep*, 38: 4603-11.

Yang, Y., F. X. Reichl, J. Shi, X. He, R. Hickel, and C. Högg. 2018. 'Cytotoxicity and DNA double-strand breaks in human gingival fibroblasts exposed to eluates of dental composites', *Dent Mater*, 34: 201-08.

IJAE
ITALIAN JOURNAL OF ANATOMY AND EMBRYOLOGY

Firenze University Press
www.fupress.com/ijae

OPEN ACCESS

Citation: D'Angiolini, S., Trubiani, O., & Mazzon, E. (2023). Role of toll-like receptor signaling pathway in a rat model of spinal cord injury: a transcriptomic analysis. *Italian Journal of Anatomy and Embryology* 127(2): 65-68. doi: 10.36253/ijae-14689

Data Availability Statement: All relevant data are within the paper and its Supporting Information files.

Competing Interests: The Author(s) declare(s) no conflict of interest.

Role of toll-like receptor signaling pathway in a rat model of spinal cord injury: a transcriptomic analysis

Simone D'Angiolini[1,2,*], Oriana Trubiani[1], Emanuela Mazzon[2]

[1] *Department of Innovative Technologies in Medicine & Dentistry, University "Gabriele d'Annunzio", Chieti-Pescara, 66100 Chieti, Italy*
[2] *IRCCS Centro Neurolesi "Bonino-Pulejo", 98123 Messina, Italy*
*Corresponding author. E-mail: simone.dangiolini@irccsme.it

Abstract. Spinal cord injury (SCI) is a debilitating condition characterized by primary and secondary damage to the spinal cord tissue encompassing the site of injury. In this study, we analyzed transcriptomic data from Rattus norvegicus with SCI induced by aneurysm clip impact-compression at seventh thoracic vertebra to explore the main alterations in pathways expression. RNA was extracted from the specific SCI region after 2 weeks and hybridized on Affymetrix GeneChip arrays. Differential gene expression analysis identified 5213 DEGs among which 25 showing a fold change < -2 or > 2. Over-representation analysis was performed using the 25 DEGs above mentioned and revealed the toll-like receptor (TLR) signaling pathway signaling pathway (rno04620) as the only significantly enriched pathway (q-value < 0.05). Further examination of the regulation of this pathway unveiled upregulation of MyD88, *Tlr2*, and *Tlr4*, activating NF-κB and MAPK pathways, leading to proinflammatory cytokine synthesis and cellular apoptosis. Upregulation of *Cd80* and *Cd86* indicated T-cell activation, while IFN-β downstream regulation showed increased expression of JAK-STAT signaling pathway genes. This transcriptomic perspective highlights the dysregulation of the TLR signaling pathway in SCI at 2 weeks and emphasizes its potential role in the pathology.

Keywords: spinal cord injury, toll-like receptor signaling pathway, transcriptomic analysis, microarray.

INTRODUCTION

Spinal cord injury (SCI) is a traumatic event that can cause primary and secondary damage to the spinal cord tissue surrounding the lesion site (Ahuja et al., 2017). The primary injury is caused by the initial impact, which can lead to the rupture of nerve fibres. This damage is often irreversible and results in the loss of both motor and sensory capabilities below the site of injury (Eckert & Martin, 2017; Ortega et al., 2023). The secondary injury occurs within a short period after the initial impact causing progressive damage to the surrounding spinal cord tissue at the site of injury (Alizadeh et al., 2019). Approximately 500.000 individuals experience a SCI annually, resulting in a higher

risk of premature mortality ("Spinal Cord Injury (SCI) Facts and Figures at a Glance," 2016). An important overview in the SCI was obtained using animal models to replicate this pathological condition (Cheriyan et al., 2014) (Sharif-Alhoseini et al., 2017). In this publication we chosen to explore the pathways that can play a role in the ongoing of the SCI through 2 group of samples of rats. We compared the genes expression of sham group and SCI group after 2 weeks from the damage to highlights gene that can act an important role in the disease.

MATERIALS AND METHODS

Dataset selection

All the data analyzed in this study were obtained from the Gene Expression Omnibus repository (Barrett et al., 2013). The dataset with the accession number GSE45006 was downloaded. This dataset contains information regarding samples of Rattus norvegicus belonging to either the sham group and group related to 2 weeks after SCI induced by aneurysm clip impact-compression at seventh thoracic vertebra. The specific region of the SCI was isolated to extract RNA. Subsequently, the extracted RNA underwent processing and hybridization on Affymetrix GeneChip arrays.

Bioinformatic analysis

The analysis conducted to explore the differentially expressed genes (DEGs) was performed using R (R Core Team) with the limma package (Ritchie et al., 2015) from Bioconductor (Gentleman et al., 2004). A background correction, followed by quantile normalization, was applied to the transcriptomic data. The normalized data were then subjected to a principal components analysis (PCA). Transcriptomic profiles of our groups were then compared to highlights the DEGs with associated the information about fold change and q-value. DEGs were filtered for fold change and those with fold change < -2 or > 2 was used for the over-representation analysis (ORA) of the pathways, performed through the package clusterProfiler (Wu et al., 2021). List and information about pathways used for the analysis were retrieved using the KEGG database (Kanehisa & Goto, 2000).

RESULT

The analysis started considering the 31099 transcripts included in the array. The matrix used for the study was composed by the transcripts on the rows and the 8 samples (4 related to sham group and 4 SCI) on the columns. All the data mentioned were used to perform the different steps of background correction and normalization and then, from this data, was possible to carry out the PCA analysis. The results of PCA analysis are showed in Figure 1.

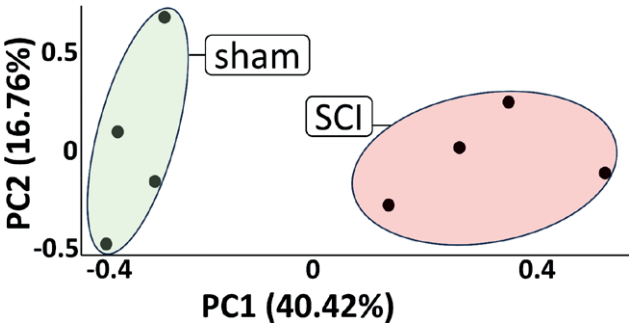

Figure 1. PCA of sham and SCI groups. In the figure, on the axes, are reported the principal component 1 and 2 that respectively describe the 40.42% and 16.76% of the variance. In green are highlighted the area that includes the sham samples and in red the area that includes the SCI samples.

Figure 1 suggests an important difference at transcriptomic level among the samples of each group. To explore this difference and observe which genes results as DEGs we carried out the comparison among sham and SCI. We considered DEGs all those genes that had a q-value, obtained through the Benjamini-Hochberg post-hoc correction of the p-value, <0.05. This investigation results in 5213 DEGs. The 5213 DEGs were further inspected to identify those that exhibited a better fold change in the comparison and, to accomplish this, DEGs

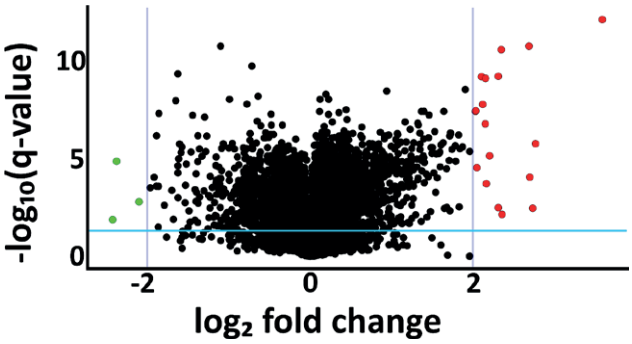

Figure 2. Dot plot distribution of all the transcript after comparison among sham and SCI. The dots represent the transcripts and, upper the horizontal light blue line, are differentially expressed (q-value < 0.05). Vertical blue lines indicate the fold change values of -2 and 2. In red are reported the DEGs upregulated in SCI conditions with a fold change > 2 and in green are reported the DEGs downregulated in SCI conditions with a fold change < -2.

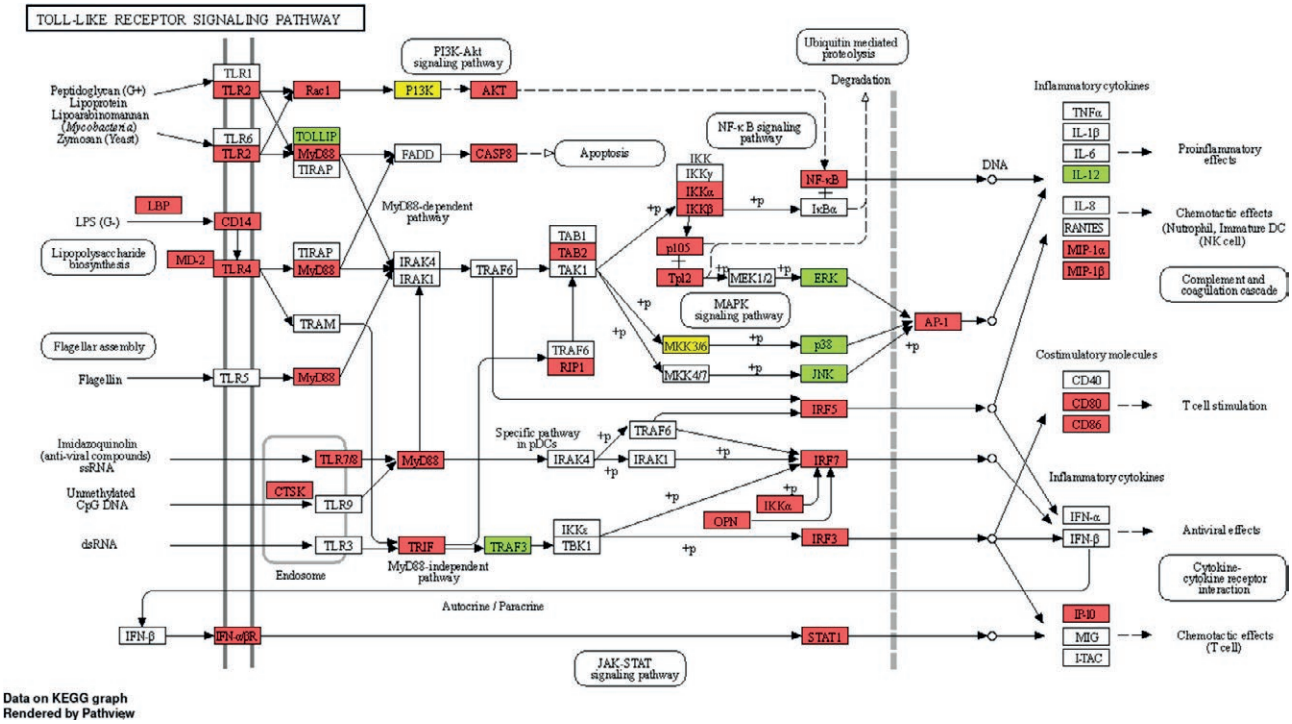

Figure 3. Toll-like receptor signaling pathway. In the pathway are highlighted in red the transcripts obtained from upregulated DEGs in SCI condition and in green the downregulated in SCI condition.

with fold change >2 or <-2 were filtered out. Data related to fold change and q-value of the transcripts are reported in Figure 2.

Figure 2 shows that 25 DEGs have a fold change > 2 o < -2. These DEGs with extreme fold change were used to perform the ORA. The aim was to discover some pathway that can result as over-represented to give us information about some possible biological focus altered in SCI condition. Results of ORA indicate that the only one pathway resulted enriched is "rno04620" related to toll-like receptor (TLR) signaling pathway with a q-value of 0.02. In Figure 3 are reported the pathway with the up and down regulated DEGs resulted involved. All the DEGs reported in the Figure 3 are not filtered for fold change to better understand every change in SCI condition.

As reported in Figure 3, it is possible to see that a significant portion of the pathway is altered. The pathway involves a total of 94 genes out of which 44 resulted DEGs. Among these DEGs, 37 genes are upregulated in the SCI condition, while 10 genes are upregulated.

DISCUSSION

The presence of just 1 pathway from ORA can indicates an important involvement of TLR signaling pathway in this stage of SCI. Is reported that TLR signaling pathways can be divided into two distinct categories: a MyD88-dependent and a MyD88-independent pathway. MyD88-dependent pathway triggers the rapid activation of NF-κB and MAPK, leading to the synthesis of proinflammatory cytokines. MyD88-independent pathway is linked to the initiation of IFN- and IFN-inducible gene expression (Kawai & Akira, 2007; Uematsu & Akira, 2007). As showed in the results, MyD88 is upregulated and this upregulation appears to be a consequence of upstream upregulation of *Tlr2* and *Trl4*. Among the downstream effects, there is an upregulation of *Casp8*, which leads to cellular apoptosis, as well as an upregulation of NF-kB. Following our results, we can also observe that, downstream of the pathway, there is an increase in the expression of *Cd80* and *Cd86* the products of which are known for their activation of T cells (Halliday et al., 2020). In addition to what has been reported so far, the regulation downstream of IFN-β shows an increase in regulation of genes involved in the JAK-STAT signaling pathways. Several genes in this pathway have already been associated with SCI (Heiman et al., 2014; Kigerl & Popovich, 2009; Li et al., 2021) but this study highlights the overall dysregulation of the pathway from a transcriptomic perspective. Significance of our discussion is reinforced by the fact that TLR sign-

aling pathway it is the only pathway found to be over-represented. Future investigations are required to ascertain whether the observed gene expression pattern in this analysis is maintained at various temporal stages or how it may potentially evolve.

FUNDING

This research was funded by PhD InTEchMed Course of the University "G. d'Annunzio" of Chieti-Pescara.

REFERENCES

Ahuja C. S., Wilson J. R., Nori S., Kotter M. R. N., Druschel C., Curt A., & Fehlings M. G. (2017) Traumatic spinal cord injury. Nat Rev Dis Primers. 3: 17018.

Alizadeh A., Dyck S. M., & Karimi-Abdolrezaee S. (2019) Traumatic Spinal Cord Injury: An Overview of Pathophysiology, Models and Acute Injury Mechanisms. Front Neurol. 10: 282.

Barrett T., Wilhite S. E., Ledoux P., Evangelista C., Kim I. F., Tomashevsky M., Marshall K. A., Phillippy K. H., Sherman P. M., Holko M., Yefanov A., Lee H., Zhang N., Robertson C. L., Serova N., Davis S., & Soboleva A. (2013) NCBI GEO: archive for functional genomics data sets--update. Nucleic Acids Res. 41(Database issue): D991-995.

Cheriyan T., Ryan D. J., Weinreb J. H., Cheriyan J., Paul J. C., Lafage V., Kirsch T., & Errico T. J. (2014) Spinal cord injury models: a review. Spinal Cord. 52(8): 588-595.

Eckert M. J., & Martin M. J. (2017) Trauma: Spinal Cord Injury. Surg Clin North Am. 97(5): 1031-1045.

Gentleman R. C., Carey V. J., Bates D. M., Bolstad B., Dettling M., Dudoit S., Ellis B., Gautier L., Ge Y., Gentry J., Hornik K., Hothorn T., Huber W., Iacus S., Irizarry R., Leisch F., Li C., Maechler M., Rossini A. J., Sawitzki G., Smith C., Smyth G., Tierney L., Yang J. Y., & Zhang J. (2004) Bioconductor: open software development for computational biology and bioinformatics. Genome Biol. 5(10): R80.

Halliday N., Williams C., Kennedy A., Waters E., Pesenacker A. M., Soskic B., Hinze C., Hou T. Z., Rowshanravan B., Janman D., Walker L. S. K., & Sansom D. M. (2020) CD86 Is a Selective CD28 Ligand Supporting FoxP3+ Regulatory T Cell Homeostasis in the Presence of High Levels of CTLA-4. Front Immunol. 11: 600000.

Heiman A., Pallottie A., Heary R. F., & Elkabes S. (2014) Toll-like receptors in central nervous system injury and disease: a focus on the spinal cord. Brain Behav Immun. 42: 232-245.

Kanehisa M., & Goto S. (2000) KEGG: kyoto encyclopedia of genes and genomes. Nucleic Acids Res. 28(1): 27-30.

Kawai T., & Akira S. (2007) TLR signaling. Semin Immunol. 19(1): 24-32.

Kigerl K. A., & Popovich P. G. (2009) Toll-like receptors in spinal cord injury. Curr Top Microbiol Immunol. 336: 121-136.

Li L., Acioglu C., Heary R. F., & Elkabes S. (2021) Role of astroglial toll-like receptors (TLRs) in central nervous system infections, injury and neurodegenerative diseases. Brain Behav Immun. 91: 740-755.

Ortega M. A., Fraile-Martinez O., Garcia-Montero C., Haro S., Alvarez-Mon M. A., De Leon-Oliva D., Gomez-Lahoz A. M., Monserrat J., Atienza-Perez M., Diaz D., Lopez-Dolado E., & Alvarez-Mon M. (2023) A comprehensive look at the psychoneuroimmunoendocrinology of spinal cord injury and its progression: mechanisms and clinical opportunities. Mil Med Res. 10(1): 26.

Ritchie M. E., Phipson B., Wu D., Hu Y., Law C. W., Shi W., & Smyth G. K. (2015) limma powers differential expression analyses for RNA-sequencing and microarray studies. Nucleic Acids Res. 43(7): e47.

Sharif-Alhoseini M., Khormali M., Rezaei M., Safdarian M., Hajighadery A., Khalatbari M. M., Safdarian M., Meknatkhah S., Rezvan M., Chalangari M., Derakhshan P., & Rahimi-Movaghar V. (2017) Animal models of spinal cord injury: a systematic review. Spinal Cord. 55(8): 714-721.

Spinal Cord Injury (SCI) Facts and Figures at a Glance. (2016). The Journal of Spinal Cord Medicine. 39(1): 123-124.

Uematsu S., & Akira S. (2007) Toll-like receptors and Type I interferons. J Biol Chem. 282(21): 15319-15323.

Wu T., Hu E., Xu S., Chen M., Guo P., Dai Z., Feng T., Zhou L., Tang W., Zhan L., Fu X., Liu S., Bo X., & Yu G. (2021) clusterProfiler 4.0: A universal enrichment tool for interpreting omics data. Innovation (Camb). 2(3): 100141.

IJAE
ITALIAN JOURNAL OF ANATOMY AND EMBRYOLOGY

Firenze University Press
www.fupress.com/ijae

Citation: Botondi, V., D'Adamo, E., Trubiani, O., & Gazzolo, D. (2023). Effects of temperature on presepsin assessment in biological fluids. *Italian Journal of Anatomy and Embryology* 127(2): 69-72. doi: 10.36253/ijae-14690

Data Availability Statement: All relevant data are within the paper and its Supporting Information files.

Competing Interests: The Author(s) declare(s) no conflict of interest.

Effects of temperature on presepsin assessment in biological fluids

Valentina Botondi[1], Ebe D'Adamo[1], Oriana Trubiani[2], Diego Gazzolo[1]

[1] *Neonatal Intensive Care Unit, G. d'Annunzio University, Chieti, Italy*
[2]*Department of Innovative Technologies in Medicine & Dentistry, University "G. D'Annunzio", Chieti, Italy*
*Corresponding author. E-mail: valentina.botondi.91@gmail.com

Abstract. Thermal stabilization is important for assuring a sample quality and prevent protein denaturation. Presepsin is a new reliable biomarker of sepsis produced in response to bacterial infections. However, before its inclusion into clinical practice several criteria need to be fulfilled. One of these regards the samples thermostability after a long-term refrigeration in different biological fluids (blood, urine, saliva) that can constitute a confounding factor for Presepsin reliability as diagnostic test. On this light, this review offers an update of studies analyzing presepsin after sample thawing.

Keywords: presepsin, temperature, biological fluids, sample storage.

1. INTRODUCTION

A proper sample management (collection, processing and storage) is essential for assuring a consistent quality for the intended analyses and study goal. In particular, consideration must be given to the storage condition to maintain sample quality until analyses are completed (Vaught J.B. et al).

Thermal stabilization is essential to prevent protein denaturation; in human fluids, slow freezing and fast thawing represent the recommended procedure (He X; Cuhadar S. et al).

Presepsin (P-SEP) is a protein produced in response to bacterial infections (Botondi V et al). P-SEP is a reliable biomarker for bacterial infections in adults, infants and newborns because of its measurability in biological fluids (i.e. blood, urine, saliva), its rapid activation and quick result output (Botondi V et al; Koh J.H. et al; Prester L. et al).

Recently, specific criteria for biomarkers inclusion in clinical practice have been stated according to official institutions (Food and Drug Administration, FDA; European Medicine Agency, EMA; the National Institute of Health, NIH) including the thermostability and results reproducibility (U.S Department of Health and Human Services et al; Hunter D.J. et al).

There are several studies in Literature focused on P-SEP detection, in which samples have been frozen (from -20°C to -80°C) until analysis (Kim S.Y.

et al; Lee S. et al; Aliu-Bejta A. et al; Al-Kindi S.G. et al). Nonetheless, according to some Authors and to the package insert of different P-SEP kit (PATHFAST and ELISA) a long-term refrigeration could somewhat represent a bias for P-SEP stability (Lee S. et al; Wagner B. et al, Khan M.).

In the present review we offer an overview of studies using refrigeration as a sample storage method before P-SEP analysis.

2. RESEARCH STRATEGY

We searched in the PubMed database for the period 2010 to 2023 all records matching the terms "Temperature", "sCD14", "storage conditions" and "frozen samples". We found 10 records in whom P-SEP samples were stored from -20 to -80 °C.

3. CONTENT

3.1 P-SEP molecule

P-SEP is a truncated form of a cell surface glycoprotein (CD14) expressed by innate immunity cells such as monocytes and neutrophils. CD14 receptor has a high-affinity for bacterial lipopolysaccharides (LPS) and activates the proinflammatory signaling cascade. At the end of the process, P-SEP is released in the blood stream (Botondi V et al).

3.2 P-SEP sampling and storage

Characteristics of Studies in which P-SEP samples have been frozen for maintenance are shown in Table 1.

In detail, P-SEP was collected in different study-population such as:

i) adults, in 5 out of the 10 series (Aliu-Bejta A. et al; Kim S.Y et al; Al-Kindi S.G. et al; Khan M. et al),
ii) children, in 3 out of 10 series (Nishana E. et al; Maya-Barrios A. et al; Bhat S.S. et al),
iii) newborns 2 out of 10 series (Topcuoglu S. et al; Pons S. et al).

Moreover, P-SEP was measured/stored in different biological fluids such as:

iv) blood, in 7 out of 10 series (Topcuoglu S. et al; Aliu-Bejta A. et al; Kim S.Y et al; Pons S. et al; Al-Kindi S.G. et al; Lee S. et al; Khan M. et al)
v) saliva, in 3 out of 10 series (Nishana E. et al; Maya-Barrios A. et al; Bhat S.S. et al),

Notably, CLEIA assay was performed in 3 out of 10 studies (Topcuoglu S. et al; Kim S.Y et al; Lee S. et al) and ELISA assay in 7 out of 10 reports (Aliu-Bejta A. et al; Pons S. et al; Al-Kindi S.G. et al; Al-Kindi S.G. et al; Nishana E. et al; Maya-Barrios A. et al; Bhat S.S. et al).

In all studies, samples were stored at a temperature of ≤-20°C and only 4 out of 10 studies provide information on the duration of freezing (Aliu-Bejta A. et al; Al-Kindi S.G. et al; Lee S. et al; Khan M. et al).

Finally, none of the studies object of evaluation analyzed the samples at different times after thawing.

4. DISCUSSION

Today, the determination of thermostability constitutes an important issue in the evaluation of biomarkers suitable for inclusion in clinical daily practice. The aim is to guarantee sample quality preventing protein denaturation and subsequent reliability of out-put results (He

Table 1. Characteristics of studies.

Population	BF	Assay	Storage T(°C)	Freezing Time	Ref
N	B	C	-80°C	NA	Topcuoglu S. et al
A	B	E	-40°C	7 d	Aliu-Bejta A. et al
A	B	C	-70°C	NA	Kim S.Y et al
N	B	E	-80°C	NA	Pons S. et al
A	B	E	-70/-80 °C	> 2 y	Al-Kindi S.G. et al
C	S	E	-20°C	NA	Nishana E. et al
C	S	E	-80°C	NA	Maya-Barrios A. et al
A	B	C	-80°C	3 m	Lee S. et al
C	S	E	-20°C	NA	Bhat S.S. et al
A	B	E	-20/-80 °C	34 d / 311 d	Khan M. et al

Abbreviations: BF, biological fluid; A, adults; C, children; N, newborn; B, blood; S, saliva; C, CLEIA; E, ELISA; d, days; y, years; m, months NA, not available.

X; Cuhadar S. et al). The issue is noteworthy especially for assessment, storage and measurement of P-SEP, a new promising early sepsis biomarker (Botondi V et al).

Among a series of assays currently used for P-SEP measurement the most available is the PATHFAST P-SEP device. Data on sample storage modalities and potential bias are at this controversial and still matter of debate. For example, according to manufacturer' instructions plasma samples are reported to be stable for 3 days at +2 to +8 °C and 9 months at –20 °C or lower, respectively. Notably, when samples are stored for a period > 9 months the result output reliability can somewhat be affected.

Data is corroborated by those reported by Khan M. et al who stored P-SEP samples at a prolonged temperature ranging from -20 to -80 °C and reported that caution should be exercised while analyzing samples for sCD14 after a so prolonged time-storage length.

Another issue that still require further investigation was within which time-period the samples were frozen from collection or were analyzed for the first time soon after thawing. Literature data showed in Table 1 report that samples were stored at a temperature ≤ -20°C in all the studies. It is important to underline that only 4 out of 10 studies (Aliu-Bejta A. et al; Al-Kindi S.G. et al; Lee S. et al) provided information about the duration of sample freezing, moreover no study has analyzed the P-SEP at different time points after thawing.

In conclusion, on the basis of the present data:

i) there are no studies focusing on the effects of thawing samples after a long-term storage on the P-SEP stability;
ii) there are no series investigating the P-SEP thermostability at short/long time from refreshment, and
iii) further research is needed in order to clarify the biomarker's stability at different time points and at different storage conditions.

REFERENCES

1. Vaught J.B., & Henderson M.K. (2011) Biological sample collection, processing, storage and information management. IARC Sci Publ.163(163):23-42.
2. He X. (2011) Thermostability of biological systems: fundamentals, challenges, and quantification. The open biomedical engineering journal.5:47–73.
3. Cuhadar S., Koseoglu M., Atay A., Dirican A. (2013) The effect of storage time and freeze-thaw cycles on the stability of serum samples. Biochemia medica.23(1): 70–77.
4. Botondi V., D'Adamo E., Plebani M., Trubiani O., Perrotta M., Di Ricco L., Spagnuolo C., De Sanctis S., Barbante E., Strozzi M.C., Maconi A., Gazzolo F., Betti M., Roveta A., Levantini G., Gazzolo D. (2022). Perinatal presepsin assessment: a new sepsis diagnostic tool?. Clinical chemistry and laboratory medicine. 60(8):1136–1144.
5. Koh J.H., Lee S., Kim H.S., Lee K., Lee C.S., Yoo S.A., Lee N., Kim W.U. (2020). Development of Monitoring System for Assessing Rheumatoid Arthritis within 5 Minutes Using a Drop of Bio-Fluids. Journal of clinical medicine. 9(11):3499.
6. Prester L., Protrka N., Macan J., Katunarić M. (2017) Salivary sCD14 as a potential biomarker of dental caries activity in adults. Arhiv za higijenu rada i toksikologiju. 68(4):315–321.
7. Lee S., Song J., Park D.W., Seok H., Ahn S., Kim J., Park J., Cho H.J., Moon S. (2022) Diagnostic and prognostic value of presepsin and procalcitonin in non-infectious organ failure, sepsis, and septic shock: a prospective observational study according to the Sepsis-3 definitions. BMC infectious diseases, 22(1):8.
8. Wagner B., Ainsworth D.M., Freer H. (2013) Analysis of soluble CD14 and its use as a biomarker in neonatal foals with septicemia and horses with recurrent airway obstruction. Veterinary immunology and immunopathology. 155(1-2):124–128.
9. Kim S.Y., Hong D.Y., Lee K.R., Paik J.H., Jung H.M. (2022) Plasma presepsin level predicts acute kidney injury in patients with sepsis in the emergency department. Medicine. 101(28):e29919.
10. Aliu-Bejta A., Kurshumliu M., Namani S., Dreshaj S., Baršić B. (2023) Ability of presepsin concentrations to predict mortality in adult patients with sepsis. Journal of clinical and translational science. 7(1):e121.
11. Al-Kindi S.G., Buzkova P., Shitole S.G., Reiner A.P., Garg P.K., Gottdiener J.S., Psaty B.M., Kizer J.R. (2020).Soluble CD14 and Risk of Heart Failure and Its Subtypes in Older Adults. Journal of cardiac failure. 26(5):410–419.
12. U.S Department of Health and Human Services; Food and Drug Administration Center for Drug Evaluation and Research (CDER); Center for Biologics Evaluation and Research (CBER). Biomarker qualification: Evidentiary Framework Guidance for Industry and FDA Staff. 2018.
13. European, Medicines, Agency. 2017. Essential Considerations for Successful Qualification of Novel Methodologies EMA/750178/2017.
14. Hunter D.J., Losina E., Guermazi A., Burstein D., Lassere M.N., Kraus V. (2010) A pathway and approach to biomarker validation and qualification

for osteoarthritis clinical trials. Curr Drug Targets. 11:536-545.
15. Topcuoglu S., Arslanbuga C., Gursoy T., Aktas A., Karatekin G., Uluhan R., Ovali F. (2016). Role of presepsin in the diagnosis of late-onset neonatal sepsis in preterm infants. The journal of maternal-fetal & neonatal medicine : the official journal of the European Association of Perinatal Medicine, the Federation of Asia and Oceania Perinatal Societies, the International Society of Perinatal Obstetricians. 29(11):1834–1839.
16. Pons S., Trouillet-Assant S., Subtil F., Abbas-Chorfa F., Cornaton E., Berthiot A., Galletti S., Plat A., Rapin S., Trapes L., et al. (2023) Performance of 11 Host Biomarkers Alone or in Combination in the Diagnosis of Late-Onset Sepsis in Hospitalized Neonates: The Prospective EMERAUDE Study. Biomedicines. 11(6):1703.
17. Nishana E., Bhat S.S., Sahana K.S., Hegde S.K., Bhat V., Kalal B.S. (2019). Estimation of Salivary sCD14 in Children with Early Childhood Caries in Association with Pneumonia. Reports of biochemistry and molecular biology. 8(2):132–138.
18. Maya-Barrios, A., Lira-Hernandez, K., Jiménez-Escobar, I., Hernández, L., Ortiz-Hernandez, A., Jiménez-Gutiérrez, C., López-Velázquez, G., Gutiérrez-Castrellón, P. (2021). Limosilactobacillus reuteri ATCC PTA 5289 and DSM 17938 as adjuvants to improve evolution of pharyngitis/tonsillitis in children: randomised controlled trial. Beneficial microbes. 12(2), 137–145.
19. Bhat S.S., Kalal B.S., Veena K.M., Kakunje A., Sahana K.S.R., Rekha P.D., Chandra J., Nasreen I. (2021). Serum and salivary immunoglobulin G4 levels in children with autism spectrum disorder from south India: a case-control study. American journal of clinical and experimental immunology. 10(4):103–111.
20. Khan M. (2010) Adaptation of fit-for-purpose biomarker assay validation using commercial kits: A CRO perspective. Drug Research. 11/12:33-34.

IJAE
ITALIAN JOURNAL OF ANATOMY AND EMBRYOLOGY

Firenze University Press
www.fupress.com/ijae

OPEN ACCESS

Citation: Oliva, S., Trubiani, O., Piattelli, M., Capogreco, M., & Murmura, G. (2023). Antibacterial activity of titanium nitride coating: a mini review. *Italian Journal of Anatomy and Embryology* 127(2): 73-76. doi: 10.36253/ijae-14692

Data Availability Statement: All relevant data are within the paper and its Supporting Information files.

Competing Interests: The Author(s) declare(s) no conflict of interest.

Antibacterial activity of titanium nitride coating: a mini review

Stefano Oliva[1,*], Oriana Trubiani[1], Maurizio Piattelli[1], Mario Capogreco[2], Giovanna Murmura[1]

[1] *Department of Innovative Technologies in Medicine and Dentistry, University "G. d'Annunzio" of Chieti-Pescara, 66100 Chieti, Italy*
[2] *Department of Life, Health and Environmental Sciences, University of L'Aquila, 67100 L'Aquila, Italy*
*Corresponding author. E-mail: oliva.stefano@hotmail.com

Abstract. Bacterial adhesion to the implant surface was the first step of peri-implant inflammation. Changes in the properties of the implant surface represent a way to reduce plaque colonization. The aim of this study was to evaluate the actual efficacy of titanium nitride (TiN) coated implants on antibacterial activity. Data were collected after identification of PICO. A search was performed in PubMed-Medline, Embase, Web of Knowledge, and Google Scholar using the following keywords: "Titanium nitride, dental implant coating, antibacterial activity, biofilm formation, plaque formation, modified implant surfaces, implant abutments". The original search included 107 articles. After title and abstract screening, the number was reduced to 12. These articles were read in full text, and finally 5 articles were included in the mini-review. TiN-coated titanium appears to reduce bacterial adhesion and growth and may represent a real possibility for preventing peri-implantitis and mucositis. However, further clinical studies need to be conducted.

Keywords: systematic review, titanium nitride, antibacterial activity, dental implant coating, peri-implantitis, bacterial adhesion.

INTRODUCTION

The long- term stability of dental implants depends on the integration of the biomaterial with the tissues surrounding the implants, i.e., bone and soft tissue, epithelium and fibrocollagenous connective tissue. Maintenance of a healthy connective tissue-implant interface is a critical issue for long-term implant survival. (Adell et al. 1981) Peri-implant inflammation, mucositis and peri-implantitis, represent the most common complications of dental implants (22%) and may be responsible for implant loss. (Derks and Tomasi 2015) The initial stage in the pathogenesis of peri-implant inflammation is caused by plaque colonization and bacterial adhesion to the implant surface. Therefore, it is essential to prevent bacterial adhesion to hard or soft tissue.(Abrahamsson et al. 1996) (Abrahamsson et al. 2002) Modifications of

implant surface characteristics could affect the biocompatibility and osteointegration of dental implants. TiN coating was introduced in dentistry in the 1980s. The aim of the coating is to achieve greater surface hardness, abrasion/wear resistance and corrosion resistance, lower friction, and better interaction with adjacent biological and material substrates. Physical vapor deposition (PVD) is the most common method for depositing TiN on orthopedic implants, and TiN is formed by the reaction of pure titanium and nitrogen gas in a vapor phase prior to deposition («Mezger, P.R.; Creugers, 1992) (Yeniyol et al. 2013).The aim of this study was to evaluate the antibacterial properties of TiN coating on dental implants on microbial biofilm adhesion and bacterial growth suppression.

MATERIAL AND METHODS

This review was performed in accordance with the PRISMA (Preferred Reporting Items for Systematic Reviews and Meta-analyses) statement (Fig. 1).

A search was performed on PubMed-Medline, Embase, Web of Knowledge, Google Scholar including the following keywords: "Titanium nitride, dental implant coating, antibacterial activity, biofilm formation, plaque formation, modified implant surfaces, implant abutments".

The review included in vitro studies comparing the antibacterial activity of titanium nitride coatings with that of pure titanium, evaluating the percentage of titanium surface covered by bacteria.

In vitro studies were selected based on title and abstract. The participants, intervention, comparison, and outcomes (PICO) were determined to formulate a specific question: How effective is the antibacterial effect of TiN?

RESULTS

The initial search included 105 articles. It was reduced to 11 after title and abstract screening. These articles were full-text read and finally 5 articles were included in the mini review (Fig. 1).

All the studies included in this review were in vitro study (Table 1).

DISCUSSION

The main objective of this study was to determine the efficacy of the antibacterial activity of TiN used as a coating for implant abutments. The investigation was based on in vitro studies comparing TiN-coated titanium disks with uncoated pure titanium disks.

Großner-Schreiber et al. (2001) investigated the effect of titanium nitride coating on bacterial adhesion of S. sanguis and S. mutans compared to a pure titanium surface and concluded that "a significant reduction in the number of adherent bacteria was observed on inherently stable titanium hard materials such as TiN compared to polished titanium"," with a statistically significant difference (p=0.0036) (Größner-Schreiber et al. 2001).

Zhang et al. (2015) showed no difference in biofilm formation between TiN-coated disks and pure titanium disks (Zhang et al. 2015).

Ji et al. (2015) showed that the number of S.mutans colonies on TiN significantly decreased ($p < 0.05$) compared to the control group (Ji et al. 2015).

Brunello et al. (2018) showed that the percentage of dead bacteria in the biofilms that grew on the TiN-coated disks was higher than in the pure titanium disks (Brunello et al. 2018).

Finally,Camargo et al. (2020) concluded their study by stating that biofilm coverage was lower on TiN (24.22%) compared to uncoated samples (85.2%). $p < 0.05$ (Camargo et al. 2020).

The results of this mini-review demonstrate that TiN-coated titanium can effectively reduce bacterial adhesion and the percentage of titanium surface covered by bacteria.

CONCLUSION

We were able to answer the PICO question "How effective is TiN in terms of antibacterial activity?" and confirm that TiN coating suppresses bacterial adhesion and growth on the titanium surface compared to pure titanium.

TiN-coated implants and abutments could be an effective way to reduce mucositis and peri-implantitis, thus improving the long-term stability of implants.

Furthermore, only in vitro studies were performed in this study; further clinical investigations need to be performed to confirm these results.

REFERENCES

Abrahamsson et al. "The mucosal attachment to titanium implants with different surface characteristics: an experimental study in dogs." *Journal of Clinical Periodontol*ogy 2002

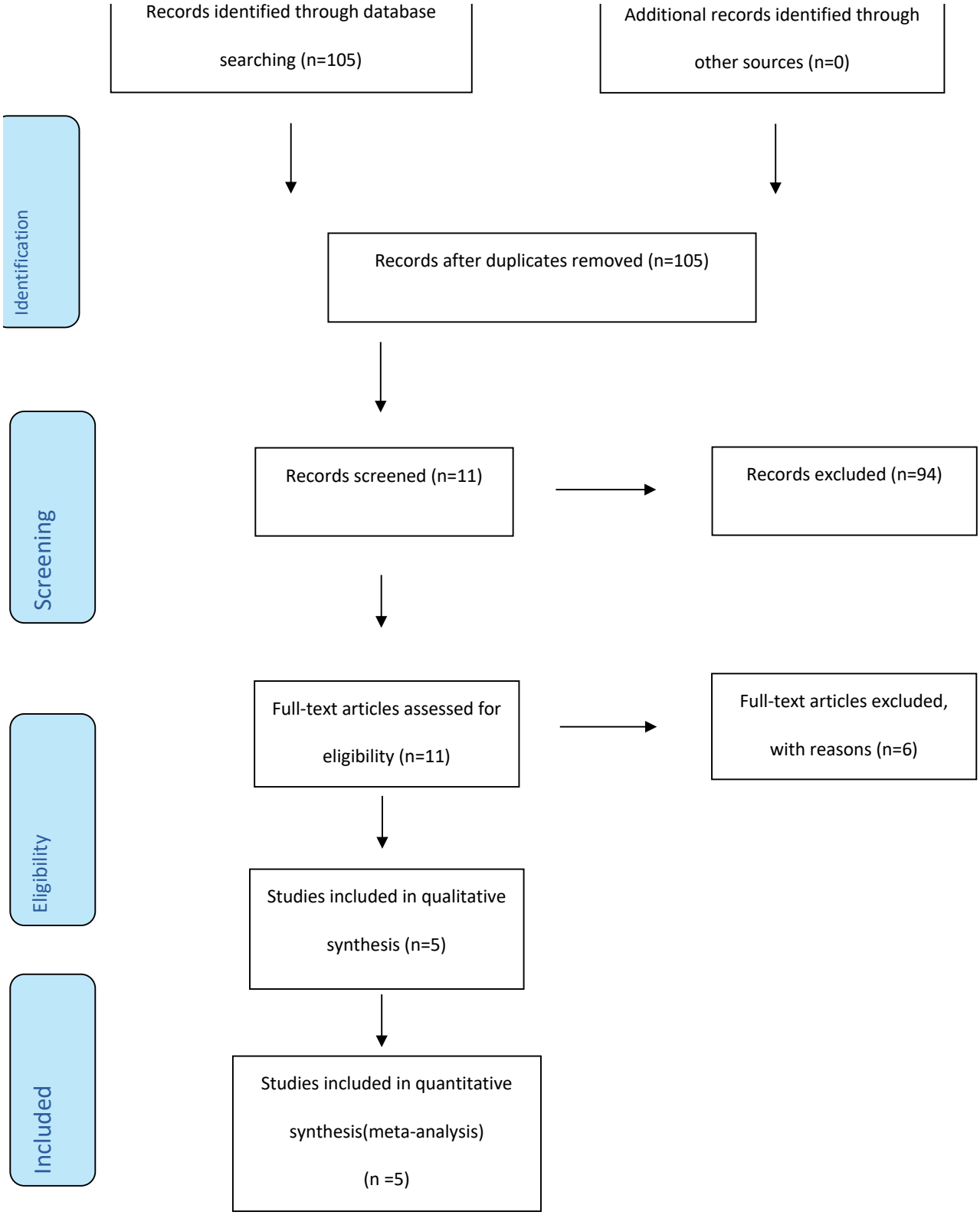

Figure 1. PRISMA Flow Diagram.

Table 1.

Author (Year)	Study design	Coating	Control group	Bacteria used	Influence of coating on bacteria
Großner-Schreiber et al. (2000)	In vitro	TiN	Pure titanium discs grade 2	*S. sanguis* *S. mutans*	Significantly lower number of bacteria on TiN coated discs (p=0.0036)
Zhang et al. (2015)	In vitro	TiN	Commercial pure titanium grade 2	*S. mutans* *A. viscosus* *P. gingivalis*	No difference in biofilm formation
Ji et al. (2015)	In vitro	TiN	Commercially pure titanium grade 2	*S. mutans* *P. gingivalis*	Number of S.mutans colonies on TiN decreased significantly (p<0.05)
Brunello et al. (2018)	In vitro	TiN	TiAl6V4, grade 5, disks	*S. sanguis* *S. salivarius* *S. mutans* *S. sobrinus* *S. oralis*	Percentage of dead bacteria was higher in the biofilms grown on the TiN coated disks
Camargo et al. (2020)	In vitro	TiN	High pure titanium	*P. gingivalis*	Biofilm coverage was lower in TiN (24.22%) compared to uncoated samples (85.2%) p<0.05

Abrahamsson et al. "The peri-implant hard and soft tissues at different implant systems. A comparative study in the dog." *Clin Oral Implants Res*. 1996

Adell et al." A 15-year study of osseointegrated implants in the treatment of the edentulous jaw." *Int J Oral Surg*. 1981

Brunello et al. "Biocompatibility and antibacterial properties of zirconium nitride coating on titanium abutments: An invitro study" *Plos One 2018*

Camargo et al. "Novel Coatings to Minimize Bacterial Adhesion and Promote Osteoblast Activity for Titanium Implants" *Materials 2021, 14, 342*.

Derks J.; Tomasi C. "Peri-implant health and disease. A systematic review of current epidemiology." *Journal of Clinical Periodontology 2014*

Großner-Schreiber et al. "Plaque formation on surface modified dental implants: An in vitro study" *Clinical Oral Implants Research* 2001

Ji et al. "Evaluation of antibacterial activity and osteoblast-like cell viability of TiN, ZrN and (Ti1-xZrx)N coating on titanium" *J Adv Prosthodont 2015;7:166-71*

Mezger, P.R.; Creugers, N.H. "Titanium nitride coatings in clinical dentistry." *J. Dent. 1992*

Yeniol et al. "Relative Contributions of Surface Roughness and Crystalline Structure to the Biocompatibility of Titanium Nitride and Titanium Oxide Coatings Deposited by PVD and TPS Coatings" *ISRN Biomaterials 2013*

Zhang et al. "Tantalum Nitride-Decorated Titanium with Enhanced Resistance to Microbiologically Induced Corrosion and Mechanical Property for Dental Application" *Plos One 2015*

IJAE
ITALIAN JOURNAL OF ANATOMY AND EMBRYOLOGY

Firenze University Press
www.fupress.com/ijae

OPEN ACCESS

Citation: Mazzone, A., Della Rocca, Y., Pizzicannella, J., Diomede, F., Marconi, G.D., & Trubiani, O. (2023). Modulation of inflammatory pathway in human gingival fibroblasts exposed to resinous materials. *Italian Journal of Anatomy and Embryology* 127(2): 77-82. doi: 10.36253/ijae-14694

Data Availability Statement: All relevant data are within the paper and its Supporting Information files.

Competing Interests: The Author(s) declare(s) no conflict of interest.

Modulation of inflammatory pathway in human gingival fibroblasts exposed to resinous materials

Antonella Mazzone[1,*], Ylenia Della Rocca[1], Jacopo Pizzicannella[2], Francesca Diomede[1], Guya Diletta Marconi[1], Oriana Trubiani[1]

[1] *Department of Innovative Technologies in Medicine & Dentistry, University "G. d'Annunzio" Chieti-Pescara, Via dei Vestini, 31, 66100 Chieti, Italy*
[2] *Department of Engineering and Geology, University "G. d' Annunzio" Chieti-Pescara, Viale Pindaro, 42, 65127 Pescara, Italy*
*Corresponding author. E-mail: antonella.mazzone@unich.it

Abstract. The goal of this work was to evaluate the anti-inflammatory effects of two resins, Bis-GMA-based resin (ProTemp 4™) and PMMA-based resin (Coldpac), used in dentistry for temporary prosthetics treatments, in the modulation of the inflammatory pathway NFkBp65/NLRP3/IL-1β. The protein expression of inflammatory markers was evaluated in an *in vitro* model of primary human gingival fibroblasts (hGFs) by immunofluorescence analysis while the study of the ultra-morphological analysis was performed through scanning electron microscopy. Taken together these results may suggest that ProTemp 4™ resin exerts a better performance in terms of inflammatory modulation.

Keywords: hGFs, ProTemp 4™, Coldpac, inflammation, biocompatibility.

INTRODUCTION

The advent of new technologies in the dental field has allowed the development of more resistant and easy-to-use resinous materials with innovative features.

One of the most important uses of composite resins is the development of temporary restorations, which is a fundamental step in the prosthetic treatment plan. Each type of resinous material has specific properties depending on the structure and molecular composition [1].

The main problem using these resinous materials is the incomplete polymerization process that leads to leakage of monomers [2] the substances released by these resinous materials may have important adverse reactions such as irritation or allergy to the oral mucosa [3-5]Previous studies reported that the toxicity of dental resin composite can be due to the release of monomers during the auto-polymerization process [6]. For this reason, there is an increased interest in the development of novel biocompatible resinous mate-

rials in the dental field [7-9] the present work aimed to evaluate the biological effects of the ProTemp 4™ resin, containing bisphenol A glycidyl methacrylate (Bis-GMA), and of the Coldpac resin, containing polymethyl methacrylate (PMMA), in an *in vitro* model of hGFs.

Protein expression and scanning electron microscopy were performed to understand the biological effects of provisional resins in contact with the oral fibroblasts. The expression of the inflammatory pathway nuclear factor kappa-light-chain-enhancer of activated B cells (NF-κB), the inflammasome protein NOD-, LRR- and pyrin domain-containing 3 (NLRP3), and the pro-inflammatory cytokine interleukin-1 beta (IL-1β) [10,11] were evaluated using the immunofluorescence analysis.

MATERIALS AND METHODS

Preparation of resin disc samples to evaluate cell adhesion

Two materials used for temporary restorations were compared: ProTemp 4™ (ProtempTM 4 Temporization Material, 3M ESPE, St. Paul, USA) and Coldpac self-curing PMMA (Coldpac tooth acrylic, Yates Motloid, Chicago, USA).

After mixing and polymerization according to the manufacturer's instructions, round section bars of 10 mm in diameter were produced.

Discs with a thickness of 0.3mm were obtained using two glass plates, while using a core drill bit with an internal diameter of 0.5mm, approximately 50 disks were obtained for each resin under examination. Each disc was then finished and polished according to the procedures described by the manufacturer. To eliminate any finishing residues, the disks were placed in distilled water and sonicated for 30 minutes. The samples were dried and placed in an autoclave at 134 °C for 50 minutes to obtain complete disinfection.

Cell culture of hGFs

Human gingival fibroblasts (hGFs PCS-201-018 ATCC, Manassas, Virginia, US) were cultured in basal medium (Fibroblast Growth Kit-Low Serum, (PCS-201-041, ATCC), containing 5 ng/mL rh FGF-β (fibroblast growth factor beta), 7.5 mM L-glutamine, 50 μg/mL ascorbic acid, 1 μg/mL hydrocortisone hemisuccinate, 5 μg/mL rh insulin and 2% fetal bovine serum [12,13]. The culture was maintained in an incubator at 37°C in a humidified atmosphere of 5% CO2 and 95% air [13,14]

Once the cells reached 75-80% confluency, subcultures were made.

Confocal Microscopy Analysis

The hGFs cells were seeded at 8500/well on 8-well culture glass slides (Corning, Glendale, Arizona, USA) and treated with ProTemp 4™ and Coldpac resins, for 24 hours and 1 week, replacing the medium every 2 days. The cells were then fixed for 10 min at room temperature (RT) with 4% paraformaldehyde in 0.1 M PBS (pH 7.4); after washing, samples were processed for immunofluorescence staining.

The Confocal Microscopy analysis was performed using NFkB (1:500, sc-8008, Santa Cruz Biotechnology, CA), NLRP3 (1:500, NBP1 77080, Novus, Milan, Italy), and Il-1b (1:500, sc-32294, Santa Cruz) as primary mouses monoclonal antibodies [16] and Alexa Fluor 568 red fluorescence conjugated goat anti-mouse antibody (A11031, Invitrogen, Eugene, OR, USA) as a secondary antibody. The microscope used is Zeiss LSM800 confocal system (Zeiss, Jena, Germany) [17].

SEM

SEM analyses were then performed to evaluate the relationship between hGFs and the resin disks.

After 24 hours and 1 week of culture, the samples were fixed for 1 hour 4 °C in 2.5% glutaraldehyde (Electron Microscopy Sciences, EMS, Hatfield, PA, USA), in 0.1 M sodium phosphate buffer (PB), pH 7.3, rinsed three times with PB, and post-fixed for 1 h in 1% aqueous osmium tetroxide (EMS) at 4 °C. The cells were dehydrated through an ethanol series (30%, 50%, 70%, 90%, 95%, and two times 100%) followed by drying in air and carbon. Specimens were mounted on aluminum stubs and gold-coated in an Emitech K550 sputter-coater (Emitech Ltd., Ashford, UK). SEM EVO 50 (Zeiss, Jena, Germany) was used for analysis [20].

Design of the experimental study

The experimental steps featured in this study were performed in triplicate with hGFs (Figure 1):

- hGFs cultured alone as negative control for 24 hours and 7 days.
- hGFs cultured with ProTemp 4™ resin disk for 24 hours and 7 days
- hGFs cultured with Coldpac resin disk for 24 hours and 7 days

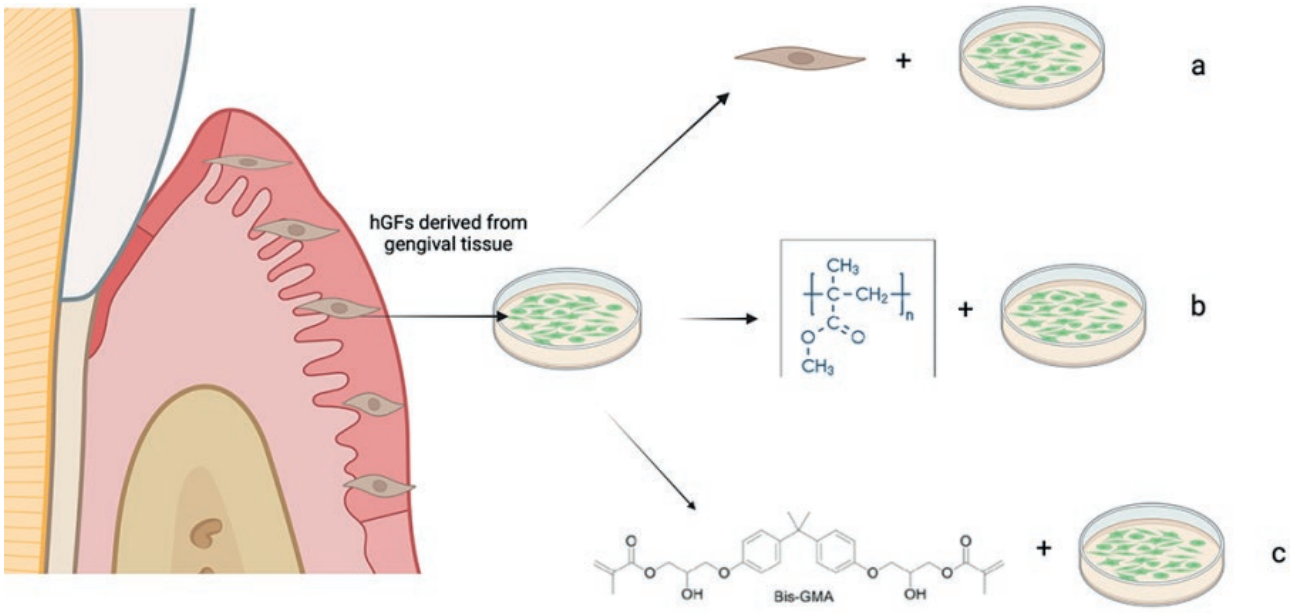

Figure 1. Design of the experimental study. 1a) hGFs cultured alone; 1b) hGFs cultured with Coldpac; 1c) hGFs cultured with ProTemp 4™.

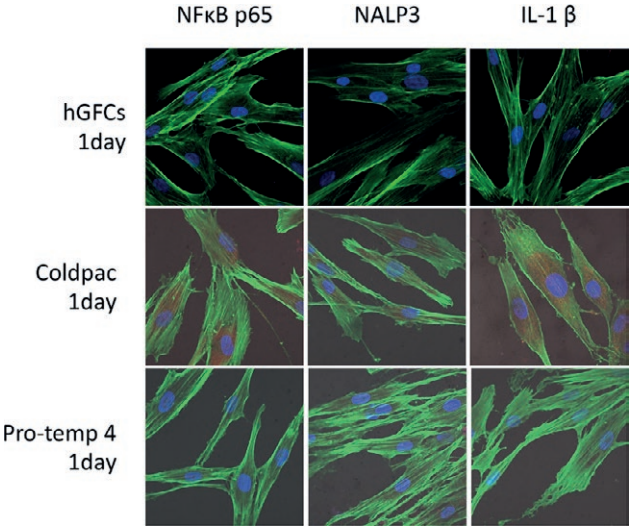

Figure 2. Protein Expression evidenced by CLSM in hGFs, in hGFs cultured on Coldpac and in hGFs cultured on ProTemp 4™ after 24 h.

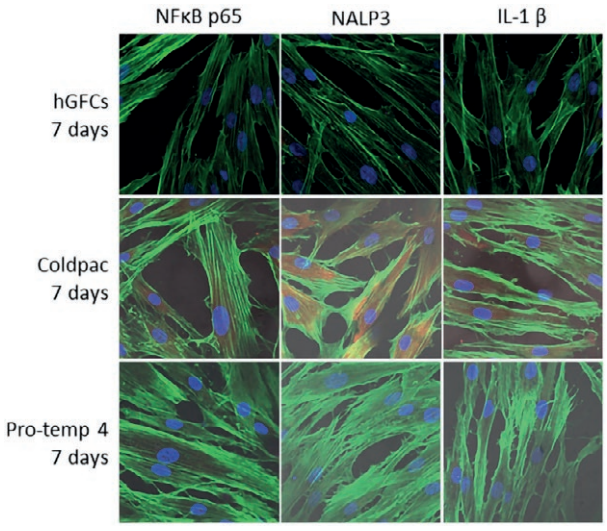

Figure 3. Protein Expression evidenced by CLSM in hGFs, in hGFs cultured on Coldpac, and in hGFs cultured on ProTemp 4™ after 1 week.

RESULTS

The immunofluorescence analysis showed that the pathway NFkBp65/NLRP3/IL-1β was significantly downregulated in hGFs alone and in hGFs cultured with ProTemp 4™ disks compared to hGFs cultured with Coldpac disks, after 24 h (Figure 2) and 1 week of treatment (Figure 3).

The immunofluorescence figures show the NFκB p65/NLRP3/IL-1β expression in hGFs alone, cultured with Coldpac and with ProTemp 4™ for 24 hours. The results show that the NFκBp65/NLRP3/IL-1β pathway was significantly upregulated in hGFs cultured with Coldpac after 24h compared to hGFs cultured with Pro-Temp 4™ and hGFs alone.

The immunofluorescence figures show the NFκB p65/NLRP3/IL-1β expression in hGFs alone, cultured with Coldpac and with ProTemp 4™ after 1 week. The results

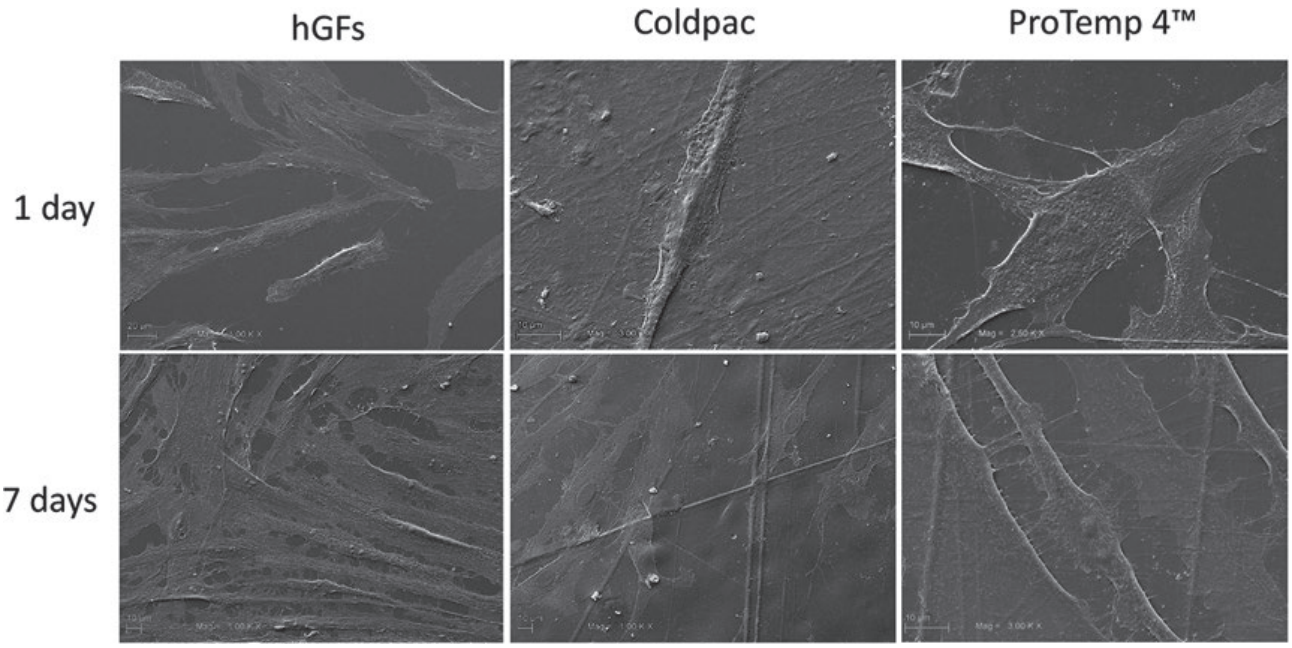

Figure 4. Representative SEM images of hGFs cultured alone, with Coldpac, and with ProTemp 4™ after 24 hours and 7 days.

show that the NFκBp65/NLRP3/IL-1β pathway was significantly upregulated in hGFs cultured with Coldpac after 1 week compared to hGFs cultured with ProTemp 4™ and hGFs alone.

Regarding the morphological analysis, hGFs cultured on ProTemp 4™ showed a similar morphology as hGFs evidencing nucleo and nucleoli, after 24h and 1 week; on the contrary, cells cultured on Coldpac showed a different morphological feature (Figure 4).

DISCUSSION

Over the last few years, new technologies have developed biologically compatible resins with optimum safety profiles and physical properties.

In our study, we focused on the ProTemp 4™ and Coldpac resins that are particularly used for the development of prosthetic implants [21]. The incomplete polymerization process of these materials may induce toxic effects on the oral cavity cells [22].

The *in vitro* model hGFs was used to understand which provisional resin can lead to better biocompatibility, after 24 hours and 1 week of culture.

Scanning electron microscopy was performed to understand the cell adhesion capacity on the resin disks, on the other hand, confocal laser scanning microscopy was performed to analyze inflammatory modulation.

The NFkB p65/NLRP3/ IL-1β inflammatory pathway was found to be downregulated in hGFs cultured with ProTemp 4™ resin when compared with cells cultured with Coldpac resin, after 24h and 7 days of cultured. In parallel, SEM analysis showed that the fibroblastic morphology was preserved in hGFs treated with Protemp 4™ while compared with hFGs treated with Coldpac.

According to our results, ProTemp 4™ resin could be less inflammatory when compared to Coldpac resin; this could mean that the ProTemp 4™ resin could lead to better biocompatibility and better performance in terms of cell/material interaction.

REFERENCES

1. Wei, X.; Gao, L.J.; Wu, K.; Pan, Y.; Jiang, L.; Lin, H.L.; Wang, Y.H.; Cheng, H. In vitro study of surface properties and microbial adhesion of various dental polymers fabricated by different manufacturing techniques after thermocycling. *Clinical oral investigations* **2022**, *26*, 7287-7297, doi:10.1007/s00784-022-04689-2.
2. Mazzaoui, S.A.; Burrow, M.F.; Tyas, M.J.; Rooney, F.R.; Capon, R.J. Long-term quantification of the release of monomers from dental resin composites and a resin-modified glass ionomer cement. *J Biomed Mater Res* **2002**, *63*, 299-305, doi:10.1002/jbm.10184.
3. Hatton, P.V.; Mulligan, S.; Martin, N. The safety and biocompatibility of direct aesthetic restorative materials. *Brit Dent J* **2022**, *232*, 611-614, doi:10.1038/s41415-022-4198-6.

4. Marconi, G.D.; Diomede, F.; Pizzicannella, J.; Fonticoli, L.; Merciaro, I.; Pierdomenico, S.D.; Mazzon, E.; Piattelli, A.; Trubiani, O. Enhanced VEGF/VEGF-R and RUNX2 Expression in Human Periodontal Ligament Stem Cells Cultured on Sandblasted/Etched Titanium Disk. *Front Cell Dev Biol* **2020**, *8*, doi: 10.3389/Fcell.2020.00315.
5. Diomede, F.; Marconi, G.D.; Cavalcanti, M.F.X.B.; Pizzicannella, J.; Pierdomenico, S.D.; Fonticoli, L.; Piattelli, A.; Trubiani, O. VEGF/VEGF-R/RUNX2 Upregulation in Human Periodontal Ligament Stem Cells Seeded on Dual Acid Etched Titanium Disk. *Materials* **2020**, *13*, doi: 10.3390/Ma13030706.
6. Camassa, L.M.A.; Ervik, T.K.; Zegeye, F.D.; Mdala, I.; Valen, H.; Ansteinssond, V.; Zienolddiny-Narui, S. Characterization and toxicity evaluation of airborne particles released by grinding from two dental resin composites in vitro (vol 37, pg 1121, 2021). *Dent Mater* **2022**, *38*, 1564-1564, doi:10.1016/j.dental.2022.07.007.
7. Zizzari, V.L.; Marconi, G.D.; De Colli, M.; Zara, S.; Zavan, B.; Salini, V.; Fontana, A.; Cataldi, A.; Piattelli, A. In Vitro Behavior of Primary Human Osteoblasts Onto Microrough Titanium Surface. *Implant Dent* **2015**, *24*, 377-383, doi:10.1097/Id.0000000000000268.
8. Marconi, G.D.; Fonticoli, L.; Rocca, Y.D.; Rajan, T.S.; Piattelli, A.; Trubiani, O.; Pizzicannella, J.; Diomede, F. Human Periodontal Ligament Stem Cells Response to Titanium Implant Surface: Extracellular Matrix Deposition (vol 10, 931, 2022). *Biology-Basel* **2023**, *12*, doi: 10.3390/Biology12020306.
9. Marconi, G.D.; Fonticoli, L.; Della Rocca, Y.; Oliva, S.; Rajan, T.S.; Trubiani, O.; Murmura, G.; Diomede, F.; Pizzicannella, J. Enhanced Extracellular Matrix Deposition on Titanium Implant Surfaces: Cellular and Molecular Evidences. *Biomedicines* **2021**, *9*, doi:ARTN 1710
10.3390/biomedicines9111710.
10. Kelley, N.; Jeltema, D.; Duan, Y.; He, Y. The NLRP3 Inflammasome: An Overview of Mechanisms of Activation and Regulation. *Int J Mol Sci* **2019**, *20*, doi:10.3390/ijms20133328.
11. Pizzicannella, J.; Fonticoli, L.; Guarnieri, S.; Marconi, G.D.; Rajan, T.S.; Trubiani, O.; Diomede, F. Antioxidant Ascorbic Acid Modulates NLRP3 Inflammasome in LPS-G Treated Oral Stem Cells through NFkappaB/Caspase-1/IL-1beta Pathway. *Antioxidants* **2021**, *10*, doi:10.3390/antiox10050797.
12. Marconi, G.D.; Fonticoli, L.; Rajan, T.S.; Lanuti, P.; Della Rocca, Y.; Pierdomenico, S.D.; Trubiani, O.; Pizzicannella, J.; Diomede, F. Transforming Growth Factor-Beta1 and Human Gingival Fibroblast-to-Myofibroblast Differentiation: Molecular and Morphological Modifications. *Frontiers in physiology* **2021**, *12*, doi: 10.3389/Fphys.2021.676512.
13. Marconi, G.D.; Gallorini, M.; Carradori, S.; Guglielmi, P.; Cataldi, A.; Zara, S. The Up-Regulation of Oxidative Stress as a Potential Mechanism of Novel MAO-B Inhibitors for Glioblastoma Treatment. *Molecules* **2019**, *24*, doi: 10.3390/Molecules24102005.
14. De Colli, M.; Tortorella, P.; Marconi, G.D.; Agamennone, M.; Campestre, C.; Tauro, M.; Cataldi, A.; Zara, S. In vitro comparison of new bisphosphonic acids and zoledronate effects on human gingival fibroblasts viability, inflammation and matrix turnover. *Clinical oral investigations* **2016**, *20*, 2013-2021, doi:10.1007/s00784-015-1690-2.
15. Pizzicannella, J.; Marconi, G.D.; Guarnieri, S.; Fonticoli, L.; Della Rocca, Y.; Konstantinidou, F.; Rajan, T.S.; Gatta, V.; Trubiani, O.; Diomede, F. Role of ascorbic acid in the regulation of epigenetic processes induced by Porphyromonas gingivalis in endothelial-committed oral stem cells. *Histochemistry and cell biology* **2021**, *156*, 423-436, doi:10.1007/s00418-021-02014-8.
16. Diomede, F.; Fonticoli, L.; Marconi, G.D.; Della Rocca, Y.; Rajan, T.S.; Trubiani, O.; Murmura, G.; Pizzicannella, J. Decellularized Dental Pulp, Extracellular Vesicles, and 5-Azacytidine: A New Tool for Endodontic Regeneration. *Biomedicines* **2022**, *10*, doi:10.3390/biomedicines10020403.
17. Zara, S.; De Colli, M.; Rapino, M.; Di Valerio, V.; Marconi, G.D.; Cataldi, A.; Macchi, V.; De Caro, R.; Porzionato, A. NF-kappaB involvement in hyperoxia-induced myocardial damage in newborn rat hearts. *Histochemistry and cell biology* **2013**, *140*, 575-583, doi:10.1007/s00418-013-1092-y.
18. Marconi, G.D.; Diomede, F.; Pizzicannella, J.; Fonticoli, L.; Merciaro, I.; Pierdomenico, S.D.; Mazzon, E.; Piattelli, A.; Trubiani, O. Enhanced VEGF/VEGF-R and RUNX2 Expression in Human Periodontal Ligament Stem Cells Cultured on Sandblasted/Etched Titanium Disk. *Front Cell Dev Biol* **2020**, *8*, 315, doi:10.3389/fcell.2020.00315.
19. Diomede, F.; Marconi, G.D.; Cavalcanti, M.; Pizzicannella, J.; Pierdomenico, S.D.; Fonticoli, L.; Piattelli, A.; Trubiani, O. VEGF/VEGF-R/RUNX2 Upregulation in Human Periodontal Ligament Stem Cells Seeded on Dual Acid Etched Titanium Disk. *Materials* **2020**, *13*, doi:10.3390/ma13030706.
20. Zizzari, V.L.; Marconi, G.D.; De Colli, M.; Zara, S.; Zavan, B.; Salini, V.; Fontana, A.; Cataldi, A.; Piattelli, A. In Vitro Behavior of Primary Human Osteoblasts Onto Microrough Titanium Surface. *Implant Dent* **2015**, *24*, 377-383, doi:10.1097/ID.0000000000000268.

21. Poonacha, V.; Poonacha, S.; Salagundi, B.; Rupesh, P.L.; Raghavan, R. In vitro comparison of flexural strength and elastic modulus of three provisional crown materials used in fixed prosthodontics. *Journal of clinical and experimental dentistry* **2013**, *5*, e212-217, doi:10.4317/jced.51136.
22. Hampe, T.; Wiessner, A.; Frauendorf, H.; Alhussein, M.; Karlovsky, P.; Burgers, R.; Krohn, S. Monomer Release from Dental Resins: The Current Status on Study Setup, Detection and Quantification for In Vitro Testing. *Polymers* **2022**, *14*, doi:10.3390/polym14091790.

IJAE
ITALIAN JOURNAL OF ANATOMY AND EMBRYOLOGY

Firenze University Press
www.fupress.com/ijae

OPEN ACCESS

Citation: Foglietta, M., D'Antonio, F., Pierdomenico, S.D., Bacigalupi, E., & Pizzicannella, J. (2023). Twin pregnancies and maternal cardiovascular function: literature review and future prospects. *Italian Journal of Anatomy and Embryology* 127(2): 83-87. doi: 10.36253/ijae-14700

Data Availability Statement: All relevant data are within the paper and its Supporting Information files.

Competing Interests: The Author(s) declare(s) no conflict of interest.

Twin pregnancies and maternal cardiovascular function: literature review and future prospects

Melissa Foglietta[1,*], Francesco D'Antonio[2], Sante Donato Pierdomenico[1], Elena Bacigalupi[3], Jacopo Pizzicannella[4]

[1] *Department of Innovative Technologies in Medicine & Dentistry, University "G. d'Annunzio" Chieti-Pescara, Via dei Vestini, 31, 66100 Chieti, Italy*
[2] *Department of Medicine and Aging Sciences, University "G. d' Annunzio" Chieti-Pescara, Italy*
[3] *Department of Neuroscience, Imaging and Clinical Sciences, University "G.D'Annunzio",Chieti-Pescara, Italy*
[4] *Department of Engineering and Geology, University "G. d' Annunzio" Chieti-Pescara, Viale Pindaro, 42, 65127 Pescara, Italy*
*Corresponding author. E-mail: melissa.foglietta11@gmail.com

Abstract. Twin pregnancy – with a prevalence nearly doubled in the last decades due to the use of assisted reproductive technology and the increasing age of conception – is associated with physiological cardiovascular adaptations to meet the hemodynamic demands of pregnancy. Compared to singleton pregnancies, increased and earlier in pregnancy risk of developing perinatal complications and maternal cardiac disease is demonstrated due to additional stress on the maternal cardiovascular system due to higher circulation volume. Knowledge on maternal adaptation in twin pregnancies are still lacking and often data derive from research studies on singleton pregnancy and including twins without differentiations. Only a few trials considered the impact of twin pregnancies on the maternal cardiovascular system and included echocardiographic evaluations showing how the changes in left ventricular geometry, systolic and diastolic function were comparable to those observed later in uncomplicated singleton pregnancies or in presence of hypertensive disorders. The present work aimed to review the current state of research on maternal cardiovascular function in twin pregnancies as the basis for a new study focused to find premature echocardiographic parameters able to contribute to the design of effective preventive strategies of complications – such as hypertensive disorders – in pregnancies, particularly on twin pregnancy.

Keywords: twin, pregnancy, cardiovascular system, diastolic function, systolic function.

INTRODUCTION

The Worldwide incidence of multiple pregnancies, especially twins is growing – nearly doubled in the last decades in USA – due to the wide use of assisted reproductive technology and the increased age of conception.

During pregnancy – singleton or multiple – mother's anatomical, metabolic, and physiological changes are necessary for the benefit of the foetus-

es; in fact, physiological cardiac remodelling permits to increase cardiac output and blood volume on one side and decrease the peripherical vascular resistances from the other side (Melchiorre et al., 2016).

Women failing to meet the haemodynamic demands of pregnancy are more likely to develop perinatal or maternal complications and have also an increased risk to develop cardiovascular disease later in life. (Bellamy et al., 2007).

Compared with singleton pregnancy, uncomplicated twin pregnancy has a more pronounced and altered maternal cardiac function, haemodynamic changes, and additional stress on the maternal cardiovascular system due to higher circulation volume; therefore, in twin pregnancies mother's heart has a higher risk of decompensation correlating to increased risk of complication such as pre-eclampsia (Francisco et al., 2017 and Li X et al., 2016).

Trials demonstrated the proportionality of the occurrence of pre-eclampsia and the number of foetuses with a prevalence of 6.5%, 12.7% and 20% in singleton, twin and triples pregnancies respectively (DayMC Barton et al., 2005 and Adank MC et al., 2020) and occurrence at an earlier gestation age, a more quickly progression and an atypical presentation in twin pregnancies; the larger placental size and mass, the stronger inflammatory response, and the possibility to a larger area of placental perfusion damage are the major causes of these findings (Wang et al.2021 and Narang et al., 2021).

We conducted an extensive literature search through PubMed (NCBI) up to 20 June 2023 based on journals evaluating maternal echocardiographic cardiovascular function in twin pregnancies. The keywords used were: twin, pregnancy, echocardiography, systolic and diastolic function (Table 1).

HYPOTHESIS AND THEORY ON MATERNAL CARDIOVASCULAR FUNCTION

Knowledge on maternal cardiovascular function during twin pregnancies are still lacking, women with multiple gestations were often excluded from research studies or included in studies with singletons without differentiation, despite the disproportionate incidence of pregnancy changes and complications in twin pregnancies.

Two of the most dated studies (Robson et al.,1989 and Veille et al.,1985) and then other more recent studies (Kametas et al.,2003 and Kuleva et at,2011) reported variations of the left ventricular (LV) function during gestation such as the increase of cardiac output, stroke volume (SV), heart rate, LV end-diastolic volume and of left atrial area, related to the more hyperdynamic maternal circulation, increased plasma volume and venous return in twin pregnancies.

Moreover, a recent trial (Orabona et al.,2022) added information on maternal LV dimensions, volumes and LV mass during twin pregnancies demonstrating the progressively increased trend from the first to the third trimester, like in singletons.

Regarding the LV diastolic function, at first, Ghi and Degli Esposti et al (2015) observed the deterioration of diastolic parameters characterized by the reduction of mitral E wave and the increase of mitral A wave and of left atrial pressures.

Recently, Nunez et al confirmed all previous data and taking into consideration the increase of cardiac output, myocardial performance index, LV mass, relative wall thickness (RWT) and the progressive LV diastolic dysfunction demonstrating the increase of isovolumetric relaxation time (IVRT), left atrial area and, the decrease of mitral E/A ratio in twin – dichorionic and monochorionic – pregnancies. No differences were observed in LV myocardial deformation between twin and singleton pregnancies.

Moreover, the impact of chorionicity on the cardiovascular system was examined (Nunez et al and Ghi and Dall'Asta et al.,2019) and dichorionic twin pregnancies seemed to be associated with more accentuated mother cardiac changes.

The impact of pregnancy on maternal right ventricular (RV) systolic and diastolic function was investigated in a recent longitudinal study (Orabona et al.,2022) involving 30 twin pregnancies and no significant differences in RV function (all the parameters such as fractional area change FAC, TAPSE, sPAP, E and A waves, E/A, DT, E/e', IVCT, myocardial performance index and 2D longitudinal strain) were found in twins pregnancies compared to singleton pregnancies.

In general, all trials demonstrated how the maternal cardiovascular changes in twin pregnancies anticipated those encountered in singleton pregnancy later in gestation, suggesting the physiological remodelling in response to the increase in volume loading rather than decompensation of the maternal cardiovascular system.

Recently Giorgione et al (2022) – considering around 830 pregnant women – demonstrated how changes in LV geometry, function and haemodynamics in normotensive twin pregnancy were comparable to those observed in singleton pregnancies complicated by hypertensive disorders of pregnancy (HDP); the cardiac maladaptation in twin pregnancies seemed to be exacerbated in the presence of HDP, compared to normotensive twin pregnancies.

The importance of these findings is related to the precocious evaluation of the functional and structural cardiac changes that could precede complications in pregnancy.

Table 1. Summary of studies on twin pregnancies.

Author	Country	Year	Experimental model	Results
Robson et al.	UK	1989	10 and 13 women with twin and singleton pregnancies respectively.	Heart rate (HR), SV, cardiac output, LV end-diastolic volume, left atrial dimension, RWT, LV mass, systolic and diastolic blood pressure were increased and TVR were reduced compared to non-pregnant values. In twin pregnancies, only heart rate, cardiac output, left atrial dimension were significantly higher compared to singleton pregnancies.
Veille et al.	USA	1985	6 and 16 women with twin and singleton pregnancies respectively.	Heart rate, cardiac index, SV, fractional shortening were increased in the second and third trimester of twin pregnancies. Blood pressure and end-diastolic ventricular size were not affected differently by twin pregnancies.
Kametas et al.	UK	2003	119 women with twin pregnancies and 128 women with singleton pregnancies.	In twin pregnancies, compared to singletons, cardiac output, SV, HR, LV end-diastolic dimensions, ejection fraction, long axis shortening were increased.
Kuleva et al.	Italy	2011	20 women with twin pregnancies and 10 women with singleton pregnancies.	Cardiac output increased during pregnancies, in both twins and singletons. TVR decreased during pregnancy.
Ghi and Degli Esposti et al.	Italy	2015	30 (24 dichorionic and 6 monochorionic) twin pregnancies.	During pregnancy, a reduction of LV ejection fraction, a progressive reduction of pulsed Doppler E-wave velocity and an increase of A-wave were showed from first to third trimester. Higher left atrial pressure was demonstrated.
Ghi and Dall'Asta et al.	Italy	2018	67 twin pregnancies (48 dichorionic and 19 monochorionic).	Compared to dichorionic pregnancies, in the monochorionic sets lower cardiac output and higher TVR were observed. Regarding the diastolic function, higher values were observed for mitral E/A ratio, septal mitral E'/A' ratio, lateral mitral E' in monochorionic pregnancies.
Nunez et al.	UK	2022	155 women with twin pregnancies (86 dichorionic and 69 monochorionic).	In both types of twin pregnancies, compared to singletons, IVRT, left atrial area, RWT, myocardial performance index and LV mass were increased, and mitral E/A ratio decreased.
Orabona et al.	Italy	2022	30 women with uncomplicated singleton and 30 women with uncomplicated twin pregnancies.	During twin pregnancy, maternal LV dimensions and mass increased from first to third trimester, like singletons, while LVEF remained stable. Diastolic function worsened with no differences between twins and singletons, except for higher LV filling pressure in the second trimester in twins. Two-dimensional strains did not vary during gestation in either group, while GLS was altered in one-fourth/one-third in both groups.
Orabona et al.	Italy	2022	30 women with uncomplicated singleton and 30 women with uncomplicated twin pregnancies.	RV function parameters (FAC, TAPSE, sPAP, E, A, E/A, DT, E/E', IVA, IVCT, MPI and 2D longitudinal strain) in twin pregnancies were similar to singletons. Left atrial dimension increased throughout gestation in both twins and singletons.
Giorgione et al.	UK	2022	119 HDP singleton pregnancies, 52 normotensive twin pregnancies and 24 HDP twin pregnancies.	LV mass did not differ between singleton pregnancies complicated by HDP and normotensive twin pregnancies but was higher in HDP twin compared with HDP singleton pregnancies. Left atrial volume and E/e' were higher in HDP twin compared with normotensive twin pregnancies. In normotensive twin compared with HDP singleton pregnancies SV was higher and TVR lower.

Heart rate (HR), cardiac output (CO), total vascular resistances (TVR), hypertensive disorders of pregnancy (HDP).

POTENTIAL FUTURE DEVELOPMENTS IN THE TWIN PREGNANCIES FIELD

Although data on twin pregnancies are still missing, recent knowledge about physiological and pathophysiological changes are emerging.

During singleton and multiple pregnancies physiological adaptations are necessary to ensure adequate uteroplacental circulation for foetal growth and development and to respond to higher circulation volume of mothers. In twin pregnancies – compared with singletons – LV mass, end-diastolic volume, SV, cardiac output, and left atrium dimensions increase, but there are also other subtle changes in systolic and diastolic LV function parameters. The typical cardiovascular adaptations in twin pregnancies resemble to those seen in singletons in late gesta-

tion and this concept suggests physiological remodelling in response to the increase in volume.

When mother's physiological changes fail to meet the haemodynamic demands, the risk of complication increases.

Moreover, twin pregnancies have an increased risk of cardiovascular complications -such as pre-eclampsia-, at an earlier gestation age and, a more quickly progression compared to singleton pregnancies.

Understanding the normal cardiovascular changes occurring during pregnancies is essential not only for caring patients with cardiovascular disease but also to try to anticipate the occurrence of complications in the pregnancies of subjects with no pre-pregnancy disorders.

Therefore, we retain that could be useful to establish a new longitudinal study based on transthoracic echocardiography evaluations during the three trimesters of pregnancy to find premature parameters able to contribute to the design of effective preventative strategies for prevention of maternal cardiovascular diseases in high-risk pregnancies such as twins ones.

LEGENDS

HDP hypertensive disorders of pregnancy
IVCT isovolumetric contraction time
IVRT isovolumetric relaxation time
LAVi left atrial volume
LV left ventricle
RV right ventricle
RWT relative wall thickness
SV stroke volume
TTE Transthoracic echocardiography
TVR total vascular resistance

REFERENCES

Adank MC, Broere-Brown ZA, Goncalves R, Kamran Ikram M, Jaddoe VW, Steegers EAP, Schalekamp-Timmermans S. 2020, Maternal cardiovascular adaptation to twin pregnancy: a population-based prospective cohort study, BMC Pregnancy and Childbirth.

Bellamy L, Casas JP, Hingorani AD, William DJ.2007 Pre-eclampsia and risk of cardiovascular disease and cancer in later life: systematic review and metaanalysis. BMJ.

DayMC, Barton JR, O'Brien JM, Istwan NB, SibaiBM. 2005. The effect of fetal number on the development of hypertensive conditions of pregnancy. Obstet Gynecol. 106(5 Pt 1):927–31.

Francisco C, Wright D, Benk ¨o Z, Syngelaki A, Nicolaides KH. 2017. Hidden high rate of pre-eclampsia in twin compared with singleton pregnancy. Ultrasound Obstet Gynecol; 50: 88–92.

Ghi T, degli Esposti D, Montaguti E, Rosticci M, Tancredi S, Youssef A, di Giovanni MV, Pilu G, Borghi C, Rizzo N. 2015. Maternal cardiac evaluation during uncomplicated twin pregnancy with emphasis on the diastolic function. Am J Obstet Gynecol; 213: 376. e1–8.

Ghi T, Dall'Asta A, Franchi L, Fieni S, Gaibazzi N, Siniscalchi C, Pedrazzi G, Montaguti E, Degli Esposti D, Carpano MG, Suprani A, Orabona R, Prefumo F, Vizzardi E, Bonadei I, Sciatti E, Borghi C, Frusca T. 2019. The effect of chorionicity on maternal cardiac adaptation to uncomplicated twin pregnancy: A prospective longitudinal study. Fetal Diagn Ther; 45: 394–402.

Giorgione V, Melichiorre K, O'Driscoll J, Khalil A, Sharma R, Thilaganathan B. 2022. Maternal echocardiographic changes in twin pregnancies with and without pre-eclampsia, Ultrasound Obstet Gynecol.

Kametas N, Mcauliffe F, Krampl E, Chambers J, Nicolaides KH. 2003. Maternal cardiac function in twin pregnancy. Obstet Gynecol; 102: 806–815.

Kuleva M, Youssef A,Maroni E, Contro E, Pilu G, Rizzo N, Pelusi G, Ghi T. 2011. Maternal cardiac function in normal twin pregnancy: a longitudinal study. Ultrasound Obstet Gynecol; 38: 575–580.

Li X, Tan H, Huang X, Zhou S, Hu S, Wang X, Xu X, Liu Q, Wen SW. 2016. Similarities and differences between the risk factors for gestational hypertension and preeclampsia: a population based cohort study in south China. *Pregnancy Hypertens*. 6(1):66–71.

Melchiorre K, Sharma R, Khalil A, Thilaganathan B. 2016. Maternal cardiovascular function in normal pregnancy: Evidence of maladaptation to chronic volume overload. Hypertension; 67: 754–762.

Narang K, Szymanski LM, 2021, Multiple Gestation and hypertensive disorders of pregnancy: what do we know? Current Hypertensions reports.

Nunez E, Huluta I, Gallardo Arozena M, Wright A, Nicolaides KH, Charakida M. 2022. Maternal cardiac function in twin pregnancy at 19-23 weeks' gestation, Ultrasound Obstet Gynecol,

Orabona R, Sciatti E, Vizzardi E, Bonadei I, Metra M, Sartori E, Fusca T, Pinna A, Bellocco R, Prefumo F. 2022 Maternal left ventricular function in uncomplicated pregnancies: a speckle-tacking imaging longitudinal study. Journal of Clinical Medicine.

Orabona R, Sciatti E, Vizzardi E, Bonadei I, Metra M, Sartori E, Fusca T, Pinna A, Bellocco R, Prefumo F.

2022. Maternal right ventricular and left atrial function in uncomplicated twin pregnancies: a longitudinal study. Journal of Clinical Medicine.

Robson SC, Hunter S, Boys RJ, Dunlop W. 1989. Haemodynamic changes during twin pregnancy. A Doppler and M-mode echocardiographic study. Am J Obstet Gynecol. 161:1273–1278.

Veille JC, Morton MJ, Burry KJ. 1985. Maternal cardiovascular adaptations to twin pregnancy. Am J Obstet Gynecol; 153: 261–263

Wang Y, Wu N, Shen H. 2021. A review of Research process of pregnancy with twins with pre-eclampsia. Risk management and healthcare policy.

IJAE
ITALIAN JOURNAL OF ANATOMY AND EMBRYOLOGY

Firenze University Press
www.fupress.com/ijae

Citation: Della Rocca, Y., Mazzone, A., Pizzicannella, J., Marconi, G.D., Trubiani, O., & Diomede, F. (2023). Reprogramming methods for induced pluripotent stem cells generation. *Italian Journal of Anatomy and Embryology* 127(2): 89-93. doi: 10.36253/ijae-14702

Data Availability Statement: All relevant data are within the paper and its Supporting Information files.

Competing Interests: The Author(s) declare(s) no conflict of interest.

Reprogramming methods for induced pluripotent stem cells generation

Ylenia Della Rocca[1,*], Antonella Mazzone[1], Jacopo Pizzicannella[2], Guya Dilletta Marconi[1], Oriana Trubiani[1], Francesca Diomede[1]

[1] *Department of Innovative Technologies in Medicine & Dentistry, University "G. d'Annunzio" Chieti-Pescara, via dei Vestini, 31, 66100 Chieti, Italy*
[2] *Department of Engineering and Geology, University "G. d' Annunzio" Chieti-Pescara, Viale Pindaro, 42, 65127 Pescara, Italy*
*Corresponding author. E-mail: ylenia.dellarocca@unich.it

Abstract. Regenerative medicine expects to replace the function of tissue or organs damaged by disease, trauma, or congenital issues. The tools used to realize these outcomes are tissue engineering and cellular therapies. Cellular therapy is considered a regenerative medicine strategy based on the use of stem cells. Pluripotent stem cells are the hotspots of cellular therapy due to their features that have been showed promising results. Embryonic stem cells (ESCs) are pluripotent, self-renewing cells that are derived from the inner cell mass (ICM) of the developing blastocyst. Pluripotency is the main feature that lead single cell to generate all cell lineages of the developing and adult organism. The use of human ESC (hESC) is ethically controversial, to overcome this problem the induced pluripotent stem cells (iPSCs) were developed. The aim of the present mini-review is to report a comprehensive summary of the different cellular reprogramming techniques from its initial conception to the present day.

Keywords: embryonic stem cells, pluripotency, human ESC, reprogramming.

INTRODUCTION

Embryonic stem cells (ESCs) are pluripotent cells with the property to grow indefinitely maintaining pluripotency and to differente into cells of all three germ layers. ESCs derived from the inner cell mass of mammalian blastocysts [1] [2] [3]. Human ESCs (hESCs) could be a therapeutic perspective for the treatment of various pathologies but there are ethical problems with the use of human embryos, and clinical difficulties such as post-transplant tissue rejection. In recent years, the necessity of therapeutic purposes with greater regenerative potential, bypassing the ethical problems of the use of ESCs, led to the establishment of induced pluripotent stem cell lines (iPSCs). The iPSCs are cells with pluripotent properties obtained from differentiated cells by reprogramming. It results in a similar embryonic stem cell state [4] [5]. Yamanaka and Takahashi were the first to hypothesize the central factors to the induction of pluripotency in somatic cells and for the

maintenance of pluripotency in ESCs [6]. They selected 24 genes as candidate factors, starting from other previous studies in which it was demonstrated that several transcription factors, including Oct3/4, Sox2, Nanog are involved in the maintenance of pluripotency at the level of ESCs, as well as some genes demonstrated upregulated in ESCs. Tumors markers, such as Stat3, E-Ras, c-myc, Klf4 and β-catenin, contribute to the maintenance of ESCs phenotype in culture and their rapid proliferation. By combining four selected factors (OCT3/4, SOX2, c-Myc, and KLF4), it was possible to generate pluripotent cells directly from mouse embryonic or adult fibroblasts cultures, generating iPSCs [6]. Since the characteristics of iPSCs are similar to those of embryonic stem cells; they can be expanded indefinitely in vitro and differentiated into the three germ layers: endoderm, mesoderm and ectoderm. Takahashi and Yamanaka's revolutionary discovery has led to the extensive use of iPSCs and their differentiated cells in various research areas, especially in regenerative and personalized medicine. Among the reprogramming methods that allow to obtain iPS there are: nuclear transplantation, cell fusion, reprogramming by cell extracts, and direct reprogramming through gene manipulation [7]. Among the direct reprogramming methodologies, we can make a further distinction between integrating vector methods and genomic non-integrating methods. These two types of direct reprogramming are the most widely used methods today to generate iPSCs [8].

NUCLEAR TRANSPLANTATION

Nuclear transfer allows to obtain cells with embryonic characteristics through the reprogramming of differentiated somatic cells by transplanting cell nuclei into an enucleated oocyte [9] [10]. At this point, the cloned embryo reaches the blastocyst stage, from which ESCs can differentiate into pluripotent cells and thus into cells of the three embryonic layers and then in different tissues. However, this method has several limitations for clinical applications since it presupposes an unfertilized egg cell and, in addition, there is the risk of immunological rejection. In 2007, only 2 cells out of a total of 304 oocytes were successfully created as ES cells by nuclear transfer, demonstrating a low efficiency of the method [11].

CELL FUSION

Cell fusion is the reprogramming method which generate cells with pluripotency characteristics through the hybridization of an adult somatic cell with an embryonic stem cell. The resulting hybrid is determined by rearrangement in the DNA during cell division of the formed syncytium. ESCs therefore can induce somatic cell reprogramming, overwriting the somatic cell genome with ESC genetic information [11]. Hybrids thus formed have been seen to generate chimera embryos after blastocyst injection, demonstrating their pluripotency [12]. It is not clear whether the cytoplasmic elements of ESCs are sufficient to obtain pluripotent cells through this methodology or whether the nuclear elements are also necessary. Since it would be desirable to selectively remove only ESCs chromosomes from the melted nuclei, and it is practically difficult, this technique is still far from its possible use in clinical applications [13].

REPROGRAMMING BY CELL EXTRACTS

This method of reprogramming involves inserting cell extracts obtained from pluripotent stem cells into somatic cells. The cellular extract, chemically isolated from ESCs, consists of a set of reprogramming factors which, once inside somatic cells, induce their reprogramming. This technique has been shown to increase the expression levels of pluripotent markers such as Oct4 in host cells. Although these cells were able to differentiate into different cell lines, they were not able to give rise to the three germ layers [14], fundamental property for a pluripotent cell. For this reason, this method does not allow a complete reprogramming.

INTEGRATING VECTOR METHODS

Methods that use integrating vectors to induce pluripotency can first be distinguished based on whether they use viral or non-viral vectors.

As regards the viral delivery systems, the gene factors inducing pluripotency are inserted into the cells to be reprogrammed through a viral vector. The determining factor for efficient delivery is the infection system utilized by the virus, especially for entry into the host cell, into the nucleus, and for cytoplasmic trafficking. These processes change and vary according to different types of viruses. Persistent gene expression requires the use of integrating vectors such as lentiviruses or retroviruses. For transient expression, however, it may be sufficient to use an adenovirus since they are episomically maintained and do not integrate into the genome [15].

The original system for obtaining iPSCs is using retroviral vectors, which integrate the transgenes into the

host genome [16]. Adenovirus vectors are generally quite poor in cell gene transfer, probably due to the availability of primary receptors and/or co-receptors required for *in vitro* cell binding and internalization [17,18]. Stem cells gene delivery by these vectors is relatively weak, although there are capsid modification techniques that improve delivery efficiency [19]. Retroviruses are vectors that induce long-term expression through DNA integration. They have been used with exceptional effect in the reprogramming of mouse and human dermal fibroblasts into iPSCs [20] [6]. However, they have the important limitation related to their propensity for cellular transduction limited to actively dividing cells. Due to retrovirus limitations, the research has shifted to lentiviruses for several reasons. First, the lentivirus transduces both dividing and non-dividing cells. This distinguishes it from classic retroviruses [21]. Furthermore, unlike native adenoviruses which are selective for CD4 on T cells, recombinant lentiviruses can be pseudo typed with other envelope proteins to make them less selective and broaden the viral tropism [22]. Finally, producing lentiviruses in the laboratory is not overly complicated. The lentivirus allows a very efficient, stable, and reproducible gene delivery.

However, since viral integration methods lead to host genomic integration and bring safety risk associated with genetic manipulation, they are not ideal methods to obtain iPSCs for therapeutic purposes.

Therefore, a non-viral approach can be considered as an alternative to developing iPSCs.

The non-viral system usually employs plasmids, through which genes for pluripotency induction are transported. For delivery, the plasmid is encapsulated by lipid or cationic polymers which are needed to transfect the cells to be reprogrammed. Plasmids are episomically maintained and result in short-term gene expression [23].

In 2008 mouse iPSCs were generated with a plasmid vector, demonstrating that transient expression of reprogramming factors can be induced, identifying three essential reprogramming factors: Oct3/4, Sox2 and Klf4 [24]. These three factors were linked in a single plasmid with a constitutively active CAG promoter, allowing an high expression of multiple proteins from a single RNA transcript. The transfection trough plasmids was repeated several times to obtain the necessary expression for generating iPSCs. After four weeks, colonies of iPSCs were obtained, but with a low frequency: one third of the iPSCs clones did not integrate the transgene. The iPSCs clones lacking integration had the potential to differentiate into different cell types of the three germ layers. Furthermore, when transplanted into blastocysts, they were able to form chimeric mice, competent for germline transmission [25].

NON-INTEGRATING METHODS.

One of alternative reprogramming methods for obtaining iPSCs trough non-integrating methods is by episomal vectors derived from the Epstein-Barr virus without the viral packaging. It is seen that with this method the reprogramming efficiency was low although sufficient to have enough starting cells for culture. Furthermore, the addition of chemical compounds could increase the reprogramming efficiency of these episomal vectors [26]. Another method is the constitution of a minicircle vector. This is a small size double-stranded circular DNA. A mini-circle DNA vector was developed with a constituted single cassette of four reprogramming factors (Oct4, Sox2, Lin28 and Nanog) together with the GFP reporter gene, each separated by self-cleaving 2A peptide sequences [27]. This construct exhibits better transfection efficiency besides longer ectopic transcription factors expression, probably because it less activates exogenous silencing mechanisms. In the delivery of the minicircle vector electrotransfer gave the best results [28]. Furthermore, this method showed low cytotoxicity when electroporation was performed with minicircle DNA. Although these non-viral methods represent an important advance, they show poor reprogramming efficiency. Among the more recent non-integrating methods is synthetic transfection of mRNA, which has resulted in efficient and controlled gene expression in human cells, without genomic integration. Treatment with speific mRNA cocktail induces pluripotency in somatic cells [29]. Transfection with mammalian cell mRNA results in severe cytotoxicity which can be reduce by substituting cytidine and uridine with pseudo UTP and 5 methyl CTP respectively, still achieving stable transfection [30]. Furthermore, more recently iPSCs have been efficiently generated using synthetic self-replicating RNAs [31]. With this method it is avoided repeated mRNA transfection, so cytotoxicity is limited. More recently, these pluripotency-inducing nucleic acid have been placed inside state-of-the-art nanoparticles that interact with the membrane allowing target cell transfection [32].

CONCLUSION

Regenerative medicine has made great progress. Reprogramming tools represent a recent area of research with promising results. Although encouraging data have been obtained, further studies are needed, especially to establish the efficacy and safety of reprogramming methods. Cellular reprogramming is one of the most promising cell therapy approach for treatment of several diseases.

REFERENCES

1. Evans, M.J.; Kaufman, M.H. Establishment in culture of pluripotential cells from mouse embryos. *Nature* **1981**, *292*, 154-156, doi:10.1038/292154a0.
2. Diomede, F.; Fonticoli, L.; Marconi, G.D.; Della Rocca, Y.; Rajan, T.S.; Trubiani, O.; Murmura, G.; Pizzicannella, J. Decellularized Dental Pulp, Extracellular Vesicles, and 5-Azacytidine: A New Tool for Endodontic Regeneration. *Biomedicines* **2022**, *10*, doi:10.3390/biomedicines10020403.
3. Pizzicannella, J.; Marconi, G.D.; Guarnieri, S.; Fonticoli, L.; Della Rocca, Y.; Konstantinidou, F.; Rajan, T.S.; Gatta, V.; Trubiani, O.; Diomede, F. Role of ascorbic acid in the regulation of epigenetic processes induced by Porphyromonas gingivalis in endothelial-committed oral stem cells. *Histochem Cell Biol* **2021**, 10.1007/s00418-021-02014-8, doi:10.1007/s00418-021-02014-8.
4. Kumar, D.; Talluri, T.R.; Anand, T.; Kues, W.A. Induced pluripotent stem cells: Mechanisms, achievements and perspectives in farm animals. *World journal of stem cells* **2015**, *7*, 315-328, doi:10.4252/wjsc.v7.i2.315.
5. Della Rocca, Y.; Fonticoli, L.; Rajan, T.S.; Trubiani, O.; Caputi, S.; Diomede, F.; Pizzicannella, J.; Marconi, G.D. Hypoxia: molecular pathophysiological mechanisms in human diseases. *Journal of physiology and biochemistry* **2022**, *78*, 739-752, doi:10.1007/s13105-022-00912-6.
6. Takahashi, K.; Yamanaka, S. Induction of pluripotent stem cells from mouse embryonic and adult fibroblast cultures by defined factors. *Cell* **2006**, *126*, 663-676, doi:10.1016/j.cell.2006.07.024.
7. Miyazaki, S.; Yamamoto, H.; Miyoshi, N.; Takahashi, H.; Suzuki, Y.; Haraguchi, N.; Ishii, H.; Doki, Y.; Mori, M. Emerging methods for preparing iPS cells. *Jpn J Clin Oncol* **2012**, *42*, 773-779, doi:10.1093/jjco/hys108.
8. Panda, A.; Gurusamy, N.; Rajasingh, S.; Carter, H.K.; Thomas, E.L.; Rajasingh, J. Non-viral reprogramming and induced pluripotent stem cells for cardiovascular therapy. *Differentiation* **2020**, *112*, 58-66, doi:10.1016/j.diff.2019.12.001.
9. Robl, J.M.; Gilligan, B.; Critser, E.S.; First, N.L. Nuclear transplantation in mouse embryos: assessment of recipient cell stage. *Biology of reproduction* **1986**, *34*, 733-739, doi:10.1095/biolreprod34.4.733.
10. Tsunoda, Y.; Yasui, T.; Shioda, Y.; Nakamura, K.; Uchida, T.; Sugie, T. Full-Term Development of Mouse Blastomere Nuclei Transplanted into Enucleated 2-Cell Embryos. *J Exp Zool* **1987**, *242*, 147-151, doi:DOI 10.1002/jez.1402420205.
11. Byrne, J.A.; Pedersen, D.A.; Clepper, L.L.; Nelson, M.; Sanger, W.G.; Gokhale, S.; Wolf, D.P.; Mitalipov, S.M. Producing primate embryonic stem cells by somatic cell nuclear transfer. *Nature* **2007**, *450*, 497-502, doi:10.1038/nature06357.
12. Tada, M.; Morizane, A.; Kimura, H.; Kawasaki, H.; Ainscough, J.F.; Sasai, Y.; Nakatsuji, N.; Tada, T. Pluripotency of reprogrammed somatic genomes in embryonic stem hybrid cells. *Developmental dynamics : an official publication of the American Association of Anatomists* **2003**, *227*, 504-510, doi:10.1002/dvdy.10337.
13. Pralong, D.; Mrozik, K.; Occhiodoro, F.; Wijesundara, N.; Sumer, H.; Van Boxtel, A.L.; Trounson, A.; Verma, P.J. A novel method for somatic cell nuclear transfer to mouse embryonic stem cells. *Cloning and stem cells* **2005**, *7*, 265-271, doi:10.1089/clo.2005.7.265.
14. Taranger, C.K.; Noer, A.; Sorensen, A.L.; Hakelien, A.M.; Boquest, A.C.; Collas, P. Induction of dedifferentiation, genomewide transcriptional programming, and epigenetic reprogramming by extracts of carcinoma and embryonic stem cells. *Mol Biol Cell* **2005**, *16*, 5719-5735, doi:10.1091/mbc.e05-06-0572.
15. Viral and non-viral gene delivery and its role in pluripotent stem cell engineering. *Drug discovery today. Technologies* **2008**, *5*, e105-148, doi:10.1016/j.ddtec.2008.10.002.
16. Okita, K.; Yamanaka, S. Induced pluripotent stem cells: opportunities and challenges. *Philosophical transactions of the Royal Society of London. Series B, Biological sciences* **2011**, *366*, 2198-2207, doi:10.1098/rstb.2011.0016.
17. Bergelson, J.M.; Cunningham, J.A.; Droguett, G.; Kurt-Jones, E.A.; Krithivas, A.; Hong, J.S.; Horwitz, M.S.; Crowell, R.L.; Finberg, R.W. Isolation of a common receptor for Coxsackie B viruses and adenoviruses 2 and 5. *Science* **1997**, *275*, 1320-1323, doi:10.1126/science.275.5304.1320.
18. Wickham, T.J.; Mathias, P.; Cheresh, D.A.; Nemerow, G.R. Integrins alpha v beta 3 and alpha v beta 5 promote adenovirus internalization but not virus attachment. *Cell* **1993**, *73*, 309-319, doi:10.1016/0092-8674(93)90231-e.
19. Shayakhmetov, D.M.; Papayannopoulou, T.; Stamatoyannopoulos, G.; Lieber, A. Efficient gene transfer into human CD34(+) cells by a retargeted adenovirus vector. *Journal of virology* **2000**, *74*, 2567-2583, doi:10.1128/jvi.74.6.2567-2583.2000.
20. Takahashi, K.; Tanabe, K.; Ohnuki, M.; Narita, M.; Ichisaka, T.; Tomoda, K.; Yamanaka, S. Induction of pluripotent stem cells from adult human fibro-

blasts by defined factors. *Cell* **2007**, *131*, 861-872, doi:10.1016/j.cell.2007.11.019.
21. Ma, Y.; Ramezani, A.; Lewis, R.; Hawley, R.G.; Thomson, J.A. High-level sustained transgene expression in human embryonic stem cells using lentiviral vectors. *Stem cells* **2003**, *21*, 111-117, doi:10.1634/stemcells.21-1-111.
22. Carneiro, F.A.; Bianconi, M.L.; Weissmuller, G.; Stauffer, F.; Da Poian, A.T. Membrane recognition by vesicular stomatitis virus involves enthalpy-driven protein-lipid interactions. *Journal of virology* **2002**, *76*, 3756-3764, doi:10.1128/jvi.76.8.3756-3764.2002.
23. Lai, M.I.; Wendy-Yeo, W.Y.; Ramasamy, R.; Nordin, N.; Rosli, R.; Veerakumarasivam, A.; Abdullah, S. Advancements in reprogramming strategies for the generation of induced pluripotent stem cells. *J Assist Reprod Genet* **2011**, *28*, 291-301, doi:10.1007/s10815-011-9552-6.
24. Okita, K.; Nakagawa, M.; Hyenjong, H.; Ichisaka, T.; Yamanaka, S. Generation of mouse induced pluripotent stem cells without viral vectors. *Science* **2008**, *322*, 949-953, doi:10.1126/science.1164270.
25. Niwa, H.; Yamamura, K.; Miyazaki, J. Efficient selection for high-expression transfectants with a novel eukaryotic vector. *Gene* **1991**, *108*, 193-199, doi:10.1016/0378-1119(91)90434-d.
26. Yu, J.; Hu, K.; Smuga-Otto, K.; Tian, S.; Stewart, R.; Slukvin, II; Thomson, J.A. Human induced pluripotent stem cells free of vector and transgene sequences. *Science* **2009**, *324*, 797-801, doi:10.1126/science.1172482.
27. Jia, F.; Wilson, K.D.; Sun, N.; Gupta, D.M.; Huang, M.; Li, Z.; Panetta, N.J.; Chen, Z.Y.; Robbins, R.C.; Kay, M.A., et al. A nonviral minicircle vector for deriving human iPS cells. *Nature methods* **2010**, *7*, 197-199, doi:10.1038/nmeth.1426.
28. Chabot, S.; Orio, J.; Schmeer, M.; Schleef, M.; Golzio, M.; Teissie, J. Minicircle DNA electrotransfer for efficient tissue-targeted gene delivery. *Gene therapy* **2013**, *20*, 62-68, doi:10.1038/gt.2011.215.
29. Grudzien-Nogalska, E.; Kowalska, J.; Su, W.; Kuhn, A.N.; Slepenkov, S.V.; Darzynkiewicz, E.; Sahin, U.; Jemielity, J.; Rhoads, R.E. Synthetic mRNAs with superior translation and stability properties. *Methods in molecular biology* **2013**, *969*, 55-72, doi:10.1007/978-1-62703-260-5_4.
30. Warren, L.; Manos, P.D.; Ahfeldt, T.; Loh, Y.H.; Li, H.; Lau, F.; Ebina, W.; Mandal, P.K.; Smith, Z.D.; Meissner, A., et al. Highly efficient reprogramming to pluripotency and directed differentiation of human cells with synthetic modified mRNA. *Cell stem cell* **2010**, *7*, 618-630, doi:10.1016/j.stem.2010.08.012.
31. Yoshioka, N.; Gros, E.; Li, H.R.; Kumar, S.; Deacon, D.C.; Maron, C.; Muotri, A.R.; Chi, N.C.; Fu, X.D.; Yu, B.D., et al. Efficient generation of human iPSCs by a synthetic self-replicative RNA. *Cell stem cell* **2013**, *13*, 246-254, doi:10.1016/j.stem.2013.06.001.
32. Soppimath, K.S.; Aminabhavi, T.M.; Kulkarni, A.R.; Rudzinski, W.E. Biodegradable polymeric nanoparticles as drug delivery devices. *Journal of controlled release : official journal of the Controlled Release Society* **2001**, *70*, 1-20, doi:10.1016/s0168-3659(00)00339-4.

IJAE
ITALIAN JOURNAL OF ANATOMY AND EMBRYOLOGY

Firenze University Press
www.fupress.com/ijae

OPEN ACCESS

Citation: Ruggieri, A.G., & Sallese, M. (2023). Motor behavioural tests for phenotype evaluation of mouse models of ataxia: the case of Marinesco-Sjögren Syndrome. *Italian Journal of Anatomy and Embryology* 127(2): 95-98. doi: 10.36253/ijae-14705

Data Availability Statement: All relevant data are within the paper and its Supporting Information files.

Competing Interests: The Author(s) declare(s) no conflict of interest.

Motor behavioural tests for phenotype evaluation of mouse models of ataxia: the case of Marinesco-Sjögren Syndrome

Anna Giulia Ruggieri, Michele Sallese*

Department of Innovative Technologies in Medicine and Dentistry, "G. d'Annunzio" University of Chieti-Pescara, 66100 Chieti, Italy
Center for Advanced Studies and Technology (CAST), "G. d'Annunzio" University of Chieti-Pescara, 66100 Chieti, Italy
*Corresponding author. E-mail: michele.sallese@unich.i

Abstract. Ataxias are a clinically relevant group of neurological diseases characterized by impaired motor coordination that affects both static and dynamic control of body movements. Among the autosomal recessive ataxias there is Marinesco-Sjogren syndrome (MSS). The main clinical signs of MSS are incoordination with cerebellar atrophy, and myopathy associated to hypotonia. Mouse models of MSS (e.g. woozy mouse) closely mimic human pathology and are widely used to study this disease. In fact, the woozy mouse was helpful in understanding that molecular alteration occurs before clinical signs. To data, several motor behavioural tests have been developed including rotarod, beam walking, and grip-strength. Some of these tests were effective to reveal MSS ataxia only at specific stages of the disease. To achieve these results, it is important to apply the most appropriate motor behavioural tests that are able to sensitively assess the specific phenotype. However, the administration of additional motor tests would be useful to better define the coordination and motor problems in MSS. Cognitive tests should also be considered to examine whether the woozy model has mental retardation. In conclusion, motor and cognitive tests are essential for the assessment of disease stage and future therapies in ataxias, including MSS.

Keywords: ataxia, Marinesco-Sjögren Syndrome, SIL1, mouse model, motor test.

INTRODUCTION

The cerebellum is the region of the brain responsible for motor movement coordination, balance and walking. Impairments of this area lead to deficits in controlling voluntary muscle activity, maintaining posture and motor learning (Jimsheleishvili and Dididze, 2023). These symptoms can be enclosed in the term "ataxia", which refers to a physical finding due to cerebellar dysfunction.

Ataxias are classified mainly in hereditary and acquired. Autosomal dominant ataxias are identified as spinocerebellar ataxias (SCA), while autosomal recessive cerebellar ataxias (ARCAs) are classified according to the presence and the severity of sensory neuropathy (Kuo, 2019).

ARCAs are characterized by high genetic heterogeneity and variable phenotypes (Beaudin et al., 2017). Among them, Friedreich's ataxia is the most common form, and it is used as referring point. Indeed, it is possible to distinguish between Friedreich's ataxia like disorders, with and without cerebellar atrophy, and early-onset ataxias with cerebellar atrophy, such as ataxia telangiectasia, and Marinesco-Sjögren Syndrome (MSS) (Fogel and Perlman, 2007).

MSS is characterized by cerebellar ataxia due to degeneration of Purkinje cells, associated with myopathy and congenital cataracts. Symptomatology may include also mental retardation, short stature, skeletal deformities, hypergonadotropic hypogonadism and intention tremor (Anna-Kaisa Anttonen, 2006).

SIL1 gene mutation is the major cause of MSS (Anttonen et al., 2005; Senderek et al., 2005). This gene encodes the endoplasmic reticulum (ER) cochaperone Sil1, required for ADP-ATP exchange from the chaperone BiP, which in turn is able to release folded proteins.

Non-functional Sil1 protein is responsible of the accumulation of unfolded proteins into the ER, thus triggering the activation of the unfolded protein response (UPR), which contributes to neurodegeneration and myopathy (Figure 1) (Chiesa and Sallese, 2020; Potenza et al., 2021; Restelli et al., 2019). Both cell lines and mouse models (e.g. woozy mice) carrying the SIL1 mutation are useful for studying MSS (Roos et al., 2014; Ruggieri and Sallese, 2022; Zhao et al., 2005).

In this work we focus our attention on the study of mouse models and in particular on motor behavioural tests, which are considered powerful tools in the case of neurological diseases (Brooks and Dunnett, 2009). A more comprehensive characterization of the motor functions of woozy mouse may be useful to better understand MSS and its progression, and to evaluate the efficacy of potential therapeutic treatments.

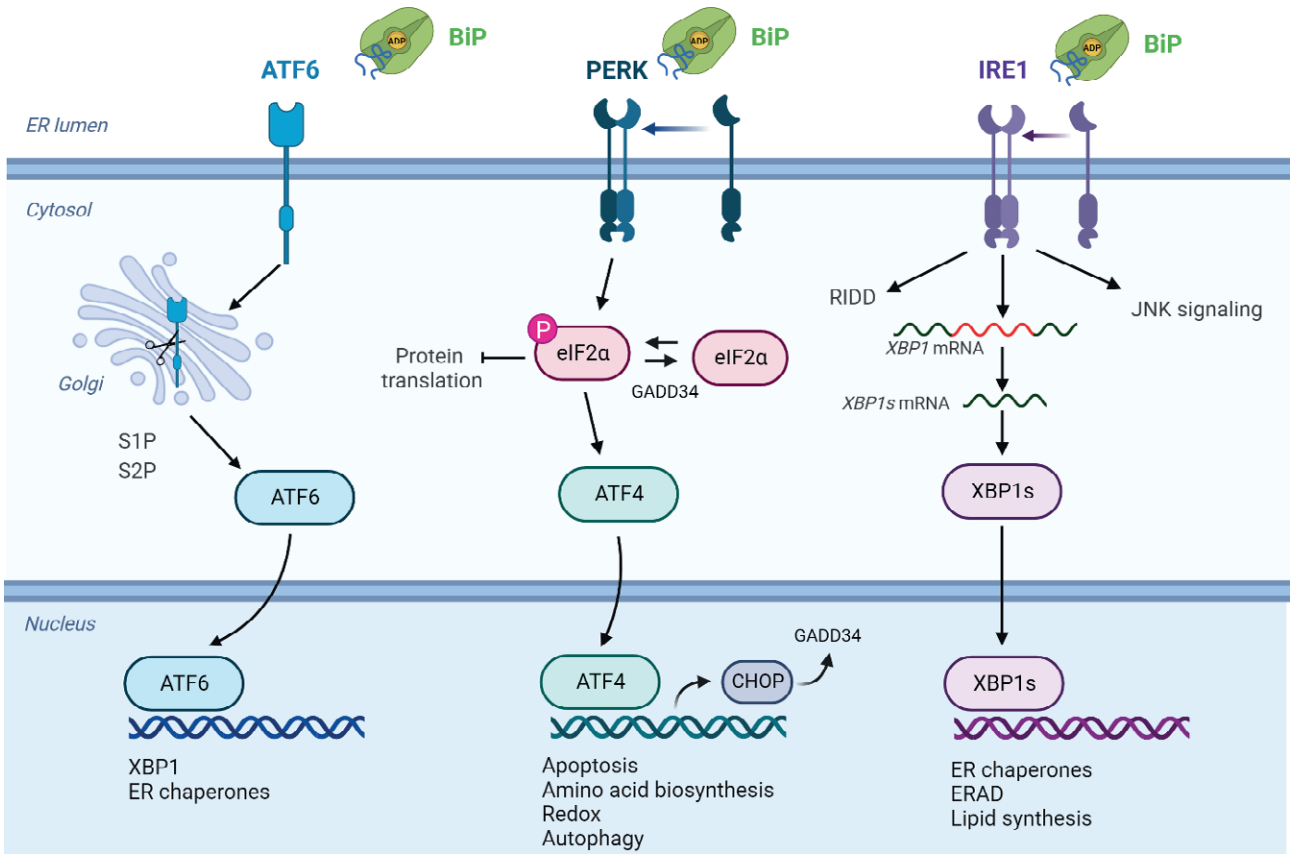

Figure 1. Unfolded protein response is a cellular defense mechanism whose purpose is to reestablish the normal protein homeostasis in the ER, through the activation of three ER transmembrane sensors: inositol-requiring enzyme 1 (IRE1), activating transcription factor 6 (ATF6), and protein kinase R (PKR)-like endoplasmic reticulum kinase (PERK). Their signaling pathways result in enhanced ER protein folding potential, increased degradation of unfolded proteins, and decreased protein synthesis. Figure adapted from "UPR Signaling (ATF6, PERK, IRE1)", by BioRender.com (2023). Retrieved from https://app.biorender.com/biorender-templates.

MOTOR BEHAVIOURAL TESTS

Motor behavioural tests are essential for assessing motor capabilities of mice, such as coordination and balance, muscle strength and locomotor activity. Because of the high number of existing tests, a correct selection should be made on four criteria: validity, reliability, sensitivity and utility (Brooks and Dunnett, 2009). Here we present the presumably most representative motor behavioural tests for characterizing the woozy mouse phenotype.

Rotarod test

Rotarod is a simple and common test for a first evaluation of locomotor deficits and coordination of mice. It consists of a circular rod turning at a constant or accelerating speed. Before the test, mice undergo a training trial at low speed, then the real trial is repeated two or three times and latency to fall is recorded (Brooks and Dunnett, 2009). The rotarod test can be performed multiple times at different stages of disease. As drawbacks, animals' weight could affect the performance, it is difficult to distinguish between fatigue and coordination deficits and some animals refuse to stay on the rotating rod.

Grande et al. tested woozy mice on rotarod from 6 to 34 weeks of age, to determine the first manifestations of motor dysfunction and to follow its progression. They found no significative differences from controls until 10 weeks, by which time woozy mice showed a shorter latency to fall up to 16 weeks (Grande et al., 2018). Therefore, the rotarod test is confirmed to be a valid tool to evaluate locomotor deficits but in the case of MSS it is not able to detect alterations in the initial stages of the disease.

Beam walking test

Beam walking assay is useful for assessing fine motor coordination and sense of balance. Mice have to walk across an elevated narrow beam and reach the cage. This test needs two days of training, and then performance is evaluated by measuring the time taken to cross the beam and the occurred number of paw slips (Brooks and Dunnett, 2009; Luong et al., 2011). Beam walking assay is more sensitive than rotarod and does not require expensive equipment, but sometimes mice refuse to walk across the beam or are unable to balance on it. In woozy mice this test is able to reveal subtle deficits in motor functions and balance only at the beginning of the disease, because it is hard to perform with severe ataxic mice (Grande et al., 2018)

Grip strength test

Grip strength test is used to evaluate neuromuscular function by measuring the muscle strength. There are three ways to perform this test: by assessing the ability of the mouse to stick to an inverted wire grid using the four limbs; by measuring the time a mouse can hang on a wire only with its forelimbs; by determining the force needed to pull the mouse off a narrow bar connected to a force transducer (Brooks and Dunnett, 2009). Grip strength test is easy to carry on and effective in monitoring the progression of motor dysfunctions, but its performance could be affected by diet restrictions, handling, body weight and muscle fatigue. Woozy mice show first signs of myopathy at 16 weeks of age (Grande et al., 2018), therefore grip strength assay could be useful to measure the progression of skeletal muscle degeneration in these animals.

CONCLUSIONS

Mouse models are extremely important for the study of disorders affecting movement, such as ataxias, and for the development of effective treatments. A large number of motor behavioural assays has been validated to assess motor capabilities of mice, and the combined use of these tests could provide useful information about MSS. Cognitive tests that are able to evaluate memory, learning process and attention, should be taken into account for a more comprehensive characterization of woozy mouse phenotype.

ACKNOWLEDGEMENTS

This research was funded by the Italian Telethon ONLUS Foundation, Rome, Italy, grants N° GGP20092 to M.S.

REFERENCES

Anna-Kaisa Anttonen, 2006. Marinesco-Sjögren Syndrome. GeneReviews 12.

Anttonen, A.-K., Mahjneh, I., Hämäläinen, R.H., Lagier-Tourenne, C., Kopra, O., Waris, L., Anttonen, M., Joensuu, T., Kalimo, H., Paetau, A., Tranebjaerg, L., Chaigne, D., Koenig, M., Eeg-Olofsson, O., Udd, B., Somer, M., Somer, H., Lehesjoki, A.-E., 2005. The gene disrupted in Marinesco-Sjögren syndrome encodes SIL1, an HSPA5 cochaperone. Nat. Genet. 37, 1309–1311. https://doi.org/10.1038/ng1677

Beaudin, M., Klein, C.J., Rouleau, G.A., Dupré, N., 2017. Systematic review of autosomal recessive ataxias and proposal for a classification. Cerebellum Ataxias 4, 3. https://doi.org/10.1186/s40673-017-0061-y

Brooks, S.P., Dunnett, S.B., 2009. Tests to assess motor phenotype in mice: a user's guide. Nat. Rev. Neurosci. 10, 519–529. https://doi.org/10.1038/nrn2652

Chiesa, R., Sallese, M., 2020. Review: Protein misfolding diseases – the rare case of Marinesco-Sjögren syndrome. Neuropathol. Appl. Neurobiol. 46, 323–343. https://doi.org/10.1111/nan.12588

Fogel, B.L., Perlman, S., 2007. Clinical features and molecular genetics of autosomal recessive cerebellar ataxias. Lancet Neurol. 6, 245–257. https://doi.org/10.1016/S1474-4422(07)70054-6

Grande, V., Ornaghi, F., Comerio, L., Restelli, E., Masone, A., Corbelli, A., Tolomeo, D., Capone, V., Axten, J.M., Laping, N.J., Fiordaliso, F., Sallese, M., Chiesa, R., 2018. PERK inhibition delays neurodegeneration and improves motor function in a mouse model of Marinesco-Sjögren syndrome. Hum. Mol. Genet. 27, 2477–2489. https://doi.org/10.1093/hmg/ddy152

Jimsheleishvili, S., Dididze, M., 2023. Neuroanatomy, Cerebellum, in: StatPearls. StatPearls Publishing, Treasure Island (FL).

Kuo, S.-H., 2019. Ataxia. Contin. Lifelong Learn. Neurol. 25, 1036. https://doi.org/10.1212/CON.0000000000000753

Luong, T.N., Carlisle, H.J., Southwell, A., Patterson, P.H., 2011. Assessment of Motor Balance and Coordination in Mice using the Balance Beam. J. Vis. Exp. JoVE 2376. https://doi.org/10.3791/2376

Potenza, F., Cufaro, M.C., Di Biase, L., Panella, V., Di Campli, A., Ruggieri, A.G., Dufrusine, B., Restelli, E., Pietrangelo, L., Protasi, F., Pieragostino, D., De Laurenzi, V., Federici, L., Chiesa, R., Sallese, M., 2021. Proteomic analysis of marinesco–sjogren syndrome fibroblasts indicates pro-survival metabolic adaptation to SIL1 loss. Int. J. Mol. Sci. 22. https://doi.org/10.3390/ijms222212449

Restelli, E., Masone, A., Sallese, M., Chiesa, R., 2019. Neuroprotective modulation of the unfolded protein response in Marinesco-Sjögren syndrome: PERK signaling inhibition and beyond. Neural Regen. Res. 14, 62–64. https://doi.org/10.4103/1673-5374.243708

Roos, A., Buchkremer, S., Kollipara, L., Labisch, T., Gatz, C., Zitzelsberger, M., Brauers, E., Nolte, K., Schröder, J.M., Kirschner, J., Jesse, C.M., Goebel, H.H., Goswami, A., Zimmermann, R., Zahedi, R.P., Senderek, J., Weis, J., 2014. Myopathy in Marinesco–Sjögren syndrome links endoplasmic reticulum chaperone dysfunction to nuclear envelope pathology. Acta Neuropathol. (Berl.) 127, 761–777. https://doi.org/10.1007/s00401-013-1224-4

Ruggieri, A.G., Sallese, M., 2022. Genotype-phenotype correlation and adaptive proteome reorganization in Marinesco-Sjögren syndrome. Ital. J. Anat. Embryol. 126, 71–75. https://doi.org/10.36253/ijae-13802

Senderek, J., Krieger, M., Stendel, C., Bergmann, C., Moser, M., Breitbach-Faller, N., Rudnik-Schöneborn, S., Blaschek, A., Wolf, N.I., Harting, I., North, K., Smith, J., Muntoni, F., Brockington, M., Quijano-Roy, S., Renault, F., Herrmann, R., Hendershot, L.M., Schröder, J.M., Lochmüller, H., Topaloglu, H., Voit, T., Weis, J., Ebinger, F., Zerres, K., 2005. Mutations in SIL1 cause Marinesco-Sjögren syndrome, a cerebellar ataxia with cataract and myopathy. Nat. Genet. 37, 1312–1314. https://doi.org/10.1038/ng1678

Zhao, L., Longo-Guess, C., Harris, B.S., Lee, J.-W., Ackerman, S.L., 2005. Protein accumulation and neurodegeneration in the woozy mutant mouse is caused by disruption of SIL1, a cochaperone of BiP. Nat. Genet. 37, 974–979. https://doi.org/10.1038/ng1620

IJAE
ITALIAN JOURNAL OF ANATOMY AND EMBRYOLOGY

Firenze University Press
www.fupress.com/ijae

OPEN ACCESS

Citation: Valente, F., Falconio, L., Falcinelli, C., Roy, S., Trubiani, O., & Traini, T. (2023). Artificial intelligence and finite element analysis: applications in implant dentistry. *Italian Journal of Anatomy and Embryology* 127(2): 99-103. doi: 10.36253/ijae-14708

Data Availability Statement: All relevant data are within the paper and its Supporting Information files.

Competing Interests: The Author(s) declare(s) no conflict of interest.

Artificial intelligence and finite element analysis: applications in implant dentistry

Francesco Valente[1,2,*,A], Luigi Falconio[1,2,A], Cristina Falcinelli[3], Sandipan Roy[4], Oriana Trubiani[1,2], Tonino Traini[1,2]

[1] *Department of Innovative Technologies in Medicine & Dentistry, University "G. d'Annunzio" of Chieti-Pescara, Via dei Vestini 31, 66100 Chieti, Italy*
[2] *Electron Microscopy Laboratory, University "G. d'Annunzio" of Chieti-Pescara, Via dei Vestini 31, 66100 Chieti, Italy*
[3] *Department of Engineering and Geology, University "G. d'Annunzio" of Chieti-Pescara, Viale Pindaro 42, Pescara 65127, Italy*
[4] *Department of Mechanical Engineering, SRM Institute of Science and Technology, Kattankulathur, Tamil Nadu 603203, India*
*Corresponding author. E-mail: francesco.valente@unich.it
[A] These authors equally contribute to this work.

Abstract. Artificial intelligence (AI) has shown great potential across scientific disciplines, including implant dentistry. This review investigates the applications of AI in Finite Element Analysis (FEA) of dental implants, examining implications, limitations, and future directions. By following Preferred Reporting Items for Systematic Reviews and Meta-Analyses (PRISMA) guidelines, relevant articles were obtained from PubMed, Scopus, Web of Science, and Google Scholar databases. Six articles were included, covering topics such as osseointegration assessment, implant design optimization, and bone healing prediction. Integrating AI and FEA can improve parameter optimization, computational efficiency, and analysis time. FEA simulations were consistently used to train AI models, which were then validated against FEA-calculated data. While AI in dental implantology is still in its early stages, opportunities for innovation and refinement are apparent. Challenges, such as algorithmic misconduct and interpretation of AI outputs, need to be addressed through collaborative efforts between clinicians and computer engineers. Future research should explore incorporating factors like bone homeostasis and multiscale analysis to enhance understanding of peri-implant bone response. Long-term clinical studies are necessary to validate AI model predictions in real-world scenarios.

Keywords: artificial intelligence, machine learning, deep learning, finite element analysis, dental implants.

INTRODUCTION

Artificial intelligence (AI) is an interdisciplinary field of computer science that focuses on the development of intelligent systems and algorithms capable of emulating human cognitive abilities. Its fundamental goal is to

design and create computational models and algorithms that can acquire, process, analyze, and interpret vast amounts of data, enabling machines to perform complex tasks that traditionally require human intelligence (Aiken and Epstein 2000). In recent years, the integration of artificial intelligence in the field of implant dentistry has witnessed significant advancements (Revilla-León et al. 2021). Finite Element Analysis (FEA) plays a crucial role in evaluating the biomechanical behavior of dental implants and supporting bone, aiding in the design and optimization of implant-supported restorations. However, traditional FEA approaches rely on manual inputs and assumptions, which may introduce limitations, potential inaccuracies, and long testing times (Falcinelli et al. 2023). By incorporating AI techniques, such as machine learning and deep learning algorithms, FEA can leverage large datasets and complex models to enhance its predictive capabilities and overcome these limitations.

This mini-review aims to explore the applications of AI in FEA within the field of implant dentistry, highlighting its implications for scientific research, the current limitations, and the possible paths for future development.

MATERIALS AND METHODS

Reporting of this review follows the Preferred Reporting Items for Systematic Reviews and Meta-Analyses (PRISMA) guidelines (Moher et al. 2010). The search included articles about AI and FEA in implant dentistry: all study types excluding reviews, only English-language articles, and articles published until June 2023 were included. The literature search was performed on electronic databases via PubMed, Scopus, Web of Science, and Google Scholar. The search strategy used a combination of MeSH terms: (artificial intelligence OR machine learning OR deep learning) AND finite element analysis AND dental implant. The articles were selected based on their title and abstract, and then the full text was evaluated by two different reviewers (F.V., L.F.). Cohen's K test was used to assess the agreement between the two reviewers. Disagreements were resolved by consensus with a third examiner (C.F.) to identify studies that passed the selection criteria.

RESULTS

The results of the literature search are shown in Figure 1. Six articles were included in the review. One article was published in 2009 and five articles from 2018. There was substantial agreement between the two investigators for the articles that were selected, both for the title/abstract and the full-text screening (Cohen's K value=0.90 and 1, respectively). The articles and their main findings are summarized in Table 1.

DISCUSSION

Upon initial observation, it can be observed, except for the publication by Zaw and coworkers (Zaw et al. 2009), all the articles analyzed in this review were published in very recent years. This confirms the recent significant growth in interest regarding AI technologies. Consequently, there has been a notable rise in research endeavors focused on incorporating this captivating technology into various scientific domains. The articles surveyed in relation to the integration of AI into FEA exhibit a common approach, irrespective of subject matter, analyzed variables, or AI methodologies employed. The general method entails the use of FEA for initial simulations, employing predetermined parameters and variables. Subsequently, the obtained FEA data are extrapolated and employed to train the AI model. The output generated by the AI is then validated and compared against the FEA-calculated data. Consequently, the overarching objective of these studies primarily revolves around substituting FEA calculations with AI computations, with a view to enhancing parameter optimization, computational efficiency, and overall time required for analysis. The exception was the study performed by Kwak et al. (Kwak et al. 2021). In the context of their study, advanced image recognition techniques were adopted, and ultrasonic signals were inverted using a Convolutional Neural Network (CNN) to assess the osseointegration phenomena. The main topics investigated by the different studies were: osseointegration assessment (Kwak et al. 2021), implant design optimization (Zaw et al. 2009; Roy et al. 2018; Li et al. 2019; Choudhury et al. 2022), and prediction of bone healing around dental implants (Kung et al. 2023).

From this review it can be noticed that AI applied to in silico studies in in dental implantology is still in the early stages, but its potential is very promising. AI's main limitation is its inability to provide direct interpretation, making misinterpretations possible due to algorithmic misconduct and training method. To mitigate risks, collaboration between experienced clinicians and expert computer engineers is essential in the development of AI programs. Further evaluations should encompass the actual knowledge on bone homeostasis (Valente et al. 2022) and the recent recognition of the need for a multiscale analysis to predict peri-implant

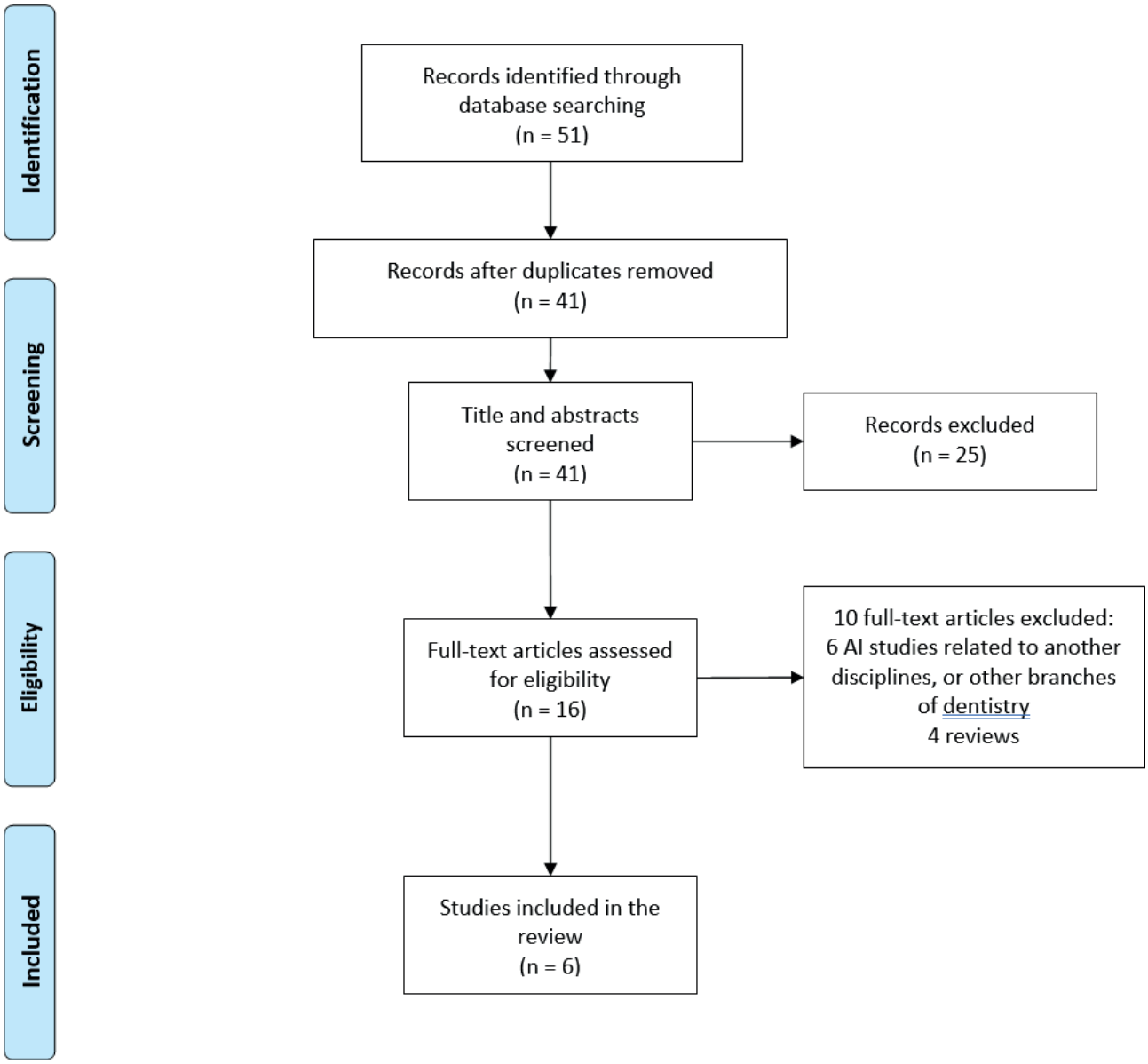

Figure 1. PRISMA flow diagram with information through phases of study selection (Moher et al. 2010).

bone response (Falcinelli et al. 2023). The incorporation of such aspects could help obtain information about the relation among implant design, distribution of stress applied to the bone, bone growth and histological arrangement. The integration of AI will allow for continuous observation of these parameters and their interrelated development, which is difficult to achieve through traditional clinical experiments, and can provide predictions prior to the insertion surgery, reducing the need for costly trial and error procedures. This can potentially save time and resources for both patients and healthcare providers.

CONCLUSIONS

The conclusion of this mini-review can be summarized as follows:

1. AI integration with FEA in dental implantology is still in its early stages.
2. FEA is mainly used to extrapolate data for AI training.
3. The main topics covered by the studies include osseointegration assessment, implant design optimization, and prediction of bone healing around dental implants.

Table 1. Overview of the studies included in the review and their main features.

Reference	AI models used	Study's purposes	Main outcomes
Zaw et al. 2009	- Neural Network (NN)	To validate a rapid inverse analysis approach based on the Reduced-Basis Method (RBM) and Neural Network to identify the elastic modulus (Young's modulus) of the interfacial tissue between a dental implant and the surrounding bones	Results identified by trained NN are very accurate, reliable, and the computational saving is very significant
Roy et al. 2018	- Genetic Algorithm (GA) - Artificial Neural Network (ANN)	To present a novel approach for designing patient-specific dental implants using FEA and computational intelligence techniques	Genetic algorithm is successfully used for designing dental implant to achieve the desired microstrain and implant stress
Li et al. 2019	- Support Vector Regression (SVR) - GA	To propose an uncertainty optimization approach for dental implants to reduce stress at the implant-bone interface	SVR model optimizes the implant design variables to minimize the stress at the implant-bone interface. There is a reduction of 36.6% of the stress at the implant-bone interface compared with the FEA model
Kwak et al. 2021	- Convolutional Neural Network (CNN)	To present a method to assess the soft tissue thickness at the bone-implant interface (BII) based on the analysis of its ultrasonic response using a simulation-based CNN	The linear correlation between actual and estimated soft tissue thickness shows correlation values equal to 99.52% and 99.65% for microscopic and macroscopic roughness, supporting the reliability of the proposed assessment of osseointegration phenomena
Choudhury et al. 2022	- ANN - GA	To present a methodology for designing patient-specific basal dental implants using FEA and ANN	The ANN metamodel developed from the FE simulation data is found to be able to formulate the fitness function for the optimization using GA to achieve desired microstrain in the peri-implant bone for a better osseointegration
Kung et al. 2023	- Deep Learning Network (DLN)	To present a DLN model that can predict tissue differentiation around dental implants in patients with different ages, genders, and occlusal forces	The network successfully surrogated the finite element (FE) calculation and mechano-regulation algorithm and significantly increased the calculation efficiency with an accuracy of 97.23%

4. All studies demonstrated the accuracy and efficiency of AI output compared to FEA.
5. Incorporating additional factors such as multiscale analysis can provide a more comprehensive understanding of the peri-implant bone response.
6. Long-term clinical studies are needed to validate the predictions made by AI models and assess their reliability in real-world scenarios.
7. The cooperation among researchers, clinicians, and AI developers is crucial for addressing technical obstacles and successfully implementing AI technology in the field of dental implantology.

ACKNOWLEDGMENTS

This research was funded by Tonino Traini ex 60% University of Chieti funds.

Cristina Falcinelli acknowledges the funding by the European Union - Fondo Sociale Europeo - PON Ricerca e Innovazione 2014–2020 (azioneIV.6) - FSE-REACT EU and the support of the Italian National Group for Mathematical Physics (GNFM-INdAM).

BIBLIOGRAPHY

Aiken R, Epstein R. 2000. Ethical guidelines for AI in education: Starting a conversation. International Journal of Artificial Intelligence in Education. 11:163–176.

Choudhury S, Rana M, Chakraborty A, Majumder S, Roy S, RoyChowdhury A, Datta S. 2022. Design of patient specific basal dental implant using Finite Element method and Artificial Neural Network technique. Proc Inst Mech Eng H. 236(9):1375–1387.

Falcinelli C, Valente F, Vasta M, Traini T. 2023. Finite element analysis in implant dentistry: State of the art and future directions. Dental Materials. 39(6):539–556. https://www.sciencedirect.com/science/article/pii/S0109564123000921.

Kung P-C, Hsu C-W, Yang A-C, Chen N-Y, Tsou N-T. 2023. Prediction of Bone Healing around Dental

Implants in Various Boundary Conditions by Deep Learning Network. Int J Mol Sci. 24(3):1948.

Kwak Y, Nguyen V-H, Hériveaux Y, Belanger P, Park J, Haïat G. 2021. Ultrasonic assessment of osseointegration phenomena at the bone-implant interface using convolutional neural network. J Acoust Soc Am. 149(6):4337.

Li H, Shi M, Liu X, Shi Y. 2019. Uncertainty optimization of dental implant based on finite element method, global sensitivity analysis and support vector regression. Proc Inst Mech Eng H. 233(2):232–243.

Moher D, Liberati A, Tetzlaff J, Altman DG. 2010. Preferred reporting items for systematic reviews and meta-analyses: The PRISMA statement. International Journal of Surgery. 8(5):336–341. https://linkinghub.elsevier.com/retrieve/pii/S1743919110000403.

Revilla-León M, Gómez-Polo M, Vyas S, Barmak BA, Galluci GO, Att W, Krishnamurthy VR. 2021. Artificial intelligence applications in implant dentistry: A systematic review. J Prosthet Dent. 129(2):293–300.

Roy S, Dey S, Khutia N, Roy Chowdhury A, Datta S. 2018. Design of patient specific dental implant using FE analysis and computational intelligence techniques. Applied Soft Computing Journal. 65:272–279. https://www.scopus.com/inward/record.uri?eid=2-s2.0-85041419810&doi=10.1016%2fj.asoc.2018.01.025&partnerID=40&md5=afeb3749d12788f70ce5f4b34cf2228b.

Valente F, Trubiani O, Traini T. 2022. The role of the applied load in bone homeostasis and its implications in implant dentistry: a mini-review. Italian Journal of Anatomy and Embryology. 126(2):39–42. https://oajournals.fupress.net/index.php/ijae/article/view/13786.

Zaw K, Liu GR, Deng B, Tan KBC. 2009. Rapid identification of elastic modulus of the interface tissue on dental implants surfaces using reduced-basis method and a neural network. J Biomech. 42(5):634–641.

IJAE
ITALIAN JOURNAL OF ANATOMY AND EMBRYOLOGY

Firenze University Press
www.fupress.com/ijae

OPEN ACCESS

Citation: Ceci, M., Trerotola, M., & Iezzi, M. (2023). STING agonists in cancer immunotherapy: a brief review. *Italian Journal of Anatomy and Embryology* 127(2): 105-107. doi: 10.36253/ijae-14710

Data Availability Statement: All relevant data are within the paper and its Supporting Information files.

Competing Interests: The Author(s) declare(s) no conflict of interest.

STING agonists in cancer immunotherapy: a brief review

Martina Ceci[1,3,*], Marco Trerotola[1,2], Manuela Iezzi[1,3]

[1] *Center for Advanced Studies and Technology (CAST), University "G. d'Annunzio", 66100 Chieti, Italy*
[2] *Department of Medical, Oral and Biotechnological Sciences, University "G. d' Annunzio", 66100 Chieti, Italy*
[3] *Department of Neurosciences, Imaging and Clinical Sciences, University "G. d' Annunzio", 66100 Chieti, Italy*
* Corresponding author. E-mail: martina.ceci@unich.it

Abstract. The "STimulator of INterferon Genes" (STING) represents the primary sensors of cytosolic double-stranded DNA (dsDNA). The STING cellular signaling pathway is considered an attractive pharmacological target for cancer immunotherapy due to its immunostimulatory potential. In fact, activation of the intracellular STING protein triggers the secretion of type I IFNs, which results in immune-mediated tumor elimination and generation of antitumor immune memory. Two types of STING agonists were developed: cyclic dinucleotides (CDNs) and non-nucleotide small molecule agonists. Preclinical studies of STING agonists have demonstrated remarkable results in many tumor models, resulting in complete and durable therapeutic responses in a majority of treated mice. This review provides a brief summary of the latest research findings on STING agonists, their delivery to the tumor and the strategies being employed to enhance their efficacy in cancer immunotherapy.

Keywords: STimulator of INterferon Genes, STING agonists, type I interferon, antitumor response, drug delivery.

INTRODUCTION

The innate immune system is the first defense line in mammals. One of the significant immune responses is the pattern recognition receptors (PRRs), which recognize the different pathogen and damage-associated molecular patterns (PAMPs and DAMPs). PRRs are germline-encoded, and they play a crucial role in the immune system's function (Hopfner *et al.*, 2020). PAMPs and DAMPs derived from bacteria, viruses, or endogenous cytosolic self-DNA from tumor cells activate PRRs, leading to the production of soluble mediators such as type I interferons and pro-inflammatory cytokines (Amouzegar *et al.*, 2021).

The "STimulator of INterferon Genes" (STING) family of PRRs was discovered in 2008, and they are considered the primary sensors of cytosolic

double-stranded DNA (dsDNA) (Ishikawa *et al.,* 2008). STING protein is expressed in both innate and adaptive immune cells, and non-immune cells, including endothelial cells, epithelial cells, and cancer cells (Garland *et al*., 2022). STING activation has immunological effects that are mediated by the secretion of IFNs, especially type I IFNs (IFN-I) such as IFN-ß. The therapeutic responses to STING activation include dendritic cell maturation, antitumor macrophage polarization, enhanced priming and activation of T cells, improved T cell infiltration in tumor sites, and promotion of natural killer (NK) cell activation (Garland *et al*., 2022). These responses to the STING pathway activation result in immune-mediated tumor elimination and the generation of antitumor immune memory. Therefore, the STING pathway is considered an attractive pharmacological target for cancer immunotherapy due to its immunostimulatory potential. This review provides an overview of the latest research findings on STING agonists in cancer treatment. It also discusses their delivery to the tumor and the strategies being employed to enhance their efficacy in cancer immunotherapy.

STING CELLULAR SIGNALING PATHWAY

Typically, cytosolic nucleases break down foreign DNA in cells. However, if there is abnormal dsDNA in the cytosol due to pathogenic infections or cellular damage, this activates the cyclic guanosine monophosphate-adenosine monophosphate synthase cGAS (discovered by Sun *et al.* in 2013), which synthesizes a cyclic dinucleotide called cGAMP (2'-3'-cyclic GMP-AMP). This signals the STING protein in the endoplasmic reticulum, which moves to the perinuclear Golgi and binds the TANK-binding kinase 1 (TBK1). Together, the complex phosphorylates transcription factors like IRF3 and NF-κB, which leads to the production of IFN-I in the cell.

STING AGONISTS IN CANCER IMMUNOTHERAPY

To achieve anti-cancer effects by mimicking the activation of STING pathway signaling, STING agonists have been developed. STING agonists come in two types: cyclic dinucleotides (CDNs) and non-nucleotide small molecule agonists. CDNs are the natural ligands of the STING protein but face limitations in clinical applications due to their chemical properties. Synthetic CDNs are being formulated to improve their performance, with ADU-S100 being tested in clinical trials for head and neck squamous cell carcinoma and lymphomas (Zandberg *et al.,* 2020). Among the non-nucleotide small molecule agonists, dimeric amidobenzimidazole (diABZI) is one of the most promising. Discovered in 2018 by Ramanjulu *et al.,* diABZI is the first effective non-nucleotide STING agonist used worldwide, with great potential to enhance human cancer immunotherapy. In immunocompetent mice with syngeneic colorectal tumors (CT-26), intravenous injection of diABZI has demonstrated tumor regression and increased overall survival time. In fact, 80% of treated animals were tumor-free until the end of the study (Ramanjulu *et al.,* 2018).

DELIVERY AND COMBINATION STRATEGIES FOR STING AGONISTS

The STING protein is located on the endoplasmic reticulum. To interact with STING, CDNs STING agonists need to passively diffuse through the lipophilic plasma membrane, which is challenging due to their anionic phosphate groups and high aqueous solubility (Garland *et al*., 2022).

Recent research shows that using liposomal delivery for STING agonists could have significant benefits. Different approaches are also in development: one study, led by Tse and colleagues, utilized lipid nanoparticles to deliver mRNA vaccines that encode a gain-of-function mutation of STING. This mutation allows for the expression of constitutively active STING, even without STING ligands. The researchers found that mice vaccinated with mRNA encoding $STING^{V155M}$, and inoculated with TC-1 tumors transformed with oncoproteins, experienced suppressed tumor growth and longer survival (Tse *et al.,* 2021).

A different team has created a cancer vaccine called STINGVAX that uses a CDNs STING agonist and granulocyte-macrophage colony-stimulating Factor (GM-CSF)-secreting cancer cells (Fu *et al.,* 2015). The study found that STINGVAX was able to successfully slow down the growth of tumors in mice with B16 melanoma, with just one injection. Tumors from mice who received STINGVAX had more $CD8^+$ IFN-γ^+ T cells compared to mice who were given a cancer cell vaccine without CDNs.

Moreover, the idea of combining STING agonists with existing immunotherapies is quite attractive. While CTLA-4 and PD-L1 blockades can successfully revive faltered T-cell responses, they rely on the availability of T cells and entry to the tumor core. STING agonists may act as an on-site vaccine, stimulating the T-cell response and reducing the threshold of myelosuppression that causes immune exclusion.

CONCLUSIONS

Currently, a crucial goal in the field of immuno-oncology is to discover new immunotherapeutic approaches that boost the immune system's ability to recognize and eliminate tumors that do not respond to FDA-approved immune checkpoint inhibitor antibodies.

The STING cellular signaling pathway is highly promising in this regard. Since the discovery of the STING protein in 2008, academic interest in this area has grown exponentially, as evidenced by the rapidly increasing number of publications, and by the development of an expanding number of STING agonists.

Significant advancements have been made also to improve the delivery of STING ligands: nanoparticles improve cytosolic cellular uptake and increase local retention of CDNs, offering a suitable approach for addressing the pharmacological shortcomings of locally administered CDNs.

Preclinical studies of an increasing number of STING agonists have demonstrated remarkable results in many tumor models, sometimes resulting in complete and durable therapeutic responses in a majority of treated mice.

There are still many open-ended questions regarding STING agonist therapy in human patients at this time, but the immense potential justifies the large number of researchers engaged on the topic.

REFERENCES

Amouzegar A, Chelvanambi M, Filderman JN et al. (2021) STING Agonists as Cancer Therapeutics. Cancers. 13: 1-24

Fu J, Kanne DB, Leong M, et al. (2015) STING agonist formulated cancer vaccines can cure established tumors resistant to PD-1 blockade. Sci Transl Med. 7(283): 1-24.

Garland KM, Sheehy Tl, Wilson JT. (2022) Chemical and Biomolecular Strategies for STING Pathway Activation in Cancer Immunotherapy. Chem Rev. 122: 5977-6039.

Hopfner KP, Hornung V. (2020) Molecular mechanisms and cellular functions of cGAS–STING signalling. Nat Rev Mol Cell Biol. 21:501-521.

Ishikawa H, Barber GN (2008) STING is an endoplasmic reticulum adaptor that facilitates innate immune signalling. Nature. 455:674-678.

Ramanjulu JM, Pesiridis GS, Yang J, et al. (2018) Design of amidobenzimidazole STING receptor agonists with systemic activity. Nature. 564:439-443.

Sun L, Wu J, Du F, et al. (2013) Cyclic GMP-AMP Synthase is a Cytosolic DNA Sensor that activates the Type-I Interferon Pathway. Science. 339: 1-15.

Tse SW, McKinney K, Walker W, et al. (2021) mRNA-encoded, constitutively active STING^{V155M} is a potent genetic adjuvant of antigen-specific CD8^{+} T cell response. Mol Ther. 29(7):2227-2238.

Zandberg DP, Ferris R, Laux D, et al. (2020) 71P A phase II study of ADU-S100 in combination with pembrolizumab in adult patients with PD-L1+ recurrent or metastatic HNSCC: Preliminary safety, efficacy and PK/PD results. Ann Onc. 31(7):S1446-S1447

IJAE
ITALIAN JOURNAL OF ANATOMY AND EMBRYOLOGY

Firenze University Press
www.fupress.com/ijae

OPEN ACCESS

Citation: Mastrangelo, G., Santodirocco, M., Semerano, L., Palena, G., Sciannelli, V., Magistro, G., Marinucci, R., Di Sebastiano, P., & Palazzo, V. (2023). Clinical efficacy of cord blood platelet gel in chronic limb-threatening ischaemia patients: a case series. *Italian Journal of Anatomy and Embryology* 127(2): 109-113. doi: 10.36253/ijae-14713

Data Availability Statement: All relevant data are within the paper and its Supporting Information files.

Competing Interests: The Author(s) declare(s) no conflict of interest.

Clinical efficacy of cord blood platelet gel in chronic limb-threatening ischaemia patients: a case series

Giovanni Mastrangelo[1,2,*], Michele Santodirocco[3], Luigi Semerano[1], Giancarlo Palena[1], Vincenzo Sciannelli[1], Gabriele Magistro[1], Roberto Marinucci[1], Pierluigi Di Sebastiano[2], Vincenzo Palazzo[1]

[1] *Unit of Vascular Surgery, Fondazione IRCCS Casa Sollievo della Sofferenza, San Giovanni Rotondo (FG), 71013, Italy*
[2] *Department of Innovative Technologies in Medicine and Dentistry, University "G.D'Annunzio" Chieti-Pescara, 66100 Chieti, Italy*
[3] *Apulia Cord Blood Bank, Fondazione IRCCS Casa Sollievo della Sofferenza, San Giovanni Rotondo (FG), 71013, Italy*
*Corresponding author. E-mail: g.mastrangelo@operapadrepio.it

Abstract. The cord blood platelet gel (CBPG), rich in growth factors and chemoattractans molecules, is a useful tool to treat lesions with tissue loss as it accelerates remission and ensures the functional recovery of the limb. The results obtained in a series of 10 patients treated at the "Fondazione IRCCS Casa Sollievo della Sofferenza" in San Giovanni Rotondo (Italy) with CBPG in the treatment of revascularized patients with chronic limb-threatening ischemia (CLTI) are presented here. In the period 2017-2021, they were treated with surgical toileting of the ulcers and application of CBPG. As a general scheme, CBPG was applied once every 21 days for 3 times; 8 out of 10 patients observed had diabetes mellitus, of these 4 were on insulin therapy. One patient underwent a major amputation; two patients died for non-infectious causes. Studies in the literature show that CBPG is safe for patients affected by CLTI and undergoing revascularization, promoting faster healing. Our results appear to overlap this data, also showing CBPG as an effective therapeutic option for the treatment of vascularized patients with foot lesions for CLTI, reducing the risk of major amputation. In perspective, multicenter randomized studies are needed to evaluate immediate and late results.

Keywords: chronic limb-threatening ischemia, diabetic foot, human umbilical blood, platelet, thromboangiitis obliterans, regenerative medicine.

INTRODUCTION

Chronic limb-threatening ischemia (CLTI) is the end stage of peripheral artery disease (PAD). Moreover, it is a highly morbid disease, including significant mortality rates, limb loss, pain, and diminished health-related quality of life among those affected (Goodney et al.). For this reason, the management of CLTI in patients with foot lesions requires, after revascularia-

tion interventions, a long painful and expensive wound care. In the last years, CBPG has been successfully used for regenerative medicine in skin lesions (Piccin et al. 2017; Bisceglia et al. 2020), oral mucositis (Gelmetti et al. 2018) and orthopedics (Caiaffa et al. 2020).

PATIENTS AND METHODS

We report the case of 10 patients suffering from CLTI treated with vascularization intervention, ulcer's debridement and/or minor amputation and then cord blood platelet gel application (CBPG) in the Department of Vascular Surgery of the "Fondazione IRCCS Casa Sollievo della Sofferenza", located in San Giovanni Rotondo (Italy) between 2017 and 2021. As many as 8 patients had a type II diabetes; 2 patients had Buerger disease, also known as thromboangiitis obliterans; all patients had non-infected wounds prior to CBPG application and no local and systemic clinical signs of sepsis. Exclusion criteria included ongoing chemotherapy and oral corticosteroid therapy, a history of malignant tumors with a disease-free interval of 3 years or less. Informed consent was obtained from the patients prior to CBPG application and after approval of the Ethics Committee of our Hospital. Demographic characteristics, comorbidities, WIFi score, the type of treatment and outcome are listed in Table 1. Vascular lab testing after arterial revascularization demonstrated improved tibial artery flow in all patients with improved pulsatility and peak systolic velocity > 40 cm/s (Figure 1). Thereafter, each patient is addressed to standard wound care (normal saline solution and the surrounding skin was cleansed with betadine solution) and CBPG wound applications. First of all, it is determined the count 'ABO' cord group of the patient because the CBPG should be hemocompatible with the patient's blood (as well virological markers for HIV, HCB and HBV). The CBPG was applied topically on the wound and covered with sterile gauze. The CBPG protocol in our Department provides for one application each 21 days for 3 times. At the end of the protocol, patients underwent follow-up in the vascular lab on a monthly basis. Our clinical outcomes were: the survival of the patient and the preservation of the limb. CBPG is prepared from Cord Blood (CB) units collected after the informed consent has been collected from the mothers. The units were placed into plastic bags containing 25-30 mL of citrate-phosphate-dextrose anticoagulant by trained midwives, before and after placental delivery in natural deliveries and in Caesarean sections, respectively, according to the validated and standard Apulian Cord Blood Bank (located in the Casa Sollievo della Sofferenza Hospital) operating procedures. After storage and transportation at monitored room temperature to the CB banks were performed, the units were processed within 48 hours of collection. Units containing less than

Table 1 Demographic characteristics, comorbidities, Rutherford stage, the type of treatment, ulcer's characteristics of our cases (1 Peripheral artery disease 1=Buerger Disease, 2=type II diabetes; 2 coronary artery disease, 3 chronic kidney disease, 4 Wound-Ischemia-Foot Infection classification system ; 5 below-the-knee femoro-popliteal bypass, 6 Plain Old Balloon Angiopasty, 7 Drug Eluting Balloon, 8 endoarterectomy, 9 Above-the-knee femoro-popliteal bypass, 10 wound healing

Patient (year)	PAD[1]	Age	CAD[2]	CKD[3]	HbAc1 (mmol/L)	WIFi score[4]	Revascularization surgery strategy	Foot lesion	Outcome
1 (2017)	2	86	No	No	53	222	F-P bypass BK[5]	Gangrene I finger, 6 cm lenght medial ulcer	1th-toe amputation 72-month-follow-up died for cardiovascular disease
2 (2021)	2	74	Yes	Yes	54	131	F-P bypass BK	Two dorsalis ulcers	1th trans-metatarsal amputation
3 (2019)	2	62	Yes	No	51	222	PTA stenting	Forefoot amputation stump dehiscence	Complete WH[10]
4 (2020)	2	78	No	No	53	221	POBA[6]	I finger amputation stump dehiscence	Complete WH
5 (2018)	2	73	Yes	No	99	121	DEB[7]	10 cm length plantar ulcer	Complete WH 50-month-follow up died for cardiovascular disease
6 (2020)	2	83	Yes	No	57	231	POBA	I-II-III finger amputation stump dehiscence	Complete WH
7 (2020)	2	81	Yes	No	97	332	EA[8]	Infected heel ulcer	Tigh amputation
8 (2018)	2	72	Yes	Yes	55	221	F-P bypass AK[9]	External heel ulcer	Complete WH
9 (2020)	1	73	No	No	No diabetic	121	F-P bypass AK	Intergidital ulcers	Complete WH
10 (2018)	1	41	No	No	No diabetic	221	F-P bypass AK	Acral ulcers	Complete WH

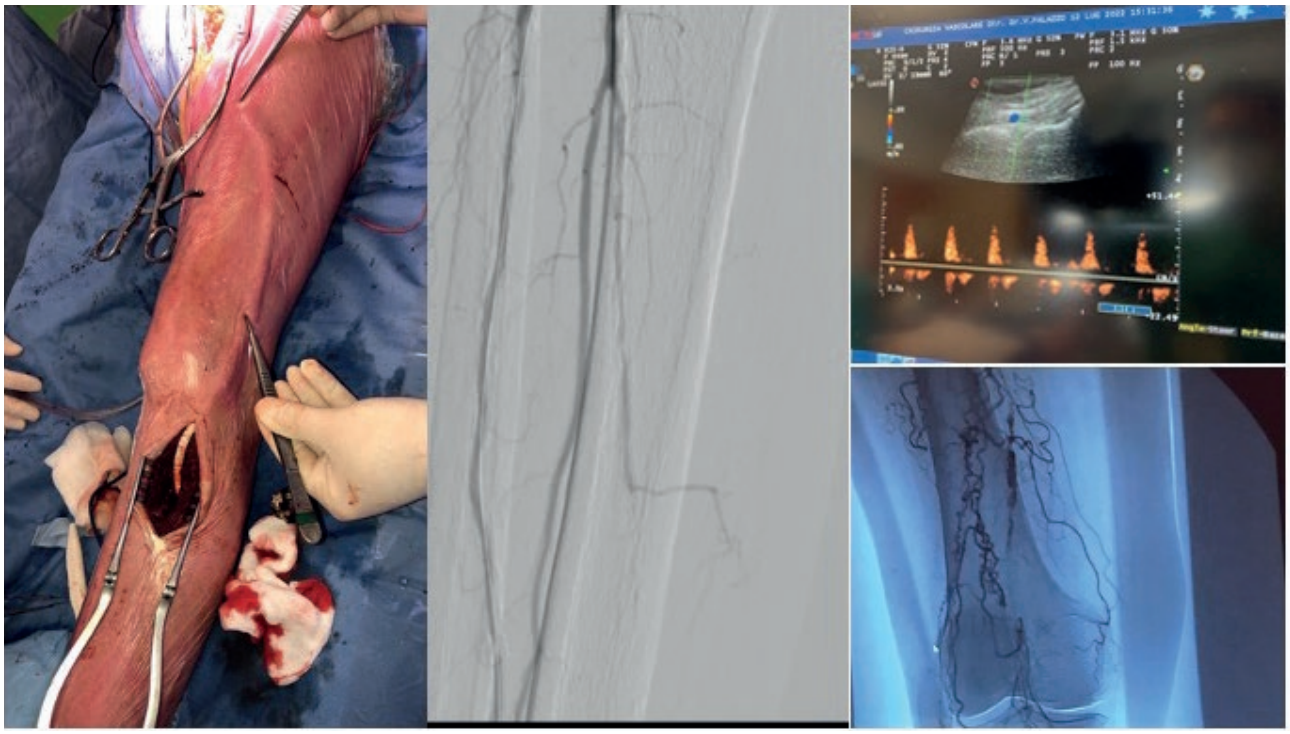

Figure 1. Vascular interventions realized in our case series are finalized to improve tibial distal arterial flow.

1.5 x 10^9 nucleated cells (which are not routinely banked for allogeneic hematopoietic transplantation purposes), a platelet count of 150 x 10^9/L or greater and a volume of 50 mL or greater were processed into CBPG within 48 hours of collection by the blood bank staff. The units are centrifuged at 200 to 210 x g for 10 to 15 minutes, and the platelet-rich plasma is collected in a transfer bag, which is centrifuged at 1800 to 2600 x g for 15 minutes. Most of the supernatant platelet-poor plasma is then removed, and the platelets are resuspended at a concentration of 1 +/- 0.2 x 10^6/ mL. The platelet concentrate, with an average volume of approximately 10 mL, is finally transferred into a storage bag and cryopreserved without cryoprotectant in a mechanical freezer at a temperature below -24°C. At the time of use, the platelet concentrate is thawed, and a platelet gel is formed by the addition of 10% calcium gluconate in a 1:3 ratio (Figure 2).

RESULTS

As many as 7 out of 10 patients had complete wound healing (WH). Two patients died of cardiovascular disease (table 1). Unfortunately, 1 out of 10 patients (patient n. 7) underwent a major amputation because of a gangrene of the limb at the 25-month follow-up.

DISCUSSION

Few are the clinical trials in the Literature (Samarkanova et al. 2020, Volpe et al. 2017) on the CBPG application to the diabetic foot, and our case series presents the results on foot lesion also in thromboangiitis obliterans, which is a nonatherosclerotic, inflammatory and thrombotic involvement of distal vessels of the extremities, most commonly affecting young male smokers. After vascular intervention, in selected patients, other adjuncts therapies can be used, including spinal cord stimulation (De Caridi et al 2016 feb, De Caridi et al. 2016 Apr) and vacuum-assisted wound (VAC) therapy (De Caridi et al 2016 Jun.; De Caridi et al. 2016 Oct.) and recently bioengineered tissues or skin substitutes and growth factors (Mannari et al. 2002, Serra et al 2013), have been used to improve WH. Impaired WH in PAD patients is due to poor angiogenesis, diminished leukocyte migration, early fibroblast senescence, extended inflammatory phase and decreased skin tensile strength, which enables wound recurrence. The interest of our group is focused on CBPG factors for the complex implication on wound healing: Platelet-Derived Growth Factor, Insulin-Like Growth Factor 1, Fibroblast Growth Factor, Epithelial Growth Factor, Vascular Endothelial Growth Factor, Transforming Growth Factor β1,

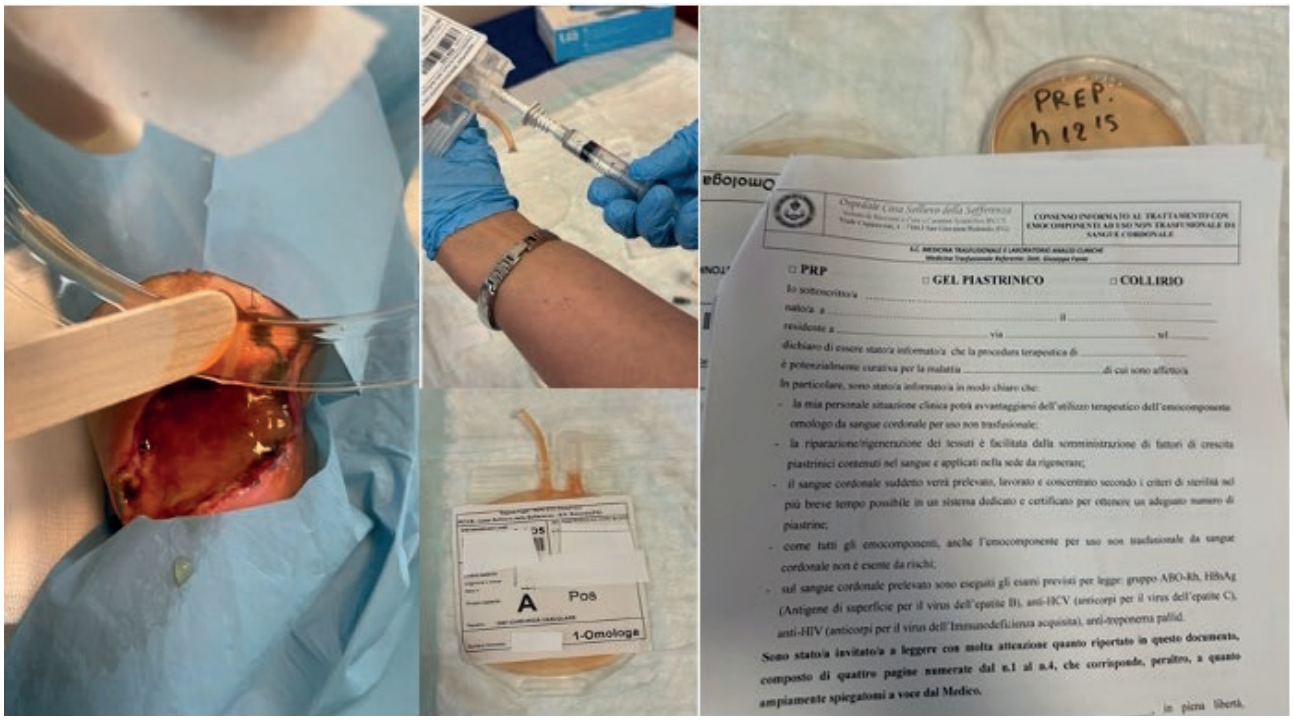

Figure 2. CBPG activation for implantation on patient's ulcers.

Hepatocyte Growth Factor and cytokines (IL-1, IL-6, IL-4)(Leme et al, 2022). In addition, CPBG seems to play a role in pain relief, as observed in diabetic patients, through immunomodulation and by stimulating neural regeneration in damaged fibers (Rosenberger et al. 2019; Bouhlel et al. 2007; Sandireddy et al. 2014, Rubio et al 2017; Rah et al 2017, Tsuda et al. 2019).

CONCLUSION

CBPG treatment protocol in foot lesions of CLTI patients after vascularization intervention in our experience appears safe and effective. Multicenter randomized studies are needed to evaluate late results, in particular for a national protocol of outpatient treatment.

ACKNOWLEDGMENTS

We would like to thank Chiara Di Giorgio (Fondazione IRCCS Casa Sollievo della Sofferenza) for editing and reviewing this manuscript for English language.

REFERENCES

1. Serra R, Buffone G, Dominijanni A, et al. Application of platelet-rich gel to enhance healing of transmetatarsal amputations in diabetic dysvascular patients. Int Wound J 2013;10:612–5.
2. Bisceglia G, Santodirocco M, Faienza A, Mastrodonato N, Urbano F, Totaro A, Bazzocchi F, Mauro LD. First endocavitary treatment with cord blood platelet gel for perianal fistula. Regen Med. 2020 Jan;15(1):1171-1176.
3. Bouhlel MA, Derudas B, Rigamonti E, et al. PPAR gamma activation primes human monocytes into alternative M2 macrophages with anti-inflammatory properties. Cell Metab. 2007;6(2):137-143.
4. Brownlee M. The pathobiology of diabetic complications: a unifying mechanism. Diabetes.2005;54(6):1615-1625.
5. Caiaffa V, Ippolito F, Abate A, Nappi V, Santodirocco M, Visceglie D. Allogenic platelet concentrates from umbilical cord blood for knee osteoarthritis: preliminary results. Med Glas (Zenica). 2021 Feb 1;18(1):260-266.
6. De Caridi G, Massara M, Benedetto F, et al. Adjuvant spinal cord stimulation improves wound healing of peripheral tissue loss due to steal syndrome of the hand: clinical challenge treating a difficult case. Int Wound J. 2016 Feb;13(1):72-6.

7. De Caridi G, Massara M, David A, et al. Spinal cord stimulation to achieve wound healing in a primary lower limb critical ischemia referral centre. Int Wound J.2016 Apr;13(2):220
8. De Caridi G, Massara M, Greco M, et al. VAC therapy to promote wound healing after surgical revascularization for Critical Lower Limb Ischemia. Int Wound J. 2016 Jun;13(3):336-42.
9. De Caridi G, Serra R, Massara M, et al. VAC therapy for the treatment of complex wounds after cardiothoracic surgery. Int Wound J. 2016 Oct;13(5):759-62.
10. Gelmetti A, Greppi N, Guez S, Grassi F, Rebulla P, Tadini G. Cord blood platelet gel for the treatment of inherited epidermolysis bullosa. Transfus Apher Sci. 2018 Jun;57(3):370-373.
11. Goodney PP, Holman K, Henke PK, Travis LL, Dimick JB, Stukel TA, et al. (2013) Regional intensity of vascular care and lower extremity amputation rates. J Vasc Surg 2013;57: 1471-9. 1480.e1-3; discussion: 1479-80.
12. Leme KC, Neri GM, Biscaro GG, Bulgareli AA, Duran N, Parisi MCR, Luzo ÂCM. Full Diabetic Foot Ulcer Healing and Pain Relief Based on Platelet-Rich-Plasma gel Formulation Treatment and the Involved Pathways. Int J Low Extrem Wounds. 2022 Jul 3:15347346221109758.
13. Mannari RJ, Payne WG, Ochs DE, et al. Successful treatment of recalcitrant, diabetic heel ulcers with topical becaplermin (rhPDGF-BB) gel. Wounds 2002;14:116–21.
14. Piccin A, Rebulla P, Pupella S, Tagnin M, Marano G, Di Pierro AM, Santodirocco M, Di Mauro L, Beqiri L, Kob M, Primerano M, Casini M, Billio A, Eisendle K, Fontanella F. Impressive tissue regeneration of severe oral mucositis post stem cell transplantation using cord blood platelet gel. Transfusion. 2017 Sep;57(9):2220-2224
15. Pietro Volpe, Daniela Marcuccio, Giuseppe Stilo, Antonino Alberti, Giovanni Foti, Alberto Volpe, Domenica Princi, Rosangela Surace, Giulia Pucci and Mafalda Massara, Efficacy of cord blood platelet gel application to enhance diabetic foot ulcer healing after lower limb revascularization, Seminars in Vascular Surgery
16. Rah DK, Min HJ, Kim YW, Cheon YW. Effect of platelet-rich plasma on ischemia-reperfusion injury in a skin flap mouse model. Int J Med Sci. 2017;14(9):829-839. Published 2017 Jul 19.
17. Rosenberger DC, Blechschmidt V, Timmerman H, Wolff A, Treede RD. Challenges of neuropathic pain: focus on diabetic neuropathy. J Neural Transm (Vienna). 2020;127(4):589-624.
18. Rubio JA. Plasma growth factors in neuronal regeneration. Austin J Clin Neurol. 2017;4(3):1111.
19. Sandireddy R, Yerra VG, Areti A, Komirishetty P, Kumar A. Neuroinflammation and oxidative stress in diabetic neuropa- thy: futuristic strategies based on these targets. Int J Endocrinol. 2014;2014:1-10. doi:10.1155/2014/674987.
20. Tsuda M. Microglia-Mediated regulation of neuropathic pain: molecular and cellular mechanisms. Biol Pharm Bull. 2019;42(12):1959-1968.

IJAE
ITALIAN JOURNAL OF ANATOMY AND EMBRYOLOGY

Firenze University Press
www.fupress.com/ijae

OPEN ACCESS

Citation: De Cecco, F., Franceschelli, S., Panella, V., Maggi, M., Bisti, S., & Speranza, L. (2023). Anti-Inflammatory effect of the Saffron Stigma and Saffron Petal Extract on LPS stimulated human Caco-2 cell by transductional signal modulation of FBW7/IKBα. *Italian Journal of Anatomy and Embryology* 127(2): 115-119. doi: 10.36253/ijae-14717

Data Availability Statement: All relevant data are within the paper and its Supporting Information files.

Competing Interests: The Author(s) declare(s) no conflict of interest.

Anti-Inflammatory effect of the Saffron Stigma and Saffron Petal Extract on LPS stimulated human Caco-2 cell by transductional signal modulation of FBW7/IKBα

Federica De Cecco[1,2,*], Sara Franceschelli[2,3], Valeria Panella[2], Maria Maggi[4,5], Silvia Bisti[6], Lorenza Speranza[2,3]

[1] *Department of Innovative Technologies in Medicine & Dentistry, University "G. d'Annunzio" Chieti- Pescara, Via dei Vestini 31, 66100 Chieti, Italy*
[2] *Department of Medicine and Aging Sciences, University "G. d'Annunzio" Chieti- Pescara, Via dei Vestini 31, 66100 Chieti, Italy*
[3] *Uda-TechLab, Research Center, University "G. d'Annunzio" of Chieti-Pescara, 66100 Chieti, Italy*
[4] *Hortus Novus srl, Colle Pietro L'Aquila, 67050, Italy*
[5] *Department of Physical and Chemical Sciences, University of L'Aquila, Coppito, 67100, Italy*
[6] *National Institute of Biostructure and Biosystem (INBB), V. le Medaglie D'Oro 305, 00136 Roma, Italy*
*Corresponding author. E-mail: federica.dececco@unich.it

Abstract. Although the progression of IBD therapy is controlled with chemical drugs and biological therapies, healing results cannot yet be achieved, along with the inevitable side effects. As a result, a variety of research have focused on exploring novel therapies and found that natural products can serve as promising therapeutic agents for IBD through their anti-inflammatory and antioxidant effect. Recently, the chemical constituents of the main saffron processing bio-product, the petals of C. sativus, have attracted the attention of researchers. We compare the anti-inflammatory effect of the Saffron Stigma Extract (SSE), Saffon Petal Extract (SPE) and Petals/Stigma Extract (SPE/SSE) on lipopolysaccharide (LPS)-stimulated human Caco-2 cell monolayers by analyzing FBW7/ signaling IkBα, upstream of the activation of inducible molecules such as iNOS and COX-2. The results of this study provide further support for the possible use of SPE in medicine, raising awareness of the potential of the waste product generated in the production of the saffron spice. Compared to the SPE/SSE is not able to attenuate the pro-inflammatory response, and further investigations should be undertaken to understand what kind of negative interaction is triggered between the two components of the spice.

Keywords: IBD, inflammation, intestinal epithelial cells, saffron petals extract, saffron stigma extract.

1. INTRODUCTION

Crocus sativus L., commonly known as saffron, is, widely cultivated in many Mediterranean countries and parts of Asia (De Cecco, F et al., 2022). Recently, the chemical constituents of the main saffron processing by-product, the petals of C. sativus, have attracted the attention of researchers. In the flowering stage, both stigmas and petals of C. sativus contain various bioactive flavonoids, alkaloids, and coumarins. Although the stigmas and petals are similar in composition, there are differences in their metabolite content. Interestingly, a total of 147 flavonoid metabolites were detected in the stigmas and petals, of which 23 were significantly upregulated in the petals. Inflammatory bowel disease (IBD) is a chronic state of gastrointestinal inflammation and is mainly grouped into Crohn's disease (CD) and ulcerative colitis (UC). Although the pathophysiology of IBD are still unclear, high levels of pro-inflammatory cytokines are present in the gut of patients with IBD and have a crucial role in the dysfunction of mucosal homeostasis contributing to the pathogenesis of IBD (Chen Y, et al., 2021). In the present study, we compare the anti-inflammatory effect of the Saffron Stigma Extract (SSE), Saffon Petal Extract (SPE) and Petals/Stigma Extract (SPE/SSE) on lipopolysaccharide (LPS)-stimulated human Caco-2 cell monolayers analysing FBW7/IKBα signaling.

2. MATERIALS & METHODS

2.1 Cell culture

The human colon adenocarcinoma Caco-2 cell line (ATCC® TIB-202™ Rockville, MD, USA) was cultured as previously reported by (Wu XX, et al., 2019).

2.2 Cytotoxicity assay

The Methylthiazolyldiphenyl-tetrazolium bromide (MTT) assay (Sigma-Aldrich, St. Louis, MO, USA) was performed, as previously described (Franceschelli S, et al., 2016).

2.3 ROS Detection

An NBT (nitroblue tetrazolium) assay was performed as previously described to detect intracellular ROS levels (Franceschelli S, et al., 2019)

2.4 RNA extraction, reverse transcription, and Real-Time PCR

Cells were collected in 1mL QIAzol lysis reagent (Qiagen, Hilden, Germany), total RNA extraction and Real-Time PCR was performed as previously described (Patruno A, et al., 2015).

2.5 Western Blot Analysis

Western blot analysis was performed as described previously (Franceschelli S, et al., 2019) using the following antibodies against iNOS (OTI1E5; 1:700), IKBα (NFKBIA) (OTI1D4; 1:400), FBXW7 (OTI6B1; 1:1000), COX-2 (ab52237; 1:500), and β-actin (Santa Cruz Biotechnology).

2.6 Statistical analysis

Quantitative variables are summarized as the mean value and standard deviations (SD) in the Tables and Figures. To assess the accuracy of fold change data, the 95% confidence interval (95% CI) and standard error (SE) were determined. A Student's t-test for unpaired data was applied to evaluate the significance of differences. All tests were two-tailed. The threshold of statistical significance was set at p=0.05. Data analysis was performed on GraphPad Prism 6 Software, version 6.01, 2012.

3. RESULTS

3.1 Saffron Stigma Extract and Stigma/Petals Extract does not affect the viability of epithelial cells.

In order to determine the concentrations of SSE and of SPE/SSE which has nontoxic to cells, we examined the cell viability in Caco-2 cells after incubation with different concentrations of SSE (50ng/ml, 100ng/ml, 500 ng/ml, 1ug/ml, 5ug/ml, 10ug/ml, 25ug/ml, 50ug/ml, 100ug/ml, 250 ug/mL, 500ug/ml, 1mg/ml) and of SPE/SSE (we used petals and stigmas in the ratio of 2:1- range to 50 and 25 ng/ml from 1 and 0.5 mg/ml), for 24 h. MTT assay showed that SSE and SPE/SSE did not affect the viability of Caco-2 cells at concentrations lower than 1mg/ml and 1-0.5 mg/ml, respectively (Fig. 1A, B). Furthermore, the superoxide anion radical-scavenging activity was also measured in a non-enzymatic method at 24h. The generation of superoxide anions was markedly inhibited (~50%) from the concentration of 25 µg/ml of SSE and 50-25 ug/ml of SPE/SSE in respect to cells

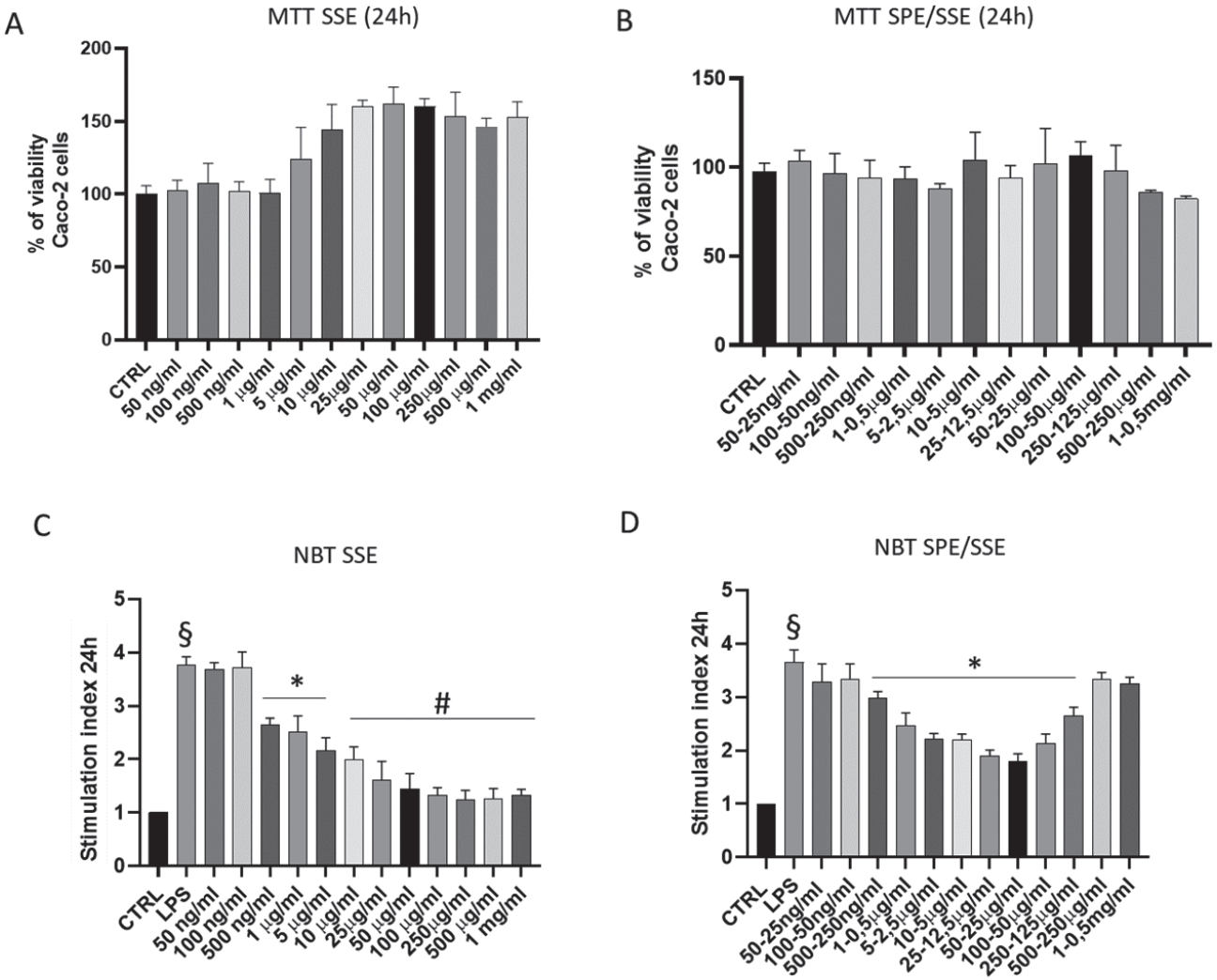

Figure 1. Cytotoxyc effect of SSE and SPE/SSE on Caco-2 cells. Cells were treated with SSE (A) and SPE/SSE (B) for 24h. Cells viability was measured by MTT assay as reported in Materials and Methods. Date are reported as % of viability in respect to control cells. Each bar represent means ±SEM (n=3); (C) Antioxidant activity of SSE (C) or SPE/SSE (D) against oxidative stress LPS-induced measured by NBT test. Results were registered as stimulation index (SI). SI value of 1 was assigned to control cells. Each bar represent means ±SEM (n=3). §p<0.005 vs CTRL; #p<0.05 and*p<0.01 vs LPS. (SSE: Saffron Stigma Extact; SPE/SSE:Petals/Stigma Extract; LPS: Lypopolysaccharide)

stimulated with LPS (Fig. 1C,1D). Of note, SPE/SSE at concentrations above 500-250 ug/ml loses its ability to neutralise superoxide anion. Thus, SSE at 25 µg/ml and SPE/SSE 50-25 ug/ml was more often used in the following experiments to test its activity against LPS-induced inflammation. SPE was used at a concentration of 50 ug/ml which, as per our previous results, is non-cytotoxic and induces significative reduction of the ROS production, as well as the expression of inducible iNOS and COX-2 (De Cecco, F et al., 2022).

3.2 Effect of Saffron Stigma, Saffron Petal and Petals/Stigma on inducible molecules

To compare the effects of SSE, SPE and SPE/SSE on epithelial cells, the expression of inducible proteins, known to be controlled by NF-kB (p65) and up-regulated in the inflammatory process, were checked. As shown in Figure 2, in Caco-2 cells exposed to LPS, SSE and SPE induce a down-regulation of both mRNA and protein expression of iNOS (Fig. 2A) and COX-2 (Fig. 2B) compared to activated cells. Instead, the combined extract of SPE/SSE, is not able to induce the down-regulation of the pro-inflammatory molecules analysed (Fig.2A,2B).

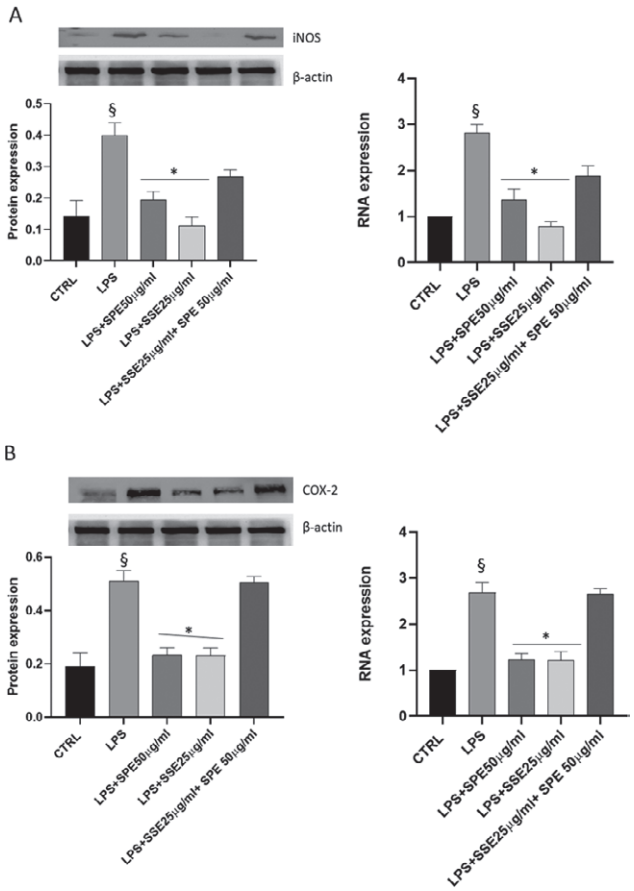

Figure 2. Effect of SPE, SSE, SPE/SSE on inducible molecules in Caco-2 cells. Representative image of Western blot analysis (left) with relative densitometry and real-Time PCR analysis (rigth) for iNOS (A), COX-2 (B). To the left, in the densitometric analysis (n = 3), each bar is reported as the intensity of optical density (IOD) ± SD. The following primer pair sequence was used: iNOS (F:5'- CATTGCTGTGCTCCATAGTTTC-3'-, R:5'- CAGGACGTAGTTCAGCATCTC-3'); COX-2 (F:5'-CGATGCTGTGGAGCTGTAT-3'; R:5'-CATTGCTGTGCTCCATAGTTTCG-3'); §P < 0.05, vs control cells and *P < 0.05 vs LPS-stimulated cells. (SSE: Saffron Stigma Extact; SPE: Saffron Petals Extract; SPE/SSE:Petals/Stigma Extract; LPS: Lypopolysaccharide)

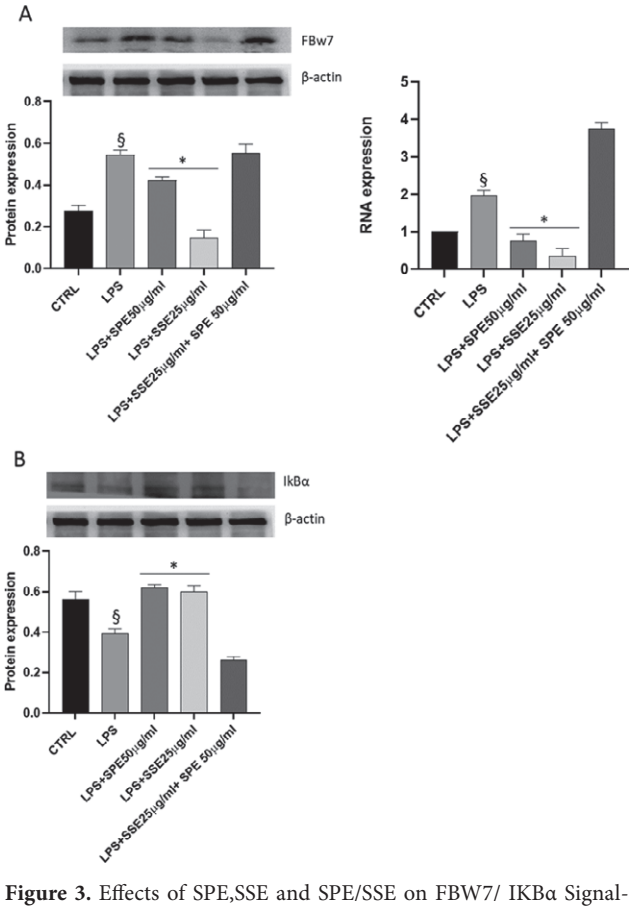

Figure 3. Effects of SPE,SSE and SPE/SSE on FBW7/ IKBα Signaling in Caco-2 cells. Representative image of Western blot analysis for FBW7 (A) and IKBα (B). To the left, in the densitometric analysis (n = 3), each bar is reported as the intensity of optical density (IOD) ± SD. §P < 0.05, significance *vs* control cells. For qRT-PCR analysis, the following primer pair sequence was used: FBW7 (F:5'-CAGTCCGCTGTGTTCAATATG-3', R:5'-GCCCTGTTAACGTGTGAATG-3'); 18S (F:5'- CTTTGCCATCACTGCCATTAAG -3', R:5'-TCCATCCTTTACATCCTTCTGTC-3'). *P < 0.05 significance *vs* LPS-stimulated cells.

3.3 Effect of Saffron Stigma and Petals on FBW7/IkBα signaling

Since in our previous paper (De Cecco, F et al., 2022) we have hypothesised that SPE exerts its regulatory effect on NF-kB interfering with FBW7, we studied and compared the effect of SPE with that of SSE and SPE/SSE. Expression levels of both mRNA and FBW7 protein were significantly up-regulated in cells stimulated with LPS confirming its role in regulating the inflammatory response (Figure 3A). Treatment with selected concentration of SPE and SSE induces a down-regulation of the expression of this ubiquitin which represents a negative regulator of the inflammatory process. At the same time, the protein levels of NF-kB inhibitor as IKBα were detected. Interestingly, IKBα was significantly expressed by SPE and SSE treatment compared to LPS-activated cells, leading us to hypothesize that both exert their regulatory effect on NF-kB by interfering with FBW7 (Figure 3B). However, the treatment of the activated intestinal epithelial cells with the SPE/SSE was unable to attenuate the inflammatory response induced by LPS and mediated by FBW7/NF-kB signaling.

4. DISCUSSION

Despite the incredible progress of modern medicine, significant obstacles remain in the treatment of IBD. There is high interest in alternative natural agents in the management of IBD because they are perceived to be safer than their synthetic equivalents due to their efficacy and minimal perceived side effects. Some herbs such as saffron, may control inflammation and improve cellular homeostasis in many diseases as well as peptic ulcer and UC (Singh G, et al., 2022). In our previous study we have demonstrated the efficacy of SPE as a protective agent against inflammation interfering with the FBW7 protein (De Cecco F, et al., 2022). In this study we compare the effect of SPE, SSE and a mix of SPE/SSE. There are several studies indicating that saffron and its constituents have an important role in inhibition the NF-κB signaling, but few studies have focused on comparing the effects of saffron and its components in cellular processes. (Zeinali M, et al., 2019). Our results showed that SPE can attenuate the over-expression of the inducible proteins iNOS and COX-2, in intestinal epithelial cells, in a similar way to SSE (Figure 2). Moreover, in this study, for the first time, we demonstrated that the SSE, as SPE, by reducing the expression of protein FBW7 inhibits the degradation of the IKBα subunit in intestinal epithelial cells (Figure 3B). This protein, by maintaining NF-kB in the inactive state, can alleviate a multitude of NF-kB-driven inflammatory diseases such as IBD. Finally, SPE/SSE treatment is not able to attenuate the pro-inflammatory response mediated by the regulation of FBW7/IKBα signalling.

This study confirmed that SSE and SPE possess anti-inflammatory and antioxidant activities, raising awareness of the potential of the waste product generated in the production of the saffron spice. However, the combined use of both is not able to attenuate the inflammatory response, therefore further investigations should be undertaken to understand what kind of negative interaction is triggered between the two components of the spice. The results of this study provide further insights into the study and confirmation of the effects of SPE in a two-dimensional coculture model to evaluate its possible use to support conventional IBD therapy through a clinical trial.

REFERENCE

Chen Y, Wang J, Li J, Zhu J, Wang R, Xi Q, Wu H, Shi T, Chen W. (2021) Astragalus polysaccharide prevents ferroptosis in a murine model of experimental colitis and human Caco-2 cells via inhibiting NRF2/HO-1 pathway. Eur J Pharmacol. Nov 15;911:174518.

De Cecco, F., Franceschelli, S., & Speranza, L. (2022). Inflammatory Bowel Disease (IBD): a novel biological role of saffron petal extracts as a modulator of phlogistic pathway via FBW7/NF-kB in Caco-2 cell line LPS-stimulated. *Italian Journal of Anatomy and Embryology*, *126*(2), 65–69.

Franceschelli S, Gatta DM, Pesce M, Ferrone A, Patruno A, de Lutiis MA, Grilli A, Felaco M, Croce F, Speranza L. (2016) New Approach in Translational Medicine: Effects of Electrolyzed Reduced Water (ERW) on NF-κB/iNOS Pathway in U937 Cell Line under Altered Redox State. Int J Mol Sci. Sep 1;17(9):1461.

Franceschelli S, Gatta DMP, Pesce M, Ferrone A, Quiles JL, Genovese S, Epifano F, Fiorito S, Taddeo VA, Patruno A, Grilli A, Felaco M, Speranza L. (2019) Modulation of CAT-2B-Mediated l-Arginine Uptake and Nitric Oxide Biosynthesis in HCT116 Cell Line Through Biological Activity of 4'-Geranyloxyferulic Acid Extract from Quinoa Seeds. Int J Mol Sci. Jul 2;20(13):3262.

Franceschelli S, Lanuti P, Ferrone A, Gatta DMP, Speranza L, Pesce M, Grilli A, Cacciatore I, Ricciotti E, Di Stefano A, Miscia S, Felaco M, Patruno A. (2019) Modulation of Apoptotic Cell Death and Neuroprotective Effects of Glutathione-L-Dopa Codrug Against H_2O_2-Induced Cellular Toxicity. Antioxidants (Basel). Aug 19;8(8):319.

Patruno A, Pesce M, Grilli A, Speranza L, Franceschelli S, De Lutiis MA, Vianale G, Costantini E, Amerio P, Muraro R, Felaco M, Reale M. (2015) mTOR Activation by PI3K/Akt and ERK Signaling in Short ELF-EMF Exposed Human Keratinocytes. PLoS One. Oct 2;10(10):e0139644.

Singh G, Haileselassie Y, Ji AR, Maecker HT, Sinha SR, Brim H, Habtezion A, Ashktorab H. (2022) Protective Effect of Saffron in Mouse Colitis Models Through Immune Modulation. Dig Dis Sci. Jul;67(7):2922-2935.

Wu XX, Huang XL, Chen RR, Li T, Ye HJ, Xie W, Huang ZM, Cao GZ. (2019) Paeoniflorin Prevents Intestinal Barrier Disruption and Inhibits Lipopolysaccharide (LPS)-Induced Inflammation in Caco-2 Cell Monolayers. Inflammation. Dec;42(6):2215-2225.

Zeinali M, Zirak MR, Rezaee SA, Karimi G, Hosseinzadeh H. (2019) Immunoregulatory and anti-inflammatory properties of *Crocus sativus* (Saffron) and its main active constituents: A review. Iran J Basic Med Sci. Apr;22(4):334-344.

IJAE
ITALIAN JOURNAL OF ANATOMY AND EMBRYOLOGY

Firenze University Press
www.fupress.com/ijae

OPEN ACCESS

Citation: Bonelli, M., Catena, A.M., Pietrangelo, T., Locatelli, M., Trubiani, O., & D'Ovidio, C. (2023). Use of cadaveric stem cells: analysis of literature. *Italian Journal of Anatomy and Embryology* 127(2): 121-124. doi: 10.36253/ijae-14739

Data Availability Statement: All relevant data are within the paper and its Supporting Information files.

Competing Interests: The Author(s) declare(s) no conflict of interest.

Use of cadaveric stem cells: analysis of literature

Martina Bonelli[1,*], Antonio M. Catena[2], Tiziana Pietrangelo[3], Marcello Locatelli[4], Oriana Trubiani[5], Cristian D'Ovidio[1]

[1] *Department of Medicine and Aging Sciences, Section of Legal Medicine, University "G. d'Annunzio" of Chieti-Pescara, 66100 Chieti, Italy*
[2] *Institute of Legal Medicine, University of Rome 2 "Tor Vergata", 00133 Rome, Italy*
[3] *Department of Neuroscience, Imaging and Clinical Sciences, University "G. d'Annunzio" of Chieti-Pescara, 66100 Chieti, Italy*
[4] *Department of Pharmacy, University"G. d'Annunzio" of Chieti-Pescara, 66100 Chieti, Italy*
[5] *Department of Innovative Technologies in Medicine & Dentistry, University "G. d'Annunzio" Chieti-Pescara, 66100 Chieti, Italy*
*Corresponding author. E-mail: martinabonelli3@gmail.com

Abstract. Determination of Post Mortem Interval (PMI) has always been based on empirical analysis of microdata not always endowed with sufficient reliability. Due to its significancy in medico-legal issues, PMI estimation needs to be assessed by applying new and more reliable methods and/or biomarkers. Considering the growing interest and use of stem cells taken from cadaveric tissues and the success in their isolation from death donors, with the maintenance of vitality and regenerative capacity, we evaluated the Literature "state of the art" on this topic to understand if those stem cells could also be used for thanatochrologic estimation. The results obtained from Literature analysis show the possibility of using these cells as a marker for the post-mortal interval. In particular Mesenchymal Stem cells, isolated from adipose and muscular tissues, can be used to evaluate their regenerative capacity over time according to the PMI.

Keywords: Post Mortem Interval, PMI, stem cells, cadaveric tissue, forensic medicine.

INTRODUCTION

Post mortem interval (PMI) is defined as the elapsed time since the death of an individual. Assessing PMI is one of the most difficult task and recurrent challenge in forensic pathology due to the influence of various intrinsic and extrinsic factors, but it is of fundamental importance in medico-legal issues.

Due to its significance and complexity, PMI estimation needs to be assessed by applying new and more reliable methods and/or biomarkers and this, in recent years, is reflected by an increasing focus of research in thanatochronology.

Several methodological approaches have been proposed but, to date, none of these resulted to be reliable for forensic purposes.

Considering the growing interest of regenerative medicine in cadaveric stem cells with a view to minimize ethical problems associated with their obtainment, we evaluated the Literature "state of the art" on this topic to understand if those stem cells could also be used for thanatochrologic estimation.

MATERIALS AND METHODS:

A review of publications was performed using PubMed database. The search was limited to work and studies published in English. Key words included were: stem cells, forensic medicine and/or cadaver.

373 articles were found. Exclusion criteria were: case reports, trials, reviews, book chapters, articles with unavailable fulltext and studies performed on brain dead but beating heart donors.

A total of 91 studies were retained, involving both human and animal cadavers.

RESULTS:

15 of the analyzed articles used only animals of different specimens, 65 focused just on human cadavers, 7 compared results between human and animals cadavers while the remaining 4 compared results between human cadavers and living donors.

The most sampled tissues were the ones derived from eye ball like corneas, conjunctiva, retina and ciliary body (30 articles), followed by bone marrow (23 articles) and central nervous system (14 articles).

Considering the type of stem cells studied, large majority of Literature focused on limbal stem cells, mesenchymal stem cells and hematopoietic stem cells with 18, 16 and 13 studies respectively.

All the articles aimed at finding useful tools for regenerative medicine purposes, while 2 studies also considered data of medico-legal interest, but only as collateral observations.

DISCUSSION:

The aim of this work is to evaluate the possibility of using stem cells as a marker for post mortem interval estimation in medico-legal issues. The idea to focus on cadaveric stem cells arised from the growing interest, especially in regenerative medicine field, on deceased donors in order to avoid ethical controversies.

Literature analysis permitted to underline that cadaveric stem cells are successfully isolated from various tissues and that, within a certain timeframe, they maintain viability and proliferative capacity. To evaluate which stem cells could be most suitable for forensic purposes, we initially focused on the most studied organs in Literature which resulted to be eye, bone marrow and the central nervous system. However, none of these organs are particularly useful in medico-legal analysis as they undergo rapid degradation after death, cannot be sampled in all the contexts (i.e. site inspection) and moreover are often affected by pre-death patients clinical conditions.

We then focused on the most studied types of stem cells that resulted in limbal, mesenchymal and hematopoietic by analysing 18, 16 and 13 articles, respectively.

Of these three types of cells, the first and third ones are collected almost exclusively from eye ball tissues and bone marrow respectively, and therefore are scarcely useful for forensic purposes for the reasons afore mentioned, while mesenchymal cells are of greater interest as they derive from various tissues, (see Table 1).

In particular muscular and adipose tissues are considered superior by some studies in terms of proliferative and differentiative capacity if compared to other tissues such as bone marrow. Moreover these tissues are very resistant to ischemic insults, are easily accessible for sampling and they are little affected by the most frequently pre-existing pathological conditions and by the cause of death of an individual.

CONCLUSIONS

Despite the growing interest and use of stem cells taken from cadaveric tissues and the success in their isolation from death donors, with the maintenance of vitality and regenerative capacity, very little attention is given to their potential use in forensic medicine, in particular for thanatochronological purposes.

The results obtained from Literature analysis, although still limited, show the possibility of using these cells as a marker for the post-mortal interval. In particular adipose and muscular tissues can be used also in comparison, to evaluate the regenerative capacity over time of stem cells according to the PMI.

REFERENCES

Ahrens N., Tormin A., Paulus M., Roosterman D., Salama A., Krenn V., Neumann U., Scheding S. (2004) Mesenchymal Stem Cell Content of Human Vertebral Bone Marrow. Transplantation. 78: 925–929.

Table 1.

First author	AIM	PMI	Samples	Case number	Tissue	Main analysis
Kisiel A.H.	Compare muscle and periosteum derived MSC to adipose and ne marrow derived MSC	Immediately after euthanasia	Dogs	7	Adipose tissue, muscle, periosteum, bone marrow	Differentiation analysis
Ahrens N.	Compare MSC content in different sites of extraction	Not specified	Human	Not specified	Vertebral bone marrow	Quantification of cells
Alhadlaq A.	Create a tissue-engineered human-shaped mandibular condyle	Immediately after euthanasia	Rats	Not specified	Tibial and femural bone marrow	Isolation of MSC
Radtke C. L.	Compare proliferation capacity and osteogenic potential of muscle and periosteum derived MSCs in comparsion with bone marrow and adipose tissue-derived MSCs	Immediately after euthanasia	Horses	10	Muscle tissue, periosteal tissue, bone marrow(sternebrae) and adipose tissue	Proliferation and differentiation analysis
Eslani M.	Evaluate anti-angiogenic properties of corneal derived MSCs	Not specified	Human and Mice	Not specified	Cornea	Anti-angiogenic effects of MSC secretome
Chahla J.	Identify, characterize and compare MSCs in varous menisci zones	Immediately after death and stored at 4°C	Human	7	Menisci	Isolation and proliferation capacity analysis
Kami D.	Analysis of possible cardiac MSCs use in trasplants	24h	Mice	Not specified	Heart	Proliferation and differentiation analysis
Kamishina H.	Evaluation of cell surface neuronal and glial-specific markers presence on MSCs	Immediately after euthanasia	Dogs	5	Bone marrow(iliac crest)	Identification and expression of neuronal and glial markers
Kim J.	Investigate the immunologic properties of pancreatic islet-derived MSC compared with bone marrow MSC	Immediately after death	Human	9	Pancreas	Differentiation potential, analysis of cell surface markers, metabolism, gene expression levels
Shikh Alsook M. K.	Find out if viable MSCs colud survive in cadaveric tissue from adult equine ligaments up to 72 hours of post-mortem and to assess their ability (I) to remain in an undifferentiated state and (II) to divide and proliferate in the absence of any specific stimulus	48-72h	Horses	4	Ligaments	Proliferation and differentiation capacity
Reisbig N. A.	Create a bioactive synovium scaffold by infusing decellularized synovial-derived extracellular matrix (synECM) with synovial-derived mesenchymal stem cells (synMSCs)	Immediately after death	Horses	3	Synovium	Isolation for cotransduction
Parks K. S.	Further evaluated th MSCs coculture system for use with isolated humans islets	Not specified	Human	Not specified	Bone marrow and umbilical cord	Isolation for co-colture
Samaeekia R.	Effect of human corneal MSC-derived exosome on corneal epithelial wound healing	Not specified	Human	Not specified	Cornea	Isolation and exosome analysis
Valente S.	Find alternative source of MSC	12h	Human	3	Vascular tissue	Proliferation and differentiation capacity
Saito T.	Confirm whether human postmortem ASCs can be collected and culutre-expanded from cadavers	21-177h	Human and mice	30 (Human)	Adipose tissue	Viability of cells
Cavallo C.	Find alternative sources of MSCs	Within 24h	Human	Not specified	Adipose tissue and bone marrow	Proliferation and differentiation capacity

Alhadlaq A., Mao J.J. (2003) Tissue-engineered Neogenesis of Human-shaped Mandibular Condyle from Rat Mesenchymal Stem Cells. J Dent Res. 82: 951-956.

Cavallo C., Cuomo C., Fantini S., Ricci F., Tazzari P.L., Lucarelli E., Donati D., Facchini A., Lisignoli G., Fornasari P.M., Grigolo B., Moroni L. (2011). Comparison of alternative mesenchymal stem cell sources for cell banking and musculoskeletal advanced therapies. Journal of Cellular Biochemistry. 112(5): 1418–1430.

Chahla J., Papalamprou A., Chan V., Arabi Y., Salehi K., Nelson T.J., Limpisvasti O., Mandelbaum B.R., Tawackoli W., Metzger M.F., Sheyn D. (2021) Assessing the Resident Progenitor Cell Population and the Vascularity of the Adult Human Meniscus. Arthroscopy. 37(1): 252–265.

Eslani M., Putra I., Shen X., Hamouie J., Afsharkhamseh N., Besharat S., Rosenblatt M.I., Dana R., Hematti P., Djalilian A.R. (2017) Corneal Mesenchymal Stromal Cells Are Directly Antiangiogenic via PEDF and sFLT-1. Invest Ophthalmol Vis Sci. 58: 5507–5517.

Kami D., Kitani T., Nakata M., Gojo S. (2014) Cardiac Mesenchymal Progenitors From Postmortem Cardiac Tissues Retained Cellular Characterization. Transplantation Proceedings. 46: 1194-1197.

Kamishina H., Deng J., Oji T., Cheeseman J.A., Clemmons R.M. (2006) Expression of neural markers on bone marrow–derived canine mesenchymal stem cells. American Journal of Veterinary Research. 67(11): 1921-1928.

Kim J., Breunig M.J., Escalante L.E., Bhatia N., Denu R.A., Dollar B.A., Stein A.P., Hanson S.E., Naderi N., Radek J., Haughy D., Bloom D.D., Assadi-Porter F.M., Hematti P. (2012) Biologic and immunomodulatory properties of mesenchymal stromal cells derived from human pancreatic islets. Cytotherapy. 14(8): 925–935.

Kisiel A.H., McDuffee L.A., Masaoud E., Bailey T.R., Esparza Gonzalez B.P., Nino-Fong R. (2012) Isolation, characterization, and in vitro proliferation of canine mesenchymal stem cells derived from bone marrow, adipose tissue, muscle, and periosteum". American Journal of Veterinary Research,. 73(8): 1305-1317.

Park K.S., Kim Y.S., Kim J.H., Choi B.K., Kim S.H., Oh S.H., Ahn Y.R., Lee M.S., Lee M.K., Park J.B., Kwon C.H., Joh J.W., Kim K.W., Kim S.J. (2009) Influence of Human Allogenic Bone Marrow and Cord Blood–Derived Mesenchymal Stem Cell Secreting Trophic Factors on ATP (adenosine-5=-triphosphate)/ADP (adenosine-5=-diphosphate) Ratio and Insulin Secretory Function of Isolated Human Islets From Cadaveric Donor. Transplantation Proceedings. 41: 3813–3818.

Radtke C.L., Nino-Fong R., Esparza Gonzalez B.P., Stryhn H., McDuffee L.A. (2013) Characterization and osteogenic potential of equine muscle tissue– and periosteal tissue– derived mesenchymal stem cells in comparison with bone marrow– and adipose tissue–derived mesenchymal stem cells. AJVR. Vol 74, No. 5: 790-800.

Reisbig N.A., Hussein H.A., Pinnell E., Bertone A.L. (2018) Evaluation of equine synovial-derived extracellular matrix scaffolds seeded with equine synovial-derived mesenchymal stem cells. American Journal of Veterinary Research. 79(1): 124-133.

Saito T., Sato T., Suzuki K. (2020) Isolation and culture of human adipose-derived mesenchymal stromal/stem cells harvested from postmortem adipose tissues. Journal of Forensic and Legal Medicine. 69 101875.

Samaeekia R., Rabiee B., Putra I., Shen X., Park Y.J., Hematti P., Eslani M., Djalilian A.R. (2018) Effect of Human Corneal Mesenchymal Stromal Cellderived Exosomes on Corneal Epithelial Wound Healing. Invest Ophthalmol Vis Sci. 59: 5194–5200

Shikh Alsook M. K., Gabriel A., Piret J., Waroux O., Tonus C., Connan D., Baise E. Antoine N. (2015) Tissues from equine cadaver ligaments up to 72 hours of post-mortem: a promising reservoir of stem cells. Stem Cell Research & Therapy. 6: 253-262.

Valente S., Alviano F., Ciavarella C., Buzzi M., Ricci F., Tazzari P.L., Pagliaro P., Pasquinelli G. (2014) Human cadaver multipotent stromal/stem cells isolated from arteries stored in liquid nitrogen for 5 years. Stem Cell Research & Therapy. 5:8.

IJAE
ITALIAN JOURNAL OF ANATOMY AND EMBRYOLOGY

Firenze University Press
www.fupress.com/ijae

OPEN ACCESS

Citation: Coccina, F., Scurti, R., Trubiani, O., & Pierdomenico, S.D. (2023). Ambulatory blood pressure and risk of heart failure: a mini-review. *Italian Journal of Anatomy and Embryology* 127(2): 125-127. doi: 10.36253/ijae-14755

Data Availability Statement: All relevant data are within the paper and its Supporting Information files.

Competing Interests: The Author(s) declare(s) no conflict of interest.

Ambulatory blood pressure and risk of heart failure: a mini-review

Francesca Coccina[1,2,*], Rosa Scurti[2], Oriana Trubiani[1], Sante D. Pierdomenico[1]

[1] *Department of Innovative Technologies in Medicine & Dentistry, University "Gabriele d'Annunzio", Chieti-Pescara, Chieti, Italy*
[2] *UOC Geriatria, Ospedale Civile Santo Spirito, Pescara, Italy*
*Corresponding author. E-mail: f.coccina@gmail.com

Abstract. The aim of this mini-review is to report current knowledge about the association between ambulatory blood pressure and risk of heart failure in hypertension. We conducted a literature search through PubMed, Web of science and Cochrane Library by using terms such as ambulatory blood pressure, 24-hour blood pressure, daytime blood pressure, nighttime blood pressure, hypertension, heart failure. We identified 4 studies including 7891 patients who developed 260 cases of heart failure during the follow-up. The evaluation of published studies indicates that ambulatory blood pressure is superior to clinic blood pressure in predicting the occurrence of heart failure. Particularly, it has been reported that 24-hour blood pressure values, nighttime non-dipping blood pressure pattern and ambulatory resistant hypertension are associated with increased risk of heart failure above clinic blood pressure. Nevertheless, there are still few data in the literature on this topic. Therefore, further studies are needed to broaden our knowledge on this matter to improve our therapeutic approach to prevent HF in hypertensive patients.

Keywords: ambulatory blood pressure, hypertension, heart failure.

INTRODUCTION

A lot of studies indicate that out-of-office blood pressure (BP), detected by ambulatory BP monitoring or home BP recording, is superior to clinic BP in predicting various cardiovascular outcomes in hypertensive patients (Williams et al, Whelton et al, Pierdomenico et al, Coccina et al, Huang et al).

Heart failure (HF) is a relevant public health matter that is characterized by high mortality and costs (Roger VL). Hypertension is one of the most important causes of HF occurrence (McMurray JJ, Stewart S). Indeed, its population-attributable risk for HF has been shown to be as high as that of coronary artery disease (Dunlay et al). Nevertheless, clinic BP, as for other cardiovascular consequences, may not entirely depict the harmful effect of hypertension on HF. In this scenario, only few studies have attempted to evaluate whether ambulatory BP is superior to clinic BP in predicting HF onset.

The aim of this mini - review is to report current knowledge about the association between ambulatory BP and risk of HF in hypertension.

METHODS

We conducted a literature search through PubMed, Web of science and Cochrane Library up to June 30, 2023. The terms used to identify studies were ambulatory blood pressure, 24-hour blood pressure, daytime blood pressure, nighttime blood pressure, hypertension, heart failure. Inclusion criteria were 1) full articles published in peer-reviewed journals; 2) use of ambulatory BP monitoring; 3) data on the occurrence of HF reported as a separate outcome. We identified 4 manuscripts (Ingelsson et al, Pierdomenico et al, Kario et al, Coccina et al).

RESULTS

In a Swedish study, 951 elderly men were investigated (Ingelsson et al). Ambulatory BP monitoring was performed at baseline. Seventy men developed HF during follow-up (median 9.1 years). In multivariable Cox regression analysis adjusted for covariates, a 1-standard deviation (9 mm Hg) increase in nighttime diastolic BP (hazard ratio [HR] 1.26, 95% confidence interval [CI] 1.02-1.55) and "nondipping" (night-day BP ratio >=1; HR 2.29, 95% CI 1.16-4.52) were associated with increased risk of HF. After adjusting for clinic BP, nondipping remained a significant predictor of HF (HR 2.21, 95% CI 1.12-4.36 vs normal night-day pattern). The authors concluded that nighttime BP conveys additional risk information on HF beyond clinic BP and other risk factors.

In an Italian study, the occurrence of HF with reduced ejection fraction (HFREF) or preserved ejection fraction (HFPEF) was evaluated in 1191 elderly treated hypertensive patients who underwent ambulatory BP monitoring to evaluate 24-hour BP, dipping status, and morning surge (MS) of BP (Pierdomenico et al). During the follow-up (mean 9.1 years), 123 patients developed HF, of whom 56 had HFREF and 67 had HFPEF. After adjustment for covariates, Cox regression analysis showed that 24-hour systolic BP, but not clinic BP, was associated with risk of both HFREF (HR 1.36, 95% CI 1.14-1.63, per 10 mm Hg increment) and HFPEF (HR 1.35, 95% CI 1.13-1.61, per 10 mm Hg increment); moreover, high MS of BP (>23 mm Hg) in dippers was associated with risk of HFREF (HR 2.27, 95% CI 1.00-5.15) and nondipping was associated with risk of HFPEF (HR 2.78, 95% CI 1.38-5.63). The authors concluded that in elderly treated hypertensive patients, 24-hour systolic BP is associated with future risk of both HFREF and HFPEF, whereas high MS and nondipping are associated with risk of HFREF and HFPEF, respectively.

In a Japanese study, the authors investigated the effect of resistant hypertension, diagnosed by ambulatory BP monitoring, on the risk of HF (Kario et al). Globally, 5839 patients were studied. According to clinic BP, ambulatory BP and number of drugs used, patients were classified in those with true resistant hypertension, pseudo resistant hypertension, well-controlled nonresistant hypertension or uncontrolled nonresistant hypertension. During a mean follow-up of 4.5 years, 67 HF events occurred. The adjusted risk of HF was increased in patients with true resistant versus controlled nonresistant hypertension (HR 2.24, 95% CI 1.17–4.30) and versus uncontrolled nonresistant hypertension (HR 3.03, 95% CI 1.58–5.83). The authors concluded that true resistant hypertension diagnosed by ambulatory BP monitoring is a significant independent risk factor for HF.

In another Italian study, the risk of HF was assessed in elderly treated hypertensive patients with white coat uncontrolled hypertension (WUCH), ambulatory nonresistant hypertension (ANRH) and ambulatory resistant hypertension (ARH), compared to those with controlled hypertension (CH) (Coccina et al). Globally, 745 treated hypertensive subjects older than 65 years were investigated, of whom 153 had CH, 153 had WUCH, 307 had ANRH and 132 (18%) had ARH. During a mean follow-up of 8.4 years, 82 HF events occurred. After adjustment for covariates, when compared to CH, the HR (95% CI), for HF was 1.30 (0.51–3.32), 2.14 (1.03–4.43) and 3.52 (1.56–7.96) in WUCH, ANRH and ARH, respectively. The authors concluded that, among elderly treated hypertensive patients, those with ARH are at a considerably higher risk of HF when compared to CH.

DISCUSSION

Hypertension is one of the most frequent chronic diseases and is responsible for various cardiovascular complications. Among these, HF is an increasingly relevant problem in individuals with long-lasting hypertension and in elderly patients. However, clinic BP, as for other cardiovascular outcomes, may not completely describe the detrimental effect of hypertension on the occurrence of HF. Indeed, 24-hour ambulatory BP has repeatedly been shown to be a powerful predictor of future combined cardiovascular events, even after adjustment for clinic BP. In this context, some studies have also tried to evaluate whether ambulatory BP might

be superior to clinic BP in predicting HF. The literature analysis indicate that ambulatory BP is superior to clinic BP in predicting the occurrence of HF. Particularly, it has been reported that 24-hour BP, nondipping and ambulatory resistant hypertension are associated with increased risk of HF above clinic BP, emphasizing that traditional clinic BP does not capture all the increased risk of HF associated with hypertension. However, there are still few data in the literature on this topic. Therefore, further studies are needed to broaden our knowledge on this matter to improve our therapeutic approach to prevent HF in hypertension.

REFERENCES

1. Williams B, Mancia G, Spiering W et al. Practice Guidelines for the management of arterial hypertension of the European Society of Hypertension and the European Society of Cardiology: ESH/ESC Task Force for the Management of Arterial Hypertension. J. Hypertens. 2018; 36: 2284–2309.
2. Whelton PK, Carey RM, Aronow WS, et al. 2017 ACC/AHA/AAPA/ABC/ACPM/ AGS/APhA/ASH/ ASPC/NMA/PCNA Guideline for the Prevention, Detection, Evaluation, and Management of High Blood Pressure in Adults: A Report of the American College ofCardiology/American Heart Association Task Force on Clinical Practice Guidelines. Hypertension 2018; 71: e13–e115.
3. Pierdomenico SD, Pierdomenico AM, Coccina F, Lapenna D, Porreca E. Circadian blood pressure changes and cardiovascular risk in elderly treated hypertensive patients. Hypertens. Res. 2016; 39: 805–811.
4. Coccina F, Pierdomenico AM, Pizzicannella, J, et al. Prognostic value of daytime and nighttime blood pressure in treated hypertensive patients according to age and sex. J. Clin. Hypertens. 2020; 22: 2014–2021.
5. Huang QF, Yang WY, Asayama K, et al. Ambulatory Blood Pressure Monitoring to Diagnose and Manage Hypertension. Hypertension 2021; 77: 254–264.
6. Roger VL. Epidemiology of heart failure. Circ. Res. 2013; 113: 646–659.
7. McMurray JJ, Stewart S. Epidemiology, aetiology, and prognosis of heart failure. Heart 2000; 83: 596–602.
8. Dunlay SM, Weston SA, Jacobsen SJ, Roger VL. Risk factors for heart failure: a population-based case-control study. Am J Med 2009; 122: 1023-1028.
9. Ingelsson E, Björklund-Bodegård K, Lind L, Arnlöv J, Sundström J. Diurnal blood pressure pattern and risk of congestive heart failure. JAMA 2006; 295: 2859–2866.
10. Pierdomenico SD, Pierdomenico AM, Coccina F, Lapenna D, Porreca E. Ambulatory blood pressure parameters and heart failure with reduced or preserved ejection fraction in elderly treated hypertensive patients. Am. J. Hypertens. 2016; 29: 1001–1007.
11. Kario K, Hoshide S, Narita K, Okawara Y, Kanegae H. Investigators' network. Cardiovascular Prognosis in Drug-Resistant Hypertension Stratified by 24-Hour Ambulatory Blood Pressure: The JAMP Study. Hypertension 2021; 78: 1781–1790.
12. Coccina F, Pierdomenico AM, Cuccurullo C, Pizzicannella J, Trubiani O, Pierdomenico SD. Ambulatory Resistant Hypertension and Risk of Heart Failure in the Elderly. Diagnostics (Basel). 2023; 13 :1631.

IJAE
ITALIAN JOURNAL OF ANATOMY AND EMBRYOLOGY

Firenze University Press
www.fupress.com/ijae

OPEN ACCESS

Citation: Falconio, L., Valente, F., Mavriqi, L., Trubiani, O., & Traini, T. (2023). The implant loading influence on crestal bone remodelling around hybrid titanium implants: a prospective clinical study. *Italian Journal of Anatomy and Embryology* 127(2): 129-132. doi: 10.36253/ijae-14821

Data Availability Statement: All relevant data are within the paper and its Supporting Information files.

Competing Interests: The Author(s) declare(s) no conflict of interest.

The implant loading influence on crestal bone remodelling around hybrid titanium implants: a prospective clinical study

Luigi Falconio[1,2,*,A], Francesco Valente[1,2,A], Luan Mavriqi[3], Oriana Trubiani[1,2], Tonino Traini[1,2]

[1] *Department of Innovative Technologies in Medicine & Dentistry, University "G. d'Annunzio" of Chieti-Pescara, Via dei Vestini 31, 66100 Chieti, Italy*
[2] *Electron Microscopy Laboratory, University "G. d'Annunzio" of Chieti-Pescara, Via dei Vestini 31, 66100 Chieti, Italy*
[3] *Department of Dentistry, Albanian University, Tirana 1001, Albania*
*Corresponding author. E-mail: luigi.falconio@unich.it
[A] These authors equally contribute to this work.

Abstract. The aim of this work was to analyze the changes of the mesial and distal cortical bone peaks around the hybrid titanium implants in relation to the masticatory load up to 7 years of follow-up. The analysis aims how occlusal loads may affect the peri-implant bone years after insertion through two-dimensional analysis using intraoral digital radiographs. Twelve hybrid T3 implants (Biomet 3i) were placed in 9 healthy patients with the 2-stage surgical approach. Standardized digital Rx were taken after early loading (6-8 weeks) after placement (T0); after 12 months (T1); after 30 months (T2); after 4 years follow-up (T3), after 5 years follow-up (T4), after 6 years follow-up (T5), after 7 years follow-up (T6). The marginal bone gain and loss was digitally measured. From T2 to T4 (5 years follow-up) there was a new bone formation demonstrating that well-balanced load forces can ensure good maintenance, with a crestal bone gain during the 2.7 to 7-year follow-up period.

Keywords: correct implant loading, peri-implant bone resorption, marginal bone loss, dental implant, loading procedure.

INTRODUCTION

Prosthetic rehabilitation through the insertion of implants requires achieving osteointegration and maintaining the height of the cervical bone (6). In the analysis of the longevity of the rehabilitation treatment, occlusal biomechanics plays a fundamental role in preventing the failure of already osseointegrated implants and favouring their correct maintenance, since occlusal overload is one of the main causes of loss of bone insertion around implants (3).

In the last decade, it was already defined how the behaviour of bone structures can be predicted in the face of a constant stimulus, which trans-

lates into the preservation of bone tissue (5). An ineffective mechanical stimulus can lead to reabsorption due to disuse. Conversely, exacerbated values can lead to disorganizations, due to remodeling, which in turn cause irreversible structure micro-deformation (8).

When osseointegration processes are achieved, newly formed bone directly contacts the titanium surface, and bone remodeling allows the implant to be fixed into the vital bone during occlusion (12). Peri-implant bone preservation can be considered the paramount aspect for long-term successful treatment outcomes. The bone quantity/quality surrounding an implant, affects the osseointegration process and shape/outline of the above soft tissue, both important for treatment function and aesthetic efficacy (9).

In this light, data on a management procedure aimed at preventing or minimizing bone resorption, and short/long term is still lacking.

Therefore, it was the purpose of the present preliminary series to investigate in a cohort of 9 patients whether crestal bone changed in a time-dependent manner from early loading of hybrid implants to 7 years follow-up.

MATERIALS AND METHODS

Nine healthy patients were enrolled in the present prospective study and received 12 T3 implants (Biomet 3i, Palm Beach Gardens, FL, USA) using the 2-stage surgical approach (Table 1). A careful phase of general and specific intraoral anamnesis was performed for all patients, followed by first and second level radiographic examinations to analyze the quality and quantity of available bone.

Furthermore, diagnostic wax-ups were performed for each patient to guide the insertion of the implants from an occlusal biomechanical point of view. Surgical and prosthetic protocols followed manufacturer guidelines and were performed by a single investigator in a private clinic (T.T.). The implants had submerged healing for 3.1 ± 0.2 weeks.

The final restorations were placed 7.5 ± 0.6 weeks after implant placement (14). Six implants were restored with cemented porcelain fused to metal and six implants with cemented monolithic zirconia, on screw-retained abutments. A long-term follow-up period was established: the implants were checked 12 months (1 year), 30 months (2.7 years), 4, 5, 6, and 7 years after the final delivery of the restoration (13).

Digital intraoral radiographs and computer processing were done to measure levels of crestal bone remodeling as it was a high-quality method for scientific evaluations with an accuracy of <0.1 mm (2). X-ray recordings Radiographs were performed with a digital sensor adopting complementary metal oxide semiconductor technology capable of recording 1.92-megapixel images with a pixel size of 18.5 μm (Kodak RVG 6100 Digital Radiography System: Carestream Health Inc., Rochester, NY, USA). A multiphase follow-up method was used to identify the time course of bone changes induced by each clinical procedure up to 7 years of follow-up.

The implant was considered an individual unit to overcome possible problems resulting in a more positive outcome for patients with multiple implants.

Data were analysed after the normality assessment (Shapiro-Wilk test), using the Repeated Measures ANOVA (RMANOVA) followed by the Tukey post hoc test. Statistical significance was set at $P < 0.05$.

Table 1. General characteristics and surgical procedure parameters in patients admitted into the study.

Patient	Age	Sex	IS	OB	BD	ID (mm)	FTDD (mm)	FDUT (Ncm)	IP	IBF
1	64	F	3.6	Native	Normal	4 x 10	4.0	50	Sub.	Tight
			3.6	Native	Normal	4 x 10	4.0	50	Crestal	Firm
2	63	M	3.7	Native	Normal	4 x 10	4.0	50	Sub.	Firm
3	42	F	4.6	Native	Dense	4 x 8.5	4.0	50	Crestal	Tight
			4.5	Native	Dense	4 x 11.5	4.0	50	Crestal	Tight
4	47	M	4.7	Native	Dense	5 x 8.5	5.0	50	Crestal	Tight
5	53	M	3.4	Native	Normal	4 x 11.5	4.0	50	Crestal	Firm
6	48	M	2.5	Native	Normal	5 x 10	5.0	50	Sub.	Firm
7	42	F	3.6	Native	Normal	5 x 11.5	5.0	50	Sub.	Tight
			1.5	Augment	Dense	4 x 11.5	4.0	50	Sub.	Firm
8	40	F	1.6	Augment	Dense	4 x 13	4.0	50	Sub.	Tight
9	50	F	4.7	Native	Normal	5 x 8.5	5.0	50	Sub.	Firm

Abbreviations: IS, implant site; Sub.: Subcrestal.

RESULTS

The implants were perfectly osseointegrated and were loaded early 6-8 weeks after placement (T0) (7). Since loading the implants, no failures have been recorded and all fixed prosthetic restorations were stable at the end of the 7-year observation period. At T0 the mean peri-implant bone level was -0.43. The mean bone level at each step was 0.64 mm (T1), 0.76 mm (T2), 0.58 mm (T3), 0.47 mm (T4), 0.53 mm (T5), 0.49 mm (T6). These data showed that most of the peri-implant bone loss occurred in the period following early loading of the implants (11). There were no statistically significant differences in the comparison between T0 and the other follow-up periods in terms of crestal bone resorption around the implants (p>0,05). Therefore, implant with regular occlusal loading can maintain adequate crestal bone levels for correct long-term function.

DISCUSSION

Research in implant surgery, requires the maintenance of the crestal bone level over the years. The dependent factors are various, for example correct oral hygiene, a minimum required quantity of adherent gingiva and the occlusal load to which the implants are subjected (4). The most common problem is the absence of reference data on the peri-implant bone level over the long term in literature (>3 years). In the present study we found that in adult patients undergone to surgical procedure with Hybrid implant T3 (Biomet 3i, Palm Beach Gardens, FL, USA), longitudinal X-ray of the crestal bone level showed no differences between the short- and long-term follow-up. Most bone resorption occurred up to about 3 years (T2) (1). This supports the hypothesis that the primary reason for crestal bone loss during the first year of function, and thereafter, is the establishment of biological width. This process can therefore be considered a fast-acting factor (10). An important element is represented by the study carried out by our research group, where the behavior of the crestal bone was analyzed in the period between the second implant uncovering operation and their load. (T2) (11).

The main limitation of the present study is related to the small sample size. Furthermore, method of measuring the crestal bone level performed on digital X-rays, being operator dependent, can bring to a variability of results. In conclusion, the surprising factor that we found with this study was the crestal bone gain registered during the follow-up period from 2.7 to 7 years (T2-T6). We considered the applied load the main responsible for the bone gain stimulation, during a long period of correct functioning of the system crown-implant-bone. Future research is needed to shed lighter on these factors, such as finding a way to standardize bone response as a function of load.

REFERENCES

1. Coli, Pierluigi, and Torsten Jemt. 2021. 'On Marginal Bone Level Changes around Dental Implants'. Clinical Implant Dentistry and Related Research 23 (2): 159–69. https://doi.org/10.1111/cid.12970.
2. De Smet, E., R. Jacobs, F. Gijbels, and I. Naert. 2002. 'The Accuracy and Reliability of Radiographic Methods for the Assessment of Marginal Bone Level around Oral Implants'. Dento Maxillo Facial Radiology 31 (3): 176–81. https://doi.org/10.1038/sj/dmfr/4600694.
3. Krawiec, Maciej, Cyprian Olchowy, Paweł Kubasiewicz-Ross, Jakub Hadzik, and Marzena Dominiak. 2022. 'Role of Implant Loading Time in the Prevention of Marginal Bone Loss after Implant-Supported Restorations: A Targeted Review'. Dental and Medical Problems 59 (3): 475–81. https://doi.org/10.17219/dmp/150111.
4. Laurell, Lars, and Dan Lundgren. 2011. 'Marginal Bone Level Changes at Dental Implants after 5 Years in Function: A Meta-Analysis'. Clinical Implant Dentistry and Related Research 13 (1): 19–28. https://doi.org/10.1111/j.1708-8208.2009.00182.x.
5. Lin, Hsi-Kuei, Jerry Chin-Yi Lin, Yu-Hwa Pan, Eisner Salamanca, Yi-Ting Chang, Yung-Szu Hsu, Yi-Fan Wu, Chin-Kai Lin, Odontuya Dorj, and Wei-Jen Chang. 2022. 'Peri-Implant Marginal Bone Changes around Dental Implants with Platform-Switched and Platform-Matched Abutments: A Retrospective 5-Year Radiographic Evaluation'. Journal of Personalized Medicine 12 (8): 1226. https://doi.org/10.3390/jpm12081226.
6. Pandey, Chandrashekhar, Dinesh Rokaya, and Bishwa Prakash Bhattarai. 2022. 'Contemporary Concepts in Osseointegration of Dental Implants: A Review'. Edited by João Paulo Mendes Tribst. BioMed Research International 2022 (June): 1–11. https://doi.org/10.1155/2022/6170452.
7. Sanz-Sánchez, Ignacio, Ignacio Sanz-Martín, Elena Figuero, and Mariano Sanz. 2015. 'Clinical Efficacy of Immediate Implant Loading Protocols Compared to Conventional Loading Depending on the Type of the Restoration: A Systematic Review'. Clinical Oral Implants Research 26 (8): 964–82. https://doi.org/10.1111/clr.12428.

8. Suarez, Fernando, Hsun-Liang Chan, Alberto Monje, Pablo Galindo-Moreno, and Hom-Lay Wang. 2013. 'Effect of the Timing of Restoration on Implant Marginal Bone Loss: A Systematic Review'. Journal of Periodontology 84 (2): 159–69. https://doi.org/10.1902/jop.2012.120099.
9. Suárez-López Del Amo, Fernando, Guo-Hao Lin, Alberto Monje, Pablo Galindo-Moreno, and Hom-Lay Wang. 2016. 'Influence of Soft Tissue Thickness on Peri-Implant Marginal Bone Loss: A Systematic Review and Meta-Analysis'. Journal of Periodontology 87 (6): 690–99. https://doi.org/10.1902/jop.2016.150571.
10. Sun, Ping, Dan Yu, Xin Luo, Antian Xu, Yi Feng, and Fu-Ming He. 2022. 'The Effect of Initial Biologic Width on Marginal Bone Loss: A Retrospective Study'. The International Journal of Oral & Maxillofacial Implants 37 (1): 190–98. https://doi.org/10.11607/jomi.9169.
11. Traini, Tonino, Marco Berardini, Francesca Congedi, Bruna Sinjari, Paolo Trisi, and Sergio Caputi. 2017. 'Impact of Second Stage Surgery on Bone Remodeling Around New Hybrid Titanium Implants: A Prospective Clinical Study in Humans'. Implant Dentistry 26 (1): 121–28. https://doi.org/10.1097/ID.0000000000000525.
12. Traini, Tonino, Jörg Neugebauer, Ulf Thams, Joachim E. Zöller, Sergio Caputi, and Adriano Piattelli. 2009. 'Peri-Implant Bone Organization under Immediate Loading Conditions: Collagen Fiber Orientation and Mineral Density Analyses in the Minipig Model'. Clinical Implant Dentistry and Related Research 11 (1): 41–51. https://doi.org/10.1111/j.1708-8208.2008.00086.x.
13. Windael, Simon, Stijn Vervaeke, Lieve Wijnen, Wolfgang Jacquet, Hugo De Bruyn, and Bruno Collaert. 2018. 'Ten-Year Follow-up of Dental Implants Used for Immediate Loading in the Edentulous Mandible: A Prospective Clinical Study'. Clinical Implant Dentistry and Related Research 20 (4): 515–21. https://doi.org/10.1111/cid.12612.
14. Zuffetti, Francesco, Marco Esposito, Fabio Galli, Matteo Capelli, Giovanni Grandi, and Tiziano Testori. 2016. 'A 10-Year Report from a Multicentre Randomised Controlled Trial: Immediate Non-Occlusal versus Early Loading of Dental Implants in Partially Edentulous Patients'. European Journal of Oral Implantology 9 (3): 219–30.

Finito di stampare da
Logo s.r.l. – Borgoricco (PD) – Italia

IJAE
Italian Journal of Anatomy and Embryology
Vol. 127, N. 2 – 2023

€ 26,00 (for Italy)